THE UNIVERSITY of ADELAIDE

Engineering Novel Nano-Structured 3D-Printed Titanium Implants for Optimized Osseointegration, Antibacterial Protection and Localized Drug Delivery Applications

By

Shaheer Makar

Supervisors:

Professor Dusan Losic

Professor Gerald J. Atkins

A thesis is submitted for the degree of

Doctor of Philosophy

In

School of Chemical Engineering and Advanced Materials

The University of Adelaide, Australia

October 2021

BLANK PAGE

To my best friend and beloved wife Sally, who has always been there for me and supported me at my highest and lowest points in life, and to my beautiful strong children Nadine and Jonathan, who endured my deficiencies and who always remind me that life is beautiful. To my devoted parents, Guirguis and Amany, who constantly encouraged me and helped me to achieve my goals, and to my brother Nader who always supported me.

TABLE OF CONTENTS

LIST OF FIGURES

Chapter 1

Chapter 2

Chapter 3

Chapter 4

Chapter 5

Chapter 6

LIST OF TABLES

Chapter 2

LIST OF SCHEMES AND DIAGRAMS

Chapter 3

LIST OF ABBREVIATIONS

3 dimensional printed titanium	3D-Ti
3 dimensional printed titanium with surface nanopillars fabricated by electrochemical anodization followed by hydrothermal process	HT-TNTs-3D-Ti
3 dimensional printed titanium with titania nanotubes fabricated by electrochemical anodizationon top	TNTs-3D-Ti
3-(4,5-dimethylthiazol-2-yl)-5-(3carboxymethoxyphenyl)-2-(4-sulfophenyl)-2h tetrazolium assay	MTS assay
3-sulfopropyl methacrylate potassium salt	PSPMA
4',6-diamidino-2-phenylindole	DAPI
Additive manufacturing	AM
Alternative immersion method	AIM
American Society for Testing and Materials	ASTM
Antimicrobial resistance	AMR
Arginine–glycine-aspartic acid–cysteine	RGDC
Average roughness value	R_a
Bicinchoninic acid	BCA
Bovine serum albumin	BSA
Chemical vapor deposition	CVD
Colony forming units	CFUs
Confocal laser scanning microscopy	CLSM
Doxorubicin	DOX
Dulbecco's modified Eagle's culture medium	DMEM
Electrical stimulation therapy	EST
Electrochemical anodization (EA)	EA
Electrophoretic deposition	EPD
Energy-dispersive X-ray spectroscopy	EDX, EDS
Extracellular matrix proteins	ECM
Extracellular polymeric substance	EPS
Fibroblast growth factor	FGF
Focused-ion beam	FIB
Formation of Ti Nano-nodular Structure by Electron-Beam-Physical Vapor Deposition	EB-PVD
Gallium nitrate coated HT-tnts-3D-Ti	Ga-HT-TNTs-3D-Ti

Gallium nitrate loaded tnts-3D-Ti discs	Ga-TNTs-3D-Ti
Gentamicin- loaded TNTs	GN-TNTs
Gold	Au
Growth factors	GFs
Hexamethyl disilazane	HDMS
Horseradish peroxide	HRP
Human fibronectin fragments	hFN
Hydrothermal process	HT
Hydroxyapatite	HA, HAP
Inductively coupled plasma mass spectrometry	ICP-MS
Infrared	IR
Lactate dehydrogenase	LDH
Lactic acid	LA
Localized drug delivery	LDD
Methicillin-resistant *Staphylococcus aureus*	MRSA
Microcomputerized tomography	μCT
Nanoparticles	NP
Normal human osteoblast-like cells	NHBCs
One-way analysis of variance	ANOVA
Optical density	OD
Phosphate buffer solution	PBS
Physical vapor deposition	PVD
Plasma electrolytic oxidation	PEO
Plasma polymerization	PP
Poly (lactideglycolide acid)	PLGA
Poly (vinyl alcohol)	PVA
Pseudomonas aeruginosa	*P. aeruginosa*
Pulsed laser deposition	PLD
Radio frequency identification	RFID
Reverse transcription-quantitative polymerase chain reaction	RT-qPCR
Scanning electron microscopy	SEM
Selective laser melting	SLM
Selenium	Se
Self-assembled monolayers	SAM

Silver	Ag
Simulated body fluid	SBF
Standard deviation	SD
Staphylococcus aureus	*S. aureus*
Staphylococcus epidermidis	*S. epidermidis*
Strontium	Sr
Suture mesenchymal cells	SMCs
Thermogravimetric analysis	TGA
Three-dimensional printing	3D-printing
Ti alloy composed of 6% w/w Aluminum, 4% w/w vanadium and 90% w/w titanium	Ti6Al4V alloy
Titania	TiO_2
Titania nanotubes	TNTs
Titanium	Ti
Titanium nanotubes	TiNTs
Tris-hydroxymethyl aminomethane	Tris
Tryptone soy agar	TSA
Tumor necrosis factor	TNF
Tumor necrosis factor-related apoptosis-inducing ligand	Apo2L/TRAIL
Ultrasonic waves	USW
Vancomycin incorporated into HAP	Van HA
Water contact angle	WCA
X-ray diffraction spectra	XRD

ABSTRACT

Titanium (Ti) and its alloys have been used for decades as bone implants owing to their desirable biomechanical properties and corrosion resistance. However, they present many postoperative challenges in the body including inadequate osseointegration (*e.g.*, poor attachment and differentiation, or overgrowth of bone cells), inflammation and infection. More than 5% of bone implants are rejected requiring repeated surgeries associated with increased patient suffering and high socioeconomic expense. Moreover, the requirements and surface properties of the implant are significantly determined according to the type of application and duration of use. Permanent or long-term implants are required for ongoing fixation (*e.g.*, dental implants, hip and bone replacements), thus they should support bone cell attachment and differentiation on their surface (osseointegration) to improve mechanical stability. On the other hand, short-term implants used for temporal fracture fixing, especially in paediatrics, which are eventually removed from the body after serving their purpose, should not support osseointegration in order to facilitate their surgical removal.

Studies have indicated that the implant surface, micro- and nano-scale topography, could play a vital role in directing implant bio-integration. At the same time, the surface topography could significantly affect bacterial attachment and biofilm formation on the implant surface. This thesis aims to engineer new and advanced Ti implants featuring multiple functions including controlled cell-implant interaction (*i.e.*, enhancement or reduction), localized drug release and bactericidal activity to address the key challenges associated with implants. As a result, four specific aims are included; (i) nano-surface fabrication of nano-tubular arrays (TNTs) or nanopillars onto the surface of 3D-printed Ti implants to achieve desired combination of micro- and nano-rough surface properties, (ii) studying the drug loading capabilities of the fabricated implants using different therapeutic agents (e.g., anticancer and antibacterial agents), (iii) controlling the cell adhesion and growth on the surface of the implants

to optimize bone cell attachment for either permanent or removable implants and (iv) enhancing the antibacterial properties of the fabricated implants.

In order to address these aims, 3D-printed titanium implants were fabricated using additive manufacturing selective laser melting (SLM) technology (*i.e.*, 3D-printing) followed by low cost, scalable surface nanoengineering manufacturing technologies of electrochemical anodization and hydrothermal process. As a result, unique implants surfaces featuring hierarchical micro-nano structures were generated covered with either TNTs or nanopillars. The fabrication and physicochemical characterization of the fabricated implants were assessed using multiple techniques such as scanning electron microscope, energy-dispersive X-ray spectroscopy (EDX), X-ray diffraction spectroscopy (XRD) and water contact angle (WCA). Moreover, bone cell responses, drug delivery properties and antibacterial activity of fabricated implants were assessed *in-vitro*.

Results described herein confirmed the successful fabrication of surface nanostructures (*i.e.,* TNTs and nanopillars). The drug loading and release of anticancer (doxorubicin and Apo2L/TRAIL) and antibacterial (gallium ions) agents were successfully demonstrated. At the same time, the antibacterial activity of TNTs and nanopillars was verified against two bacterial strains that commonly cause bone infections; *Staphylococcus aureus* and *Pseudomonas aeruginosa*. Finally, the control of bone cell growth over the implant surface was successfully demonstrated by adjusting the surface nano topography of the implants.

The research studies completed in this thesis combine fundamental understanding and application of knowledge of the surface, structural and chemical characteristics of Ti implant surfaces. These findings will facilitate the engineering of the next generations of advanced bone implants that will open the door to replace conventional implant manufacturing technology.

PREFACE

This Ph.D. thesis is submitted as a "thesis by publication" in accordance to the "Specifications for Thesis 2020" of The University of Adelaide. This thesis contains the following list of publications that resulted from my Ph.D. candidature. The outcomes generated during my PhD candidature include 8 published journal articles and 4 book chapters.

List of journal publications (Published/Under Review):

1- **Shaheer Maher**, Denver Linklater, Hadi Rastin, Pei Le Yap, Elena P. Ivanova and Dusan Losic (2022), **Tailoring additively manufactured titanium implants for short-time pediatric implantations with enhanced bactericidal activity**. ChemMedChem. 17(2): e202100580. doi.org/10.1002/cmdc.202100580

2- **Shaheer Maher**, Denver Linklater, Hadi Rastin, Sandy Liao, Karolinne Martins, de Sousa, Luis Lima-Marques, Peter Kingshott, Helmut Thissen, Elena P. Ivanova and Dusan Losic (2021), **Advancing of 3D-printed titanium implants with combined antibacterial protection using ultrasharp nanostructured surface and gallium-releasing agents**. ACS Biomaterials Science & Engineering 8(1): 314–327. doi.org/10.1021/acsbiomaterials.1c01030

3- **Shaheer Maher**, Asiri R. Wijenayaka, Luis Lima-Marques, Dongqing Yang, Gerald J. Atkins and Dusan Losic (2021), **Advancing of additive-manufactured titanium implants with bioinspired micro- to nanotopographies**. ACS Biomaterials Science & Engineering 7(2): 441-450. doi.org/10.1021/acsbiomaterials.0c01210

4- **Shaeer Maher**, Arash Mazinani, Mohammad Reza Barati and Dusan Losic (2018), **Engineered titanium implants for localized drug delivery: Recent advances and perspectives of titania nanotubes arrays**. Expert Opinion on Drug Delivery **15**(10): 1021-1037. doi.org/10.1080/17425247.2018.1517743

5- **Shaheer Maher**, Tushar Kumeria, Moom Sin Aw and Dusan Losic (2018), **Diatom silica for biomedical applications: Recent progress and advances**. Advanced Healthcare Materials **7**(19): e1800552. doi.org/10.1002/adhm.201600688

6- Jie Qin, Dongqing Yang, **Shaheer Maher**, Luis Lima-Marques, Yanmin Zhou, Yujie Chen, Gerald J. Atkins and Dusan Losic (2018), **Micro- and nano-structured 3D printed titanium implants with a hydroxyapatite coating for improved osseointegration**. Journal of Materials Chemistry B **6**(19): 3136-3144. doi.org/10.1039/C7TB03251J

7- **Shaheer Maher**, Gagandeep Kaur, Luis Lima-Marques, Andreas Evdokiou and Dusan Losic (2017), **Engineering of micro- to nanostructured 3D-printed drug-releasing titanium**

implants for enhanced osseointegration and localized delivery of anticancer drugs. ACS Applied Materials & Interfaces **9**(35): 29562-29570. doi.org/10.1021/acsami.7b09916

8- Tushar Kumeria, Steven J P McInnes, **Shaheer Maher** and Abel Santos (2017), **Porous silicon for drug delivery applications and theranostics: Recent advances, critical review and perspectives**. Expert Opinion on Drug Delivery **14**(12): 1407-1422. doi.org/10.1080/17425247.2017.1317245.

List of book chapters:

1- Dusan Losic and **Shaheer Maher** (2022)**, Nanoporous anodic alumina (NAA): *In-vitro/vivo* approaches.** In Advanced Porous Biomaterials for Drug Delivery Applications, Mahaveer Kurkuri, Dusan Losic and U. T. Uthappa (Eds), CRC Press (In press)

2- **Shaheer Maher** and Dusan Losic (2022), **Surface bioengineering of nanostructured diatom biosilica and their applications in drug delivery.** In Advanced Porous Biomaterials for Drug Delivery Applications, Mahaveer Kurkuri, Dusan Losic and U. T. Uthappa (Eds), CRC Press (In press)

3- **Shaheer Maher** and Dusan Losic (2018), **Nanotechnologies for tissue engineering and regeneration: Nanoengineered titania nanotube arrays for localized drug delivery and enhanced osseointegration**. In Nanotechnologies in Preventive and Regenerative Medicine: An Emerging Big Picture, V. Uskokovic, and D. Uskokovic (Eds.), (pp. 163-193). Netherlands: Elsevier. doi.org/10.1016/B978-0-323-48063-5.00002-2

4- **Shaheer Maher**, Moom Sin Aw and Dusan Losic (2019), **Diatom silica for biomedical applications**. In Diatoms: Fundamentals and Applications, Joseph Seckbach and Richard Gordon (Eds), (pp. 511-536).Wiley. doi.org/10.1002/9781119370741.ch20

List of awards:

1- Australian Government Research and Training Program (RTP) Scholarship (2017-2021).

2- Forrest George and Sandra Lynne Young Supplementary Scholarship (2017-2021).

3- ARC Grant-funded Supplementary scholarship (2017-2021).

DECLARATION

I certify that this work contains no material which has been accepted for the award of any other degree or diploma in my name, in any university or other tertiary institution and, to the best of my knowledge and belief, contains no material previously published or written by another person, except where due reference has been made in the text. In addition, I certify that no part of this work will, in the future, be used in a submission in my name, for any other degree or diploma in any university or other tertiary institution without the prior approval of the University of Adelaide and where applicable, any partner institution responsible for the joint-award of this degree.

I acknowledge that copyright of published works contained within this thesis resides with the copyright holder(s) of those works. I also give permission for the digital version of my thesis to be made available on the web, via the University's digital research repository, the Library Search and also through web search engines, unless permission has been granted by the University to restrict access for a period of time.

I acknowledge the support I have received for my research through the provision of an Australian Government Research Training Program Scholarship.

Shaheer Makar Date: 1/10/2021

ACKNOWLEDGEMENTS

I would like to express my sincere appreciation and gratitude to the following people and organizations, without whom this thesis would have not been possible:

- My principal supervisor and mentor ***Prof. Dusan Losic***, for his constructive supervision, scientific guidance, encouragement and for exerting much of his time and effort for the fine adjustment, monitoring, and guiding my efforts in all steps in this thesis with his creative valuable advice and instructions. Without his generous advice and encouragement, this work would not have come to light. Really, I greatly respect his scientific thinking and creative mentality. His generosity, kindness and humanity are unique and everlasting.

- My co-supervisor ***Prof. Gerald J. Atkins*** for his scientific guidance, encouragement, and moral support. He kindly exerted much of his time and effort to teach me and help me improve my work, interpret results logically, and troubleshoot experimental errors. I appreciate his time and dedication in drafting and revising my thesis.

- ***Prof. Elena Ivanova and her team*** for their support and significant participation in the bacterial studies throughout my thesis that was published as two research papers.

- I would like to extend my gratitude to ***Mrs Sandra Young*** for her generous support through Forrest George and Sandra Lynne Young Supplementary Scholarship. I have met Sandra many times during the last few years and I was so touched by her kind and humble personality.

This work would not have been possible without the financial support provided by the Commonwealth through the Australian Government Research Training Program (RTP) and Australian Research Council (ARC) supplementary scholarships

- I cannot find the words to express my great thankfulness to my family, my wife and my kids who gave me plenty of love, support and kindness and have been always with me through this journey. God bless them all and convey upon them peace and happiness.

Finally, all praise is to God for granting me the power and will, relieving me during hard times, and helping me throughout my whole life.

Shaheer Makar

CHAPTER 1

INTRODUCTION

1.1 Background:

Titanium (Ti) and its alloys have been extensively utilized as implant materials in dental and orthopaedic applications (*e.g.*, fracture fixation, joint replacement) due to their desirable properties including outstanding mechanical characteristics and biocompatibility with human tissues, while also being corrosion resistant [1-4]. Despite the great progress in the design of Ti-based implants, many challenges remain related to their intended use, design and interaction with the bone tissues. In this chapter, those limitations will be discussed followed by the aims of the thesis, however, before going through the limitations associated with the use of Ti implants, it is important to understand the structure of bone.

The human skeleton is formed of numerous bone types of various shapes, including long short, flat, sesamoid and irregular bones. In addition to biomechanical functions, including mechanical support and muscle attachment allowing mobility, and acting as protective armour for vital organs, bone is increasingly recognised as performing numerous biochemical and biological functions, including calcium and phosphate homeostasis, as well as being the centre of haematogenesises [5, 6], however the extensive underlying biology of the bone is beyond the scope of this chapter.

Bone is composed of a heterogenous complex of organic materials and minerals. The main mineral is a hydroxyapatite-like calcium phosphate, which represents more than 60% of bone's mass and contributes mechanical hardness. The organic portion is mostly composed of collagen, primarily type I, which comprises 20-25 % mass, which contributes flexibility, while free or bound water forms the remaining ~10%. Microscopic examination of bone reveals a parallel array of triple-helical type I collagen fibrils, usually arranged parallel to the axis of mechanical loading, impregnated with bone mineral [6].

Bone can be also classified macroscopically as cortical or cancellous. Cortical bone, also known as compact bone, is the solid outer layer of the bone and is the major contributor to overall bone strength. In contrast, cancellous bone is found in the epiphyses and metaphyses of the long bones and between cortical layers of the flat bones. It hosts the bone marrow inside its cavity. The architecture of the cancellous bones consists of void spaces between bony trabeculae, which provide additional mechanical support without adding more weight. The compact structure of bone represents a significant challenge for drug delivery owing to poor diffusion of medications through the highly-calcified tissue. Bones are mainly supplied with blood through three main routes, nutrient artery, periosteal and epiphyseal vessels. For further details about the detailed anatomy of the bones and blood supply please refer to references [6].

Challenges facing Ti bone implants:

1- Controlling the process of osseointegration

The attachment of bone cells to the implant surface is a critical process that determines the degree of osseointegration and the ultimate fate of implants. Soon after surgical insertion, numerous processes can potentially occur at the bone-implant interface, including an inflammatory response and or host bone cell attachment. Thus, the physical and chemical properties of the implant surface can significantly influence the host response [7].

Ti implants differ according to their application and intended life span inside the body. Based on the expected duration of application, implants can be divided into two categories; permanent, which are required for long-term fixation (*e.g.*, dental implants, hip and bone replacements) and short-term, which are applied for temporal fracture fixation that ultimately need to be removed from the body (*e.g.*, implants used in paediatrics due to rapid bone growth and in some cancer treatment applications [8]).

Permanent implants (*e.g.,* joint replacement prostheses) are intended to be placed inside the body for prolonged period of times, thus they should support cell attachment and growth to allow maximum longevity in the body. In case of short-term implants, cellular on-growth is not required and may be troublesome when implant removal is due. Thus, these temporal implants should either slow or at least not support, significant bone cell growth on their surface.

Most of the current research studies focus on improving the process of osseointegration on the implant surface that is desirable for long-term implants. Several approaches have been investigated to improve the process of osseointegration [9]. One simple approach involves the application of a thin film of hydroxyapatite onto the surface of the implant, which was found to enhance bone cell function and promote osseointegration [10]. Another promising approach involves modification of surface topography (*i.e.,* roughness) where many studies asserted that surface topography of the implants significantly influence the process of osseointegration [11-14]. Previous studies demonstrated the ability of the micro-texture to promote "osteoconduction" [15] (*i.e.,* bone cell growth onto the implant surface) and "osteoinduction" [15] (*i.e.,* encouraging cells to differentiate into osteoblasts on the implant surface) [12, 16].

Beyond implant micro-texture, the advent of nanotechnology has made tools available to fabricate implants with nanometer dimensioned surface architecture (*e.g.,* nanotubes and nanopores). Many studies have determined that nano-rough surface patterns, particularly nano-tubular structures, significantly affect protein adsorption and osteoblast activity that leads to controlled osteoblast adhesion and long-term osseointegration, in comparison with smooth or micro-rough surfaces [17, 18]. In this context, titania or titanium dioxide nanotubes (TNTs) represent remarkable nanostructures with a wide range of potential applications. They are similar to hollow test tubes, vertically aligned and composed of titanium dioxide (TiO_2) [19]. They have an opening at the top and are closed at the bottom where they protrude from the underlying mass of the implant and can be prepared with strict control over resulting dimensions, with achievable diameters of 10-300 nm and lengths of 0.5 to 300 μm [4]. Previous

studies have established that TNTs, fabricated by electrochemical anodization, are cost-effective and simple modifications for conventional bone implants, with properties that can either enhance or retard bone cell on-growth and osseointegration [4, 19, 20].

It is worth mentioning that the optimal template for an implant surface design is still inconclusive [17, 21-23]. Moreover, additional research effort is urgently required towards the design and the study of short-term implants. This thesis is sought to investigate the different surface features (*e.g.*, micro-nano surface topography) that could enable Ti implants surface to either enhance or reduce bone cell attachment and proliferation, as will be discussed in Chapters 4 and 6.

2- Bacterial infection and inflammation

A common reason for the failure of orthopaedic implants is bacterial infection and inflammation [15, 24], leading to implant loosening and/or complete detachment from its place of insertion, requiring repeated surgery and eventually result in amputation or even death. Bacterial infection at the bone implant interface could arise from a variety of sources during the surgical procedure, or even after implant insertion, from infection of the surgical wound or haematogenous seeding from another site within the patient's body [32]. In this case, implants may serve as bacterial substrates that tend to form antibiotic-resistant biofilms on their surfaces [25]. **Figure 1** summarizes the main limitations related to bacterial infection causing bone implants' failure in their clinical applications.

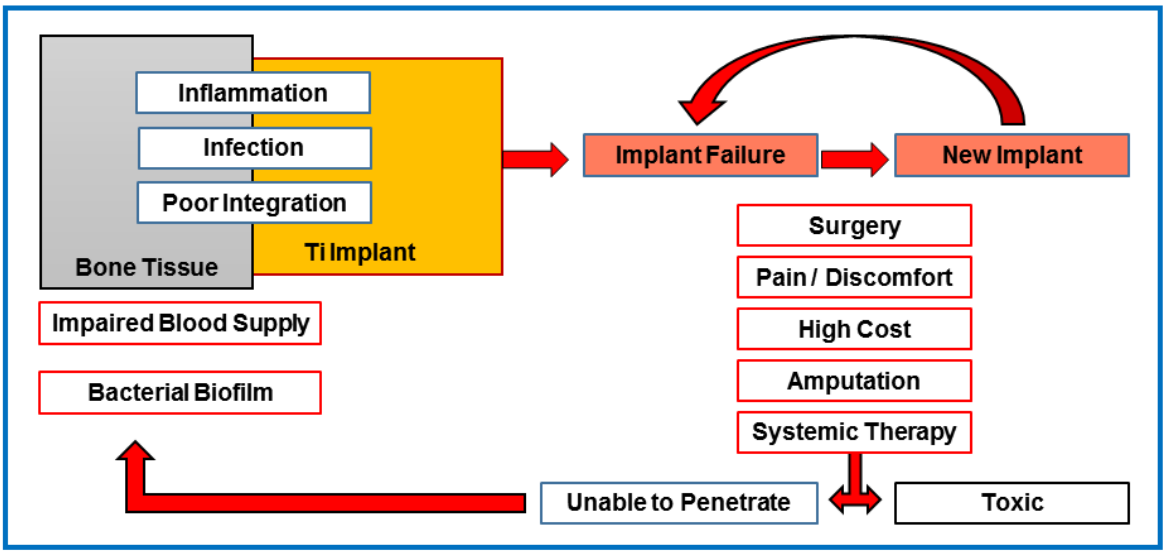

Figure 1: Illustration of common challenges associated with bone implants

One main approach, to cater for bone implants complications and rejections *(i.e.,* infection and inflammation) comprises systemic administration of potent antimicrobial agents. In order to reach the effective levels of therapeutics at the desired site (*i.e.,* the affected bone or joint), the whole body is exposed to elevated doses of drugs, which could be toxic, for example causing nephrotoxicity or disruption to the host gut microbiome. In addition, the infected bone may also suffer from compromised blood supply, which may hamper therapeutics from reaching the diseased areas [26]. Coupled with systemic administration, antibiotic-laden bone cements are commonly used when surgically revising an infected prosthesis. However, these suffer from problems with controllability, duration and extent of drug release, as well as systemic toxicity, which potentially limit the effectiveness of the antibiotics used [27]. These challenges often result in therapeutic failure and additional surgical actions to remove the implant.

Owing to the above-mentioned limitations of systemically delivered antibiotics, current research tends to focus on improvements to localized delivery of active therapeutics at the bone implant interface [28, 29]. This in turn will likely decrease dependence on systemic therapy while simultaneously providing significantly more effective local therapeutic effect and improving implant bio-integration performance [30, 31]. One key feature of drug releasing

implants is to release active therapeutics directly at the affected site, locally inside the bone micro-environment [30, 32-35]. Another key feature is that localized drug delivery has the potential to not only enhance the osseointegration and life span of the implants, but also provide effective treatment for conditions like: osteoporosis, bone infection (i.e. osteomyelitis) and related inflammation as well as malignant conditions such as bone carcinoma *etc*. [15, 20]. However, it is important to acknowledge that the excessive use of conventional antibiotics (*e.g.*, vancomycin or gentamicin) could result in the development of resistant bacterial strains [36]. As a result, many non-conventional antibacterial agents such as silver, copper or gallium ions are currently being explored to overcome this problem [37, 38].

Concerning localized drug delivery application from implants, the loading of sufficient amounts of therapeutics onto implants remains a challenge. Even after successful drug loading, the loaded therapeutics could suffer from insufficient loading amounts, uncontrollable or erratic release kinetics. To permit optimal loading of substantial amounts of active agents, the loaded therapeutics should be deeply integrated into the implant surface; and for effective therapy, a sustained and prolonged drug release is desired [29].

Another appealing approach to cater for bacterial infection is the development of surface micro/nanostructures with inherent antibacterial properties such as bioinspired nanostructures that mimic insect wings (e.g. cicadas and dragonflies), which are covered with natural nano-sharp structures that mechanically kill bacteria through disruption of their cell membranes [39, 40]. It is worth mentioning that studies also suggest that TNTs could also possess antibacterial activity [41]. This thesis will explore both approaches through designing implants that combine drug release function together with physical antibacterial properties as will be discussed in Chapters 3,4 and 6.

3- Tailoring the design of bone implants for individual patients:

Current production of Ti implants is based on conventional metal and metallurgical processing methods. Thus, one of the major limitations of currently used Ti implant is that they are fabricated with fixed shapes and dimensions and therefore they lack customization for specific cases such as children or due to cancer, where local drug delivery of anticancer is required [42]. In such cases, expensive and time-consuming implant alterations are made by post-processing. Furthermore, implant companies potentially lose millions of dollars each year through expiry of prefabricated generic implants.

A potential solution for this issue is to incorporate additive manufacturing (AM) technology in implant production. AM, for example involving 3D-printing, triggered a revolution in metal implant manufacturing [43]. It offered many improvements including design flexibility with ability to fabricate implants with complex geometries to mimic bone porosity [44]. In addition, AM could offer "on demand" production of implants specifically tailored for patients, (*e.g.*, young children) which is fast and reliable for achieving an optimal anatomical match [45]. Using AM, implants can be delivered on request instead of massive production of implants that could eventually expire. Selective laser melting (SLM) is considered the ideal AM technique for implants fabrication with ability to print a variety of metals (*e.g.*, Ti based, stainless steel, Co-Cr, Mg, Ca, Zn, Ta and Ti-Ni) while reducing waste materials and costs of implants [43, 46]. It can also print metal combinations or metal/ceramic combination implants with no post-processing required which is usually needed in conventional techniques such as casting or machining [46, 47]. Based on that, all implants studied throughout this thesis were fabricated using SLM of Ti alloy (Ti6Al4V) powder.

Research Gaps

Although many approaches have been investigated to produce the appropriate surface topography, bioactivity, antibacterial properties and localized drug delivery capabilities, these implant characteristics have not been integrated into one tailorable technology [9]. Thus, there

is an urgent need for multifunctional implants that can overcome the abovementioned challenges.

In addition, the actual impact of the surface features (*e.g.*, micro or nano), their shape (pores, tubes, particles, rods, wires, spikes, *etc.*), on bone tissue formation is still in debate, which makes it difficult to compare the influences of these topographical features [48]. For example, nanostructures of ~100 nm were capable of disrupting integrin clusters, resulting in the inhibition of cellular adhesion and proliferation [49]. On the other hand, nanoporous structures (~30 nm in diameter) enhanced adhesion of bone cells [50].

To achieve efficient loading of therapeutics together with tuning of the surface roughness, several nano-engineering techniques, to generate nano/micro-rough surfaces, have been proposed, including an electrochemically engineered anodization process, which has been investigated for many materials, such as porous silicon, porous alumina and titania nanotubes; it is worth mentioning that, this method is cost-effective and could be easily scaled up [51].

This thesis will combine fundamentals of materials science, nanotechnology, chemistry, biology and drug delivery to prepare unique bone implants manufactured using 3D-printing technology of Ti alloy powder. The implants surface will be modified using a variety of techniques including electrochemical anodization, hydrothermal process and alternative immersion method (AIM). The final implants will feature nano/micro-topography for controlled osseointegration together with drug releasing and antibacterial capabilities in an attempt to overcome current limitations of common implants.

1.2 Aims/Objectives of the project

This aims of this thesis is to engineer novel, 3D-printed Ti implants (3D-Ti) with dual micro- and nano-topography prepared by scalable, cost-effective techniques including electrochemical anodization and hydrothermal process to achieve multiple functionalities including localized drug delivery, control of bone cells growth and attachment and bactericidal

properties. 3D-printed implants are fabricated using additive manufacturing SLM to generate surface microparticles. The main nano-topographical features will include titania nanotube (TNTs) and nano-pillars. Here, commercially used Ti alloy (Ti6Al4V) was utilized for fabrication of 3D-Ti implant substrates.

The detailed objectives of the thesis are as follows:

Objective 1: Reviewing the recent challenges and research gaps of Ti based bone implants currently used in dental and orthopaedic applications.

Objective 2: Engineering of new 3D-printed drug-releasing Ti implants to achieve desired combination of micro- and nano-rough surface properties which is followed by surface characterization and optimization of the fabricated surface nano-features.

Objective 3: Studying the drug loading capabilities of the fabricated TNTs-3D-Ti implants using chemotherapeutic agents followed by investigating the *in-vitro* cytotoxicity of TNTs-drug loaded implants.

Objective 4: Tailoring implant-cell response of additively manufactured implants

Objective 5: Investigating the *in-vitro* antibacterial efficacy of surface nano-features (*i.e.*, TNTs and nanopillars) on top of 3D-printed implants.

Objective 6: Exploring the *In-vitro* cell-implant interaction in order to determine desired features to control bone cells growth and attachment.

This thesis provides innovative solutions for the most challenging limitations facing Ti bone implants, including osseointegration control, bacterial infection and localized drug delivery. This will be achieved by designing multifunctional implants which can combine drug delivery of different therapeutics (e.g., anticancer or antibacterial agents), antibacterial properties and design flexibility. The implants are fabricated using additive manufacturing technology which is combined by scalable and cost-effective surface modification techniques of

electrochemical anodization and hydrothermal process. The research results from this research offer deep insight on the significance of micro and nano surface features and their effect on cells attachment and bacterial activity not explored before. The overall outcome of this thesis will pave the way towards the design and fabrication of next generation of multifunctional implants that are capable to revolutionize Ti implants industry.

1.3 Thesis outline:

Chapter 1 presents a general overview of the challenges and research gaps facing the currently used Ti implants and possible solutions. This chapter also included the thesis objectives and outline.

Chapter 2 (**Literature Review)** includes a review of literature of recent research focusing on engineering Ti implants to address the most key challenges facing the applications of bone implants with emphasis on fabrication of titania nanotubes (TNTs) with localized drug delivery capabilities.

Chapter 3 (**Titania Nanotubes for Localized Drug Delivery of Anticancer Agents)** includes engineering of 3D-printed drug-releasing Ti implants with TNTs covering the surface with drug delivery functions for treatment of bone cancer. The fabrication process together with drug loading and release are discussed followed by *in-vitro* assessment of the cytotoxicity of the loaded therapeutics as summarized in **Figure 2**.

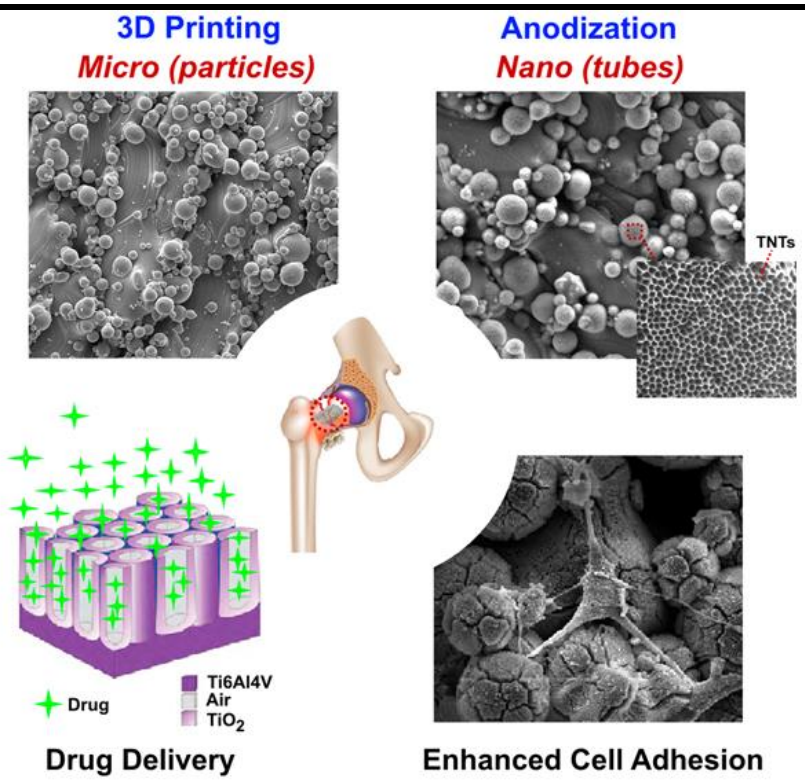

Figure 2: Graphical abstract "Engineering of Micro- to Nanostructured 3D-Printed Drug-Releasing Titanium Implants for Enhanced Osseointegration and Localized Delivery of Anticancer Drugs"

Chapter 4 (Tailoring Implant-Cell Response of Additively Manufactured Implants) includes two studies focusing on controlling (*i.e.,* reducing or enhancing) bone cells implant interaction. In the first study, TNTs were fabricated in an attempt to reduce bone cells growth on the surface so that they can be used for short-term implants applications. At the same time, the surface was coated with antibacterial agent, gallium nitrate, to add antibacterial capabilities as shown in **Figure 3**. In the second study, hydroxyapatite was used to enhance bone cells attachment on TNTs surface, **Figure 4**.

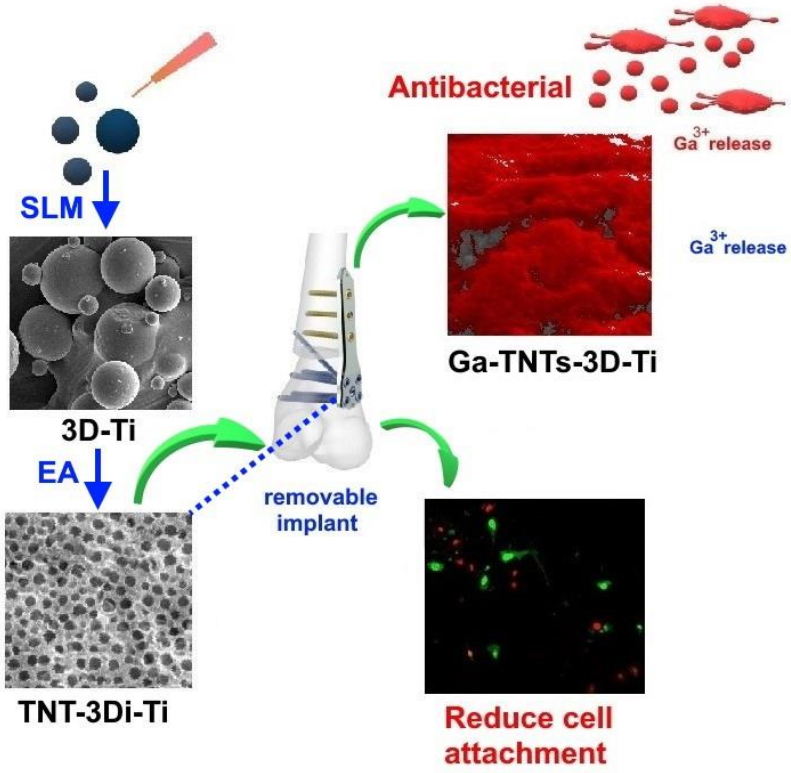

Figure 3: Graphical abstract "Tailoring additively manufactured titanium implants for short-time pediatric implantations with enhanced bactericidal activity"

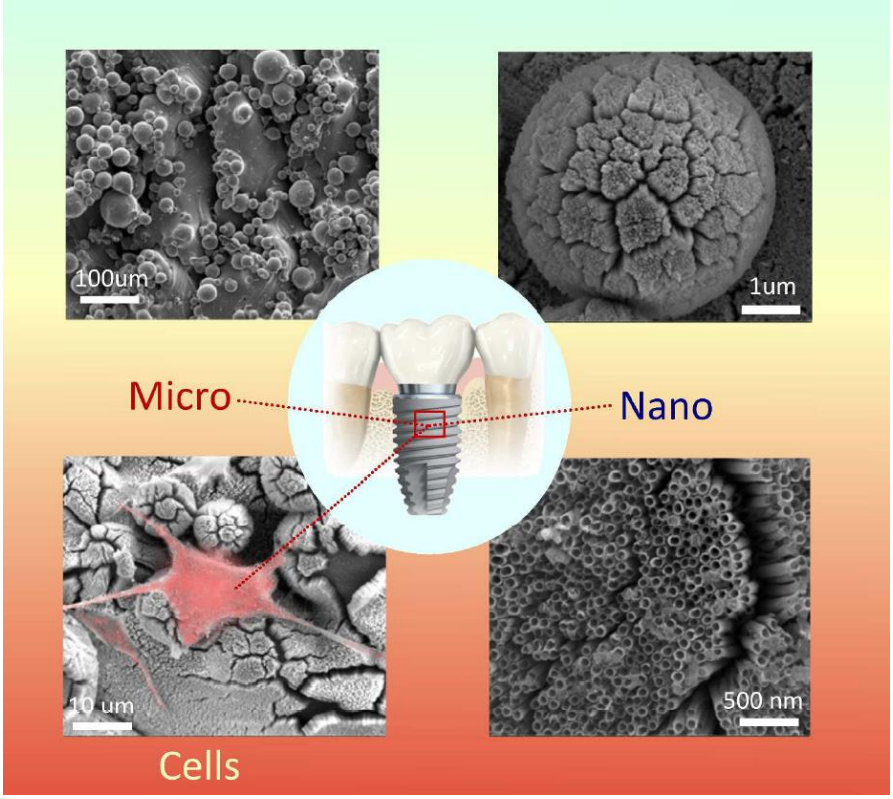

Figure 4: Graphical abstract "Micro- and Nano-structured 3D Printed Titanium Implants with Hydroxyapatite Coating for Improved Osseointegration"

Chapter 5 (Engineering of Surface Nanopillars On 3D-Printed Titanium Implants) illustrates the fabrication of 3D-printed Ti implants with unique hierarchical micro-nano topographies composed of microspheres covered with sharp nanopillars. The study compares the effect of using electrochemical anodization and hydrothermal process on the structure of the produced nanopillars. It also shows that the fabricated surfaces could enhance bone cells mineralization as shown in **Figure 5**.

Chapter 6 (Antibacterial Activity of Surface Nanopillars Fabricated On 3D-Printed Titanium Implants) involves the study of the cells attachment and antibacterial activity of the nanopillars fabricated in chapter 5, which was loaded with gallium nitrate to provide short-term antibacterial activity in an attempt to combine both physical and chemical antibacterial mechanisms, **Figure 6**.

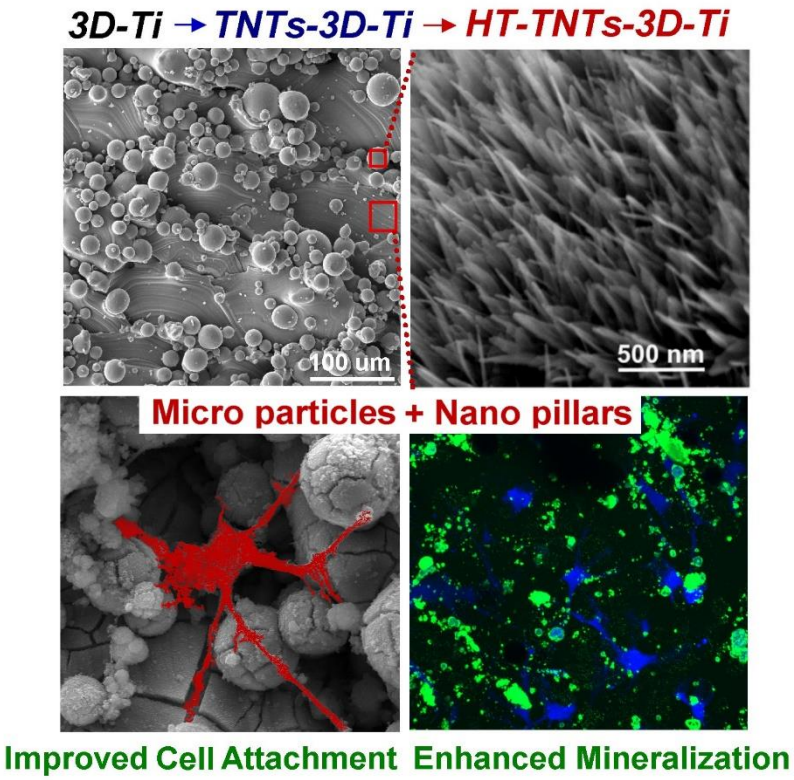

Figure 5: Graphical abstract "Advancing of Additive-Manufactured Titanium Implants with Bioinspired Micro- to Nanotopographies"

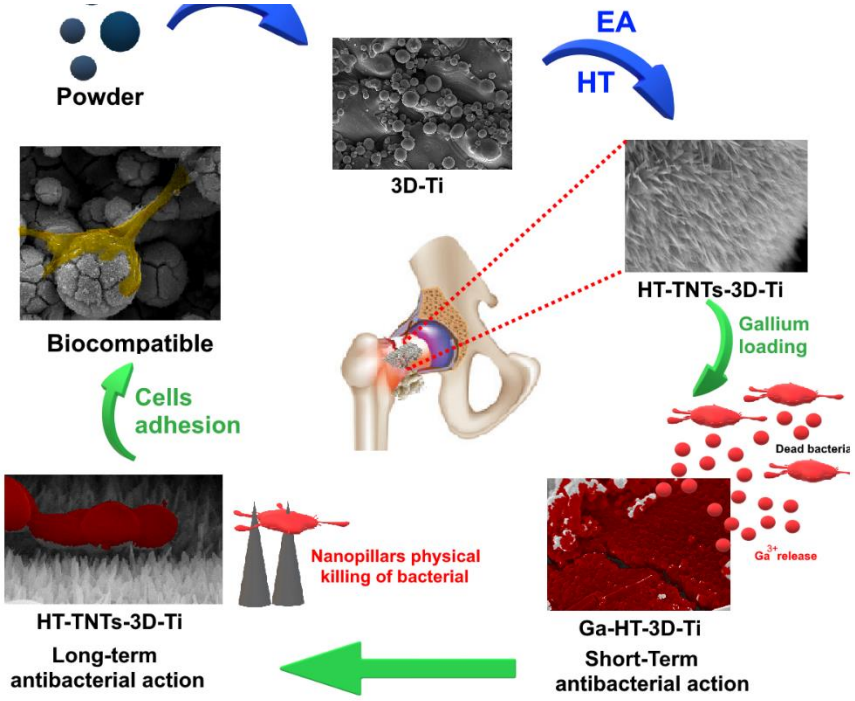

Figure 6: Graphical abstract "Advancing of 3D-printed titanium implants with combined antibacterial protection using ultra-sharp nanostructured surface and gallium releasing agents"

Chapter 7 (Conclusions and Perspectives) includes a summary of the most significant findings obtained throughout this thesis which is then followed by several recommendations for future research in order to move this research towards the next phase of *in-vivo* and clinical studies which could eventually result in the development of multifunctional new generation of bone implants.

8. References

[1] H. Chouirfa, H. Bouloussa, V. Migonney, C. Falentin-Daudré, Review of titanium surface modification techniques and coatings for antibacterial applications, Acta Biomater. 83 (2019) 37-54.

[2] M. Geetha, A.K. Singh, R. Asokamani, A.K. Gogia, Ti based biomaterials, the ultimate choice for orthopaedic implants – A review, Prog. Mater Sci. 54(3) (2009) 397-425.

[3] R. Bosco, J. Van Den Beucken, S. Leeuwenburgh, J. Jansen, Surface Engineering for Bone Implants: A Trend from Passive to Active Surfaces, Coatings 2(3) (2012) 95-119.

[4] K. Gulati, M.S. Aw, D. Findlay, D. Losic, Local drug delivery to the bone by drug-releasing implants: perspectives of nano-engineered titania nanotube arrays, Ther. Deliv. 3(7) (2012) 857-873.

[5] N. Su, J. Yang, Y. Xie, X. Du, H. Chen, H. Zhou, L. Chen, Bone function, dysfunction and its role in diseases including critical illness, International journal of biological sciences 15(4) (2019) 776-787.

[6] D.B. Burr, O. Akkus, Chapter 1 - Bone Morphology and Organization, in: D.B. Burr, M.R. Allen (Eds.), Basic and Applied Bone Biology, Academic Press, San Diego, 2014, pp. 3-25.

[7] J.E. Lemons, Biomaterials, biomechanics, tissue healing, and immediate-function dental implants, J. Oral Implantol. 30(5) (2004) 318-24.

[8] J.S. Hayes, I.M. Khan, C.W. Archer, R.G. Richards, The role of surface microtopography in the modulation of osteoblast differentiation, Eur Cell Mater 20 (2010) 98-108.

[9] M. Sarraf, B. Abdul Razak, A. Dabbagh, B. Nasiri-Tabrizi, N.H. Abu Kasim, W.J. Basirun, Optimizing PVD conditions for electrochemical anodization growth of well-adherent Ta2O5nanotubes on Ti-6Al-4V alloy, RSC Advances 6(82) (2016) 78999-79015.

[10] A. Chug, S. Shukla, L. Mahesh, S. Jadwani, Osseointegration—Molecular events at the bone–implant interface: A review, Journal of Oral and Maxillofacial Surgery, Medicine, and Pathology 25(1) (2013) 1-4.

[11] A. Wennerberg, T. Albrektsson, Effects of titanium surface topography on bone integration: a systematic review, Clin. Oral Implants Res. 20 Suppl 4 (2009) 172-84.

[12] T. Albrektsson, C. Johansson, Osteoinduction, osteoconduction and osseointegration, Eur. Spine J. 10 Suppl 2 (2001) S96-101.

[13] D.M. Findlay, K. Welldon, G.J. Atkins, D.W. Howie, A.C. Zannettino, D. Bobyn, The proliferation and phenotypic expression of human osteoblasts on tantalum metal, Biomaterials 25(12) (2004) 2215-27.

[14] K.J. Welldon, G.J. Atkins, D.W. Howie, D.M. Findlay, Primary human osteoblasts grow into porous tantalum and maintain an osteoblastic phenotype, J Biomed Mater Res A 84(3) (2008) 691-701.

[15] K. Gulati, S. Maher, D.M. Findlay, D. Losic, Titania nanotubes for orchestrating osteogenesis at the bone–implant interface, Nanomedicine 11(14) (2016) 1847-1864.

[16] L. Le Guehennec, A. Soueidan, P. Layrolle, Y. Amouriq, Surface treatments of titanium dental implants for rapid osseointegration, Dent. Mater. 23(7) (2007) 844-54.

[17] G. Mendonca, D.B. Mendonca, F.J. Aragao, L.F. Cooper, Advancing dental implant surface technology from micron to nanotopography, Biomaterials 29(28) (2008) 3822-35.

[18] T.J. Webster, J.U. Ejiofor, Increased osteoblast adhesion on nanophase metals: Ti, Ti6Al4V, and CoCrMo, Biomaterials 25(19) (2004) 4731-4739.

[19] D. Losic, S. Simovic, Self-ordered nanopore and nanotube platforms for drug delivery applications, Expert Opinion on Drug Delivery 6(12) (2009) 1363-1381.

[20] D. Losic, M.S. Aw, A. Santos, K. Gulati, M. Bariana, Titania nanotube arrays for local drug delivery: recent advances and perspectives, Expert Opin Drug Deliv. (2014) 1-25.

[21] B.-S. Moon, S. Kim, H.-E. Kim, T.-S. Jang, Hierarchical micro-nano structured Ti6Al4V surface topography via two-step etching process for enhanced hydrophilicity and osteoblastic responses, Materials Science and Engineering: C 73 (2017) 90-98.

[22] L.Y. Han, C.S. Wang, J.B. Qiang, Microstructure and properties of Ti-Fe-Zr-Y alloys prepared by laser rapid prototyping, J. Alloys Compd. 700 (2017) 159-168.

[23] H. Liu, X. Huang, H. Yu, X. Yang, X. Zhang, R. Hang, B. Tang, A cytocompatible micro/nano-textured surface with Si-doped titania mesoporous arrays fabricated by a one-step anodization, Materials Science and Engineering: C 73 (2017) 120-129.

[24] S.B. Goodman, Z. Yao, M. Keeney, F. Yang, The Future of Biologic Coatings for Orthopaedic Implants, Biomaterials 34(13) (2013) 3174-3183.

[25] M.C. Sanchez, E. Fernandez, A. Llama-Palacios, E. Figuero, D. Herrera, M. Sanz, Response to antiseptic agents of periodontal pathogens in in vitro biofilms on titanium and zirconium surfaces, Dent. Mater. 33(4) (2017) 446-453.

[26] A.K. Jain, R. Panchagnula, Skeletal drug delivery systems, International journal of pharmaceutics 206(1–2) (2000) 1-12.

[27] T.A.G. van Vugt, J.J. Arts, J.A.P. Geurts, Antibiotic-Loaded Polymethylmethacrylate Beads and Spacers in Treatment of Orthopedic Infections and the Role of Biofilm Formation, Front. Microbiol. 10 (2019) 1626-1626.

[28] K. Gulati, M. Kogawa, S. Maher, G. Atkins, D. Findlay, D. Losic, Titania Nanotubes for Local Drug Delivery from Implant Surfaces, Electrochemically Engineered Nanoporous Materials, Springer International Publishing2015, pp. 307-355.

[29] D. Losic, M.S. Aw, A. Santos, K. Gulati, M. Bariana, Titania nanotube arrays for local drug delivery: recent advances and perspectives, Expert Opin Drug Deliv 12(1) (2015) 103-27.

[30] H. Buchholz, R. Elson, E. Engelbrecht, H. Lodenkamper, J. Rottger, A. Siegel, Management of deep infection of total hip replacement, J. Bone Joint Surg. 63-B(3) (1981) 342-353.

[31] P. Wu, D.W. Grainger, Drug/device combinations for local drug therapies and infection prophylaxis, Biomaterials 27(11) (2006) 2450-67.

[32] B. Trajkovski, A. Petersen, P. Strube, M. Mehta, G.N. Duda, Intra-operatively customized implant coating strategies for local and controlled drug delivery to bone, Advanced drug delivery reviews 64(12) (2012) 1142-1151.

[33] D.A. Puleo, A. Nanci, Understanding and controlling the bone–implant interface, Biomaterials 20(23–24) (1999) 2311-2321.

[34] E. Moran, I. Byren, B.L. Atkins, The diagnosis and management of prosthetic joint infections, J. Antimicrob. Chemother. 65(suppl 3) (2010) 45-54.

[35] A.B. Novaes Jr, S.L.S.d. Souza, R.R.M.d. Barros, K.K.Y. Pereira, G. Iezzi, A. Piattelli, Influence of implant surfaces on osseointegration, Braz. Dent. J. 21 (2010) 471-481.

[36] D. Campoccia, L. Montanaro, P. Speziale, C.R. Arciola, Antibiotic-loaded biomaterials and the risks for the spread of antibiotic resistance following their prophylactic and therapeutic clinical use, Biomaterials 31(25) (2010) 6363-6377.

[37] E. Zhang, X. Zhao, J. Hu, R. Wang, S. Fu, G. Qin, Antibacterial metals and alloys for potential biomedical implants, Bioactive Materials 6(8) (2021) 2569-2612.

[38] X. Qu, H. Yang, B. Jia, M. Wang, B. Yue, Y. Zheng, K. Dai, Zinc alloy-based bone internal fixation screw with antibacterial and anti-osteolytic properties, Bioactive Materials 6(12) (2021) 4607-4624.

[39] T.L. Clainche, D. Linklater, S. Wong, P. Le, S. Juodkazis, X.L. Guével, J.-L. Coll, E.P. Ivanova, V. Martel-Frachet, Mechano-Bactericidal Titanium Surfaces for Bone Tissue Engineering, ACS Applied Materials & Interfaces 12(43) (2020) 48272-48283.

[40] D.P. Linklater, V.A. Baulin, S. Juodkazis, R.J. Crawford, P. Stoodley, E.P. Ivanova, Mechano-bactericidal actions of nanostructured surfaces, Nature Reviews Microbiology (2020).

[41] Y. Li, Y. Yang, R. Li, X. Tang, D. Guo, Y. Qing, Y. Qin, Enhanced antibacterial properties of orthopedic implants by titanium nanotube surface modification: a review of current techniques, Int J Nanomedicine 14 (2019) 7217-7236.

[42] H. Fan, J. Fu, X. Li, Y. Pei, X. Li, G. Pei, Z. Guo, Implantation of customized 3-D printed titanium prosthesis in limb salvage surgery: a case series and review of the literature, World journal of surgical oncology 13 (2015) 308-308.

[43] J. Ni, H. Ling, S. Zhang, Z. Wang, Z. Peng, C. Benyshek, R. Zan, A.K. Miri, Z. Li, X. Zhang, J. Lee, K.J. Lee, H.J. Kim, P. Tebon, T. Hoffman, M.R. Dokmeci, N. Ashammakhi, X. Li, A. Khademhosseini, Three-dimensional printing of metals for biomedical applications, Materials Today Bio 3 (2019) 100024.

[44] B.V. Krishna, S. Bose, A. Bandyopadhyay, Low stiffness porous Ti structures for load-bearing implants, Acta Biomater. 3(6) (2007) 997-1006.

[45] S.A.M. Tofail, E.P. Koumoulos, A. Bandyopadhyay, S. Bose, L. O'Donoghue, C. Charitidis, Additive manufacturing: scientific and technological challenges, market uptake and opportunities, Materials Today 21(1) (2018) 22-37.

[46] J.P. Kruth, X. Wang, T. Laoui, L. Froyen, Lasers and materials in selective laser sintering, Assembly Automation 23(4) (2003) 357-371.

[47] S.H. Ko, H. Pan, C.P. Grigoropoulos, C.K. Luscombe, J.M.J. Fréchet, D. Poulikakos, All-inkjet-printed flexible electronics fabrication on a polymer substrate by low-temperature high-resolution selective laser sintering of metal nanoparticles, Nanotechnology 18(34) (2007) 345202.

[48] Y. Hou, L. Yu, W. Xie, L.C. Camacho, M. Zhang, Z. Chu, Q. Wei, R. Haag, Surface Roughness and Substrate Stiffness Synergize To Drive Cellular Mechanoresponse, Nano Letters 20(1) (2020) 748-757.

[49] E.A. Cavalcanti-Adam, T. Volberg, A. Micoulet, H. Kessler, B. Geiger, J.P. Spatz, Cell spreading and focal adhesion dynamics are regulated by spacing of integrin ligands, Biophysical journal 92(8) (2007) 2964-74.

[50] Y. He, Z. Li, X. Ding, B. Xu, J. Wang, Y. Li, F. Chen, F. Meng, W. Song, Y. Zhang, Nanoporous titanium implant surface promotes osteogenesis by suppressing osteoclastogenesis via integrin β1/FAKpY397/MAPK pathway, Bioactive Materials (2021).

[51] A. Santos, M. Sinn Aw, M. Bariana, T. Kumeria, Y. Wang, D. Losic, Drug-releasing implants: current progress, challenges and perspectives, Journal of Materials Chemistry B 2(37) (2014) 6157-6182.

CHAPTER 2

LITERATURE REVIEW

2.1. Overview

Current Ti implants draw many challenges, including inflammation, infection and poor osseointegration. The aim of this chapter is to address these challenges and discuss the recent advances on designing and engineering Ti implants surface to overcome these challenges. This chapter also highlights the fabrication and design of titania nanotubes (TNTs) with localized drug delivery capabilities. At the end, the article concludes with general overview and a prospective outlook on the future trends, challenges and perspectives in this exciting and promising research field which will be further explored in the following chapters of the thesis.

This chapter has been published as:

Shaheer Maher, Arash Mazinani, Mohammad Reza Barati and Dusan Losic (2018), Engineered titanium implants for localized drug delivery: Recent advances and perspectives of titania nanotubes arrays. Expert Opinion on Drug Delivery 15(10): 1021-1037.

Statement of Authorship

Title of Paper	Engineered titanium implants for localized drug delivery: recent advances and perspectives of Titania nanotubes arrays
Publication Status	☑ Published ☐ Accepted for Publication ☐ Submitted for Publication ☐ Unpublished and Unsubmitted w ork w ritten in manuscript style
Publication Details	S. Maher, A. Mazinani, M.R. Barati, D. Losic, Engineered titanium implants for localized drug delivery: recent advances and perspectives of Titania nanotubes arrays, Expert Opin Drug Deliv 15(10) (2018) 1021-1037.

Principal Author

Name of Principal Author (Candidate)	Shaheer Maher (*also known as* Shaheer Makar)		
Contribution to the Paper	Prepared, edited and revised the review manuscript		
Overall percentage (%)	85%		
Certification:	This paper reports on original research I conducted during the period of my Higher Degree by Research candidature and is not subject to any obligations or contractual agreements with a third party that would constrain its inclusion in this thesis. I am the primary author of this paper.		
Signature		Date	19/08/2021

Co-Author Contributions

By signing the Statement of Authorship, each author certifies that:

i. the candidate's stated contribution to the publication is accurate (as detailed above);

ii. permission is granted for the candidate in include the publication in the thesis; and

iii. the sum of all co-author contributions is equal to 100% less the candidate's stated contribution.

Name of Co-Author	Arash Mazinani		
Contribution to the Paper	Edited and revised the manuscript		
Signature		Date	19/08/20121

Name of Co-Author	Dusan Losic		
Contribution to the Paper	Supervised the development of the work, revised the manuscript and acted as corresponding author		
Signature		Date	19/08/2021

Please cut and paste additional co-author panels here as required.

Statement of Authorship

Title of Paper	Engineered titanium implants for localized drug delivery: recent advances and perspectives of Titania nanotubes arrays
Publication Status	☑ Published ☐ Accepted for Publication ☐ Submitted for Publication ☐ Unpublished and Unsubmitted w ork w ritten in manuscript style
Publication Details	S. Maher, A. Mazinani, M.R. Barati, D. Losic, Engineered titanium implants for localized drug delivery: recent advances and perspectives of Titania nanotubes arrays, Expert Opin Drug Deliv 15(10) (2018) 1021-1037.

Principal Author

Name of Principal Author (Candidate)	Shaheer Maher (*also known as* Shaheer Makar)		
Contribution to the Paper	Prepared, edited and revised the review manuscriptpe text here		
Overall percentage (%)	85%		
Certification:	This paper reports on original research I conducted during the period of my Higher Degree by Research candidature and is not subject to any obligations or contractual agreements with a third party that would constrain its inclusion in this thesis. I am the primary author of this paper.		
Signature		Date	19/08/2021

Co-Author Contributions

By signing the Statement of Authorship, each author certifies that:

i. the candidate's stated contribution to the publication is accurate (as detailed above);

ii. permission is granted for the candidate in include the publication in the thesis; and

iii. the sum of all co-author contributions is equal to 100% less the candidate's stated contribution.

Name of Co-Author	M.R. Barati		
Contribution to the Paper	Revised the final manuscript Co-author can not be reached signed by corresponding author on their behalf		
Signature		Date	19/08/2021

Name of Co-Author			
Contribution to the Paper			
Signature		Date	

Please cut and paste additional co-author panels here as required.

Expert Opinion on Drug Delivery

ISSN: 1742-5247 (Print) 1744-7593 (Online) Journal homepage: https://www.tandfonline.com/loi/iedd20

Engineered titanium implants for localized drug delivery: recent advances and perspectives of Titania nanotubes arrays

Shaheer Maher, Arash Mazinani, Mohammad Reza Barati & Dusan Losic

To cite this article: Shaheer Maher, Arash Mazinani, Mohammad Reza Barati & Dusan Losic (2018) Engineered titanium implants for localized drug delivery: recent advances and perspectives of Titania nanotubes arrays, Expert Opinion on Drug Delivery, 15:10, 1021-1037, DOI: 10.1080/17426247.2018.1617743

To link to this article: https://doi.org/10.1080/17425247.2018.1517743

Published online: 27 Sep 2018.

EXPERT OPINION ON DRUG DELIVERY
2018, VOL. 15, NO. 10, 1021–1037
https://doi.org/10.1080/17425247.2018.1517743

Taylor & Francis
Taylor & Francis Group

REVIEW

Engineered titanium implants for localized drug delivery: recent advances and perspectives of Titania nanotubes arrays

Shaheer Maher, Arash Mazinani, Mohammad Reza Barati and Dusan Losic

School of Chemical Engineering, The University of Adelaide, Adelaide, Australia

ABSTRACT

Introduction: Therapeutics delivery to bones to treat skeletal diseases or prevent postsurgical infections is challenging due to complex and solid bone structure that limits blood supply and diffusion of therapeutics administered by systemic routes to reach effective concentration. Titanium (Ti) and their alloys are employed as mainstream implant materials in orthopedics and dentistry; having superior mechanical/biocompatibility properties which could provide an alternative solution to address this problem.

Areas covered: This review presents an overview of recent development of Ti drug-releasing implants, with emphasis on nanoengineered Titania nanotubes (TNTs) structures, for solving key problems to improve implants osseointegration, overcome inflammation and infection together with providing localized drug delivery (LDD) for bone diseases including cancer. Critical analysis of the advantages/disadvantages of developed concepts is discussed, their drug loading/releasing performances and specific applications.

Expert opinion: LDD to bones can address many disorders and postsurgical conditions such as inflammation, implants rejection and infection. To this end, TNTs-Ti implants represent a potential promise for the development of new generation of multifunctional implants with drug release functions. Even this concept is extensively explored recently, there is a strong need for more preclinical studies using animal models to confirm the long-term safety and stability of TNTs-Ti implants for real-life medical applications.

ARTICLE HISTORY
Received 16 April 2018
Accepted 27 August 2018

KEYWORDS
Localized drug delivery; titanium implants; osseointegration; Titania nanotubes

1. Introduction

Bone is a remarkable organ with many key functions in human physiology including maintaining posture, movement, protection and mechanical support for muscles, visceral organs and soft tissues, blood cell production, storage of minerals, fats and growth factors, calcium homeostasis, blood acid-base regulation and housing of multiple progenitor cell (mesenchymal, hemopoietic) [1]. According to the World Health Organization, nearly ten million injuries occur each year in developed countries, which are often associated with severe soft tissue damages, bone fractures and infections [2]. Furthermore, with the increasing number of aged population, age-related orthopedic disorders, such as osteoporosis, fractures, Paget's disease and rheumatoid arthritis, are also increasing with concerning rate. This is attributed to disturbances of this dynamic behavior (i.e. new tissues are continuously formed and old, injured or unwanted tissues are removed by bone cells) [3]. Moreover, bone infections (osteomyelitis), primary and secondary cancer are most concerning skeletal diseases and have in most cases fatal ends [3,4]. The impact of such bones disorders on quality of life is significant with severe patients' suffering, high treatment costs (~10% of annual healthcare expenses) and limited ability to work and perform essential daily tasks [1]. Accordingly, millions of cases require surgical intervention each year for joint replacement, implants insertion for fracture repair, total hip or knee replacement. Even after implants insertion, patients may suffer from infection and/or inflammation of bones tissues [4]. This usually involves prolonged hospitalization, implant failure, repeated surgical procedures, and in some cases complete amputation or even death of patients.

Improved methods are therefore needed to cater for these problems with the ability to deliver therapeutic agents directly at the diseased bone tissue [2]. Treating bone disorders through application of therapeutic agents (e.g. antibiotics, anti-inflammatory, and anticancer agents) is a common approach, however, systemic drug administration suffers from many limitations such as lack of selectivity, poor bioavailability, and distribution. In addition, high drug dosages are required for prolonged periods to reach the effective levels of therapeutics at the desired site (i.e. bones) which could be toxic to other body tissues. Moreover, bone tissue differs greatly from other body tissues having a unique complex structure and composition, Figure 1(a) [1]. Drugs suffer from poor diffusion through the highly calcified tissue especially in case of fractures, trauma or cancer where blood supply is compromised.

One promising solution to address these drawbacks of systemic drug therapy is localized drug delivery (LDD) to

CONTACT Dusan Losic dusan.losic@adelaide.edu.au School of Chemical Engineering, The University of Adelaide, North Engineering Building, Adelaide, SA 5000, Australia

Article highlights

- Localized drug delivery from titanium implants represents a promising approach to treat many bone conditions which are hard be treated using systemic drug therapies.
- Titania Nanotubes (TNTs) modified implants are considered as a unique platform for combining enhanced bone integration and localized drug delivery.
- TNTs show a set of unique properties such as mechanical and thermal stability, improved osseointegration, biocompatibility, and structural flexibility.
- The fabrication of TNTs using electrochemical anodization process permits precise control over the tubular structure and dimensions which provide versatile applicability of TNTs in biomedical field.
- A wide range of therapeutics (anti-inflammatory, antibacterial, anticancer, and growth factors) was loaded inside TNTs and tested for controlled release as well as 'on demand' release kinetics.
- - 3D printing technology will open new doors for 'on demand' manufacturing of different forms of implants specially designed according to patient's needs.
- More *in-vivo* studies are required to establish the long-term toxicity and to translate this technology into clinical applications.

This box summarizes key points contained in the article.

deliver therapeutics directly to the bone [5]. Releasing drugs locally can help to minimize systemic therapy side effects while simultaneously providing more optimum drug concentration inside the bone microenvironment [6]. Another key feature is that LDD could enhance bioavailability for drugs that are either destroyed by acids of the stomach, highly bind to plasma proteins or those which have high first-pass metabolism [7,8]. Furthermore, addition of drug delivery feature to bone implants has the potential to not only enhance the osseointegration and lifespan of such implants, but also provide effective treatment for conditions like: osteoporosis, bone infection (i.e. osteomyelitis) and related inflammation as well as malignant conditions such as bone carcinoma, etc. [9]. Consequently, techniques to deliver drugs locally to diseased bones have turned out to be one of the main focus in orthopedic therapy. Several LDD systems based on polymers, ceramics and bone cements have been clinically proved to deliver bone healing or anti-inflammatory agents for bone repair or tissue engineering, but with limited performances [1]. Most popular carriers are biodegradable polymers and their composites such as poly (lactic acid) and poly (methyl methacrylate), collagen and chitosan shaped into discs or membranes where active therapeutics are integrated [10]. However, many limitations of these materials were reported including compromised implants lifespan, erratic drug release, nonreproducible preparations, and inability to provide adequate support in case of fractures due to poor mechanical strength [11]. In addition, these materials are usually drug specific and lack the flexibility to be used for a broad range of drugs with different physical and chemical properties (i.e. proteins, genes, hydrophilic, and hydrophobic drugs).

On the other hand, metal-based bone implants (e.g. orthopedic prostheses, screws, K-wires (pins) and plates, Figure 1(b), are commonly used in a variety of bone surgical procedures to treat bone conditions that also in addition to this function could be used as LDD carriers [1]. In particular, titanium (Ti) and its alloys are very suitable materials for implants fabrication since they possess good mechanical characteristics and biocompatibility with human bone tissues while being corrosion resistant [12,13]. Even though, Ti implants have a long history of successful clinical use, they still face many challenges related to their integration and longevity after insertion in the human body [14–16]. Failure of orthopedic implants can occur for various reasons, including inflammation, or poor 'osseointegration' (i.e. firm attachment of the implant's surface with bone tissues) [9], leading to implant's loosening and/or complete detachment. Therefore, there is a strong need to have bone implants to address these problems that may provide antibiotics to resistant biofilms formation to treat bacteria or provide other therapeutics to enhance bone healing or treat specific bone diseases such as cancer [17,18].

This article presents the recent advances in the LDD application of Ti-based implants with particular emphasis on Titania nanotubes (TNTs), their fabrication, improving properties and applications for localized drug-releasing drug carriers for treating various bone diseases. Finally, this review concludes with a general overview and a prospective outlook on the future

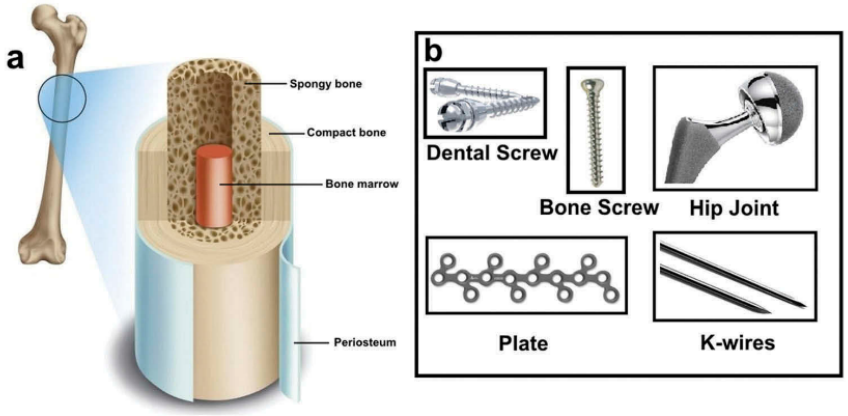

Figure 1. (a) Illustration of bone structure, (b) different forms of Ti implants (original figures, no permission required).

trends, challenges and perspectives in this exciting and promising research field.

2. Engineering approaches for modification of Ti implants

Extensive research activities on Ti implants in recent years can be divided into two categories; the first with aims to improve conventional performances of implants such as mechanical strength and corrosion stability. Engineering methods based on mechanical, chemical or electrochemical treatment were used as simplest methods to provide surfaces patterns with optimal micro to nanostructures to improve bone cells growth and better osseointegration. The second category focuses to add new functions such as therapeutic with drug delivery and antibacterial with reduced bacterial biofilm formation. A summary of common engineering approaches to achieve these goals are presented in Table 1.

With the aim to prepare Ti implants with drug delivery capabilities, the simplest and first attempts included coating/adsorption of therapeutics on the implant's surfaces. Many bioactive molecules coated onto Ti implants have been explored for inducing osseointegration, enhancing protein adsorption together and enhancing bone remodeling at the bone-implant interface [19,20]. These approaches involve impregnation of osteoinductive growth promoters like BMPs (bone morphogenetic proteins) into biocompatible polymers (e.g. polylactides, collagen, chitosan) deposited on Ti implant's surface [21]. Several studies utilized hydroxyapatite (HAP), which could promote bone growth and osseointegration, as a carrier for active agents. In this case, drugs were either mixed with HAP or adsorbed onto HAP coated Ti implants to offer dual functionality of promoting osseointegration and simultaneously inhibiting bacterial infection and/or inflammation [22]. However, such drug coatings could be easily detached and showed inadequate loading and uncontrolled release profile.

To realize sufficient drug loading, deep incorporation of payloads into the implant surface is required; and for effective therapeutic outcomes, slow and controlled release properties are desired. To achieve that it is essential to make Ti surface porous to control the amount of therapeutics loaded with easily tuning of the surface structures. Thus, nanoengineered techniques are required to fabricate nanotubular/nanoporous surfaces. To this end, simple and scalable electrochemical anodization methods have been widely explored to fabricate titania (TiO_2) nanotubular (TNTs) arrays onto Ti implants surface and successfully used to prove the concept of Ti drug-releasing implants. In last 10 years, more than several hundreds of papers and several review articles were published on their development and applications for broad range medical applications.

Electrochemical anodization process was introduced to generate nanostructured oxide layer on the implant surfaces with tunable features that can serve as optimum reservoirs for loading of active agents and subsequently permit their release. This fabrication process is low cost, simple and scalable. It has been explored and used at industrial scale for production of porous silicon and protective aluminum coatings [23]. Due to very high surface energy and surface properties of these structures compared to untreated surfaces, anodization attracted applications not only for drug delivery and implants but also for other potential biomedical applications including biosensing and tissue engineering [1,15]. Owing to the simplicity of generating electrochemically engineered TNTs, this technology is considered as an appealing strategy toward the fabrication of drug-releasing bone implant. These TNTs resemble vertically aligned nanotest tubes (open at top and closed at bottom), Figure 2(a,b) [24]. The dimensions (diameters (100–300 nm) and length (0.5–300 µm) and shape of TNTs could be easily controlled under different anodization conditions [1]. It is noteworthy that, many studies showed that implants with TNTs on top exhibit improved osseointegration properties as will be discussed later. In addition, it is more feasible to functionalize TNTs surface to control drug loading and release [15]. It is worth mentioning that electrochemical anodization process could be used not only for flat pure Ti foil, 3d-printed Ti alloys, but also for Ti substrates with other shapes (e.g. wires or meshes) [25,26]. This flexibility opens new doors for integration of this process into currently used medical implant devices.

2.1. Recent advancement on TNTs fabrication

Since most of the currently used implants in market are made of titanium or its alloys, the fabrication of TNTs by electrochemical anodization and their scale-up and translation into Ti implants industry is expected to be feasible compared with other methods such as template methods, sol-gel method, hydrothermal, and atomic layer deposition [27,28]. The anodization process involves immersing Ti implants (as anode) in an electrochemical cell containing an electrolyte solution (e.g. organic electrolyte, water, and fluoride ions) with alternate metal (Ti or Pt) acting as a cathode, Figure 2(c,d) that is with some variation used in metal processing and finishing industry [6,24]. The mechanism of TNTs formation was extensively studied and could be found elsewhere [29].

The last few years have witnessed a considerable progress in optimization of the electrochemical anodization process to fabricate TNTs providing a precise control over morphological features such as length, diameter and shapes. This progress mainly involved the alteration of the anodization electrolyte starting with aqueous acidic solutions such as chromic acid electrolyte containing HF which results in TNTs with irregular structure [30]. This was followed by TNTs fabrication in aqueous buffered electrolyte containing fluoride species; which showed significant improvements, with longer tubes up to 7 µm due to less dissolution rates [31]. Subsequently, higher growth rates were achieved using non-aqueous polar organic solvents (dimethyl sulfoxide, ethylene glycol, or diethylene glycol) containing fluoride species yielding TNTs up to 1000 µm in length [32]. It is worth mentioning that, TNTs have been also fabricated in fluoride-free electrolytes [33]. The most distinguished progress in TNTs fabrication has been realized by Schmuki group through the incorporation of weak organic acids (e.g. lactic acid (LA)) into the organic-based electrolyte which could

Table 1. Summary of surface modification approaches toward osseointegration/antibacterial resistance improvement and/or drug-delivery application for titanium implants.

Surface modification	Osseointegration enhancement	Antibacterial/ Bacteriostatic Improvement	Drug-delivery application	Refs.
Physio-chemical modification				
Physical Vapor Deposition (PVD)	✓ Formation of Ti Nano-nodular Structure by Electron-Beam-Physical Vapor Deposition (EB-PVD)	✓ Ti/Ag hard coating	✓ Coatings for controlled drug release	[115]
Chemical Vapour Deposition (CVD) technique	✓ Metal-organic (CVD)	✓ CVD of TiO_2/Ag layers	–	[116]
Acid etching	✓	–	–	[117]
Magnetron sputtering	✓ Deposition of HAP on Ti	✓ Ag-Ti	–	[118]
Laser deposition/melting	✓ Pulsed laser deposition (PLD) of Titanium carbide or HAP	✓ (e.g. copper–nickel coatings on titanium substrate)	✓ (e.g. incorporation of PLD with Anodization to coat HAP on nanostructured titanium)	[119,120]
Spin-coating	✓ Poly(vinyl acetate)/HAP composite nanofibers on Ti implants	✓ Coating Ti with chitosan	✓ TNTs/PLGA spin coated	[104,121]
UV treatment	✓	✓	–	[122,123]
Machining	✓	✓ Polishing to prevent bacterial colonization	–	[45,124]
Grit blasting	✓ Grit blasting with TiO2	✓ Ti blasted with zirconia	–	[125]
Sol-gel	✓ $Ca_3(PO_4)_2$ deposition on Ti by Discrete Crystalline Deposition	✓ TiO_2–Ag composite coating	✓ Controlled release of vancomycin from coating	[126,127]
Alkaline-heat treatment deposition	✓ Poly (vinyl alcohol) (PVA)/poly (lactide-glycolide acid) (PLGA) NPs	✓ Ti coated with vancomycin containing NPs	pH-controlled release of vancomycin	[128]
Plasma modifications				
Plasma sprayed hydroxyapatite + Antibacterial agents	✓	✓ Incorporation of Ag	–	[129,130]
Plasma sprayed hydroxyapatite	✓	–	✓ Pamidronate or zoledronate	[131]
Electrochemical Modification				
Electrophoretic Deposition (EPD)	✓ EPD of HAP on Ti	✓ Addition of AgNps during EPD	✓ Chitosan–gelatine formation by EPD on Ti	[132,133]
Anodization (TNTs formation, Nanopitting)	✓	✓ Combined with antibacterial materials such as ZnO, Ag	✓ Polymer/TNTs array system	[14,104,134]
Plasma Electrolytic Oxidation (PEO)	✓	✓ Alkaline etching/ antibacterial agents doping	✓ Loaded with bovine serum Albumin	[135,136]
Cathodic polarization	✓	✓ Binding doxycycline onto titanium surfaces	–	[137]
Hydrothermal method				
Hydrothermal treatment/ alkaline etching	✓ Combined with electrochemical methods to form Apatite	✓ Combined with Anodization and formation of Na_2TiO_3	–	[136]

prevent dielectric breakdown in the growing oxide. This allowed ultrafast TNTs growth through anodization at a significantly elevated voltage [34].

The fabrication of TNTs with altering tubes morphology have been recently demonstrated by So *et al.* [35] by successful preparation of double-walled tubes (i.e. tube in tube configuration) by anodization in lactic acid containing ethylene glycol electrolyte for 10 min at room temperature, Figure 2(e). In the same study, the inner tubes could be selectively etched out leaving larger diameter single-walled tubes [35]. Also, large diameter tubes (>500 nm) were grown through increasing the applied potential to 170 V for 4 h [36]. Such wide tubes could allow the loading of substantial amounts of drugs owing to their large void volume and wide pore opening. More recently, spaced TNTs with regular gaps, Figure 2(f), could be fabricated

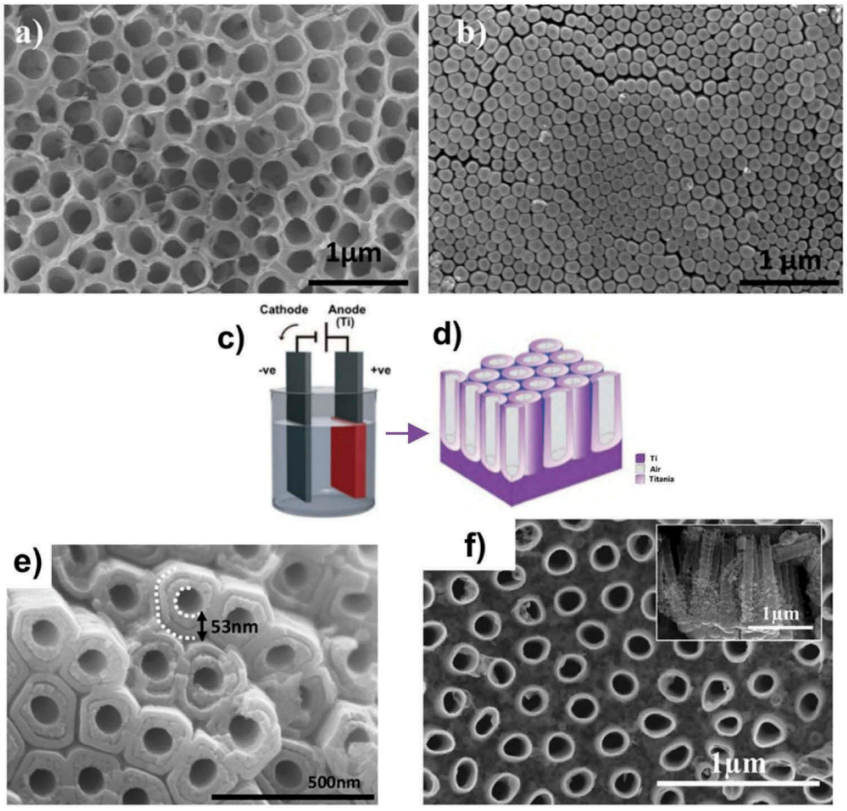

Figure 2. Titania nanotube arrays (TNTs) formation and structure. (a) SEM image showing the top view of TNTs with open pores prepared by electrochemical anodization, (b) SEM of the closed bottom view TNTs (adapted with permission from ref [113]), (c) Schematic representation of electrochemical cell setup for the formation of TNTs layer on Ti, (d) illustration of vertically aligned arrays of TNTs structures fabricated by electrochemical process, (e) double-walled NTs (adapted with permission from ref [35]), and (f) Top view and inset side view of spaced NTs (adapted with permission from ref [37]).

using electrolytes containing tri(tetra, poly)-ethylene glycol, diethylene glycol or dimethyl sulfoxide with addition of HF and NH_4F [37].

It is worth mentioning that, most of above-mentioned studies used pure titanium substrates in their experiments and only a few investigated titanium alloys. Titanium alloys are characterized by enhanced biomechanical properties as compared to pure Ti. In addition, most of implant devices, currently used in market, are made of Ti alloys. The incorporation of other metals, such as Al, V, Ta, Zr, etc. with Ti is found to add superior characteristics to the alloy such as more corrosion resistance, better hardness, lower elastic module, and higher withstand strength [38]. In one attempt, Liang *et al*. fabricated TNTs on Ti-4Zr-22Nb-2Sn alloy which were then tested for drug-delivery applications. Minocycline hydrochloride antibiotic was loaded onto TNTs and the release kinetics was compared for TNTs generated under different voltage [39].

Within the last few years, three-dimensional printing (3D printing) technology opened new doors for fabrication of various implants made of polymers and metals [40]. One of the major challenges of current Ti implants industry is that implants are manufactured with a fixed set of shapes and dimensions. Moreover, implant manufacturers may lose millions of dollars each year through expiry of the already fabricated implants. Thus, the application of 3D printing to fabricate implants will result in revolutionary improvements, among which is the design flexibility to manufacture different shapes of implants with tailored dimensions such as flat substrates, screws, wires or even a complete joint [40,41]. In addition, 3D printing will offer 'on-demand' production of implants which are designed specifically for individual patient. At the same time, implant companies will deliver implants on request instead of massive production of implants that could eventually expire. Recently our group demonstrated for the first time fabrication of TNTs on 3D-Ti implants made of Ti6Al4V alloys [41]. The implants were prepared by selective laser melting process and then were investigated for human osteoblasts adhesion. Results showed that the micro-nano rough surface featured by these implants could significantly improve cells attachment and proliferation in comparison with only nano rough TNTs/Ti wafers (i.e. no micro-roughness) [42]. In most recent work we explored the drug-releasing applicability for TNTs fabricated on 3D-Ti-implants showing loading of a bactericidal agent, vancomycin, inside TNTs and *in-vitro* bacterial culture study confirmed complete bacterial eradication [43].

3. TNTs for bone implants applications

3.1. Osseointegration, biocompatibility, and toxicity of TNTs

To ensure implant's longevity after insertion, a long-lasting and durable interaction between the implant's surface and surrounding bone tissue should be established [44]. Following the contact of the implant with bone tissues, a cascade of processes occur at the bone-implant interface. Thus, the bone response depends mainly on the chemical and physical characteristics of the implant surface [45]. It is essential to promote bone cells adhesion to the implant surface in order to minimize possibility of implant's loosening. Previous studies have confirmed that the process of osseointegration is significantly triggered by the implant's surface roughness [46]. Incorporation of nanosized features (e.g. TNTs) on the implant's surface, which resemble bone microenvironment, could augment bone cells activity and consequently strengthen cell attachment. The nanostructured surface topography showed excellent biocompatibility through enhancing apatite formation and providing sufficient space for cell anchoring, spreading, and proliferation [47]. The presence of TNTs on Ti implants surface enhanced the adsorption of large amounts of osteoblasts adhesion promoting proteins which was subsequently translated to improved cell adhesion and long term osseointegration, in comparison with smooth or micro-rough surfaces [48]. TNTs possess a net negative charge at physiological pH, thus, positively charged proteins would attach more favorably to TNTs. In addition, TNTs is characterized by large surface area which in turn promotes protein adhesion. Studies highlighted the influence of TNTs morphology (e.g. diameter and length) on protein adsorption. In one study, tubes with different diameters (15, 50 and 100 nm) and lengths (250 nm up to 10 μm) were fabricated and then adsorption of small charged proteins (albumin (negatively charged) and histone (positively charged)) was tested [49]. Longer tubes with higher total surface area were found to adsorb more proteins which is not surprising. Reports also showed that TNTs composed of anatase crystals favors the deposition of stable HAP layers from simulated body fluids, thus enhancing osseointegration, in contrast to smooth (no TNTs) Ti implant [50]. TNTs of variable lengths were tested against the stability of HAP coatings. The most stable coating was obtained on TNTs with a length of 560 nm [51]. Moreover, the viability of osteoblasts was significantly enhanced on HAP coated TNTs implants in comparison with smooth Ti implants even with HAP coating [51].

The influence of surface topography has been widely investigated to determine the most optimum surface modification technique. The optimal template for implant surface design could be fulfilled through combining micro and nano-rough surface features [52–54]. Figure 3 shows enhanced cell attachment and proliferation of pre-osteoblasts (MC3T3-E1) on the micro/nano-rough structured surface with a higher number of filopodia, and F-actin (filamentous actin) observed than in case of flat surface of the Ti6Al4V alloy [52].

Many studies explored the *in-vitro* biocompatibility and toxicity of TNTs using either osteoblasts or other types of cells. Alkaline phosphatase expression was significantly increased when mouse 3T3 embryonic fibroblast cell were

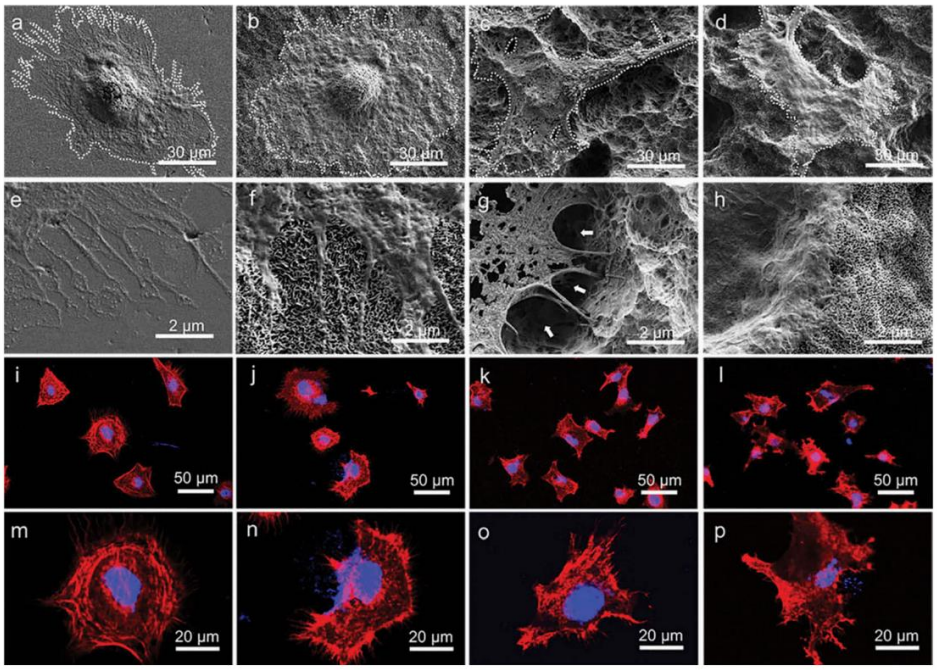

Figure 3. FESEM (above) and confocal laser scanning microscopy (CLSM) images (below) of MC3T3-E1 cells attached on (a, e, i, m) flat, (b, f, j, n) nano-, (c, g, k, o) micro-, and (d, h, l, p) hierarchical nano/microstructures with low and high magnifications. The white arrows indicate poorly attached and torn cell membranes (reproduced with permission from ref [52]).

seeded on TNTs substrates as compared to pure Ti ones indicating improved cell differentiation [55]. In the same context, MTT assay confirmed significantly higher viability of pre-osteoblast MC3T3 on TNTs/Ti substrates after 7 days compared to untreated ones [47]. In a former study, ciliated protozoan, T. pyriformis, was used as an alternative to cell culture to study TNTs toxicity [56]. Results showed no observable toxic effect of the tested TNTs, either amorphous or crystalline, on the protozoan population. The cytocompatibility of chitosan-coated TNTs/Ti implants was recently tested with human bone marrow-derived mesenchymal stem cells. Results confirmed the improved cell activity in case of chitosan-coated TNTs when compared with uncoated TNTs and flat Ti substrates [57].

The biocompatibility was also assessed *in-vivo*, Park et al. confirmed the ability of TNTs, loaded with fibroblast growth factor (FGF) and human fibronectin fragments ($hFNIII_{9-10}$), to promote osseointegration into rabbit tibia for 3 months. No toxicity or inflammatory reactions were observed in response to TNTs/Ti implants. TNTs/Ti substrates were also implanted subcutaneously into male Lewis rats and histological analysis confirmed the absence of any chronic toxicity or fibrosis [58]. In the same context, TNTs significantly enhanced bone attachment in rat tibia after 4 weeks as confirmed by pull-out test in comparison to TiO_2 gritblasted control surface [59]. This was attributed to higher calcium and phosphate level, larger attachment area and more new bone formation. Recently, Mi *et al.* prepared strontium (Sr) loaded TNTs via hydrothermal treatment of TNTs/Ti substrates in $Sr(OH)_2$ [60]. They used ovariectomized rat model with osteoporosis to investigate the effect of the prepared implants on bone loss. After 8 weeks, results showed that Sr-TNTs/Ti implants could prevent further bone loss through inhibition the activity of osteoclasts. Similar results were also obtained by Cheng *et al.* who combined silver ions with Sr to add antibacterial properties to the implant [61]. Osteoblastic cell responses to TNTs was also tested after isolation of Sprague–Dawley rats. The cells showed better proliferation and differentiation on TNTs/Ti specimens with higher calcium mineralization compared to flat Ti [62]. It is worth mentioning that all the above-mentioned studies were carried out over a short period, 1–3 months, and more long-term studies are required to explore the prolonged healing periods of these implants to reflect the clinical situation. Also, it is important to state that most of these studies focused only on surface topography (nano- vs. micro-rough) with little or no emphasis on surface chemistry (e.g. TiO_2 vs. pure Ti).

Another major concern for TNTs application is the *in-vivo* delamination of TNTs from the implant's surface which could result in severe inflammation in the surrounding bone tissues and eventually could lead to systemic toxicity. To this end, a recent study explored the mechanical damage that could occur to TNTs after implantation into equine cadaver bone [63]. A hole equivalent to the implant's diameter was made into the bone using a drilling machine. Then TNTs/Ti rods were placed and implant-bone contact was ensured by hammering on the bone before removing the rods for testing. Results showed that, TNTs, up to 1 µm in length, remained intact with no obvious deformation or detachment. This confirms the stability of TNTs fabricated on top of Ti implants with no concern of delamination.

3.2. TNTs as a platform for localized drug delivery applications

Integration of TNTs onto Ti implants surface resulted in a new concept of drug-releasing implants that can combine bone support and localized drug release functions to solve many implant challenges and hard to reach conditions like bone infection, inflammation, and cancers [23,64]. TNTs are considered a unique platform for delivering therapeutics, as its void volume can be loaded with considerable amounts of therapeutic which can later be eluted with controlled kinetics. Various therapeutic agents such as antibiotics, proteins, growth factors etc., exhibiting variable water solubilities, chemical groups, molecular weight, were loaded into TNTs to cater for wide range of bone problems [14]. In the following sections, we will highlight the most relevant applications and studies involving TNTs to cope with critical bone conditions such as inflammation, bacterial infection, and cancer.

3.2.1. TNTs implants and inflammation

The adhesion of the extracellular matrix proteins (ECM) and blood components onto the surface of the implant surface could cause either immediate or delayed trigger of the immune system causing inflammation [4]. The role of TNTs in modulating the immune response, compared to flat Ti implants, was confirmed [65]. The macrophages (RAW 264.7) response to either TNTs (78 nm in diameter) and pure Ti sheets was investigated under both standard and pro-inflammatory conditions. Results showed that, TNTs exhibited a significantly reduced macrophage inflammatory response in terms of cytokine and chemokine gene expression/protein secretion. Ainslie *et al.* also explored the influence of Ti implant nano-rough surface on the inflammatory response. They measured the human monocyte viability, inflammatory cytokines and reactive oxygen species generation in case of flat and nanostructured (i.e. TNTs) surfaces. Results showed that inflammation could be significantly reduced when nano-roughness is present [66]. Comparable results were concluded by Smith *et al.*, in which both immediate and delayed *in-vitro* immune reactions to TNTs were investigated using human blood lysate (with leukocytes, thrombocytes and erythrocytes) [67].

Several studies were dedicated to loading/releasing of anti-inflammatory drugs from TNTs/Ti implants in order to modulate the immune responses. In this context, dexamethasone, penicillin, and streptomycin were simultaneously loaded inside TNTs via physical adsorption from simulated body fluid (SBF) [68]. The results showed improved osteoblast numbers as compared to unmodified Ti implants. In the same context, other anti-inflammatory drugs like ibuprofen, sodium naproxen, etc. have been explored to obtain desirable release properties from TNTs [69,70].

3.2.2. TNTs implants and bacterial infection

Bacteria may invade bone tissues through different pathways, directly from bloodstream or after fractures, leading to serious infection. In addition, bacterial invasion may occur during implant surgeries, despite of strict sterile conditions applied. High incidence of triggering infection was reported with estimates up to 2.5% of primary hip and knee implants and about

20% of revision arthroplasties are complicated by infection [71]. *Staphylococcus aureus* (*S. aureus*), *Staphylococcus epidermidis* (*S. epidermidis*), *and Pseudomonas aeruginosa* are the most common pathogens involved in bone infections [72]. Pathogenic bacteria usually firmly stick on the implant surface forming a biofilm which makes them very resistant to antibacterial agents and this could eventually cause implant rejection/failure [73,74]. Moreover, some studies highlight the role of surface properties on bacterial adhesion in which both bones cells and pathogenic bacteria compete together to adhere to the implant's surface which determines the fate of the implant. This presents 'the race for the surface' concept [71]. When the effect of TNTs diameters (15, 50, 100 nm) on bacterial attachment was investigated, the lowest adhesion was observed for the smallest TNTs (i.e. 15 nm) as compared to other TNTs [75]. Puckett *et al*. postulated three main reasons behind bacterial attachment on TNTs: (1) Fluoride ions remaining from anodization process, (2) presence of dead bacteria on TNTs surface which induces the attachment of viable bacteria through release of intracellular proteins upon their death and at the same time, inflammation is usually triggered due to the presence of dead bacteria, and (3) amorphous TNTs [73].

To prevent bacterial infection, loading of antibacterial agents onto TNTs seems an appealing approach. Many antibacterial molecules (e.g. antibiotics and anti-microbial peptides) have been loaded inside TNTs in an attempt to achieve substantial release kinetics to render the surfaces bactericidal without compromising the bone cell activity [2,76–78]. The antibacterial effect of vancomycin incorporated into HAP (Ti/Van HA) and biomimetic HAP-collagen (Ti/Van HA-Col) coatings on Ti substrates was compared with that of vancomycin loaded TNTs. Results showed that TNTs lead to 78% release compared to 92 and 85% for Ti/Van HA and Ti/Van HA-Col coating, respectively. At the same time, all types of drug loading showed effective bacterial inhibition against *S. aureus* as shown in Figure 4(a,b) [18]. *In-vivo* activity of gentamicin-loaded TNTs (GN-TNTs) was confirmed using Sprague Dawley rats infected with *Staph. Aureus* into the medullary cavity of the femur [79]. GN-TNTs rods were inserted at the infected site and the antibacterial effect was compared with drug-free TNTs and flat rods. Signs of bone infection including osteolysis and periosteal reaction significantly appeared when Ti rods were used. However, drug free TNTs/Ti rods slightly reduced the infection signs while no signs were observed in case of GN-TNTs indicating complete bacterial eradication. Recently, new molecules called biofilm disruptors has been discovered. Their integration into TNTs/Ti implants might not only prevent bacteria from forming biofilms but could also disrupt any existing biofilms [78].

In addition to antibiotics, metal ions especially silver (Ag) ions and nanoparticles (NPs), has also been explored. AgNPs were loaded into TNTs using 3-sulfopropyl methacrylate potassium salt (PSPMA) via atom transfer radical

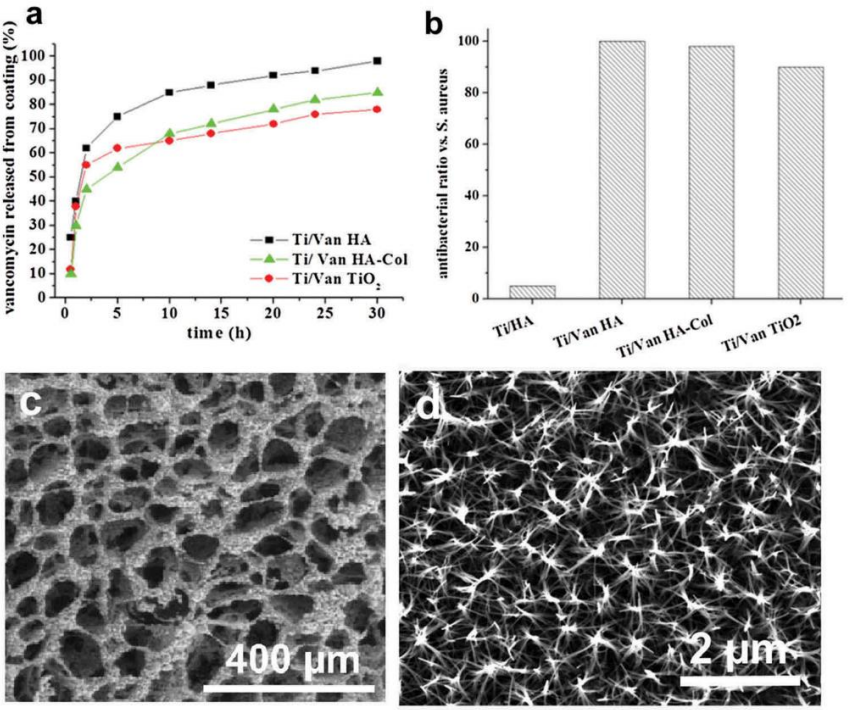

Figure 4. (a) release profiles of vancomycin from the different coatings, (b) antibacterial ratio of Ti/HA, Ti/Van HA, Ti/Van HA-Col, and Ti/Van TiO_2 against *S. aureus* (adopted with permission from ref [18]), (c) FESEM image of chitosan-TNTs scaffolds (adopted with permission from ref [86]), and (d) hydrothermal treatment for 2.5 h of titania (TiO_2) surfaces changed the texture of the surface forming a homogeneously dense coverage of spike-like structures (adopted from ref [114], no permission required).

polymerization [80]. Ag loaded TNTs were able to kill bacteria *in-vitro* and hamper the growth of new bacteria. In another attempt, excellent antibacterial activity was obtained when Ag was doped into TNTs through immersing TNTs/Ti implants into $AgNO_3$ solution followed by xenon lamp irradiation [81]. Other metal ions used include zinc and copper ions which could simultaneously enhance the process of osseointegration [82–84].

As mentioned above, one of the extensively investigated strategies to allow localized drug delivery of therapeutics from TNTs is the application of polymeric coatings. Some polymers, such as chitosan [85], exhibit antibacterial properties and thus coating TNTs with such polymers could results in long-lasting antibacterial effects, Figure 4(c) [86]. Our group adopted this strategy to illustrate long-term antibacterial activity of chitosan-coated TNTs against *S. epidermidis* [87]. First, gentamicin was loaded inside TNTs which was then covered with chitosan. The presence of chitosan not only significantly decreased bacterial adhesion, but also lead to delayed gentamicin release and enhanced bone cells attachment as well. Similar results were recently obtained after *in-vivo* assessment of chitosan-coated TNTs/Ti implants inserted into rats' femoral medullary cavity infected with *methicillin-resistant Staph. aureus* [57]. Radiographical, microbiological, and histopathological examination confirmed that chitosan-coated TNTs/Ti implants possess anti-infection potential; however, the study also suggested the importance of systemic antibiotic administration for complete eradication of the bacterial infection.

Recently, a new concept of self-antibacterial surface was introduced to design a suitable surface setting that could itself act either as bactericidal or bacteria repelling surface. This approach are expected to possess antibacterial properties without incorporation of any antibacterial drug or metal ions and is based on physical mode of action (structure, charge, hydrophobicity) that would prevent bacteria colonization and reduce risk of infection [88]. In addition, if the self-antibacterial TNTs and the antibiotics are combined together, long-lasting anti-bacterial effects can be reached, even after the loaded drug is completely released. In this aspect, annealing of TNTs at high temperature (650–750°C) was found to reduce the bacterial growth of *S. aureus* and *Pseudomonas aeruginosa* [89].

In addition to TNTs, other nanotreatment of implants surface is currently of great interest. Novel nanoscale surface modifications have been adopted to fabricate self-killing antibacterial implants as a replica of dragonfly wing structures. The antibacterial activity of these implants depends on the formation of ordered nanopillars, spikes pits on Ti implants. In addition, these nanotopographical cues mimic the natural bone architecture which could, in turn, promotes the process of osseointegration [90]. This can be achieved via hydrothermal treatment of Ti implants which appears to be a promising surface modification process. This process is simple, cost-effective with scale-up potential which involves heating implants immersed in a suitable alkaline solution (e.g. NaOH or KOH) to generate titanate nanostructures. Lorenzetti *et al.* employed this process to produce implants with better corrosion resistance with 50% less adhesion of *E. coli* compared to untreated Ti implants [91]. In another study, TiO_2 nanowires were hydrothermally grown on Ti substrates immersed in alkaline solution at 240°C for different times (2, 2.5, or 3 h). After that, bone cells growth and bacterial colonization were assessed using scanning electron microscopy and confocal microscopy. Results revealed that nanowires formed after 2 h supported bone cells growth and differentiation and at the same time significantly reduced *Pseudomonas aeruginosa* viability,

3.2.3. Delivery of Growth Factors

Different types of growth factors (GFs) are used including osteogenic (e.g. BMPs), angiogenic (vascular endothelial growth factor) and systemic factors (calcitonin and Vitamin D) [92]. Since administration of GFs via systemic routes faces many limitations, GFs local delivery from implants can directly promote bone tissue repair and permit normal cellular functions, especially when targeting multiple conditions such as osteoporosis-induced fractures with compromised normal repair mechanism [64]. Lai *et al.* chemically functionalized TNTs by BMP-2. Wistar rats MSCs were seeded onto BMP-2-TNTs (30, 60, and 100 nm in diameter) and control substrates. BMP-2-TNTs showed significantly improved cell viability, differentiation and proliferation [93]. Furthermore, the smallest diameter TNTs (30 nm) provided much better adhesion to MSCs as compared to wider TNTs. Other *in-vitro* studies reported improved bone formation through chemical incorporation of various GFs inside TNTs, including bisphosphonate and peptide sequences, such as arginine–glycine-aspartic acid–cysteine (RGDC) [94,95]. A more feasible way to load GFs inside TNTs is via immersing TNTs into a solution containing the active biomolecules. This method was employed to load ibandronate (class of bisphosphonates), followed by exploring osseointegration *in-vivo* [96]. Three substrates: control, drug free TNTs and ibandronate loaded TNTs, were implanted in rats tibia. After 2 and 4 weeks, osseointegration was assessed by removal toque test and microcomputerized tomography (μCT). Ibandronate loaded TNTs showed the best values for removal torque, and denser bone tissue growth as compared to other tested substrates. In a similar recent study, alendronate, anti-osteoporosis agent, was loaded on TNTs and tested in rabbits [97]. First, ovaries were removed to induce osteoporosis. Ti, TNTs/Ti, HAP-coated TNTs/Ti, and alendronate HAP TNTs/Ti implants were placed into the femoral epiphysis. 3 months later, rabbits were sacrificed then push-put test, μCT and histological analysis were performed. Alendronate HAP TNTs/Ti implants group showed the highest interfacial strength compared to the other groups. At the same time, more new bones and trabecular thickness were noticed in case alendronate loaded implants.

TNTs/Ti implants were also assessed *in-vivo* for dental applications [98]. Four groups of implants were used; TNTs loaded with recombinant human bone morphogenetic protein-2 (rhBMP-2), Ti implants with machined surface, sandblasted large-grit and acid-etched surface while TNTs/Ti implants with no loaded proteins were used as control. The implants were inserted into proximal tibia of New Zealand white rabbits. rhBMP-2 loaded TNTs showed the highest value of bone remodeling and bone-implant contact ratio compared to the other groups. This confirms that TNTs could serve as a reservoir for different growth proteins to reinforce bone growth.

Recently, our group prepared antagonizing proteins (glypicans) loaded TNTs/Ti implants to treat newborn craniosynostosis (premature ossification of fibrous sutures of infant's skull) [99]. Children suffering from this problem are subjected to repeated surgical procedures which are very painful and expensive. Our results showed prolonged delivery of the loaded protein *in-vitro* and downregulation of BMP2 bioactivity (ossteoinducing pathway) in transfected cells, Figure 5. This proposed that LDD could significantly enhance the affected children's quality of life and improve the treatment success.

3.2.4. Anticancer drug delivery

Bone tumors (either primary or secondary) is one of the common reasons of pathological bone fractures. This occurs as a result of disruption of the normal bone activity due to the presence of tumor cells which disrupts the bones architecture making them susceptible to break even in absence of any accidents or trauma [24]. Such condition is commonly treated by tumors removal, implant fixation, and systemic chemotherapy. However, in case of chemotherapy, the indiscriminate distribution of anticancer agents, usually lead to severe side effects to healthy tissues which limits the applications of these agents. To this end, our group developed 3D-printed Ti implants with TNTs on top. Anticancer agents, doxorubicin and tumor necrosis factor-related apoptosis-inducing ligand (Apo2L/TRAIL) were loaded inside TNTs. *In-vitro* cell study confirmed an enhanced anticancer effect of loaded therapeutics for 3 days period [24].

3.2.5. Combined osteogenic, antibacterial, and anticancer effects

Application of multiple therapeutics is sometimes required in some cases like cancer in order to realize effective healing. Drugs acting by different mechanisms are employed to improve treatment outcomes, reduce individual drugs dosage and minimize side effects. Furthermore, loading more than one therapeutic agent inside TNTs could allow simultaneous treatment of several issues. These multidrug-loaded implants can significantly improve current implant development as it can cater to common implant challenges such as infection, inflammatory response and poor integration at the same time. For example, anticancer selenium (Se) was electrodeposited into TNTs, followed by chitosan spin coating on top. This yielded implant that combines antibacterial, enhanced osseointegration and anticancer activities [100]. In this study, chitosan provided long-term antibacterial effect against *E. coli* and allowed controlled release of Se. In addition, Se served two functions; inhibition of the growth of cancer cells and improving osteoblasts adhesion.

3.3. Electrical stimulation therapy

Clinical evidence showed that electrical stimulation therapy (EST) can accelerate the healing process of bone fractures [101]. Parl *et al.* studied the mechanism of direct current electric field to induce mesenchymal stem cell differentiation seeded on TNTs [102]. They showed that electric field triggered the osteogenic induction of mesenchymal cells. This was explained due to increased Ca^{2+} influx into cells through formation of membrane protrusions with Connexin 43 hemichannels on plasma membrane in response to the applied electric field. However, the presence of TiO_2 of TNTs, TNTs/Ti implants are not expected to be good electrical conductors for EST applications. Gulati *et al.* recently demonstrated the conversion of TNTs into TiNTs (titanium nanotubes), to increase its conductivity [103]. In this study, TiO_2 (TNTs) were reduced to more conducting Ti using magnesiothermic process. The structure of nanotubes (now TiNTs) was retained with significant increase in the conductivity. TiNTs allowed dual EST and local drug-releasing properties which can be used for improved local therapeutic effects.

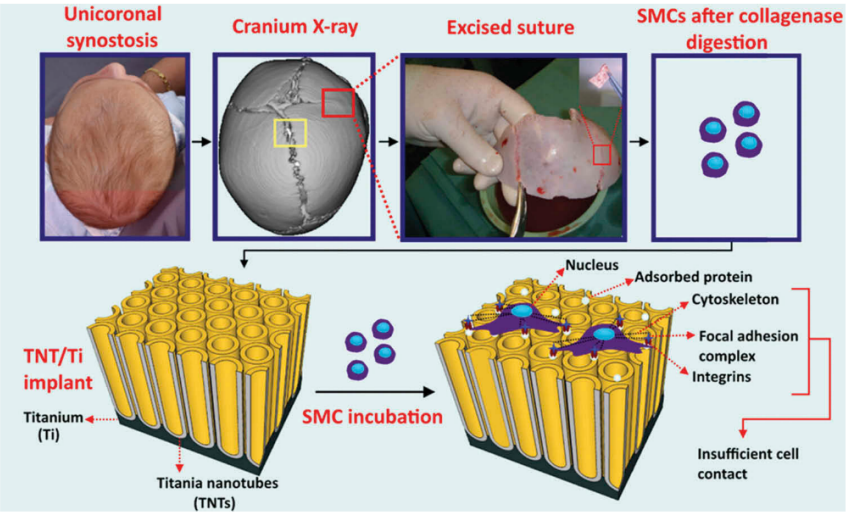

Figure 5. Schematic diagram summarizing the excision of human calvarial suture tissue and extraction of suture mesenchymal cells (SMCs) from a patient undergoing craniofacial reconstruction surgery at ACFU. The lower part of the scheme shows the TNTs/Ti implant with SMCs cultured on the top. It further depicts the cell-biomaterial interface with protein adsorption, integrin clustering, focal contact formation, and initial cell adhesion (adapted with permission from ref [99]).

3.4. Advances on improving drug releasing TNTs implants

Many studies which considered loading of TNTs with antibiotics, antibacterial metal ions, anti-inflammatory agents or anticancer drugs, neglected the control of the release kinetics. Ideal LDD system should offer controlled drug release including sufficient initial release to reach effective drug concentration followed by sustained release over a prolonged period of time. In addition, on-demand release features are sometimes required where recurrence of some conditions may occur (e.g. cancer). Rapid drop in the effective concentration of loaded therapeutics can re-trigger condition (e.g. the bacterial growth or cancer cells recovery), on the other hand, very high concentration of therapeutics can be toxic to bone cells, which can interfere with the healing mechanism. Such tunable/on-demand release kinetics could be achieved using various techniques such as varying TNTs dimensions, polymer coating or chemical functionalization. The next section will focus on various approaches to achieve controlled drug release kinetics from TNTs.

3.4.1. Varying TNTs dimensions

Drug release from drug loaded TNTs occurs through diffusion into the surrounding medium. Thus, the rate of release will depend on TNTs dimensions (i.e. pore diameter and length). The amount of drug loaded will depend on the available vacant volume of TNTs; longer nanotubes will offer more space for drug to be deeply loaded, thus prolonged drug release is achieved [9]. Since the dimensions could be precisely controlled by anodization process, varying TNTs dimensions was adopted for manipulating the drug release. This approach is limited by the relation between amounts loaded and release behavior. Maximum drug entrapment could be achieved with longer and wider TNTs but with burst drug elution while shorter and narrower TNTs mean less drug amounts with significantly less burst release. Accordingly, further trials toward increasing drug loading and at same time reducing TNTs pore diameters are desired for better control over the release kinetics. TNTs with diameters ranging from 30 to 140 nm were fabricated on Ti substrates [104]. The diameter of TNTs played a vital role in drug loading and release with least loading obtained with 30 nm TNTs. In this study, *in-vitro* release data of ibuprofen loaded TNTs showed that the 80 nm tubes provided the optimum drug loading and release properties. It is worth mentioning that, drug loading and release can be also controlled through alterations in TNTs structure (e.g. periodic, double-walled, bamboo-type, nanolace and branched TiO_2 nanostructures) which can be generated by periodic anodization conditions [105,106].

3.4.2. Altering TNTs properties by chemical functionalization

Chemical functionalization of TNTs surface can significantly influence the drug release kinetics. Rendering the surface hydrophilic using 2-carboxyethyl-phosphonic acid (2-phos) resulted in easier indomethacin diffusion inside TNTs (higher loading efficiency) and prolonged release compared to unmodified TNTs and hydrophobic TNTs functionalized with 16-phosphono hexadecanoic acid (16-phos) [107].

Song et al. represented another approach for chemical modification to fabricate hydrophilic TNTs with hydrophobic cap [108]. The fabrication process involved two anodization steps, hydrophobic cap modification was applied using (octadecylphosphonic acid) after first adonization step, while hydrophilic modification was imparted using 3-aminopropyl triethoxysilane after the second anodization step, thereby a unique amphiphilic structure was generated. After that, horseradish peroxide (HRP) was loaded according to different methods: (a) soaking, (b) soaking + hydrophobic cap, (c) covalently attached HRP, and (d) covalently attached HRP + hydrophobic cap. The presence of the hydrophobic cap significantly reduced the burst release. Moreover, a controlled release was achieved upon UV irradiation to remove the hydrophobic cap. This approach demonstrated the capacity to trigger the release of drugs from TNTs based on chemical functionalization in response UV illumination.

3.4.3. Polymeric modifications

Polymer modification of TNTs permits several benefits including ease of controlling the thickness of the TNTs covering, and also the incorporation of additional functions such as anti-bacterial and improved osseointegration characteristics [45]. Losic *et al.* extensively explored single step and scalable plasma polymerization (PP) to prolong the release of therapeutics from TNTs [107]. However, PP suffers from a few limitations including prolonged optimization time (to reach proper thickness), expensive hardware, and technical expertise requirement; which can possibly mean difficulty for its integration into the current TNTs biomedical applications [109].

Alternative approaches are reported to overcome the limitations of PP and simultaneously enhance bioactivity and osseointegrating ability such as dip coating of biopolymers (e.g. chitosan and PLGA) on the surface of drug-loaded TNTs. In addition, simple application of polymers on top of drug loaded TNTs can also provide controlled release properties. PLGA was applied on the surface of ibuprofen-loaded TNTs and then were tested for drug-releasing properties. Burst release was significantly reduced for PLGA coated TNTs samples compared to uncoated ones. In addition, the application of PLGA prolonged the release to 40 days compared to only 5 days for uncoated samples. When tested with MC3T3-E1 mouse cells, PLGA favored the proliferation and osteogenesis of the cells at an earlier stage [104].

3.4.4. Triggered drug release

Triggered release of therapeutics can offer many befits such as reduced drug loss, non-invasive 'on-demand' drug release, reduced costs, and side effects. Many investigators have included triggering features that respond to temperature, magnetic or electric fields, radio or ultrasonic frequencies, etc. into TNTs drug-releasing implants, Table 2.

Table 2. Summary of strategies of controlled/triggered drug release (original table, no permission required).

System	Example of system	Drug/Drugs loaded	Refs.
Triggered drug release			
Radiofrequency-triggered release	Gold nanoparticles used as energy transducers.	Indomethacin	[138]
Ultra-sonication triggered drug release	Super hydrophobic TNTs with ultrasonic-controlled drug release	Tetracycline hydrochloride	[112]
pH-sensitive drug release	ZnO-Folic acid sealed TNTs system PLGA/TNTs	Vancomycin Carprofen and lidocaine	[139 140]
UV light sensitive drug release	(UV)-induced chain cutting of cap of Amphiphilic TNTs covered by octadecylphosphonic acid	Horseradish peroxidase (HRP)	[108]
Infrared (IR) laser irradiation	Immobilized gold Nanorods (GNRs) onto the surface of TNTs triggered by near-IR laser irradiation	Tetracycline	[141]
Magnetic-sensitive drug delivery	Modified iron oxide MNPs (DOPA–Fe_3O_4) placed at bottom of TNTs	Indomethacin	[142]
Voltage-induced drug release	Hydrocarbon monolayers detachment due to electrochemical reaction	Horseradish peroxidase (HRP)	[143]
Functionalizing the surface of TNTs by a specific functional group	Self-assembled monolayers (SAM) of organo-silanes and organic acids	Ibuprofen	[107]
Structural modification of TNTs features			
Pore size modification	Pore widening procedure applied on TNTs	Indomethacin	[107]
TNTs length modification	Alteration of anodization time	Indomethacin	[107]
Periodically tailored titania nanotubes	Periodically modulated (p-TNTs) internal structures	Indomethacin	[144]
Controlling pore openings by depositing a layer of biopolymer via plasma polymerization	Poly(allylamine) (PAa) layer is deposited by plasma polymerization	Anti-inflammatory drugs	[145]
Multi-drug delivery with polymeric micelle act as drug nanocarriers	Sequential drug release using TNTs arrays	Gentamicin sulfate	[146]
Degradation of biopolymer film which covers the TNTs surface	Dip coating in chitosan and poly(lactic-co-glycolic acid)	Indomethacin	[109]

Visible light-triggered release of ampicillin from TNTs was successfully achieved. First, TNTs were fabricated and the walls were decorated with gold (Au) NPs followed by attachment of hydrophobic monolayer cap of octadecylphosphonic acid. After that, a second anodization was performed which allowed the growth of a second bottom layer of TNTs. Finally, ampicillin was attached to the walls of the lower tubes by forming a silane linker with 3-glycidyloxypropyl) trimethoxysilane. *In-vitro* study showed no ampicillin release in dark. In contrast, upon application of visible light, through a xenon light source, ampicillin was effectively released as a result of cap removal by AuNPs Plasmon resonance which induced chain breakdown of the hydrophobic cap [110].

Another form of triggered drug release utilizing electric field was developed by Sirvisoot *et al*. Antibiotics (penicillin and streptomycin) and anti-inflammatory drug (dexamethasone) were first conjugated with polypyrrole, which was then attached on multi-walled carbon nanotubes modified TNTs surface via electrodeposition. On applying external voltage, about 80% of the loaded drugs could be eluted [111]. In another study by *Zhou et al*.; drug release was triggered in response to ultrasonic waves (USW) which could permit urgent tetracyclin hydrochloride release. Super hydrophilic TNTs implants were prepared by immersing in methanol solution of hydrolyzed 1 wt% 1H,1H,2H,2H-perfluorooctyl-triethoxysilane. USW were produced from sonication probe dipped inside the releasing medium (PBS). The release could be controlled by varying USW time and intensity; thus, tailored to meet different patients' requirements. It is noteworthy that integrating USW into local drug-releasing implants is an attractive approach since USW could be transferred through the body without causing any damage to tissues or cells [112].

4. Conclusion and future perspectives

This review article highlighted recent advances demonstrating the potential of integrating LDD features into Ti implants which would address both the limitations of conventional systemic drug treatment and bone implants postoperative complications. Studies showed that TNTs drug releasing implants could be employed in the development of a variety of LDD systems and therapies providing controlled release kinetics and therapeutic conditions not possible with systemic drug administrations. The TNTs structured surface could be fabricated on the surface of currently used medical implants regardless of their shape by well-established, low cost, and scalable electrochemical anodization with high control over their structure and physicochemical properties. TNTs possess many unique features including tunable dimensions, ability to control drug release kinetics, incorporation of triggering mechanism (magnetic, ultrasonic, temperature). Furthermore, TNTs has shown superior biomedical characteristics such as biocompatibility, enhanced cell adhesion and proliferation, corrosion resistance and mechanical stability.

Studies mentioned throughout this article also confirmed the possibility of loading various drugs inside TNTs with different properties (e.g. solubility and molecular weight) which could cater for a variety of bone conditions. All the above mentioned demonstrates that TNTs could be described as a new generation of drug-releasing implants. However, their

implementation in practical use is slow and still far from clinical trials. Although many recent *in-vitro*, *ex-vivo*, and *in-vivo* experiments confirmed their biocompatibility, further in-depth and long-term studies are required to translate this technology from research to real human clinical trials. In addition, its long-term toxicity *in-vivo* is yet to be explored. In the near future, localized bone implants will not be able to replace systemic drug therapy, but based on the facts shown by the reviewed studies, it is rational to expect that these systems could eventually replace the conventional therapy regimens.

5. Experts opinion

Localized drug delivery represents a simple and reliable solution to many critical bone disorders that are difficult to be treated with conventional routes of drug administration such as topical or systemic routes. Owing to the versatile use of Ti implants, integrating drug delivery features into such implants will bring new opportunities to deal with resilient bone conditions such as inflammation and bacterial infection. This review highlighted the most representative studies and key findings related to the application of titanium implants for LDD with special emphasis on TNTs. This new technology could bring real opportunities to the transition of the current research into real clinical applications. TNTs have shown many advantages over other localized bone drug delivery systems (e.g. polymers and ceramics). TNTs are highly ordered arrays with precise controllable dimensions. They also mimic the bone microstructure which results in improved osseointegration. Furthermore, compared to other drug carriers, they offer higher loading efficiency and higher control in terms of drug release and loading multiple drugs with no limitations for hydrophobicity/hydrophilicity allowing a variety of drugs, proteins, genes, micelles or nanoparticles to be added. In addition, the low cost and scalability of electrochemical anodization into industrial scale make TNTs/Ti promising candidates for new generation of drug-releasing implants. Despite these features, it is worth mentioning that, translating this technology into real implants, faces many fundamental challenges. Although extensive research has been investigating the performance of TNTs-based implants (e.g. stability, toxicity, ability to enhance osseointegration, and control drug release), potential delamination and degradation in the biological milieu; long-term toxicity and longevity after implantation are yet to be confirmed through further long-term studies and clinical trials. Moreover, the commercial value of these drug-releasing implants will not be achieved unless they move to clinical trials and pass the regulatory approval stages which requires substantial financial support. TNTs-based implants are still in their early development stage which is not mature enough to attract potential industry investors. At the same time, the increasing competition by pharmaceutical companies in developing systemically administered drug delivery systems that could target bone tissues will reduce the market share of TNTs-based drug-releasing implants. Yet, in contrast to other drug-delivery systems, LDD to bones based on TNTs implants have broad applicability making them an attractive alternative to treat a variety of conditions. TNTs/Ti implants offer unique approaches that are markedly different from existing competitive technology such as polymer-based implants. Finally, the incorporation of 3D printing technology to fabricate implants with tunable design and dimensions will further present TNTs/Ti implants as a potential platform for localized drug-delivery applications.

Acknowledgments

The authors acknowledge the financial support provided to S. Maher by the Australian Government Training Program Scholarship, and Forrest George and Sandra Lynne Young Supplementary Scholarship.

Funding

This paper was not funded.

Declaration of interest

The authors have no relevant affiliations or financial involvement with any organization or entity with a financial interest in or financial conflict with the subject matter or materials discussed in the manuscript. This includes employment, consultancies, honoraria, stock ownership or options, expert testimony, grants or patents received or pending, or royalties.

Reviewer disclosures

Peer reviewers on this manuscript have no relevant financial or other relationships to disclose.

References

Papers of special note have been highlighted as either of interest (•) or of considerable interest (••) to readers.

1. Gulati K, Aw MS, Findlay D, et al. Local drug delivery to the bone by drug-releasing implants: perspectives of nano-engineered titania nanotube arrays. Ther Delivery. 2012;3(7):857–873.
2. Lu H, Liu Y, Guo J, et al. Biomaterials with antibacterial and osteoinductive properties to repair infected bone defects. Int J Mol Sci. 2016;17(3):334.
3. Gheno R, Cepparo JM, Rosca CE, et al. Musculoskeletal disorders in the elderly. J Clin Imaging Sci. 2012;2:39.
4. Binkowska AM, Michalak G, Słotwiński R. Current views on the mechanisms of immune responses to trauma and infection. Central-Eur J Immunol. 2015;40(2):206–216.
5. Wu S, Weng Z, Liu X, et al. Functionalized TiO_2 based nanomaterials for biomedical applications. Adv Funct Mater. 2014;24(35):5464–5481.
6. Maher S, Losic D. Nano-engineered titania nanotube arrays for localized drug delivery and enhanced osseointegration. In: Uskocovic V, editor. Nanotechnologies in preventive and regenerative medicine. Vol. 1. Ma, USA: Elsevier; 2017.
7. Trajkovski B, Petersen A, Strube P, et al. Intra-operatively customized implant coating strategies for local and controlled drug delivery to bone. Adv Drug Deliv Rev. 2012;64(12):1142–1151.
8. Moran E, Byren I, Atkins BL. The diagnosis and management of prosthetic joint infections. J Antimicrob Chemother. 2010;65(suppl 3):45–54.
9. Gulati K, Maher S, Findlay DM, et al. Titania nanotubes for orchestrating osteogenesis at the bone–implant interface. Nanomedicine. 2016;11(14):1847–1864.
   •• Important contribution showing roles of titania nanotubes on osteogeneis process.
10. Hendriks JGE, van Horn JR, van der Mei HC, et al. Backgrounds of antibiotic-loaded bone cement and prosthesis-related infection. Biomaterials. 2004;25(3):545–556.

11. Parvizi J, Saleh KJ, Ragland PS, et al. Efficacy of antibiotic-impregnated cement in total hip replacement. Acta Orthop. 2008;79(3):335–341.
12. Manam NS, Harun WSW, Shri DNA, et al. Study of corrosion in biocompatible metals for implants: a review. J Alloys Compd. 2017;701:698–715.
• **A comprehensive review on corrosion problems of bone implants**
13. Yongsug T, Byoung-Gu L, Jaemin K, et al. Effect of surface treatment on surface roughness and Ni content of nitinol stents. Int J Surf Sci Eng. 2016;10(4):389–399.
14. Gulati K, Kogawa M, Maher S, et al. Titania nanotubes for local drug delivery from implant surfaces. In: Losic D. and Santos A., editors. Electrochemically engineered nanoporous materials. Switzerland: Springer International Publishing; 2015. p. 307–355.
15. Losic D, Aw MS, Santos A, et al. Titania nanotube arrays for local drug delivery: recent advances and perspectives. Expert Opin Drug Delivery. 2015;12(1):103–127.
16. Hao C, Wei X, Zhong F, et al. Strontium (Sr) and silver (Ag) loaded nanotubular structures with combined osteoinductive and antimicrobial activities. Acta Biomater. 2016;31:388–400.
17. Sanchez MC, Fernandez E, Llama-Palacios A, et al. Response to antiseptic agents of periodontal pathogens in in vitro biofilms on titanium and zirconium surfaces. Dent Mater. 2017;33(4):446–453.
18. Ionita D, Bajenaru-Georgescu D, Totea G, et al. Activity of vancomycin release from bioinspired coatings of hydroxyapatite or TiO_2 nanotubes. Int J Pharm. 2017;517(1):296–302.
19. Tejero R, Anitua E, Orive G. Toward the biomimetic implant surface: biopolymers on titanium-based implants for bone regeneration. Prog Polym Sci. 2014;39(7):1406–1447.
• **Excellent review on titania based implants for bone regeneration.**
20. Hallab NJ, Vermes C, Messina C, et al. Concentration- and composition-dependent effects of metal ions on human MG-63 osteoblasts. J Biomed Mater Res. 2002;60(3):420–433.
21. Schmidmaier G, Wildemann B, Cromme F, et al. Bone morphogenetic protein-2 coating of titanium implants increases biomechanical strength and accelerates bone remodeling in fracture treatment: a biomechanical and histological study in rats. Bone. 2002;30(6):816–822.
22. Shirtliff ME, Calhoun JH, Mader JT. Experimental osteomyelitis treatment with antibiotic-impregnated hydroxyapatite. Clin Orthop Relat Res. 2002;401:239–247.
23. Santos A, Sinn Aw M, Bariana M, et al. Drug-releasing implants: current progress, challenges and perspectives. J Mater Chem B. 2014;2(37):6157–6182.
24. Maher S, Kaur G, Lima-Marques L, et al. Engineering of micro- to nanostructured 3D-printed drug-releasing titanium implants for enhanced osseointegration and localized delivery of anticancer drugs. ACS Appl Mater Interfaces. 2017;9(35):29562–29570.
25. Wijeratne AB, Wijesundera DN, Paulose M, et al. Phosphopeptide separation using radially aligned titania nanotubes on titanium wire. ACS Appl Mater Interfaces. 2015;7(21):11155–11164.
26. Jayamohan H, Smith YR, Gale BK, et al. Photocatalytic microfluidic reactors utilizing titania nanotubes on titanium mesh for degradation of organic and biological contaminants. J Environ Chem Eng. 2016;4(1):657–663.
27. Leskelä M, Ritala M. Atomic layer deposition chemistry: recent developments and future challenges. Angew Chem Int Ed. 2003;42(45):5548–5554.
28. Kulkarni M, Mazare A, Gongadze E, et al. Titanium nanostructures for biomedical applications. Nanotechnology. 2015;26(6):062002.
29. Roy P, Berger S, Schmuki P. TiO2 nanotubes: synthesis and applications. Angew Chem Int Ed. 2011;50(13):2904–2939.
• **Excellent review on titania nanotube showing progress on fabrications and applications.**
30. Zwilling V, Darque-Ceretti E, Boutry-Forveille A, et al. Structure and physicochemistry of anodic oxide films on titanium and TA6V alloy. Surf Interface Anal. 1999;27(7):629–637.
• **The first demonstration of fabrication and properties of titania nanotubes.**
31. Macak JM, Tsuchiya H, Schmuki P. High-aspect-ratio TiO_2 nanotubes by anodization of titanium. Angew Chem Int Ed. 2005;44(14):2100–2102.
32. Paulose M, Prakasam HE, Varghese OK, et al. TiO2 nanotube arrays of 1000 μm length by anodization of titanium foil: phenol red diffusion. J Phys Chem C. 2007;111(41):14992–14997.
33. Allam NK, Grimes CA. Formation of vertically oriented TiO_2 nanotube arrays using a fluoride free HCl aqueous electrolyte. J Phys Chem C. 2007;111(35):13028–13032.
34. So S, Lee K, Schmuki P. Ultrafast growth of highly ordered anodic TiO_2 nanotubes in lactic acid electrolytes. J Am Chem Soc. 2012;134(28):11316–11318.
35. So S, Riboni F, Hwang I, et al. The double-walled nature of TiO_2 nanotubes and formation of tube-in-tube structures – a characterization of different tube morphologies. Electrochim Acta. 2017;231:721–731.
36. Elzarka A, Liu N, Hwang I, et al. Large-diameter TiO_2 nanotubes enable wall engineering with conformal hierarchical decoration and blocking layers for enhanced efficiency in dye-sensitized solar cells (DSSC). Chemistry. 2017;23(53):12995–12999.
37. Ozkan S, Mazare A, Schmuki P. Critical parameters and factors in the formation of spaced TiO_2 nanotubes by self-organizing anodization. Electrochim Acta. 2018;268:435–447.
38. Guillemot F. Recent advances in the design of titanium alloys for orthopedic applications. Expert Rev Med Devices. 2005;2(6):741–748.
39. Liang YQ, Cui ZD, Zhu SL, et al. Characterization of self-organized TiO_2 nanotubes on Ti–4Zr–22Nb–2Sn alloys and the application in drug delivery system. J Mater Science Mater Med. 2011;22(3):461–467.
40. Xiong Y, Qian C, Sun J. Fabrication of porous titanium implants by three-dimensional printing and sintering at different temperatures. Dent Mater J. 2012;31(5):815–820.
41. Cheng A, Humayun A, Cohen DJ, et al. Additively manufactured 3D porous Ti-6Al-4V constructs mimic trabecular bone structure and regulate osteoblast proliferation, differentiation and local factor production in a porosity and surface roughness dependent manner. Biofabrication. 2014;6(4):045007.
42. Gulati K, Prideaux M, Kogawa M, et al. Anodized 3D-printed titanium implants with dual micro- and nano-scale topography promote interaction with human osteoblasts and osteocyte-like cells. J Tissue Eng Regen Med. 2016;11(12):3313–3325.
43. Maher S, Qin J, Gulati K, et al. 3D printed titanium implants with nano-engineered surface titania nanotubes for localized drug delivery Chemeca 2016: Chemical Engineering - Regeneration, Recovery and Reinvention; Adelaide, SA, Australia: Engineers Australia; 2016. p. 65–76.
44. Peng W, Qiao Z, Zhang Q, et al. Micropatterned TiO2 nanotubes: fabrication, characterization and in vitro protein/cell responses. J Mater Chem B. 2013;1(28):3506–3512.
45. Civantos A, Martínez-Campos E, Ramos V, et al. Titanium coatings and surface modifications: toward clinically useful bioactive implants. ACS Biomater Sci Eng. 2017;3(7):1245–1261.
46. Wennerberg A, Albrektsson T. Effects of titanium surface topography on bone integration: a systematic review. Clin Oral Implants Res. 2009;20(Suppl 4):172–184.
47. Wang H, Lai Y-K, Zheng R-Y, et al. Tuning the surface microstructure of titanate coatings on titanium implants for enhancing bioactivity of implants. Int J Nanomedicine. 2015;10(1):3887—3896.
48. Kulkarni M, Flašker A, Lokar M, et al. Binding of plasma proteins to titanium dioxide nanotubes with different diameters. Int J Nanomedicine. 2015;10:1359–1373.
49. Kulkarni M, Mazare A, Park J, et al. Protein interactions with layers of TiO_2 nanotube and nanopore arrays: morphology and surface charge influence. Acta Biomater. 2016;45:357–366.
50. Kunze J, Müller L, Macak JM, et al. Time-dependent growth of biomimetic apatite on anodic TiO_2 nanotubes. Electrochim Acta. 2008;53(23):6995–7003.

51. Parcharoen Y, Kajitvichyanukul P, Sirivisoot S, et al. Hydroxyapatite electrodeposition on anodized titanium nanotubes for orthopedic applications. Appl Surf Sci. 2014;311:54–61.
52. Moon B-S, Kim S, Kim H-E, et al. Hierarchical micro-nano structured Ti6Al4V surface topography via two-step etching process for enhanced hydrophilicity and osteoblastic responses. Mater Sci Eng C. 2017;73:90–98.
53. Han LY, Wang CS, Qiang JB. Microstructure and properties of Ti-Fe-Zr-Y alloys prepared by laser rapid prototyping. J Alloys Compd. 2017;700:159–168.
54. Liu H, Huang X, Yu H, et al. A cytocompatible micro/nano-textured surface with Si-doped titania mesoporous arrays fabricated by a one-step anodization. Mater Sci Eng C. 2017;73:120–129.
55. Lai Y, Lin L, Pan F, et al. Bioinspired patterning with extreme wettability contrast on TiO2 nanotube array surface: a versatile platform for biomedical applications. Small. 2013;9(17):2945–2953.
56. Feschet-Chassot E, Raspal V, Sibaud Y, et al. Tunable functionality and toxicity studies of titanium dioxide nanotube layers. Thin Solid Films. 2011;519(8):2564–2568.
57. Yang Y, Ao H, Wang Y, et al. Cytocompatibility with osteogenic cells and enhanced in vivo anti-infection potential of quaternized chitosan-loaded titania nanotubes. Bone Res. 2016;4:16027.
• **This review discusses the mechanism of TNTs formation and their applications other than drug delivery**
58. Popat KC, Leoni L, Grimes CA, et al. Influence of engineered titania nanotubular surfaces on bone cells. Biomaterials. 2007;28(21):3188–3197.
• **This is considered one of the first attempts to generate TNTs.**
59. Bjursten LM, Rasmusson L, Oh S, et al. Titanium dioxide nanotubes enhance bone bonding in vivo. J Biomed Mater Res Part. 2010;92(3):1218–1224.
60. Mi B, Xiong W, Xu N, et al. Strontium-loaded titania nanotube arrays repress osteoclast differentiation through multiple signalling pathways: in vitro and in vivo studies. Sci Rep. 2017;7(1):2328.
61. Cheng H, Xiong W, Fang Z, et al. Strontium (Sr) and silver (Ag) loaded nanotubular structures with combined osteoinductive and antimicrobial activities. Acta Biomater. 2016;31:388–400.
62. Zhang Y, Luo R, Tan J, et al. Osteoblast behaviors on titania nanotube and mesopore layers. Regenerative Biomater. 2017;4(2):81–87.
63. Shivaram A, Bose S, Bandyopadhyay A. Mechanical degradation of TiO2 nanotubes with and without nanoparticulate silver coating. J Mech Behav Biomed Mater. 2016;59:508–518.
64. Kyllonen L, D'Este M, Alini M, et al. Local drug delivery for enhancing fracture healing in osteoporotic bone. Acta Biomater. 2015;11:412–434.
65. Neacsu P, Mazare A, Cimpean A, et al. Reduced inflammatory activity of RAW 264.7 macrophages on titania nanotube modified Ti surface. Int J Biochem Cell Biol. 2014;55:187–195.
•• **Important evaluation showing reduced inflammatory activity on modified Titania nanotube surface.**
66. Ainslie KM, Tao SL, Popat KC, et al. In vitro inflammatory response of nanostructured titania, silicon oxide, and polycaprolactone. J Biomed Mater Res Part A. 2009;91A(3):647–655.
67. Smith BS, Capellato P, Kelley S, et al. Reduced in vitro immune response on titania nanotube arrays compared to titanium surface. Biomater Sci. 2013;1(3):322–332.
68. Aninwene GE, Yao C, Webster TJ. Enhanced osteoblast adhesion to drug-coated anodized nanotubular titanium surfaces. Int J Nanomedicine. 2008;3(2):257–264.
69. Mandal SS, Jose D, Bhattacharyya AJ. Role of surface chemistry in modulating drug release kinetics in titania nanotubes. Mater Chem Phys. 2014;147(1–2):247–253.
70. Shokuhfar T, Sinha-Ray S, Sukotjo C, et al. Intercalation of anti-inflammatory drug molecules within TiO_2 nanotubes. RSC Adv. 2013;3(38):17380–17386.
71. Gallo J, Holinka M, Moucha CS. Antibacterial surface treatment for orthopaedic implants. Int J Mol Sci. 2014;15(8):13849–13880.
72. Rogers SS, van der Walle C, Waigh TA. Microrheology of bacterial biofilms in vitro: staphylococcus aureus and Pseudomonas aeruginosa. Langmuir. 2008;24(23):13549–13555.
73. Puckett SD, Taylor E, Raimondo T, et al. The relationship between the nanostructure of titanium surfaces and bacterial attachment. Biomaterials. 2010;31(4):706–713.
74. Wei C-K, Ding S-J. Dual-functional bone implants with antibacterial ability and osteogenic activity. J Mater Chem B. 2017;5(10):1943–1953.
75. Narendrakumar K, Kulkarni M, Addison O, et al. Adherence of oral streptococci to nanostructured titanium surfaces. Dent Mater. 2015;31(12):1460–1468.
76. Popat KC, Eltgroth M, LaTempa TJ, et al. Decreased Staphylococcus epidermis adhesion and increased osteoblast functionality on antibiotic-loaded titania nanotubes. Biomaterials. 2007;28(32):4880–4888.
77. Zhang H, Sun Y, Tian A, et al. Improved antibacterial activity and biocompatibility on vancomycin-loaded TiO(2)nanotubes: in vivo and in vitro studies. Int J Nanomedicine. 2013;8:4379–4389.
78. Böttcher T, Kolodkin-Gal I, Kolter R, et al. Synthesis and activity of biomimetic biofilm disruptors. J Am Chem Soc. 2013;135(8):2927–2930.
79. Yang Y, Ao H-Y, Yang S-B, et al. In vivo evaluation of the anti-infection potential of gentamicin-loaded nanotubes on titania implants. Int J Nanomedicine. 2016;11:2223—2234.
•• **Important study showing combined impact of drugs and titania nanotubes to reducde infection of medical implants.**
80. Zhang M, Wei M, Wang D, et al. Preparation and characterization of a drug vehicle: polymer brush immobilized Ag nanoparticles onto titanium nanotubes. Mater Lett. 2014;135:51–54.
81. Li G, Zhao Q-M, Yang H-L, et al. Antibacterial and microstructure properties of titanium surfaces modified with Ag-incorporated nanotube arrays. Mater Res. 2016;19:735–740.
82. Liu R, Memarzadeh K, Chang B, et al. Antibacterial effect of copper-bearing titanium alloy (Ti-Cu) against Streptococcus mutans and Porphyromonas gingivalis. Sci Rep. 2016;6:29985.
83. Huo K, Zhang X, Wang H, et al. Osteogenic activity and antibacterial effects on titanium surfaces modified with Zn-incorporated nanotube arrays. Biomaterials. 2013;34(13):3467–3478.
84. Wang T, Liu X, Zhu Y, et al. Metal ion coordination polymer-capped pH-triggered drug release system on titania nanotubes for enhancing self-antibacterial capability of Ti implants. ACS Biomater Sci Eng. 2017;3(5):816–825.
85. Zizhou F, Xiangmei L, Lei T, et al. Electrophoretic deposited stable Chitosan@MoS2 coating with rapid in situ bacteria-killing ability under dual-light irradiation. Small. 2018;14(21):1704347.
86. Lim SS, Chai CY, Loh H-S. In vitro evaluation of osteoblast adhesion, proliferation and differentiation on chitosan-TiO2 nanotubes scaffolds with Ca2+ ions. Mater Sci Eng, C. 2017;76:144–152.
87. Kumeria T, Mon H, Aw MS, et al. Advanced biopolymer-coated drug-releasing titania nanotubes (TNTs) implants with simultaneously enhanced osteoblast adhesion and antibacterial properties. Colloids Surf B. 2015;130:255–263.
88. Zhang F, Zhang Z, Zhu X, et al. Silk-functionalized titanium surfaces for enhancing osteoblast functions and reducing bacterial adhesion. Biomaterials. 2008;29(36):4751–4759.
89. Mazare A, Totea G, Burnei C, et al. Corrosion, antibacterial activity and haemocompatibility of TiO_2 nanotubes as a function of their annealing temperature. Corrosion Sci. 2016;103:215–222.
90. Bhadra CM, Truong VK, Pham VT, et al. Antibacterial titanium nanopatterned arrays inspired by dragonfly wings. Sci Rep. 2015;5:16817.
• **This paper shows that TNTs could have a beneficial role in reducing inflammation after implant insertion which is one of major challenges to current implants**
91. Lorenzetti M, Dogša I, Stošicki T, et al. The influence of surface modification on bacterial adhesion to titanium-based substrates. ACS Appl Mater Interfaces. 2015;7(3):1644–1651.
92. Vo TN, Kasper FK, Mikos AG. Strategies for controlled delivery of growth factors and cells for bone regeneration. Adv Drug Deliv Rev. 2012;64(12):1292–1309.
93. Lai M, Cai K, Zhao L, et al. Surface functionalization of TiO2 nanotubes with bone morphogenetic protein 2 and its synergistic effect on the differentiation of mesenchymal stem cells. Biomacromolecules. 2011;12(4):1097–1105.
94. Cao X, Yu WQ, Qiu J, et al. RGD peptide immobilized on TiO_2 nanotubes for increased bone marrow stromal cells adhesion and

osteogenic gene expression. J Mater Science Mater Med. 2012;23(2):527–536.
95. Sun S, Yu W, Zhang Y, et al. Increased preosteoblast adhesion and osteogenic gene expression on TiO_2 nanotubes modified with KRSR. J Mater Science Mater Med. 2013;24(4):1079–1091.
96. Lee SJ, Oh TJ, Bae TS, et al. Effect of bisphosphonates on anodized and heat-treated titanium surfaces: an animal experimental study. J Periodontol. 2010;82(7):1035–1042.
97. Shen X, Ma P, Hu Y, et al. Alendronate-loaded hydroxyapatite-TiO_2 nanotubes for improved bone formation in osteoporotic rabbits. J Mater Chem B. 2016;4(8):1423–1436.
98. Lee J-K, Choi D-S, Jang I, et al. Improved osseointegration of dental titanium implants by TiO(2) nanotube arrays with recombinant human bone morphogenetic protein-2: a pilot in vivo study. Int J Nanomed. 2015;10:1145–1154.
99. Bariana M, Dwivedi P, Ranjitkar S, et al. Biological response of human suture mesenchymal cells to Titania nanotube-based implants for advanced craniosynostosis therapy. Colloids Surf B. 2017;150:59–67.
100. Chen X, Cai K, Fang J, et al. Fabrication of selenium-deposited and chitosan-coated titania nanotubes with anticancer and antibacterial properties. Colloids Surf B Biointerfaces. 2013;103:149–157.
101. Ozguclu E, Cetin A, Cetin M, et al. Additional effect of pulsed electromagnetic field therapy on knee osteoarthritis treatment: a randomized, placebo-controlled study. Clin Rheumatol. 2010;29(8):927–931.
102. Park J, Mazare A, Schneider H, et al. Electric field-induced osteogenic differentiation on TiO2 nanotubular layer. Tissue Eng Part C Methods. 2016;22(8):809–821.
103. Gulati K, Maher S, Chandrasekaran S, et al. Conversion of titania (TiO2) into conductive titanium (Ti) nanotube arrays for combined drug-delivery and electrical stimulation therapy. J Mater Chem B. 2016;4(3):371–375.
104. Wang T, Weng Z, Liu X, et al. Controlled release and biocompatibility of polymer/titania nanotube array system on titanium implants. Bioactive Mater. 2017;2(1):44–50.
•• **This paper include in-vivo study showing that loading antibiotics inside TNTs could significantly reduce bacterial infection which might result in implant's failure.**
105. Chen B, Lu K. Hierarchically branched titania nanotubes with tailored diameters and branch numbers. Langmuir. 2012;28(5):2937–2943.
106. Li S, Zhang G, Guo D, et al. Anodization fabrication of highly ordered TiO2 nanotubes. J Phys Chem C. 2009;113(29):12759–12765.
107. Aw MS, Kurian M, Losic D. Non-eroding drug-releasing implants with ordered nanoporous and nanotubular structures: concepts for controlling drug release. Biomater Sci. 2014;2(1):10–34.
108. Song YY, Schmidt-Stein F, Bauer S, et al. Amphiphilic TiO2 nanotube arrays: an actively controllable drug delivery system. J Am Chem Soc. 2009;131(12):4230–4232.
109. Gulati K, Ramakrishnan S, Aw MS, et al. Biocompatible polymer coating of titania nanotube arrays for improved drug elution and osteoblast adhesion. Acta Biomater. 2012;8(1):449–456.
110. Xu J, Zhou X, Gao Z, et al. Visible-light-triggered drug release from TiO2 nanotube arrays: a controllable antibacterial platform. Angew Chem Int Ed Engl. 2016;55(2):593–597.
111. Sirivisoot S, Pareta RA, Webster TJ. A conductive nanostructured polymer electrodeposited on titanium as a controllable, local drug delivery platform. J Biomed Mater Res Part A. 2011;99A(4):586–597.
112. Zhou J, Frank MA, Yang Y, et al. A novel local drug delivery system: superhydrophobic titanium oxide nanotube arrays serve as the drug reservoir and ultrasonication functions as the drug release trigger. Mater Sci Eng C. 2018;82:277–283.
113. Mohajernia S, Mazare A, Gongadze E, et al. Self-organized, free-standing TiO_2 nanotube membranes: effect of surface electrokinetic properties on flow-through membranes. Electrochim Acta. 2017;245:25–31.
114. Tsimbouri PM, Fisher L, Holloway N, et al. Osteogenic and bactericidal surfaces from hydrothermal titania nanowires on titanium substrates. Sci Rep. 2016;6:36857.
115. Brohede U, Forsgren J, Roos S, et al. Multifunctional implant coatings providing possibilities for fast antibiotics loading with subsequent slow release. J Mater Science Mater Med. 2009;20(9):1859–1867.
116. Piszczek P, Muchewicz Ż, Radtke A, et al. CVD of TiO_2 and TiO_2/Ag antimicrobial layers: deposition from the hexanuclear μ-oxo Ti(IV) complex as a precursor, and the characterization. Surface and Coatings Technology. 2013;222:38–43.
117. Zahran R, Rosales Leal JI, Rodríguez Valverde MA, et al. Effect of hydrofluoric acid etching time on titanium topography, chemistry, wettability, and cell adhesion. PLoS One. 2016;11(11):e0165296.
118. Zhang X, Wang H, Li J, et al. The fabrication of Ag-containing hierarchical micro/nano-structure on titanium and its antibacterial activity. Mater Lett. 2017;193:97–100.
119. Rajesh P, Mohan N, Yokogawa Y, et al. Pulsed laser deposition of hydroxyapatite on nanostructured titanium towards drug eluting implants. Mater Sci Eng C. 2013;33(5):2899–2904.
120. Hassanin H, Finet L, Cox SC, et al. Tailoring selective laser melting process for titanium drug-delivering implants with releasing microchannels. Additive Manufacturing. 2018;20:144–155.
121. Abdal-Hay A, Hamdy AS, Khalil KA, et al. A novel simple one-step air jet spinning approach for deposition of poly(vinyl acetate)/hydroxyapatite composite nanofibers on Ti implants. Mater Sci Eng C. 2015;49:681–690.
122. Smeets R, Stadlinger B, Schwarz F, et al. Impact of dental implant surface modifications on osseointegration. Biomed Res Int. 2016;2016:16.
123. Gallardo-Moreno AM, Pacha-Olivenza MA, Saldaña L, et al. In vitro biocompatibility and bacterial adhesion of physico-chemically modified Ti6Al4V surface by means of UV irradiation. Acta Biomater. 2009;5(1):181–192.
124. Barbour ME, O'Sullivan DJ, Jenkinson HF, et al. The effects of polishing methods on surface morphology, roughness and bacterial colonisation of titanium abutments. J Mater Sci Mater Med. 2007;18(7):1439–1447.
125. Al-Radha ASD, Dymock D, Younes C, et al. Surface properties of titanium and zirconia dental implant materials and their effect on bacterial adhesion. J Dent. 2012;40(2):146–153.
126. Bonfante EA, Granato R, Marin C, et al. Biomechanical testing of microblasted, acid-etched/microblasted, anodized, and discrete crystalline deposition surfaces: an experimental study in beagle dogs. Int J Oral Maxillofac Implants. 2013;28:1.
127. Radin S, Ducheyne P. Controlled release of vancomycin from thin sol–gel films on titanium alloy fracture plate material. Biomaterials. 2007;28(9):1721–1729.
128. Liu Z, Zhu Y, Liu X, et al. Construction of poly (vinyl alcohol)/poly (lactide-glycolide acid)/vancomycin nanoparticles on titanium for enhancing the surface self-antibacterial activity and cytocompatibility. Colloids Surf B Biointerfaces. 2017;151:165–177.
129. Roy M, Fielding GA, Beyenal H, et al. Mechanical, in vitro antimicrobial, and biological properties of plasma-sprayed silver-doped hydroxyapatite coating. ACS Appl Mater Interfaces. 2012;4(3):1341–1349.
130. Szcześ A, Hołysz L, Chibowski E. Synthesis of hydroxyapatite for biomedical applications. Adv Colloid Interface Sci. 2017;249:321–330.
131. Le Guehennec L, Soueidan A, Layrolle P, et al. Surface treatments of titanium dental implants for rapid osseointegration. Dent Mater. 2007;23(7):844–854.
132. Jain P, Mandal T, Prakash P, et al. Electrophoretic deposition of nanocrystalline hydroxyapatite on Ti6Al4V/TiO 2 substrate. J Coatings Technol Res. 2013;10(2):263–275.
133. Patel KD, Singh RK, Lee E-J, et al. Tailoring solubility and drug release from electrophoretic deposited chitosan–gelatin films on titanium. Surf Coatings Technol. 2014;242:232–236.
134. Liu X, Tian A, You J, et al. Antibacterial abilities and biocompatibilities of Ti–ag alloys with nanotubular coatings. Int J Nanomed. 2016;11:5743.
135. Martínez Campos E, Santos-Coquillat A, Mingo B, et al. Albumin loaded PEO coatings on Ti — potential as drug eluting systems. Surf Coatings Technol. 2015;283:44–51.
136. Marin E, Diamanti MV, Boffelli M, et al. Effect of etching on the composition and structure of anodic spark deposition films on titanium. Mater Des. 2016;108:77–85.

137. Geissler S, Tiainen H, Haugen HJ. Effect of cathodic polarization on coating doxycycline on titanium surfaces. Mater Sci Eng C Mater Biol Appl. 2016;63:359–366.
138. Bariana M, Aw MS, Moore E, et al. Radiofrequency-triggered release for on-demand delivery of therapeutics from titania nanotube drug-eluting implants. Nanomedicine. 2013;9(8):1263–1275.
139. Xiang Y, Liu X, Mao C, et al. Infection-prevention on Ti implants by controlled drug release from folic acid/ZnO quantum dots sealed titania nanotubes. Mater Sci Eng C. 2018;85:214–224.
140. Jia H, Kerr LL. Kinetics of drug release from drug carrier of polymer/TiO2 nanotubes composite—pH dependent study. J Appl Polym Sci. 2015;132:7.
141. Moon K-S, Bae J-M, Jin S, et al. Infrared-mediated drug elution activity of gold nanorod-grafted TiO2 nanotubes. J Nanomater. 2014;2014:8.
142. Aw MS, Addai-Mensah J, Losic D. Magnetic-responsive delivery of drug-carriers using titania nanotube arrays. J Mater Chem. 2012;22(14):6561–6563.
143. Song YY, Roy P, Paramasivam I, et al. Voltage-induced payload release and wettability control on TiO2 and TiO2 nanotubes. Angew Chem Int Ed Engl. 2010;49(2):351–354.
144. Gulati K, Kant K, Findlay D, et al. Periodically tailored titania nanotubes for enhanced drug loading and releasing performances. J Mater Chem B. 2015;3(12):2553–2559.
145. Vasilev K, Poh Z, Kant K, et al. Tailoring the surface functionalities of titania nanotube arrays. Biomaterials. 2010;31(3):532–540.
146. Aw MS, Addai-Mensah J, Losic D. A multi-drug delivery system with sequential release using titania nanotube arrays. Chem Commun (Camb). 2012;48(27):3348–3350.

CHAPTER 3

TITANIA NANOTUBES FOR LOCALIZED DRUG DELIVERY OF ANTICANCER AGENTS

3.1. Overview

Systemic administration of anticancer agents is usually limited by a wide range of adverse effects due to lack of selectivity and uncontrolled distribution. In case of bone tissues, only limited amount of the systemically administered drugs can reach the desired site of action.

The aim of this chapter is to explore the potential application of titania nanotubes (TNTs) fabricated on the surface of 3D-printed Ti implants for localized drug delivery (LDD) as an effective alternative to systemic drug administration of anticancer agents which could avoid many limitations of systemic drug therapy such as systemic toxicity and uncontrolled drug distribution.

First, the detailed process of TNTs fabrication using electrochemical anodization process, which is scalable and cost effective, is included. This was followed by physicochemical characterization of the fabricated implants using a variety of techniques (e.g., SEM, EDX, XRD and water contact angle). Two anticancer drugs were used; doxorubicin and Apo2L/TRAIL. *In-vitro* data showed that TNTs were effectively loaded with anticancer agents and were capable of releasing sufficient medication to eradicate cancer cells. At the same time, Apo2L/TRAIL showed specific activity against cancer cells while sparing normal cells.

This chapter confirms that TNTs fabricated on 3D-printed implants could provide dual functionality; one is bone support and the second is to provide localized drug delivery to treat bone cancer while protecting normal bone cells.

This chapter has been published as:

- **Shaheer Maher**, Gagandeep Kaur, Luis Lima-Marques, Andreas Evdokiou and Dusan Losic (2017), Engineering of micro- to nanostructured 3d-printed drug-releasing titanium implants for enhanced osseointegration and localized delivery of anticancer drugs. ACS Applied Materials & Interfaces 9(35): 29562-29570.

Statement of Authorship

Title of Paper	Engineering of Micro- to Nanostructured 3D-Printed Drug-Releasing Titanium Implants for Enhanced Osseointegration and Localized Delivery of Anticancer Drugs
Publication Status	☑ Published ☐ Accepted for Publication ☐ Submitted for Publication ☐ Unpublished and Unsubmitted w ork w ritten in manuscript style
Publication Details	S. Maher, G. Kaur, L. Lima-Marques, A. Evdokiou, D. Losic, Engineering of Micro- to Nanostructured 3D-Printed Drug-Releasing Titanium Implants for Enhanced Osseointegration and Localized Delivery of Anticancer Drugs, ACS Applied Materials & Interfaces 9(35) (2017) 29562-29570

Principal Author

Name of Principal Author (Candidate)	Shaheer Maher (*also known* as Shaheer Makar)
Contribution to the Paper	Study design, samples preparation, performed characterization on all samples, performed cell study, interpreted data and wrote manuscript
Overall percentage (%)	85%
Certification:	This paper reports on original research I conducted during the period of my Higher Degree by Research candidature and is not subject to any obligations or contractual agreements with a third party that would constrain its inclusion in this thesis. I am the primary author of this paper.
Signature	Date 20/08/2021

Co-Author Contributions

By signing the Statement of Authorship, each author certifies that:

i. the candidate's stated contribution to the publication is accurate (as detailed above);

ii. permission is granted for the candidate in include the publication in the thesis; and

iii. the sum of all co-author contributions is equal to 100% less the candidate's stated contribution.

Name of Co-Author	Luis Lima-Marques
Contribution to the Paper	Supervised 3D-printing process
Signature	Date 20/08/2021

Name of Co-Author	G. Kaur
Contribution to the Paper	participated in cell culture study The co-author can not be reached, signed by corresponding author on their behalf
Signature	Date 20/08/2021

Please cut and paste additional co-author panels here as required.

Statement of Authorship

Title of Paper	Engineering of Micro- to Nanostructured 3D-Printed Drug-Releasing Titanium Implants for Enhanced Osseointegration and Localized Delivery of Anticancer Drugs
Publication Status	☑ Published ☐ Accepted for Publication ☐ Submitted for Publication ☐ Unpublished and Unsubmitted w ork w ritten in manuscript style
Publication Details	S. Maher, G. Kaur, L. Lima-Marques, A. Evdokiou, D. Losic, Engineering of Micro- to Nanostructured 3D-Printed Drug-Releasing Titanium Implants for Enhanced Osseointegration and Localized Delivery of Anticancer Drugs, ACS Applied Materials & Interfaces 9(35) (2017) 29562-29570

Principal Author

Name of Principal Author (Candidate)	Shaheer Maher (*also known* as Shaheer Makar)
Contribution to the Paper	Study design, samples preparation, performed characterization on all samples, performed cell study, interpreted data and wrote manuscript
Overall percentage (%)	85%
Certification:	This paper reports on original research I conducted during the period of my Higher Degree by Research candidature and is not subject to any obligations or contractual agreements with a third party that would constrain its inclusion in this thesis. I am the primary author of this paper.
Signature	Date 19/08/2021

Co-Author Contributions

By signing the Statement of Authorship, each author certifies that:

i. the candidate's stated contribution to the publication is accurate (as detailed above);

ii. permission is granted for the candidate in include the publication in the thesis; and

iii. the sum of all co-author contributions is equal to 100% less the candidate's stated contribution.

Name of Co-Author	Andreas Evdokiou
Contribution to the Paper	Supervised cell study work and revised the manuscript The co-author can not be reacher, signed by corresponding author on their behalf
Signature	Date 19/08/2021

Name of Co-Author	Dusan Losic
Contribution to the Paper	Supervised the development of work, revised and edited the manuscript and acted as the corresponding author
Signature	Date 19/08/2021

Please cut and paste additional co-author panels here as required.

ACS APPLIED MATERIALS & INTERFACES

Research Article

www.acsami.org

Engineering of Micro- to Nanostructured 3D-Printed Drug-Releasing Titanium Implants for Enhanced Osseointegration and Localized Delivery of Anticancer Drugs

Shaheer Maher,[†,‡] Gagandeep Kaur,[†] Luis Lima-Marques,[§] Andreas Evdokiou,[∥] and Dusan Losic*[,†]

[†]School of Chemical Engineering, [§]Institute for Photonics and Advanced Sensing (IPAS), and [∥]Discipline of Surgery, Basil Hetzel Institute, The University of Adelaide, 5005 Adelaide, Australia

[‡]Faculty of Pharmacy, Assiut University, 71526 Assiut, Egypt

Supporting Information

ABSTRACT: Primary and secondary bone cancers are major causes of pathological bone fractures which are usually treated through implant fixation and chemotherapy. However, both approaches face many limitations. On one hand, implants may suffer from poor osseointegration, and their rejection results in repeated surgery, patient's suffering, and extensive expenses. On the other hand, there are severe systemic adverse effects of toxic chemotherapeutics which are administrated systemically. In this paper, in order to address these two problems, we present a new type of localized drug-releasing titanium implants with enhanced implants' biointegration and drug release capabilities that could provide a high concentration of anticancer drugs locally to treat bone cancers. The implants are fabricated by 3D printing of Ti alloy followed by an anodization process featuring unique micro- (particles) and nanosurface (tubular arrays) topography. We successfully demonstrate their enhanced bone osseointegration and drug loading capabilities using two types of anticancer drugs, doxorubicin (DOX) and apoptosis-inducing ligand (Apo2L/TRAIL). In vitro study showed strong anticancer efficacy against cancer cells (MDA-MB-231-TXSA), confirming that these drug-releasing implants can be used for localized chemotherapy for treatment of primary and secondary bone cancers together with fracture support.

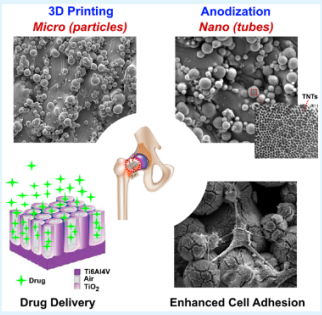

KEYWORDS: *3D printing, bone implants, titania nanotubes, anodization, bone cancer*

1. INTRODUCTION

Fracture is one of the most common complications of bone cancer. Bone cancer can either start in the bone (i.e., primary) or spread to the bone (i.e., secondary) due to metastasis of cancer cells present at other body sites. Patients suffering from either primary bone cancer, also known as osteosarcoma, or secondary bone cancer usually show a high risk of fracture especially in the first year after diagnosis.[1,2] This is attributed to the disruption of the natural bone activity and architecture due to the growth of cancer cells which in turn weakens the bones, making them vulnerable to fracture even without any accidents or trauma (i.e., pathological fracture).[3] Treatment of bone cancers usually includes two simultaneous approaches: bone fixation and administration of chemotherapeutic agents but with limited success. The fractured bones are fixed by bone implants together with removal of the cancerous part. In some cases the removed bone part is also replaced with a prosthesis.[4,2]

Moreover, primary and secondary cancer treatment also comprises systemic administration of chemotherapeutic agents.[5] This therapy usually requires high doses of anticancer drugs in order to reach their effective levels at the bone site which in turn leads to exposure of the whole body to elevated toxic doses. Besides that the fractured areas may also suffer from compromised blood supply, which may hamper therapeutics from reaching the diseased areas at effective concentrations required for therapy.[6] These limitations in systemic administration usually result in therapeutic failure and spreading bone diseases to a fatal level.[7]

One alternative solution to address the systemic toxicity of chemotherapeutics is localized delivery of active therapeutics directly inside the bone using drug-releasing bone implants,[8,6] thus avoiding systemic therapy needs.[9] The key feature of these drug-releasing implants is to release active therapeutics directly at the affected site, locally inside the bone microenvironment at the bone implant interface.[9−11] Furthermore, this localized drug delivery has the potential to provide effective treatment for multiple conditions like bone carcinoma, osteoporosis, bone infection (i.e., osteomyelitis), and related inflammation.[6,12] There is only one clinically proven system, specifically developed for treatment of brain tumor (glioblastoma), which is based on a biodegradable polymer implant impregnated with the anticancer drug carmustine (Gliadel, Guildford Pharmaceutics, UK).[13] This anticancer drug-releasing implant is

Received: July 8, 2017
Accepted: August 18, 2017
Published: August 18, 2017

DOI: 10.1021/acsami.7b09916
ACS Appl. Mater. Interfaces 2017, 9, 29562−29570

specifically designed to treat brain cancer where surgical and chemotherapeutic treatments are limited, and it is surprising that the same concept is not translated or explored for similar reasons for treatment of bone cancers.

Metal-based implants such as screws, K-wires (pins), and plates have been used in a variety of orthopedic applications over a very long time.[14,15] Titanium (Ti) is the most commonly used material for implant fabrication since it possesses good biointegration with human osteoblasts while being corrosion resistant.[14−16] However, these implants confront many challenges for integration and longevity upon insertion in the human body, especially in case of bone carcinoma.[14,8,6] Failure of orthopedic implants can occur for several reasons, including poor "osseointegration" (i.e., firm attachment of the implant following bone tissue regeneration onto implant's surface),[17,12] inflammation, or bacterial infection,[18,6,12] leading to loosening and/or complete detachment from its place which could eventually lead to repeated surgery, amputation, and even death.[19]

Several approaches have been explored to improve the process of osseointegration.[20−22] One promising approach involves the manipulation of an implant's surface topography (i.e., roughness). Studies asserted that the surface topography of the implants significantly influences the process of osseointegration.[23−26] It is worth mentioning that the optimal template for implant surface design is to combine both micro- and nanorough surface features.[27−29] Previous studies demonstrated the ability of the microtexture to promote "osteoconduction"[12] (i.e., bone cell growth onto the implant's surface) and "osteoinduction"[12] (i.e., encouraging a cell to differentiate into osteoblasts on the implant's surface).[23]

The advent of nanotechnology offers many new technologies to fabricate these implants with desired topography including a variety of nanometer surface architectures such as nanotubes, nanopores, and nanoparticles. Previous studies suggest that many of these nanorough surface patterns, particularly nanotubular structures, enhance protein adsorption and osteoblast activity that lead to improved osteoblast adhesion and long-term osseointegration, in comparison with smooth or microrough surfaces.[30,27] Titania nanotubes (TNTs) prepared by electrochemical anodization of titanium with vertically aligned nanotubular structures composed of titanium dioxide (TiO_2) represent a remarkable example of these nanostructures used for a wide range applications.[31] Similar to arrays of tiny test tubes, TNTs are open at the top and closed at the bottom and can be prepared with control over dimensions (diameters 10−300 nm and lengths 0.5−300 μm).[15] It is worth mentioning that electrochemical anodization is a scalable, cost-effective, and simple fabrication process that can be implemented for modifications of commercially fabricated bone implants at the industrial scale.[31]

Currently used bone implants in orthopeadic surgery comprise pure Ti and more often Ti alloys with Al, V, Zr, etc., since these alloys are less expensive and able to provide superior biocompatibility and mechanical characteristics in comparison to pure Ti.[32,33] The production of Ti implants is based on conventional metal and metallurgical processing techniques with limitations such as production with fixed shapes and dimensions, and therefore, they lack customization for specific cases such as children or due cancer, where local drug delivery of anticancer is required. In such cases, expensive and time-consuming implant alterations are made by postprocessing which are not acceptable where urgent interventions are required. Furthermore, the implant manufacturing companies lose millions of dollars each year through expiry of produced implants.

Recent advancements in three-dimensional printing (3D printing) technology have opened new horizons for fabrication of various implants using different materials such as polymers and metals.[34−37] Accordingly, the application of 3D printing to fabricate implants will result in revolutionary improvements, among which is the flexibility in implant design to obtain different shapes of implants with tuned dimensions such as flat substrates, screws, wires, or even a complete joint.[35,38] More importantly, 3D printing will allow "on demand" implants which are designed especially for each patient that can be fabricated very quickly in a clinical environment. At the same time, implant manufacturing companies using this technology will be able to deliver implants on request instead of massive production and storage of implants.

The aim of this work is to demonstrate engineering of new 3D-printed drug-releasing Ti implants (3D-Ti) with dual micro- and nanotopography designed to possess enhanced osseointegration and drug delivery functions. The implants are fabricated by combining 3D printing of the Ti and electrochemical anodization process, and their structures are presented in Scheme 1. The 3D printing using the selective metal laser sintering (SMLS) method was performed to fabricate Ti alloy implants (Ti6Al4V) with a specific microscale rough surface composed of randomly dispersed spherical microparticles. These 3D-printed implants were electrochemically anodized to generate an anodic layer with nanotopography on top of the implant surface composed of vertically aligned nanotubes (TNTs). Their bone integration performance was evaluated by studying the attachment of fibroblasts under physiological conditions. The drug loading and release capabilities of the fabricated 3D-Ti implants was also investigated using two chemotherapeutic agents, doxorubicin (DOX) and apoptosis-inducing ligand (Apo2L/TRAIL), followed by evaluating their in vitro anticancer efficacy against cancer cells.

Scheme 1. Illustration of Micro- and Nanostructures in TNTs-3D-Ti Drug-Releasing Implants Loaded with Anticancer Drug[a]

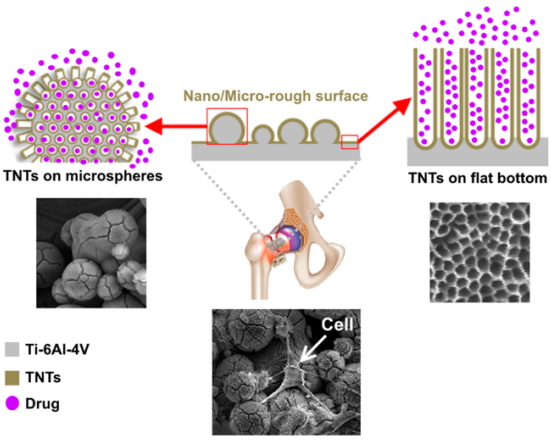

[a]SEM images show these micro- (particles) and nanostructures (titania nanotubes) and their interaction with cells.

DOI: 10.1021/acsami.7b09916
ACS Appl. Mater. Interfaces 2017, 9, 29562−29570

2. EXPERIMENTAL SECTION

2.1. Materials. Ammonium fluoride (NH_4F), ethylene glycol (EG), lactic acid (LA), and NIH 3T3 fibroblasts were purchased from Sigma-Aldrich (Australia). MDA-MB-231-TXSA Luciferase-expressing cells were kindly provided by Dr. Toshiyuki Yoneda (formerly at the University of Texas Health Sciences Centre, San Antonio, TX). Doxorubicin hydrochloride (DOX) solution (2 mg mL^{-1}) was purchased from Hospira Pty Ltd. (Australia). Tumor necrosis factor-related apoptosis-inducing ligand (Apo2L/TRAIL) was obtained from Genentech Inc. (USA). Dulbecco's modified Eagle's medium, fetal calf serum (FCS), penicillin/streptomycin, sodium pyruvate, trypsin, and phosphate buffer solution (PBS) were supplied from Life Technologies Pty Ltd. (Australia). D-Luciferin Firefly and potassium salt were obtained from Caliper Life Sciences, PerkinElmer (Australia). The standard bicinchoninic acid (BCA) protein assay kit was obtained from Pierce Chemical Co. (Australia). All chemicals and reagents were used as received without further purification steps. High-purity water Option Q-Purelabs (Australia) (18.2 MΩ) was used to prepare all solutions used throughout this study.

2.2. Fabrication of Ti Implants Using 3D Printing. Titanium wafers in the form of square strips (1.5 × 1.5 cm^2) were printed with a 3D-selective laser melting machine (ProX 200 Production 3D Printer, Phenix Systems PXM (USA) equipped with 300 W laser (1070 nm at 50% power)) under inert argon atmosphere. The alloy powder material (Ti6Al4V) used in the fabrication process is characterized by the average particles diameter as follows: $D_{[90\%]}$ = 31.32 μm, $D_{[50\%]}$ = 24.07 μm, and $D_{[10\%]}$ = 10.69 μm, where $D_{[90\%]}$ indicates 90% of the volume distribution below that value, $D_{[50\%]}$ indicates the volume 50% value of the distribution, while $D_{[10\%]}$ indicates 10% of the volume distribution below the value.

Wafers with a thickness of about 0.61 ± 0.01 mm were prepared by forming a layer of powder material (~30 μm thick), which was then selectively melted using a laser. This process was repeated to produce a successive number of melted layers in order to reach the desired thickness. The Ti wafers were removed from the build plate and then thoroughly cleaned by wiping and ultrasonication in acetone to remove any nonadhered powdered particles from the surface. The resulting implants will be referred to as "3D-Ti" throughout this paper.

2.3. Electrochemical Anodization of 3D-Ti Implants To Generate Surface TNTs. Prior to fabrication of TNTs using electrochemical anodization, 3D-Ti wafers were cleaned by sonication in acetone for 10 min and dried using a N_2 gun. After that TNTs were prepared using a temperature-controlled electrochemical cell designed in our laboratory in which the 3D-Ti wafer acts as the anode while a Ti foil acts as a counter electrode (i.e., cathode). The electrodes were immersed in ethylene glycol electrolyte solution containing lactic acid (1.5 M), water (5% v/v), and NH_4F (0.1M) at 60 °C for 15 min. The whole setup was connected to a programmable power supply (Agilent, USA) for voltage control through LabVIEW software (National Instruments, USA). After that 3D-Ti wafers with TNTs grown on top (will be referred as TNTs-3D-Ti wafers) were cleaned by sonication in Milli-Q water for 5 min to remove any remaining electrolyte.

2.4. Structural and Chemical Characterization of Prepared Implants. Surface characterization was performed using scanning electron microscopy (SEM, FEI Quanta 450 FEG-SEM, USA) and energy-dispersive X-ray spectroscopy (EDX). Samples were coated with platinum (5 nm) prior to imaging with SEM. X-ray diffraction spectra (XRD, Rigaku MiniFlex 600, Japan) and water contact angle (WCA. Attension theta optical tensiometer, KSV instruments, Finland) of the samples were also recorded.

2.5. Drug Loading. Two anticancer drugs, DOX and Apo2L/TRAIL, were separately loaded onto TNTs-3D-Ti implants under vacuum. Briefly, 10 μL of either drugs loading solution (2 mg mL^{-1}) was placed on the surface of TNTs-3D-Ti implants and allowed to dry under vacuum for 2 h at room temperature. After that the previous step was repeated 20 times. The surface was then cleaned by rinsing with Milli-Q water to remove any drug remaining on the surface so that only drug trapped inside the nanotubes hollow structure remains. In the case of implants that will be used for cell studies, they were first sterilized under UV light for 20 min; then drug loading was carried out under aseptic condition. The amount of drug loading was then detected using thermogravimetric analysis (TGA, TA Instruments Q500, USA). Samples were cut into small pieces, mounted onto a platinum pan, and heated to 550 °C at a scanning rate of 5 °C/min under constant nitrogen gas flow of 50 mL min^{-1}. 3D-Ti wafers with no TNTs on the surface and drug-free TNTs-3D-Ti implants were used as controls.

2.6. In Vitro Drug Release. The in vitro drug release was assessed by immersing drug-loaded TNTs-3D-Ti wafers in 600 μL of PBS (pH 7.4) at 37 °C. At predetermined time, 100 μL of release media was removed and replaced with fresh PBS to maintain sink conditions.[39]

The amounts of DOX released were determined by photoluminescence spectroscopy (Fluoromax-4 Horiba Jobin Yvon, Japan, equipped with a Xe lamp used as the excitation light source at room temperature), exciting the samples at 490 nm, and measuring the emission intensity at 590 nm. The concentration of drug was then calculated using a standard calibration curve constructed by measuring the fluorescence intensity of known concentrations of DOX.

Apo2L/TRAIL release was detected by standard bicinchoninic acid (BCA) assay for protein quantification.[40] Briefly, 25 μL of release samples was placed into microplate wells of a 96-wellplate. Then 200 μL of BCA working reagent was added and then placed on a plate shaker for 30 min. After that the plate was incubated at 37 °C for 30 min. The absorbance was then measured at 562 nm with a plate reader (Fluostar OPTIMA, BMG Labtech). A standard calibration curve of known concentrations of Apo2L/TRAIL was also constructed following the same steps.

Blank samples were prepared by placing TNTs-3D-Ti wafers (i.e., containing no drug) in PBS under the same conditions. All of the aforementioned experiments were repeated three times using freshly prepared samples, and averages and SD were estimated.

2.7. Cell Culture. MDA-MB-231-TXSA breast cancer cells and NIH 3T3 fibroblasts were used for cell studies of TNTs-3D-Ti implants. All cells were cultured in 75 cm^2 culture flasks (Corning Inc. Life Sciences) using Dulbecco's modified Eagle's culture medium (DMEM) supplemented with 10% fetal bovine serum, 1% glutamine (2 mM), 1% penicillin (100 IU mL^{-1}), 1% streptomycin (100 μg mL^{-1}), and 1% sodium pyruvate. The cells were maintained at 37 °C in a 5% CO_2 and 95% relative humidity. Cells were passaged every 3−4 days in order to keep them in their log phase of growth. TNTs-3D-Ti implants were sterilized under UV light for 20 min. All experiments were performed in triplicate.

2.7.1. Fibroblasts Attachment on Implants. To get insight about cell attachment on the TNTs-3D-Ti surface, sterile wafers were placed in a 12-well plate, and 5 × 10^4 NIH3T3 fibroblasts cells, suspended in 30 μL of growth media, were seeded on drug-free implant surface and allowed to attach overnight. After that cells were fixed in 4% v/v paraformaldehyde and 1.25% v/v glutaraldehyde. The cells were then washed with PBS and sequentially dehydrated in ethanol (70%, 90%, and 100% for 15 min each). Subsequently, samples were immersed in hexamethyl disilazane (HMDS):100% ethanol (1:1) solution for 10 min and then in 100% HMDS twice for 10 min. The samples were then dried and coated for SEM imaging.[41]

2.7.2. Screening the Anticancer Activity. Since we loaded two different anticancer drugs (i.e., DOX and Apo2L/TRAIL) separately on TNTs-3D-Ti implants, the cytotoxicity of the drug-loaded implants was assessed as follows:

(a) For DOX-loaded implants: MDA-MB-231-TXSA breast cancer cells (1 × 10^6) were seeded in a 12-well plate and incubated overnight. After that DOX-loaded TNTs-3D-Ti implants were added for 24 h, and then cell viability was assessed using luciferase bioluminescent cell viability assay as described in the Supporting Information.

(b) For Apo2L/TRAIL-loaded implants: After Apo2L/TRAIL loading, NIH3T3 fibroblasts (5 × 10^4 cells suspended in 30 μL of growth media) were seeded on implant surface and incubated for 24 h to allow cell adhesion. After that the wafers were transferred into the wells with a monolayer of MDA-MB-231-TXSA cells in a 12-well plate, and then cell viability was

DOI: 10.1021/acsami.7b09916
ACS Appl. Mater. Interfaces 2017, 9, 29562−29570

assessed after 24 h using luciferase bioluminescent assay as described in the Supporting Information. The same wafers were then transferred into fresh wells with MDA-MB-231-TXSA cells growing as monolayers. These steps were repeated 3 times over 72 h (i.e., repeated each 24 h) after which no cell death was observed. Finally, Ti wafers were taken out and transferred to a container containing cell fixative for SEM analysis. The aim of this experiment is to investigate whether the presence of normal cells (i.e., fibroblasts) on top of TNTs surface would allow sufficient drug release or they might block the tubes and thus no drug would be released.

For all experiments, cell cultures in growth media incubated with drug-free TNTs-3D-Ti wafers were used as negative control (i.e., 100% cell viability) and cells treated with 10 μL of DOX solution (50 μg mL^{-1}) were used as positive control.

2.8. Statistical Analysis. All results presented in this study are statistically treated and expressed as mean ± standard deviation (SD) of at least three independent experiments. ANOVA followed by a Bonferroni's multiple comparison test was used to analyze the data. The level for significance was set to $p < 0.05$ for all comparisons.

3. RESULTS AND DISCUSSION

3.1. Structural Characterization of 3D-Ti and TNTs-3D-Ti Implants. The surface of prepared Ti alloys implants with a unique morphology in which microspherical particles were randomly dispersed due to the presence of partially melted particles onto the Ti surface is shown in SEM images (Figure 1a and 1b). The size of these microparticles is in the range from

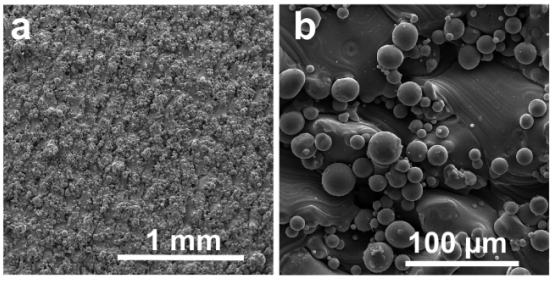

Figure 1. SEM morphology of 3D-Ti implants at different magnifications at (a) low and (b) high resolution.

5 to 20 μm (average ≈ 12 μm) in diameter. The microparticles appeared to be firmly attached to the underlying Ti surface which is confirmed by high-resolution SEM imaging. The interconnected structure of successively melted layers is shown in SEM images taken from the cross section of the fractured implants (Figure S1). During the 3D printing process the laser melts Ti alloy powder (particles) added layer by layer to create this homogeneous composite structure inside templates and microparticles on the top surface.

Electrochemical anodization was used to generate TNTs on the surface of 3D-Ti wafers involving the etching effect of fluoride ions under the effect of the applied electrical field as explained in the Supporting Information. In our previous study, we assessed the effect of different fabrication parameters (e.g., temperature, voltage, water content, and anodization time) against the properties and dimensions of the generated TNTs.[42] We showed that optimal TNTs fabrication could be obtained by anodization in ethylene glycol electrolyte containing 5% v/v water, NH_4F (0.1 M), and LA (1.5 M) under an applied potential of 60 V for 15 min at 60 °C that allows the generation of well-organized TNTs with reproducible dimensions. Figure 2 represents a series SEM images of fabricated 3D-Ti implants showing well-ordered nanotube arrays covering the whole surface. First, these images confirm that microparticles survived the anodization process and that the entire surface including microparticles and the underlying Ti surface were composed of TNTs structures (Figures 2b–e, 2g, and 2h). The length and diameter of TNTs were 3.25 ± 0.2 μm and 120 ± 10 nm, respectively. SEM images showed that the diameter of nanotubes on a flat surface is slightly large compared with TNTs formed on the particle (Figure 2e and 2f). The dimensions of the TNTs can be further tailored using various anodization parameters, if required. SEM cross-sectional images of the fractured TNTs layer confirmed the closed bottom of the nanotube structure (Figure 2f). Characteristic cracks are seen on the surface of the Ti microparticles as well as the underlying Ti surface (Figure 2c and 2d) and are a result of radial outgrowth of nanotubes on the curved surfaces that is in agreement with our previous work on formation of TNTs on curved surfaces using Ti wires.[42] These results showed that the 3D-printed Ti alloy surface consisted of two distinct features: a random array of microparticles and a flat surface, both composed with a nanotube titania layer that can be used for drug loading and providing a unique topography for enhanced cell attachment and bone integration

3.2. Chemical and Physical Characterization of Implants. Water contact angle (WCA) measurements were performed to find the effect of anodization on the interfacial properties and are presented in Figure 3a and 3b. The surface of 3D-Ti wafers showed hydrophobic properties with a WCA value of 133 ± 1°. On the contrary, after TNTs layer formation (i.e., TiO_2), the surface became superhydrophilic in which the WCA could not be measured (i.e., water droplets spread rapidly over the surface). It is noteworthy to mention that hydrophilic bone implant surfaces ensure early onset of osseointegration (i.e., quicker bone healing rates) and also reduces the number of live and dead bacteria attached to the surface.[43,44] In addition, the hydrophilic surface properties of TNTs-3D-Ti implants will allow immediate spreading of the drug solution over the surface during loading which could improve the amount of drug loading (vide infra).

EDX analysis was performed before and after electrochemical anodization. Since we are using Ti6Al4V alloy, the EDX spectrum of the 3D-Ti wafer (i.e., before anodization) showed significant peaks for Ti, Al, and V (Figure 3c). A minor peak corresponding to oxygen could also be observed which could be attributed to native oxide layer (i.e., 5–10 nm in thickness) that is spontaneously formed on metals surface. Figure 3d shows the EDX spectrum of TNTs-3D-Ti implants (i.e., after anodization) in which a prominent oxygen peak appeared confirming the formation of an oxide layer. In addition, fluoride and carbon peaks also appeared from anodization electrolyte and Pt from coating for SEM. It is noteworthy to mention that some studies suggest that the presence of F^{-1} ions, incorporated into the nanotube structures, may enhance implant integration with the healing bone.[45] These results were also confirmed by XRD analysis in which 3D-Ti showed distinct peaks of Ti while anatase TiO_2 peak appeared after anodization (Figure 3e and 3f).

3.3. Drug Loading and in Vitro Release. Two anticancer drugs, DOX and Apo2L/TRAIL, were loaded by applying a drop of loading solution onto the TNTs-3D-Ti surface followed by using vacuum forces to remove potential air gaps

DOI: 10.1021/acsami.7b09916
ACS Appl. Mater. Interfaces 2017, 9, 29562–29570

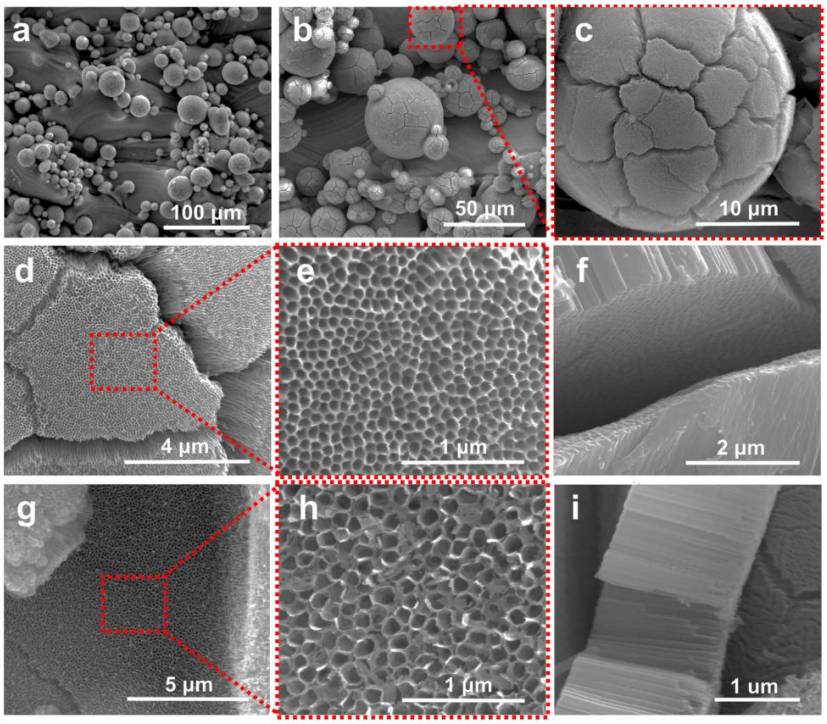

Figure 2. SEM images of TNTs fabricated by electrochemical anodization of 3D-Ti implants in ethylene glycol electrolyte containing water (5% v/v) at a voltage of 60 V for 15 min at 60 °C showing (a) low- and (b and c) high-resolution images with (d and e) TNTs structures on microparticle surface and (g and h) on flat surface; (f) cross-section view of closed TNTs ends, and (i) cross section image of fractured TNTs layer showing highly ordered and packed TNTs.

inside the hollow nanotubes structure that could prevent loading. TGA analysis was performed to determine the amount of drug loaded which was found to be 188 ± 8 and 2176 ± 25 $\mu g\ cm^{-2}$ for DOX and Apo2L/TRAIL, respectively, Figure S4, Supporting Information. The large difference in loading amount for these two drugs is explained by their different molecular size and weight where MWt. of DOX and Apo2L/TRAIL are 543.52 g $mol^{-1}$and 19.8 kDa (19 800 g mol^{-1}), respectively.

Figure 4 shows the in vitro release graphs of the drugs loaded onto TNTs-3D-Ti implants. The drug release exhibited characteristic two-phase behavior showing a burst release within the first few hours (% cumulative release of DOX and Apo2L/TRAIL after 6 h was 40% and 70%, respectively) and slow release phase of 16 days (DOX) to 4 days (Apo2L/TRAIL). Burst release is due to the release of the drug present at or near the surface of TNTs. The burst release is expected to be beneficial since the drug will be released to eradicate cancer cells for the first few days of the implant life. After complete release of the cytotoxic drug, together with cancer cells death, the healthy bone cells will be able to grow normally without interference from chemotherapeutic agents. The observed total drug release which lasted for 16 days for Dox is expected to be sufficient enough to provide high local concentration to destroy cancer cells. It is worth mentioning that drug release could be modified to reduce burst release and provide more sustained release. For example, Kumeria et al. extended the in vitro release of gentamicin for 27 days by applying a PLGA coating layer over the surface of TNTs.[46] In another study, Aw et al. were able to delay gentamicin release for 6 days by adding a layer of blank (i.e., drug free) micelles on top of the loaded drug.[47] Further confirmation of sufficient drug loading and release will be performed in the next sections in which the anticancer activity of loaded drug-loaded implants will be assessed using cell culture studies.

3.4. Cell Studies. *3.4.1. Cellular Attachment on Implants Surface.* One ultimate goal of drug-releasing bone implants is to provide support and induce bone healing. The process of bone healing is initiated by osseointegration in which cells of tissues surrounding the implant start to interact with the implant surface. Recently, studies confirmed that the micro−nano rough surface of such implants could significantly enhance cell adhesion and proliferation in comparison with smooth flat TNTs-Ti wafers (i.e., no microroughness).[28,48,29] It is important to mention that these studies did not involve any drug-loading/release properties of the implants and also that the TNTs was fabricated under different anodization conditions using a different electrolyte.

To ensure that our TNTs-3D-Ti implant will permit cell adhesion and proliferation, we studied the growth of fibroblasts on TNTs-3D-Ti surface. Fibroblasts are the most common type of cells in the human connective tissue. They play a vital role in wound and injury healing since they synthesize collagen and extracellular matrix which together form the structural framework of most body tissues.[49] Fibroblasts are commonly used in studies involving bone implants to assess properties such as cell interaction or adhesion with the implant's surface.[50−52] Figure 5 shows SEM images of fibroblasts

DOI: 10.1021/acsami.7b09916
ACS Appl. Mater. Interfaces 2017, 9, 29562−29570

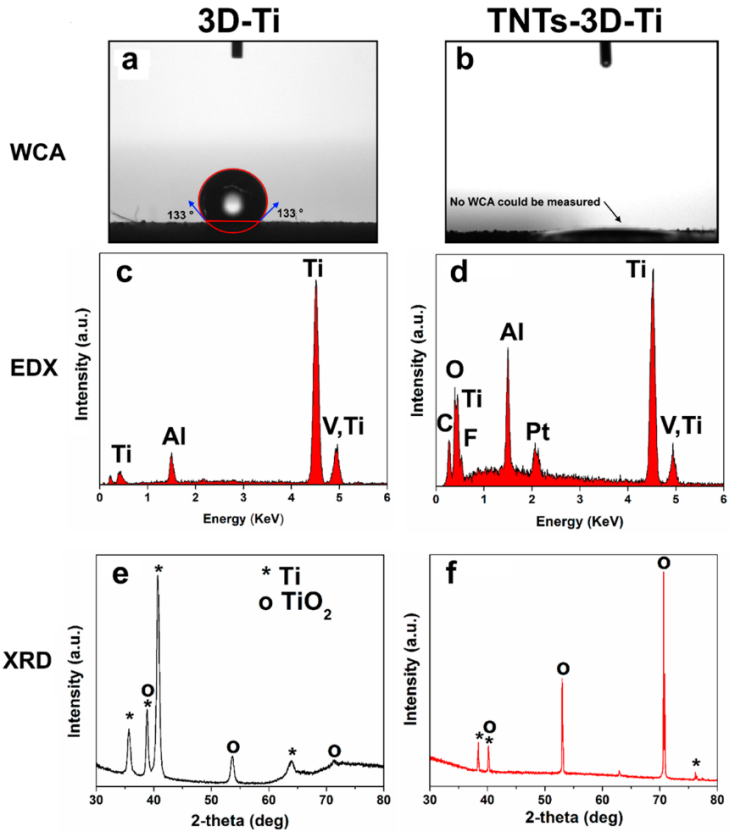

Figure 3. Surface properties and chemical characterization of 3D-Ti and TNTs-3D-Ti implants showing (a and b) water contact angle (WCA), (c and d) EDX, and (e and f) XRD graphs.

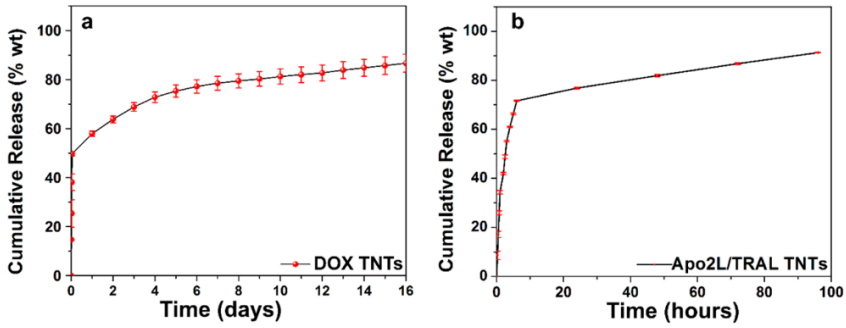

Figure 4. In vitro drug release of different drugs loaded onto TNTs-3D-Ti implants: (a) DOX and (b) Apo2L/TRAIL (n = 3 ± SD).

spreading on the "peak and valley"-like architecture and well attached to the structural features of the TNTs-3D-Ti surface. Signs of mechanical stimulation and strong/firm anchoring are evident by the appearance of stress fibers (actin-filaments) and focal cell adhesions (i.e., cell matrix adhesions) which could translate into effective osseointegration.[53] It is worth mentioning that fibroblasts appeared normal with no signs of cell death when examined under a light microscope, which confirms the compatibility of the implants material (i.e., Ti6Al4V)

3.4.2. Screening the Anticancer Activity of Drug-Loaded TNTs-3D-Ti Implants. Fracture is one of the most common complications associated with bone cancer.[54] Thus, combining bone-fixing implants with localized drug delivery, that enable anticancer release at the fracture site, is proposed to enhance disease prognosis. In our study, we loaded two anticancer agents (i.e., DOX and Apo2L/TRAIL) onto TNTs-3D-Ti implants to study the efficiency of drug loading and release of our implants.

In the case of DOX-loaded implants, when implants were incubated with TXSA cells for 24 h, the cells viability was

DOI: 10.1021/acsami.7b09916
ACS Appl. Mater. Interfaces 2017, 9, 29562−29570

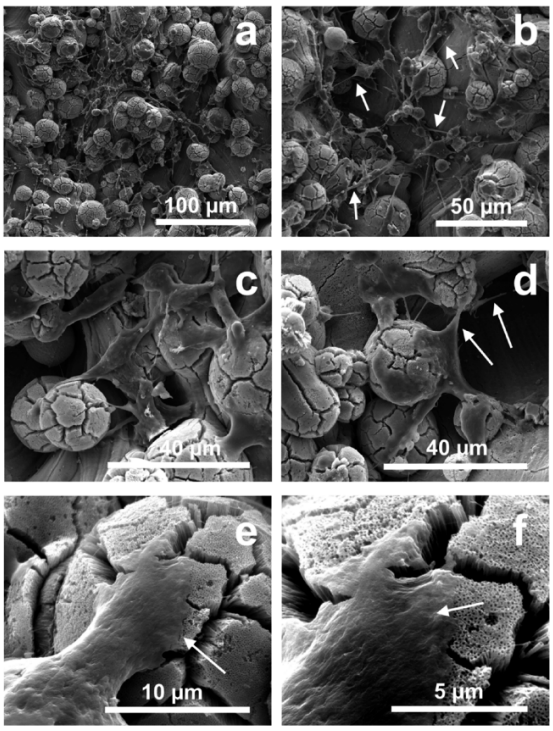

Figure 5. SEM analysis showing fibroblasts attachment on TNTs-3D-Ti implants after 24 h incubation. (a–d) Cells can be seen firmly attached on the implant surfaces and inside the cracks, which arise during anodization of the curved surfaces. White arrows show the microfilaments. (e and f) Higher magnification imaged showing ECM secreted by the attached cells.

reduced to 16.4 ± 2%, which indicates sufficient drug release for anticancer therapy. However, our investigation did not stop at this point; there are concerns TNTs could be blocked after attachment of cells onto the implant's surface after insertion into the body, which could affect the release of loaded therapeutics. Cells first secrete adhesion proteins on the implant surface which promotes cellular attachment. After that cells start to produce a collection of extracellular molecules collectively called the extracellular matrix (ECM), Figure 5e and 5f, which serves a lot of roles such as providing biochemical support, promoting cell to cell communication, and mediating cell migration. Moreover, the formation of ECM is essential for wound healing and tissue development (Figure S5).[55,56]

The presence of ECM components together with cells on top of TNTs could result in complete inhibition or at least a significant reduction in drug release due to tube blockage, and thus, the implants lose their drug-releasing properties. To this end, we loaded Apo2L/TRAIL onto TNTs-3D-Ti wafers. Apo2L/TRAIL is a tumor necrosis factor (TNF) inducing ligand that can induce apoptosis of tumor cells while sparing most normal cells (i.e., no or limited toxicity to normal cells).[57] After that we seeded fibroblasts on the wafers surface and allowed them to grow for 24 h. To check the cytotoxic effect, the wafers (i.e., with fibroblasts on top) were incubated with MDA-MB-231-TXSA cancer cells and cell viability was assessed at different time intervals (i.e., 1, 2, and 3 days).

Figure 6a–c shows SEM images of fibroblasts attached on top of TNTs loaded with Apo2L/TRAIL. Cells appear normal

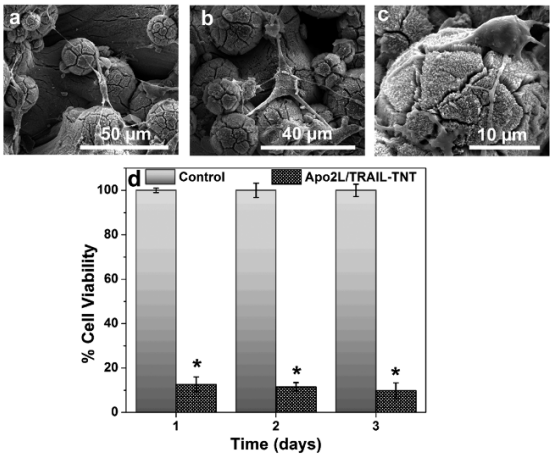

Figure 6. Anticancer activity of Apo2L/TRAIL-loaded TNTs. (a–c) SEM images of fibroblasts adhesion onto the surface of Apo2L/TRAIL-loaded TNTs-3D-Ti implant. , (d) Cell viability MDA-MB-231-TXSA cells after treatment by drug-loaded implants at different time intervals. Level of significance was set at a p value < 0.05 for asterisks in comparison to the negative control group (drug-free TNTs-3D-Ti implants) (n = 3 ± SD).

(i.e., well attached and not affected by the presence of Apo2L/TRAIL) showing stress fibers and firm adhesion. Most TNTs appeared opened, except those with cells on top, with no signs of blockage by ECM components. Figure 6d represents MDA-MB-231-TXSA cell viability after incubation with drug-loaded implants at different time intervals. The cell viability was significantly decreased for all samples which confirms that Apo2L/TRAIL was released effectively from TNTs which means that the presence of fibroblasts on top of TNTs did not prevent drug release. As a result, this proves the potential applicability of TNTs-3D-Ti implants as a multifunctional device that combines bone fracture support and localized drug delivery properties.

4. CONCLUSION

This paper presents new 3D-printed Ti alloy-based drug-releasing implants with a unique combination of microspherical and nanotopography which aims to demonstrate their enhanced cell attachment and drug loading/release performance for treatment of cancer cell for potential application for localized chemotherapy for bone cancer. The implants are produced by 3D printing based on a selective laser melting process of Ti6Al4V alloy that showed an irregular microrough particle topography on the surface. Well-organized TNTs arrays were generated on the surface by an anodization process enabling formation of additional "nanotopography" while preserving the microparticle arrangement. The drug loading and release of two anticancer agents, doxorubicin (DOX) and apoptosis-inducing ligand (Apo2L/TRAIL), were successfully confirmed showing their capacity to release locally high dosage of drugs over 16 and 4 days, respectively. Study of fibroblasts adhesion showed high affinity and adhesion to the nano/microrough features of the implant surface when examined

DOI: 10.1021/acsami.7b09916
ACS Appl. Mater. Interfaces 2017, 9, 29562–29570

using SEM. In addition, the release efficacy of chemotherapeutic agents loaded onto TNTs was not affected by cell adhesion as confirmed by in vitro cytotoxicity studies. More studies are in progress to confirm their efficacy using cancer cell tissue and animal models.

In summary, these new dual-topography 3D-Ti implants with TNTs structures are shown to perform as multifunctional drug-releasing devices with two functions related to bone cancer which is challenging to treat: one is to provide bone support and the second to provide localized drug delivery. In addition, the 3D-printing process is offering flexibility of designing implants with different shapes and dimensions specifically tailored for individual needs which are not possible to achieve with currently used implants. These results indicate potential introduction of a new type multifunctional implants to replace the conventional implants and provide an important contribution to treat more efficiently a deadly bone cancer.

■ ASSOCIATED CONTENT

Supporting Information

The Supporting Information is available free of charge on the ACS Publications website at DOI: 10.1021/acsami.7b09916.

Luciferase bioluminescent cell viability assay, SEM image showing cross section of 3D-Ti wafers, mechanism of TNTs fabrication on 3D-Ti implants surface during the electrochemical anodization process, current density−time profile during 3D-Ti wafer anodization, picture of 3D-Ti implant before and after electrochemical anodization, TGA plots of drug-loaded TNTs-3D-Ti implants, illustration of cell adhesion and ECM components secreted upon cell attachment, additional references (PDF)

■ AUTHOR INFORMATION

Corresponding Author

*Tel.: +61 8 8313 4648. E-mail: dusan.losic@adelaide.edu.au.

ORCID

Dusan Losic: 0000-0002-1930-072X

Author Contributions

The manuscript was written through contributions of all authors. All authors have given approval to the final version of the manuscript

Notes

The authors declare no competing financial interest.

■ ACKNOWLEDGMENTS

The authors acknowledge the financial support provided to S.M. by the Australian Government Training Program Scholarship, ARC grant funded supplementary scholarship, and Forrest George and Sandra Lynne Young Supplementary Scholarship. This work was done under the financial support of the Australian Research Council (ARC) through ARC grants DP120101680 and FT110100711, and of the School of Chemical Engineering, the University of Adelaide. Authors also thank Dr. Karan Gulati, School of Dentistry and Oral Health, Griffith University for his help in preparing the cell samples for SEM imaging.

■ REFERENCES

(1) Katzer, A.; Meenen, N. M.; Grabbe, F.; Rueger, J. Surgery of Skeletal Metastases. *Arch. Orthop. Unfall-Chir* **2002**, *122* (5), 251−258.

(2) Vestergaard, P.; Rejnmark, L.; Mosekilde, L. Fracture Risk in Patients with Different Types of Cancer. *Acta Oncol.* **2009**, *48* (1), 105−115.

(3) Hage, W. D.; Aboulafia, A. J.; Aboulafia, D. M. Incidence, Location, and Diagnostic Evaluation of Metastatic Bone Disease. *Orthop Clin North Am.* **2000**, *31* (4), 515−28.

(4) Sarahrudi, K.; Hora, K.; Heinz, T.; Millington, S.; Vécsei, V. Treatment Results of Pathological Fractures of the Long Bones: A Retrospective Analysis of 88 Patients. *Int. Orthop.* **2006**, *30* (6), 519−524.

(5) Rajani, R.; Gibbs, C. P. Treatment of Bone Tumors. *Surg Pathol Clin* **2012**, *5* (1), 301−318.

(6) Losic, D.; Aw, M. S.; Santos, A.; Gulati, K.; Bariana, M. Titania Nanotube Arrays for Local Drug Delivery: Recent Advances and Perspectives. *Expert Opin. Drug Delivery* **2015**, *12* (1), 103−27.

(7) Jain, A. K.; Panchagnula, R. Skeletal Drug Delivery Systems. *Int. J. Pharm.* **2000**, *206* (1−2), 1−12.

(8) Gulati, K.; Kogawa, M.; Maher, S.; Atkins, G.; Findlay, D.; Losic, D. Titania Nanotubes for Local Drug Delivery from Implant Surfaces. In *Electrochemically Engineered Nanoporous Materials*; Springer International Publishing, 2015; pp 307−355.

(9) Buchholz, H.; Elson, R.; Engelbrecht, E.; Lodenkamper, H.; Rottger, J.; Siegel, A. Management of Deep Infection of Total Hip Replacement. *J. Bone Jt. Surg.* **1981**, *63-B* (3), 342−353.

(10) Moran, E.; Byren, I.; Atkins, B. L. The Diagnosis and Management of Prosthetic Joint Infections. *J. Antimicrob. Chemother.* **2010**, *65* (Suppl 3), iii45−iii54.

(11) Novaes, A. B., Jr; Souza, S. L. S. d.; Barros, R. R. M. d.; Pereira, K. K. Y.; Iezzi, G.; Piattelli, A. Influence of Implant Surfaces on Osseointegration. *Braz. Dent. J.* **2010**, *21*, 471−481.

(12) Gulati, K.; Maher, S.; Findlay, D. M.; Losic, D. Titania Nanotubes for Orchestrating Osteogenesis at the Bone−Implant Interface. *Nanomedicine* **2016**, *11* (14), 1847−1864.

(13) Barr, J. G.; Grundy, P. L. The Effects of the Nice Technology Appraisal 121 (Gliadel and Temozolomide) on Survival in High-Grade Glioma. *Br J. Neurosurg* **2012**, *26* (6), 818−22.

(14) Bosco, R.; Van Den Beucken, J.; Leeuwenburgh, S.; Jansen, J. Surface Engineering for Bone Implants: A Trend from Passive to Active Surfaces. *Coatings* **2012**, *2* (3), 95−119.

(15) Gulati, K.; Aw, M. S.; Findlay, D.; Losic, D. Local Drug Delivery to the Bone by Drug-Releasing Implants: Perspectives of Nano-Engineered Titania Nanotube Arrays. *Ther. Delivery* **2012**, *3* (7), 857−873.

(16) Manam, N. S.; Harun, W. S. W.; Shri, D. N. A.; Ghani, S. A. C.; Kurniawan, T.; Ismail, M. H.; Ibrahim, M. H. I. Study of Corrosion in Biocompatible Metals for Implants: A Review. *J. Alloys Compd.* **2017**, *701*, 698−715.

(17) Goodman, S. B.; Yao, Z.; Keeney, M.; Yang, F. The Future of Biologic Coatings for Orthopaedic Implants. *Biomaterials* **2013**, *34* (13), 3174−3183.

(18) Lan, G.; Li, M.; Tan, Y.; Li, L.; Yang, X.; Ma, L.; Yin, Q.; Xia, H.; Zhang, Y.; Tan, G.; Ning, C. Promoting Bone Mesenchymal Stem Cells and Inhibiting Bacterial Adhesion of Acid-Etched Nanostructured Titanium by Ultraviolet Functionalization. *J. Mater. Sci. Technol.* **2015**, *31* (2), 182−190.

(19) Sanchez, M. C.; Fernandez, E.; Llama-Palacios, A.; Figuero, E.; Herrera, D.; Sanz, M. Response to Antiseptic Agents of Periodontal Pathogens in in Vitro Biofilms on Titanium and Zirconium Surfaces. *Dent. Mater.* **2017**, *33* (4), 446−453.

(20) Zhao, H.; Dong, W.; Zheng, Y.; Liu, A.; Yao, J.; Li, C.; Tang, W.; Chen, B.; Wang, G.; Shi, Z. The Structural and Biological Properties of Hydroxyapatite-Modified Titanate Nanowire Scaffolds. *Biomaterials* **2011**, *32* (25), 5837−5846.

(21) Sarraf, M.; Abdul Razak, B.; Dabbagh, A.; Nasiri-Tabrizi, B.; Abu Kasim, N. H.; Basirun, W. J. Optimizing Pvd Conditions for Electrochemical Anodization Growth of Well-Adherent Ta2o5nanotubes on Ti-6al-4v Alloy. *RSC Adv.* **2016**, *6* (82), 78999−79015.

(22) Geng, H.; Poologasundarampillai, G.; Todd, N.; Devlin-Mullin, A.; Moore, K. L.; Golrokhi, Z.; Gilchrist, J. B.; Jones, E.; Potter, R. J.;

DOI: 10.1021/acsami.7b09916
ACS Appl. Mater. Interfaces 2017, 9, 29562−29570

Sutcliffe, C.; O'Brien, M.; Hukins, D. W. L.; Cartmell, S.; Mitchell, C. A.; Lee, P. D. Biotransformation of Silver Released from Nanoparticle Coated Titanium Implants Revealed in Regenerating Bone. *ACS Appl. Mater. Interfaces* **2017**, *9* (25), 21169−21180.
(23) Albrektsson, T.; Johansson, C. Osteoinduction, Osteoconduction and Osseointegration. *Eur. Spine J.* **2001**, *10* (Suppl 2), S96−101.
(24) Welldon, K. J.; Atkins, G. J.; Howie, D. W.; Findlay, D. M. Primary Human Osteoblasts Grow into Porous Tantalum and Maintain an Osteoblastic Phenotype. *J. Biomed. Mater. Res., Part A* **2008**, *84A* (3), 691−701.
(25) Wennerberg, A.; Albrektsson, T. Effects of Titanium Surface Topography on Bone Integration: A Systematic Review. *Clin Oral Implants Res.* **2009**, *20*, 172−184.
(26) Ding, Y.-F.; Li, R. W.; Nakai, M.; Majumdar, T.; Zhang, D.-H.; Niinomi, M.; Birbilis, N.; Smith, P. N.; Chen, X.-B. Osteoanabolic Implant Materials for Orthopedic Treatment. *Adv. Healthcare Mater.* **2016**, *5* (14), 1740−1752.
(27) Mendonca, G.; Mendonca, D. B.; Aragao, F. J.; Cooper, L. F. Advancing Dental Implant Surface Technology from Micron to Nanotopography. *Biomaterials* **2008**, *29* (28), 3822−35.
(28) Liu, H.; Huang, X.; Yu, H.; Yang, X.; Zhang, X.; Hang, R.; Tang, B. A Cytocompatible Micro/Nano-Textured Surface with Si-Doped Titania Mesoporous Arrays Fabricated by a One-Step Anodization. *Mater. Sci. Eng., C* **2017**, *73*, 120−129.
(29) Moon, B.-S.; Kim, S.; Kim, H.-E.; Jang, T.-S. Hierarchical Micro-Nano Structured Ti6al4v Surface Topography Via Two-Step Etching Process for Enhanced Hydrophilicity and Osteoblastic Responses. *Mater. Sci. Eng., C* **2017**, *73*, 90−98.
(30) Webster, T. J.; Ejiofor, J. U. Increased Osteoblast Adhesion on Nanophase Metals: Ti, Ti6al4v, and Cocrmo. *Biomaterials* **2004**, *25* (19), 4731−4739.
(31) Losic, D.; Simovic, S. Self-Ordered Nanopore and Nanotube Platforms for Drug Delivery Applications. *Expert Opin. Drug Delivery* **2009**, *6* (12), 1363−1381.
(32) Guillemot, F. Recent Advances in the Design of Titanium Alloys for Orthopedic Applications. *Expert Rev. Med. Devices* **2005**, *2* (6), 741−8.
(33) Tak, Y.; Lee, B. G.; Kim, J.; Kim, J. Y. Effect of Surface Treatment on Surface Roughness and Ni Content of Nitinol Stents. *Int. J. Surf. Sci. Eng.* **2016**, *10* (4), 389−99.
(34) Fierz, F. C.; Beckmann, F.; Huser, M.; Irsen, S. H.; Leukers, B.; Witte, F.; Degistirici, O.; Andronache, A.; Thie, M.; Muller, B. The Morphology of Anisotropic 3d-Printed Hydroxyapatite Scaffolds. *Biomaterials* **2008**, *29* (28), 3799−806.
(35) Xiong, Y.; Qian, C.; Sun, J. Fabrication of Porous Titanium Implants by Three-Dimensional Printing and Sintering at Different Temperatures. *Dent. Mater. J.* **2012**, *31* (5), 815−20.
(36) Sun, X.; Lin, H.; Chen, X.; Zhang, P. Comparative Study on Electrocrystallization of Calcium Phosphate Ceramics on Commercially Pure Titanium and Selective Laser Melting Titanium. *Mater. Lett.* **2017**, *192*, 92−95.
(37) Yang, F.; Chen, C.; Zhou, Q. R.; Gong, Y. M.; Li, R. X.; Li, C. C.; Klampfl, F.; Freund, S.; Wu, X. W.; Sun, Y.; Li, X.; Schmidt, M.; Ma, D.; Yu, Y. C. Laser Beam Melting 3d Printing of Ti6al4v Based Porous Structured Dental Implants: Fabrication, Biocompatibility Analysis and Photoelastic Study. *Sci. Rep.* **2017**, *7*, 45360.
(38) Cheng, A.; Humayun, A.; Cohen, D. J.; Boyan, B. D.; Schwartz, Z. Additively Manufactured 3d Porous Ti-6al-4v Constructs Mimic Trabecular Bone Structure and Regulate Osteoblast Proliferation, Differentiation and Local Factor Production in a Porosity and Surface Roughness Dependent Manner. *Biofabrication* **2014**, *6* (4), 045007.
(39) Popat, K. C.; Eltgroth, M.; LaTempa, T. J.; Grimes, C. A.; Desai, T. A. Decreased Staphylococcus Epidermis Adhesion and Increased Osteoblast Functionality on Antibiotic-Loaded Titania Nanotubes. *Biomaterials* **2007**, *28* (32), 4880−4888.
(40) Byeon, H. J.; Choi, S. H.; Choi, J. S.; Kim, I.; Shin, B. S.; Lee, E. S.; Park, E.-S.; Lee, K. C.; Youn, Y. S. Four-Arm Peg Cross-Linked Hyaluronic Acid Hydrogels Containing Pegylated Apoptotic Trail Protein for Treating Pancreatic Cancer. *Acta Biomater.* **2014**, *10* (1), 142−150.
(41) Prideaux, M.; Wijenayaka, A. R.; Kumarasinghe, D. D.; Ormsby, R. T.; Evdokiou, A.; Findlay, D. M.; Atkins, G. J. Saos2 Osteosarcoma Cells as an in Vitro Model for Studying the Transition of Human Osteoblasts to Osteocytes. *Calcif. Tissue Int.* **2014**, *95* (2), 183−93.
(42) Maher, S.; Qin, J.; Gulati, K.; El Mekawy, A.; Kaur, G.; Lima-Marques, L.; Atkins, G. J.; Findlay, D. M.; Evdokiou, A.; Losic, D. 3d Printed Titanium Implants with Nano-Engineered Surface Titania Nanotubes for Localized Drug Delivery. *Chemeca 2016: Chemical Engineering-Regeneration, Recovery and Reinvention*; 2016; p 65.
(43) Ercan, B.; Taylor, E.; Alpaslan, E.; Webster, T. W. Diameter of Titanium Nanotubes Influences Anti-Bacterial Efficacy. *Nanotechnology* **2011**, *22* (29), 295102.
(44) Kim, K.; Lee, B.-A.; Piao, X.-H.; Chung, H.-J.; Kim, Y.-J. Surface Characteristics and Bioactivity of an Anodized Titanium Surface. *J. Periodontal Implant Sci.* **2013**, *43* (4), 198−205.
(45) Cooper, L. F.; Zhou, Y.; Takebe, J.; Guo, J.; Abron, A.; Holmén, A.; Ellingsen, J. E. Fluoride Modification Effects on Osteoblast Behavior and Bone Formation at Tio2 Grit-Blasted C.P. Titanium Endosseous Implants. *Biomaterials* **2006**, *27* (6), 926−936.
(46) Kumeria, T.; Mon, H.; Aw, M. S.; Gulati, K.; Santos, A.; Griesser, H. J.; Losic, D. Advanced Biopolymer-Coated Drug-Releasing Titania Nanotubes (Tnts) Implants with Simultaneously Enhanced Osteoblast Adhesion and Antibacterial Properties. *Colloids Surf., B* **2015**, *130*, 255−63.
(47) Aw, M. S.; Addai-Mensah, J.; Losic, D. Polymer Micelles for Delayed Release of Therapeutics from Drug-Releasing Surfaces with Nanotubular Structures. *Macromol. Biosci.* **2012**, *12* (8), 1048−1052.
(48) Miklaszewski, A.; Jurczyk, M. U.; Kaczmarek, M.; Paszel-Jaworska, A.; Romaniuk, A.; Lipińska, N.; Żurawski, J.; Urbaniak, P.; Jurczyk, M. Nanoscale Size Effect in in Situ Titanium Based Composites with Cell Viability and Cytocompatibility Studies. *Mater. Sci. Eng., C* **2017**, *73*, 525−536.
(49) Kalluri, R.; Zeisberg, M. Fibroblasts in Cancer. *Nat. Rev. Cancer* **2006**, *6* (5), 392−401.
(50) Blinova, M. I.; Yudintzeva, N. M.; Nikolaenko, N. S.; Potokin, I. L.; Raykhtsaum, G.; Pitkin, M. R.; Pinaev, G. P. Cell Cultivation on Porous Titanium Implants with Various Structures. *Cell tissue biol.* **2010**, *4* (6), 572−579.
(51) Teng, F.-Y.; Ko, C.-L.; Kuo, H.-N.; Hu, J.-J.; Lin, J.-H.; Lou, C.-W.; Hung, C.-C.; Wang, Y.-L.; Cheng, C.-Y.; Chen, W.-C. A Comparison of Epithelial Cells, Fibroblasts, and Osteoblasts in Dental Implant Titanium Topographies. *Bioinorg. Chem. Appl.* **2012**, *2012*, 687291.
(52) Wang, J.; Li, J.; Qian, S.; Guo, G.; Wang, Q.; Tang, J.; Shen, H.; Liu, X.; Zhang, X.; Chu, P. K. Antibacterial Surface Design of Titanium-Based Biomaterials for Enhanced Bacteria-Killing and Cell-Assisting Functions against Periprosthetic Joint Infection. *ACS Appl. Mater. Interfaces* **2016**, *8* (17), 11162−11178.
(53) Tojkander, S.; Gateva, G.; Lappalainen, P. Actin Stress Fibers Assembly, Dynamics and Biological Roles. *J. Cell Sci.* **2012**, *125*, 1855−64.
(54) Vestergaard, P.; Rejnmark, L.; Mosekilde, L. Fracture Risk in Patients with Different Types of Cancer. *Acta Oncol.* **2009**, *48* (1), 105−15.
(55) Hynes, R. O. Cell Adhesion: Old and New Questions. *Trends Cell Biol.* **1999**, *9* (12), M33−7.
(56) Geiger, B.; Bershadsky, A.; Pankov, R.; Yamada, K. M. Transmembrane Crosstalk between the Extracellular Matrix−Cytoskeleton Crosstalk. *Nat. Rev. Mol. Cell Biol.* **2001**, *2* (11), 793−805.
(57) Smyth, M. J.; Takeda, K.; Hayakawa, Y.; Peschon, J. J.; van den Brink, M. R. M.; Yagita, H. Nature's Trail on a Path to Cancer Immunotherapy. *Immunity* **2003**, *18* (1), 1−6.

DOI: 10.1021/acsami.7b09916
ACS Appl. Mater. Interfaces 2017, 9, 29562−29570

Supporting information

Engineering of Micro to Nano Structured 3D Printed Drug-releasing Titanium Implants for Enhanced Osseointegration and Localized Delivery of Anticancer Drugs

Shaheer Maher [a, d], *Gagandeep Kaur* [a], *Luis Lima-Marques* [b], *Andreas Evdokiou* [c], *Dusan Losic* [a,*]

[a] School of Chemical Engineering, The University of Adelaide, Engineering North Building, 5005, Adelaide, Australia

[b] Institute for Photonics and Advanced Sensing (IPAS), The University of Adelaide, 5005 Adelaide, Australia.

[c] Discipline of Surgery, Basil Hetzel Institute, The University of Adelaide, 5005, Adelaide, SA, Australia

[d] Faculty of Pharmacy, Assiut University, 71526, Assiut, Egypt.

* Corresponding author:

Prof. Dusan Losic

School of Chemical Engineering, The University of Adelaide, Engineering North Building, 5005 Adelaide, Australia; Tel (+61 8 8313 4648)

E-mail: dusan.losic@adelaide.edu.au

Luciferase bioluminescent cell viability assay:

To determine the effect of DOX loaded TNTs-3D-Ti implants on MDA-MB-231-TXSA cells, bioluminescent cell viability assay using D-luciferin firefly potassium salt was adopted. The assay is based on the oxidation of luciferin inside metabolically active cells (luciferase expressing cells) under the catalytic effects of luciferase and ATP, which results in a bluish-green light (bioluminescence). After 24 hours of implant's incubation with MDA-MB-231-TXSA cells, the culture media was removed carefully and treated with 100 µL of luciferin solution (150 µg mL-1). The cells were incubated for 20 mins at 37°C and then the bioluminescence was measured using plate reader.

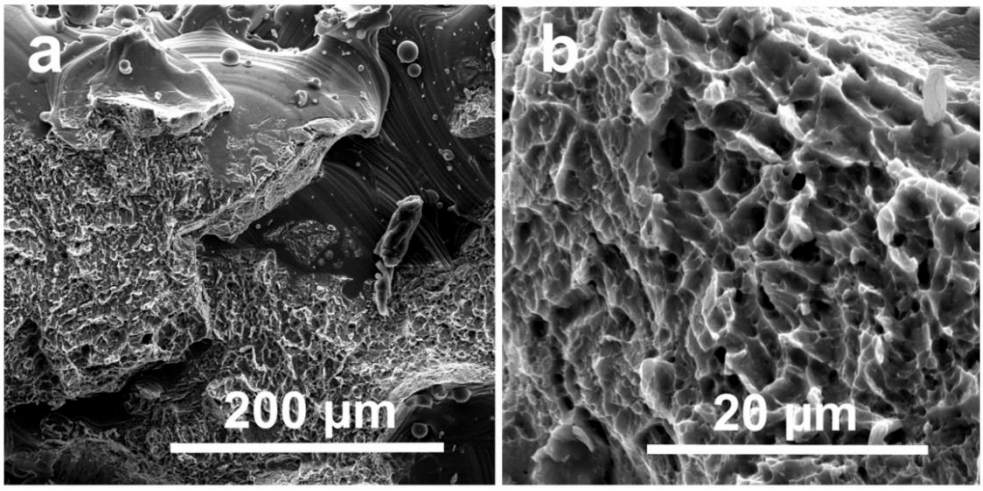

Figure S1: SEM image showing cross section of 3D-Ti wafers at (a) low and (b) high magnification

Mechanism of TNTs fabrication on 3D-Ti implants surface during the electrochemical anodization process

At anode (3D-Ti wafer):

$Ti + 2H_2O \rightarrow TiO_2 + 4H^+ + 4e^-$ **Equation 1**

$Ti^{4+} + 6F^- \rightarrow [TiF_6]^{2-}$ **Equation 2**

$TiO_2 + 6F^- + 4H^+ \rightarrow [TiF_6]^{2-} + 2H_2O$ **Equation 3**

At cathode (counter electrode):

$2H_2O + 4e^- \rightarrow 2H_2 + 4OH^-$ **Equation 4**

Under anodic voltage, titanium starts to oxidize forming Ti^{4+} which will either react with O^{2-} from water present in the electrolyte as seen in **equation 1** or with F^- from NH_4F as seen in **equation 2.** As a result of **equation 1** an initial oxide layer (TiO_2) will be formed on the surface of Ti. Small pits will be generated due to localized dissolution at the surface by the attack of fluoride ions through reaction with Ti^{4+} on the surface **(equation 2)** and also by dissolving the formed TiO_2 **(equation 3)** forming water soluble $[TiF_6]^{2-}$. A competition occurs between the formation of TiO_2 **(equation 1)** and dissolution by F^- ions **(equation 2 and 3)**. When balance is reached between these two processes, self-organised nanotubes are observed [1-3]. **Equation 4** explains the reaction that takes place at the cathode in which hydrogen ions are reduced by gaining electrons which result in release of H_2 gas [1].

To explain different anodization steps, the current through the electrochemical cell was recorded. **Figure S1** shows current density-time profile recorded during anodization of 3D-Ti samples for 15 mins under 60V at 60 ºC using ethylene glycol electrolyte containing NH_4F (0.1M), lactic acid (1.5M), water (5% v/v).

The current-time curve could be divided into three distinct stages; *stage I*, in which the current decreased rapidly due to the formation of a non-conducting TiO_2 layer (also known as a barrier layer) **(**i.e. **equation 1)**. This was followed by *stage II*, which is characterized by a slight rise in current as a result of dissolution of Ti^{4+} and TiO_2 **(equations 2 and 3)**. Finally, *stage III* starts, in which the current drops again and becomes almost stable due to equilibrium between formation and dissolution of the barrier layer [1].

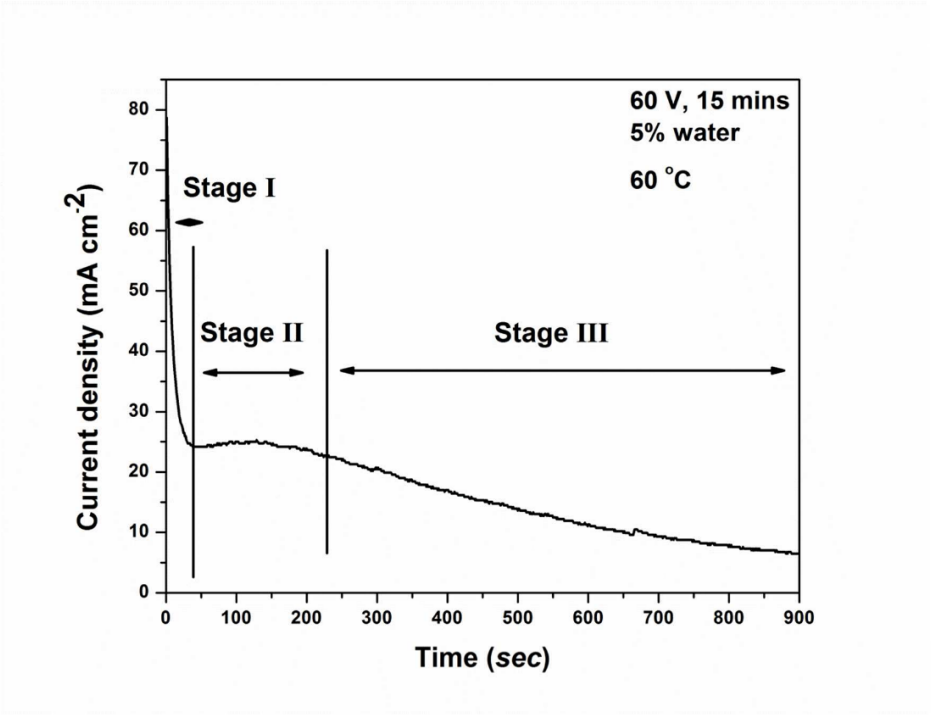

Figure S2: Current density-time profile during 3D-Ti wafer anodization at 60 V for 15 mins at temperature 60 ℃, showing different anodization stages

The use of organic viscous electrolyte, ethylene glycol, leads to reduction of diffusion speed of ions (i.e. Ti^{4+} and F^-), and therefore the equilibrium between dissolution and formation of the oxide layer could be established easier [4]. Lactic acid, on the other hand, is added to the anodization electrolyte to prevent anodic breakdown at high voltage by adsorption into the surface. Anodic breakdown occurs when ions penetrate through the formed oxide layer at weak points which results in exposure of the underneath metal together with a continuous rise in anodic current with no tubes formation. LA forms a layer that prevents ions attack, thus allow tubes to be formed at a more ordered and faster rate [5].

Figure S2 shows an image of the 3D-Ti wafer before and after anodization, TNT appear as

dark non shiny circular region (diameter =1 cm) on the wafer surface.

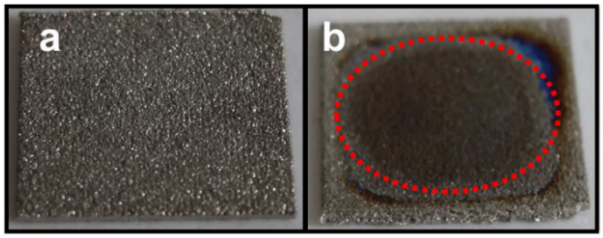

Figure S3: Picture of 3D-Ti implant (a) before and (b) after electrochemical anodization. Red dotted circle in (b) denotes the TNT region.

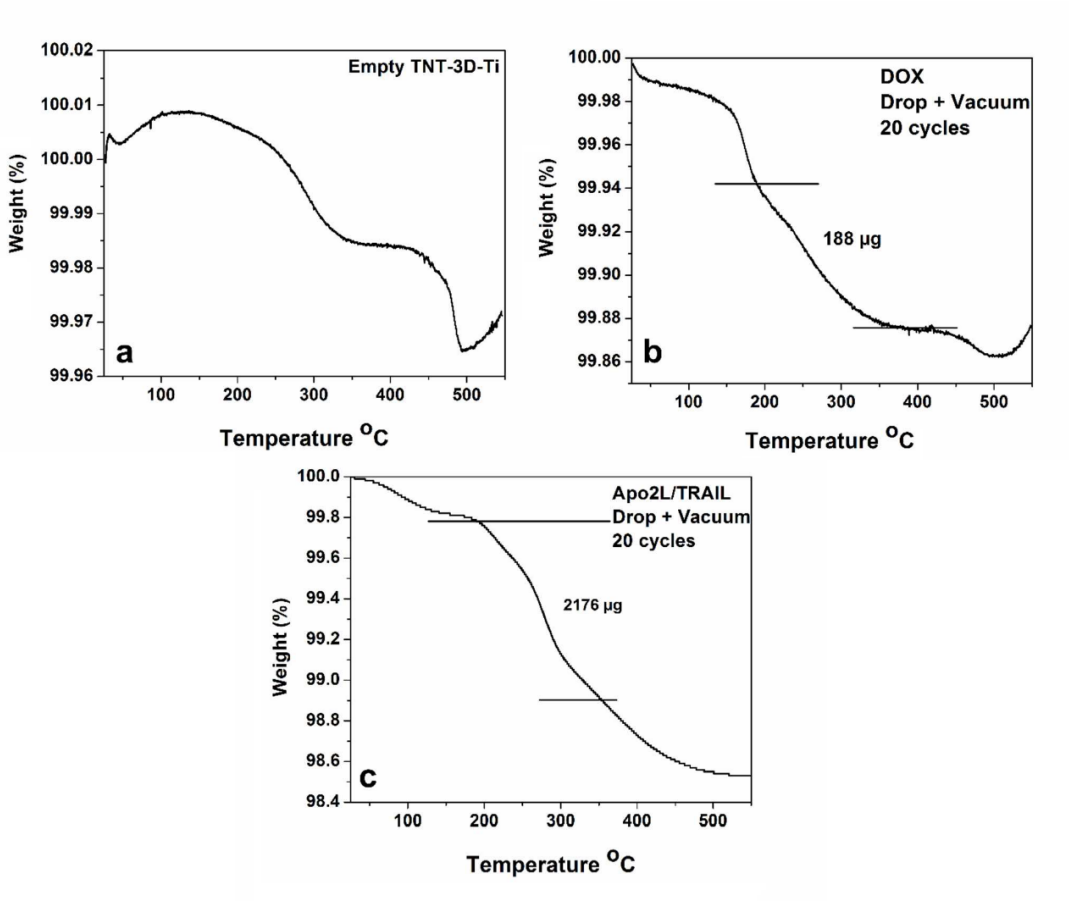

Figure S4: TGA plots of drug loaded TNT-3D-Ti implants, (a) drug free TNTs-3D-Ti implant, (b) DOX and (c) Apo2L/TRAIL

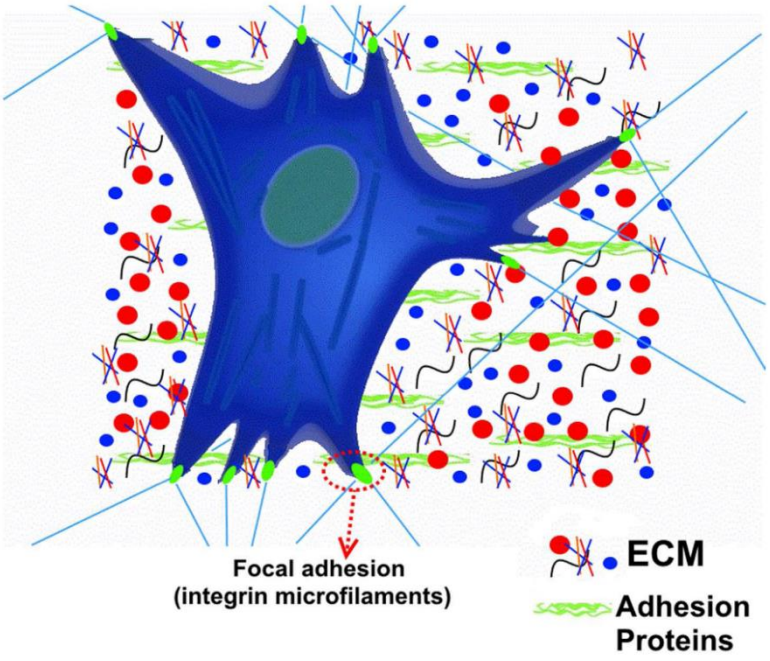

Figure S5: Illustration of cell adhesion and ECM components secreted upon cell attachment

S-8

1. Roy, P.; Berger, S.; Schmuki, P. Tio2 Nanotubes: Synthesis and Applications. *Angew. Chem., Int. Ed.* 2011, *50,* 13, 2904-2939.
2. Parcharoen, Y.; Kajitvichyanukul, P.; Sirivisoot, S.; Termsuksawad, P. Hydroxyapatite Electrodeposition on Anodized Titanium Nanotubes for Orthopedic Applications. *Appl. Surf. Sci.* 2014, *311*, 54-61.
3. Zhou, X.; Nguyen, N. T.; Özkan, S.; Schmuki, P. Anodic Tio2 Nanotube Layers: Why Does Self-Organized Growth Occur—a Mini Review. *Electrochem. Commun.* 2014, *46*, 157-162.
4. Macak, J. M.; Schmuki, P. Anodic Growth of Self-Organized Anodic Tio2 Nanotubes in Viscous Electrolytes. *Electrochim. Acta* 2006, *52,* 3, 1258-1264.
5. So, S.; Lee, K.; Schmuki, P. Ultrafast Growth of Highly Ordered Anodic Tio2 Nanotubes in Lactic Acid Electrolytes. *J. Am. Chem. Soc.* 2012, *134,* 28, 11316-11318.

CHAPTER 4

TAILORING IMPLANT-CELL RESPONSE OF ADDITIVELY MANUFACTURED IMPLANTS TNTS

4.1. Overview

One of the main challenges facing bone implant applications is the control of the process implant-cell interaction. The surface nano and micro features were confirmed to play a pivotal role in bones cells growth and attachment. Depending on the intended duration (*i.e.*, short-term or long-term) and application (permanent or removable) of the implant, it is essential to control implant-cell interaction.

This chapter will focus on the effect of titania nanotubes (TNTs) on cells response. Two separate studies were performed in order to either reduce or enhance bone cell attachment and growth on 3D-printed Ti implants.

In the first study, additively manufactured 3D-printed Ti implants were fabricated with TNTs on top. TNTs with various diameters were fabricated in attempt to generate tubes with diameter of 100 nm or more which are expected not to promote bone cell attachment. The aim of this study was to prepare bone implants that can be used for temporal fixation of bone fractures that can be easily removed after serving their function. In addition, enhanced antibacterial properties of TNTs was achieved through coating a layer of gallium nitrate. The results showed complete bacterial eradication owing to the bactericidal activity of gallium ions. At the same time, TNTs showed significant antibacterial activity against *Pseudomonas aeruginosa*. This study confirms the potential of a new generation of low-cost, removable implants that enables control of bone cell response while effectively inhibiting bacterial colonization.

The second study aims to enhance the osseointegration performance of TNTs through bioactivation by hydroxyapatite (HA) coating using alternative immersion method (AIM). Protein adsorption, cells attachment and gene expression of SaOS2 human osteoblast-like cells were evaluated. Results confirmed enhanced cell attachment, maturation and mineralization on

HA coated TNTs surface compared to uncoated surface. This confirms that functionalized TNTs could be used to support osseointegration of 3D-printed Ti implants.

This chapter confirms the potential application of TNTs to control the process of bone cell attachment and growth on TNTs for both long-term and short-term implants.

This Chapter includes the following papers:

- **Shaheer Maher**, Denver Linklater, Hadi Rastin, Pei Le Yap, Elena P. Ivanova and Dusan Losic (2022), Tailoring additively manufactured titanium implants for short-time pediatric implantations with enhanced bactericidal activity. ChemMedChem. 17(2): e202100580.

- Jie Qin, Dongqing Yang, **Shaheer Maher,** Luis Lima-Marques, Yanmin Zhou, Yujie Chen, Gerald J. Atkins and Dusan Losic (2018), Micro- and nano-structured 3D printed titanium implants with a hydroxyapatite coating for improved osseointegration. Journal of Materials Chemistry B 6(19): 3136-3144.

Statement of Authorship

Title of Paper	Tailoring Additively Manufactured Titanium Implants for Short-Time Pediatric Implantations with Enhanced Bactericidal Activity
Publication Status	☐ Published ☑ Accepted for Publication ☐ Submitted for Publication ☐ Unpublished and Unsubmitted w ork w ritten in manuscript style
Publication Details	Shaheer Maher, Denver Linklater, Hadi Rastin, Pei Le Yap, Elena P. Ivanova and Dusan LosicTailoring Additively Manufactured Titanium Implants for Short-Time Pediatric Implantations with Enhanced Bactericidal Activity, ChemMedChem

Principal Author

Name of Principal Author (Candidate)	Shaheer Makar		
Contribution to the Paper	Study design, samples preparation, performed characterization on all samples, participated in bacterial studies, interpreted data and wrote manuscript		
Overall percentage (%)	85%		
Certification:	This paper reports on original research I conducted during the period of my Higher Degree by Research candidature and is not subject to any obligations or contractual agreements with a third party that would constrain its inclusion in this thesis. I am the primary author of this paper.		
Signature		Date	09/03/2021

Co-Author Contributions

By signing the Statement of Authorship, each author certifies that:

i. the candidate's stated contribution to the publication is accurate (as detailed above);

ii. permission is granted for the candidate in include the publication in the thesis; and

iii. the sum of all co-author contributions is equal to 100% less the candidate's stated contribution.

Name of Co-Author	Denver Linklater		
Contribution to the Paper	Cell culture and bacterial study, revised the manuscript		
Signature		Date	03/09/2021

Name of Co-Author	Hadi Rastin		
Contribution to the Paper	Participated in bacterial studyType text here		
Signature		Date	03/09/2021

Please cut and paste additional co-author panels here as required.

Statement of Authorship

Title of Paper	Tailoring Additively Manufactured Titanium Implants for Short-Time Pediatric Implantations with Enhanced Bactericidal Activity
Publication Status	☐ Published ☑ Accepted for Publication ☐ Submitted for Publication ☐ Unpublished and Unsubmitted w ork w ritten in manuscript style
Publication Details	Shaheer Maher, Denver Linklater, Hadi Rastin, Pei Le Yap, Elena P. Ivanova and Dusan LosicTailoring Additively Manufactured Titanium Implants for Short-Time Pediatric Implantations with Enhanced Bactericidal Activity, ChemMedChem

Principal Author

Name of Principal Author (Candidate)	Shaheer Maher (*also known* as Shaheer Makar)
Contribution to the Paper	Study design, samples preparation, performed characterization on all samples, participated in bacterial studies, interpreted data and wrote manuscript
Overall percentage (%)	85%
Certification:	This paper reports on original research I conducted during the period of my Higher Degree by Research candidature and is not subject to any obligations or contractual agreements with a third party that would constrain its inclusion in this thesis. I am the primary author of this paper.
Signature	Date 09/03/2021

Co-Author Contributions

By signing the Statement of Authorship, each author certifies that:

i. the candidate's stated contribution to the publication is accurate (as detailed above);

ii. permission is granted for the candidate in include the publication in the thesis; and

iii. the sum of all co-author contributions is equal to 100% less the candidate's stated contribution.

Name of Co-Author	Pei Lay yap
Contribution to the Paper	Participated in ICP analysis
Signature	Date 03/09/2021

Name of Co-Author	Elena P Ivanova
Contribution to the Paper	Supervised cell and bacterial studies, revised the final manuscript
Signature	Date 03/09/2021

Please cut and paste additional co-author panels here as required.

Statement of Authorship

Title of Paper	Tailoring Additively Manufactured Titanium Implants for Short-Time Pediatric Implantations with Enhanced Bactericidal Activity
Publication Status	☐ Published ☑ Accepted for Publication ☐ Submitted for Publication ☐ Unpublished and Unsubmitted work written in manuscript style
Publication Details	Shaheer Maher, Denver Linklater, Hadi Rastin, Pei Le Yap, Elena P. Ivanova and Dusan LosicTailoring Additively Manufactured Titanium Implants for Short-Time Pediatric Implantations with Enhanced Bactericidal Activity, ChemMedChem

Principal Author

Name of Principal Author (Candidate)	Shaheer Maher (*also known* as Shaheer Makar)		
Contribution to the Paper	Study design, samples preparation, performed characterization on all samples, participated in bacterial studies, interpreted data and wrote manuscript		
Overall percentage (%)	85%		
Certification:	This paper reports on original research I conducted during the period of my Higher Degree by Research candidature and is not subject to any obligations or contractual agreements with a third party that would constrain its inclusion in this thesis. I am the primary author of this paper.		
Signature		Date	03/09/2021

Co-Author Contributions

By signing the Statement of Authorship, each author certifies that:

i. the candidate's stated contribution to the publication is accurate (as detailed above);

ii. permission is granted for the candidate in include the publication in the thesis; and

iii. the sum of all co-author contributions is equal to 100% less the candidate's stated contribution.

Name of Co-Author	Dusan Losic		
Contribution to the Paper	Supervised the development of the work, revised the manuscript and acted as corresponding author		
Signature		Date	03/09/2021

Name of Co-Author			
Contribution to the Paper			
Signature		Date	

Please cut and paste additional co-author panels here as required.

ChemMedChem
Full Papers
doi.org/10.1002/cmdc.202100580
Chemistry Europe
European Chemical Societies Publishing
www.chemmedchem.org

Special Collection

Tailoring Additively Manufactured Titanium Implants for Short-Time Pediatric Implantations with Enhanced Bactericidal Activity

Shaheer Maher,[a, b] Denver Linklater,[c] Hadi Rastin,[a] Pei Le Yap,[a] Elena P. Ivanova,[c, d] and Dusan Losic*[a]

Paediatric titanium (Ti) implants are used for the short-term fixation of fractures, after which they are removed. However, bone overgrowth on the implant surface can complicate their removal. The current Ti implants research focuses on improving their osseointegration and antibacterial properties for long-term use while overlooking the requirements of temporary implants. This paper presents the engineering of additively manufactured Ti implants with antibacterial properties and prevention of bone cell overgrowth. 3D-printed implants were fabricated followed by electrochemical anodization to generate vertically aligned titania nanotubes (TNTs) on the surface with specific diameters (~100 nm) to reduce cell attachment and proliferation. To achieve enhanced antibacterial performance, TNTs were coated with gallium nitrate as antibacterial agent. The physicochemical characteristics of these implants assessed by the attachment, growth and viability of osteoblastic MG-63 cells showed significantly reduced cell attachment and proliferation, confirming the ability of TNTs surface to avoid cell overgrowth. Gallium coated TNTs showed strong antibacterial activity against *S. aureus* and *P. aeruginosa* with reduced bacterial attachment and high rates of bacterial death. Thus a new approach for the engineering of temporary Ti implants with enhanced bactericidal properties with reduced bone cell attachment is demonstrated as a new strategy toward a new generation of short-term implants in paediatrics.

Introduction

Titanium (Ti) and its alloys have been widely utilized in pediatrics in the management of bone fractures, trauma or the correction of anatomical deformities (*e.g.*, pins, nails, plates, external fixators or frames).[1] The majority of these implantations in pediatrics requires the removal of the implants after their intended function is fulfilled in order to avoid many complications such as bone growth arrest, bone remodeling, implant fracture upon continuous pressure, implant migration or bone resorption.[2] Other reasons for implant removal also include pain, infection, dislodgement or, in some cases, carcinogenesis.[2c] Given that the implants should be removed, excessive bone growth or attachment onto the implant surface is not desirable and can be a major problem for implants removal leading to increased costs, implant breakage during its removal or excision of bone tissue, which in turn enhances the susceptibility to re-fracture.[2a] Thus, an ideal implant for pediatric applications should not support bone cell overgrowth on its surface, while achieving the desired bone fixation during its short-term application. These requirements are opposite to conventional long-term implants where fast and strong osseointegration, combined with antibacterial protection, are two of the most desirable functions and it is not surprising there is a very limited number of studies on surface modification of Ti to reduce bone growth and osseointegration.

Since the implant surface is the first site of interaction with bone cells, recent studies have confirmed the influence of its surface topography and properties on cells adhesion, proliferation and differentiation.[3] However, the impact of surface roughness (e.g. micro or nano) and surface feature geometry (pores, tubes, particles, rods, wires, spikes etc.) on bone tissue formation is still inconclusive, making it difficult to compare the influence of these topographical features.[3d] For example, Cavalacanti-Adam *et al.* showed that titania nanotubes with diameters ~100 nm can disrupt integrin clusters and thus inhibits cellular adhesion and proliferation.[4] On the other hand, He *et al.* showed that nanopores (30 nm in diameter) promoted cell adhesion and improved healing *in-vivo*.[5] It is important to mention that the majority of the research done so far focused on enhancing cells-surface interaction for the development of implants which remain in the body for an extended period (*e.g.*, hip or knee replacements)[6] with only a few studies involving the design of implants for short-term use.[2c,7]

[a] S. Maher, Dr. H. Rastin, Dr. P. Le Yap, Prof. D. Losic
School of Chemical Engineering and Advanced Materials
The University of Adelaide, Adelaide SA 5005 (Australia)
E-mail: dusan.losic@adelaide.edu.au
[b] S. Maher
Faculty of Pharmacy, Assiut University
Assiut, 71526 (Egypt)
[c] Dr. D. Linklater, Prof. E. P. Ivanova
College of STEM, School of Science
RMIT University, Melbourne VIC 3000 (Australia)
[d] Prof. E. P. Ivanova
Australian Research Council (ARC) Training Centre in Surface Engineering for Advanced Materials (SEAM)
Swinburne University of Technology
Hawthorn VIC 3122 (Australia)

This article belongs to the Special Collection "Nanomedicine: Drug Delivery and Nanodrugs".

ChemMedChem
Full Papers
doi.org/10.1002/cmdc.202100580
Chemistry Europe
European Chemical Societies Publishing

Bone overgrowth is not the only limitation that affects the performance and functionality of temporary implants in pediatrics; bacterial infection is considered another major problem that could result in implant failure or bone sepsis before complete bone healing is achieved.[6c] Systemic antibiotics administration is the most common practice to prevent and treat implants related bacterial infections.[8] However, the concentration of antibiotic reaching the site of the implant is often inadequate to infiltrate the bacterial biofilm leading to treatment failure.[9] As a result, localized drug delivery through coating of implants with antibiotics seems to be a promising approach.[3a,10] However, the local application of antibiotics at the implant site (*e.g.*, antibiotic-loaded cement) can cause localized cell toxicity and contributes to the development of antibiotic-resistant bacterial strains, such as methicillin-resistant *Staphylococcus aureus* (MRSA).[11] To address the problems of antimicrobial resistance (AMR), considerable research effort has been focused on exploring alternative approaches to conventional Ti implants. Recent advancements in the design of antibacterial Ti biomaterials include incorporating non-conventional metal antibacterial agents such as silver, copper and gallium,[12] altering surface properties such as charge, and hydrophobicity by chemical modification, or engineering of the surface topography,[8,13] physical contact killing of bacteria by sharp surface nanostructures[14] or using drug-releasing titania nanotubes (TNTs) structures loaded with antibacterial drugs.[15]

Additive manufacturing, or 3D-printing technology, has triggered a revolution in the manufacturing sector across various industries including Ti orthopedic and dental implants. Selective laser melting (SLM) is an example of a 3D-printing technique for implant fabrication with the ability to print a variety of metals (*e.g.*, Ti based, stainless steel, Mg, Zn, and Ta) while reducing manufacturing waste and the overall costs of medical implants.[16] SLM can also print metal combinations or metal/ceramic combination implants with no post-processing requirements that are usually necessary for traditional techniques such as casting or machining.[17] More importantly, 3D-printing of the implants provides design flexibility with the ability to fabricate low-cost implants with complex geometries to mimic bone porosity.[18] Moreover, it can offer "on demand" production of implants specifically tailored for children that is fast, and reliable for the best anatomical match using computer-aided design models saving time and costs.[18a,19]

Considering the above discussions, herein, we present a study to demonstrate the design of antibacterial 3D-printed Ti materials for short-term implantations, such as those used in pediatrics, that are able to prevent bacterial infection and reduce excessive cell-surface interaction to allow easier implant removal. To address this challenge, 3D-printed Ti alloy implants with micro-nano hierarchical topographies were fabricated using SLM followed by electrochemical anodization (EA) to generate TNTs on the surface with controlled diameters of 100 nm, which has been shown in previous studies to be optimal for the reduction of cell surface adhesion.[20] To simultaneously enhance the bactericidal properties, the fabricated Ti implants were coated with gallium nitrate. The release of Ga^{3-} is well known to possess strong antibacterial activity based on its ability to interfere with bacterial metabolic activity.[12c] The design and fabrication of the engineered Ti implants is shown schematically in Figure 1. The attachment, proliferation, and viability of osteoblastic MG-63 cells was assessed to evaluate the suitability of the modified Ti topography as a short-term implantable material. Furthermore, the antibacterial activity of Ga^{3-} and TNTs was evaluated against two common human bacterial pathogens; gram-positive *Staphylococcus aureus* and gram-negative *Pseudomonas aeruginosa*.[21] The results of this study provide novel insights into an innovative approach to tailor the surface of Ti implants for temporary or short-term applications, such as those used in pediatric orthopedic surgery, that is currently lacking and urgently needed.

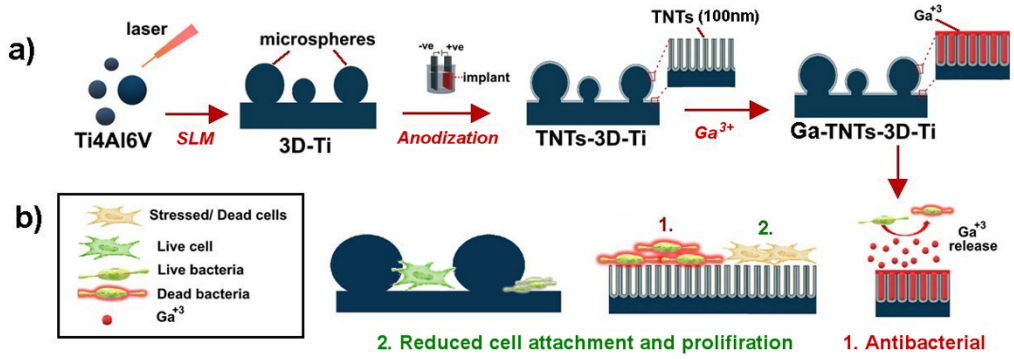

Figure 1. Illustrated representation of 3D-printed Ti implants fabrication by selective laser melting (SLM) followed by electrochemical anodization (EA) to generate a unique surface with microparticles combined with titania nanotubes (TNTs) able to control cells attachment. Ga^{3-} release used to passively kill bacteria in proximity to the implant whereas TNTs effectively reduce bone cell and bacterial attachment. The combination of microsphere and TNTs structures was designed based on the rationale to provide reduced bone cell attachment for short-term implant applications.

ChemMedChem
Full Papers
doi.org/10.1002/cmdc.202100580
Chemistry Europe
European Chemical Societies Publishing

Results and Discussion

Characterization of fabricated 3D-printed TNTs implants

To prepare TNTs structures with optimized pore diameters of ~100 nm that could provide reduced cell surface attachment, an initial study using different anodization voltages (20, 40 and 60 V) was performed. During anodization, TNTs were generated on the smooth 3D-Ti surface through etching by fluoride ions under influence of the applied electrical field.[22] SEM images, Figure 2, revealed that the TNTs diameters increased with increased voltage, in agreement with previous reports.[23] TNTs prepared at 60 V for 15 min showed the largest diameter (100 ± 20 nm) compared to those fabricated at 20 and 40 V, Figure 2d, and thus they were selected for further experiments.

The typical surface morphology of 3D-Ti implant plates before and after electrochemical anodization is shown in Figure 3 (a–c). As seen in the images, 3D-Ti is covered with microspheres possessing variable diameters ranging from *5–30* μm resulting from incomplete melting of the Ti alloy powder used during the SLM process[22] . It is important to state that the fabricated discs were subjected to extensive sonication prior to further processing to remove any loosely attached spheres and the remaining microspheres were firmly attached to the surface as we previously confirmed.[22,24]

The surface topography of selected TNTs-3D-Ti (anodized at 60 V), presented in SEM images in Figure 3 (d–f), revealed a typical array of vertically aligned TNTs structures covering the whole surface including the microspheres and underlying surface. The random cracks are observed across the entirety of the TNTs surface as a result of the mechanical expansion during the growth of the titanium oxide (TiO_2) layer initiated by the electrochemical anodization process. The images confirm that the microspheres and TNTs films with these cracks were stable and endured the conditions of the electrochemical anodization process and following sonication. After fabrication of TNTs, the surface of the TNTs-3D-Ti discs were coated with a layer of gallium nitrate for enhanced antibacterial activity. As observed in Figure 3 (g-i), the Ga^{3+} layer completely covered the TNTs surface, confirming successful coating of the antibacterial agent.

The chemical composition of the surface of fabricated 3D-Ti and TNTs-3D-Ti discs was analyzed by using EDX, as shown in Figure 4 (a-c). Typical peaks corresponding to Ti6Al4 V alloy are displayed in spectra obtained from all samples. After anodization, a prominent oxygen peak was observed as a result of TiO_2 layer (i.e., TNTs) formation on TNTs-3D-Ti, Figure 4b. In addition, a Ga peak appeared in spectra obtained for Ga-TNTs-3D-Ti after gallium nitrate coating, confirming successful coating as seen in Figure 3c. These results were also confirmed by XRD analysis, Figure 4 (d–f), in which anatase TiO_2 peaks (JCPDS 21-1272) appeared after anodization and a peak corresponding to gallium oxide appeared in Figure 3f confirming the deposition of gallium on the surface (JCPDS 06-0180).

Water contact angle (WCA) measurements on 3D-Ti surfaces confirmed their hydrophobicity with a WCA of 133 ± 1°, as presented in Figure 4g. After anodization, TNTs-3D-Ti surface showed super-hydrophilic properties as a result of TNTs formation, which is in agreement with previous reports,[22,25] Figure 4h. At the same time, the deposition of Ga^{3+} layer did not change the hydrophilic properties of the TNTs-3D-Ti surface with the WCA estimated to be < 10°, as shown in Figure 4i. Notably, surface hydrophilicity has been confirmed to reduce bacterial attachment on Ti implants.[26]

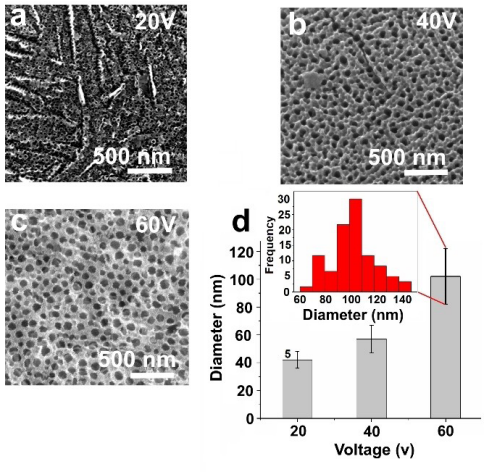

Figure 2. Effect of voltage on TNTs diameter. (a–c) High resolution SEM images showing TNTs formed under different applied voltage (20 V, 40 V and 60 V) and (d) influence of voltage on the diameter of TNTs (Values are expressed as the mean ± SD), inset showing size distribution of TNTs diameters prepared at 60 V.

Gallium coating and *in-vitro* release from Ga-TNTs-3D-Ti implants

In-vitro Ga^{3+} release from Ga-TNTs-3D-Ti was assessed following incubation in PBS at 37 °C for 5 days. The typical release kinetics are presented in Figure 5. The overall Ga^{3+} release is shown to have two characteristic patterns: 1) a burst release during the first 6 h and 2) slow release over many days. A burst release pattern was observed for the initial 6 h incubation as a result of the rapid dissolution of the gallium nitrate layer covering the top surface (Figure 5b). After that, a slower release pattern was achieved with zero order kinetics due to the dissolution of Ga^{3+} trapped inside the TNTs structures. The higher Ga^{3+} release rate (~40 μg/h) at an early stage is particularly beneficial for fast eradication of bacteria at the surgical site in order to prevent possible bacterial infection that might occur either on the implant surface or in the nearby tissues within the first few hours of the implant life. At the same time, the slow release (~3 μg/h) over following days after surgery can provide enduring bactericidal activity, preventing potential infections.

To verify the dissolution pattern of Ga^{3+} layer in physiological conditions, the prepared samples were collected at

ChemMedChem
Full Papers
doi.org/10.1002/cmdc.202100580
Chemistry Europe
European Chemical Societies Publishing

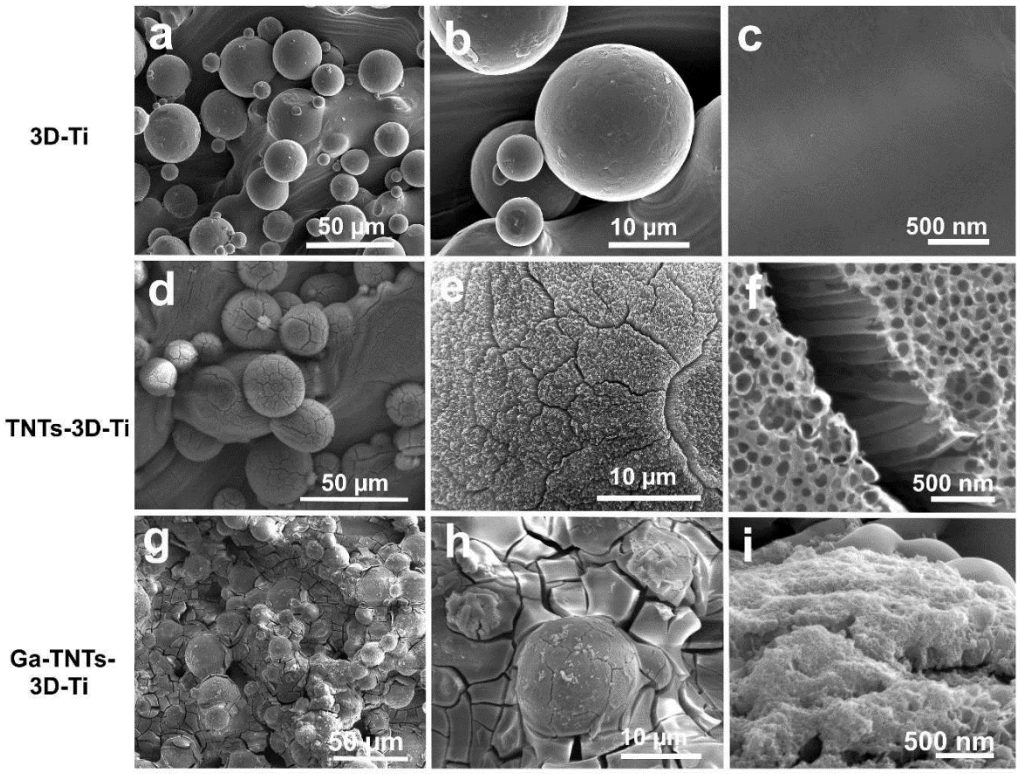

Figure 3. SEM images showing (a-c) the top surface of 3D-Ti, (d–f) TNTs-3D-Ti with arrays of titania nanotubes generated after electrochemical anodization of 3D-Ti and (g–h) Ga-HT-TNTs-3D-Ti with Ga^{3+} layer covering the whole surface. Images confirm the microstructure stability after both electrochemical anodization. (TNT: titania nanotubes, Ga: gallium).

different time points (3 and 5 days) after immersion in PBS at 37 °C and imaged using SEM, as presented in Figure 5c. SEM images clearly revealed partial dissolution of the gallium nitrate layer after 3 days, evidenced by the partial exposure of the surface TNTs. On day 5, the gallium nitrate layer was almost completely dissolved, virtually exposing the TNTs surface, as shown in Figure 5d. Only a few crystals were remaining, as denoted by the red arrows in Figure 5d. Thus, the gallium nitrate coating on modified Ti implants is expected to provide a sufficient concentration of Ga^{3+} to kill bacteria within the first few days. Following the complete dissolution of gallium nitrate layer, it is expected that the TNTs will be exposed to directly physically interact with bone cells and any remaining bacteria.

The influence of micro/nano surface topography on MG-63 viability, proliferation, and morphology

To test our hypothesis that 3D-Ti surfaces possessing TNTs with optimized diameters of ~100 nm can prevent bone cell overgrowth through excessive cell attachment and proliferation, we examined the viability and proliferation of MG-63 human osteoblastic cells on 3D-Ti and TNTs-3D-Ti discs at 1, 4 and 7 days of culture, as shown in Figure 6. Since the gallium nitrate layer dissolved within 5 days in physiological buffer, as confirmed during the *in-vitro* release study, only Ga^{3+} free samples were investigated. The cytotoxicity of Ga^{3+} ions toward human cells was previously studied for applications where Ga^{3+} can potentially make direct or indirect contact to biomaterials or human tissues. Results showed that Ga^{3+} possess no cytotoxic effect except when used in concentrations above 100 µM, which is much higher than the amount used in our experiments.[27] In addition, Ga^{3+} is currently approved by the Food and Drug Administration (FDA) as an anti-tumor and anti-hypercalcemia drug.[28]

As indicated in Figure 6a, no significant difference in cell viability was observed at day 1 between 3D-Ti and TNTs-3D-Ti. However, on days 4 and 7, the cell viability on TNTs-3D-Ti was significantly ($p < 0.0001$) reduced compared to the 3D-Ti. TNTs-3D-Ti did not show substantial cell growth at 4 and 7 days of incubation, suggesting that it might slow or hinder MG-63 cell growth. Previous studies showed that TNTs with a diameter

ChemMedChem
Full Papers
doi.org/10.1002/cmdc.202100580
Chemistry Europe
European Chemical Societies Publishing

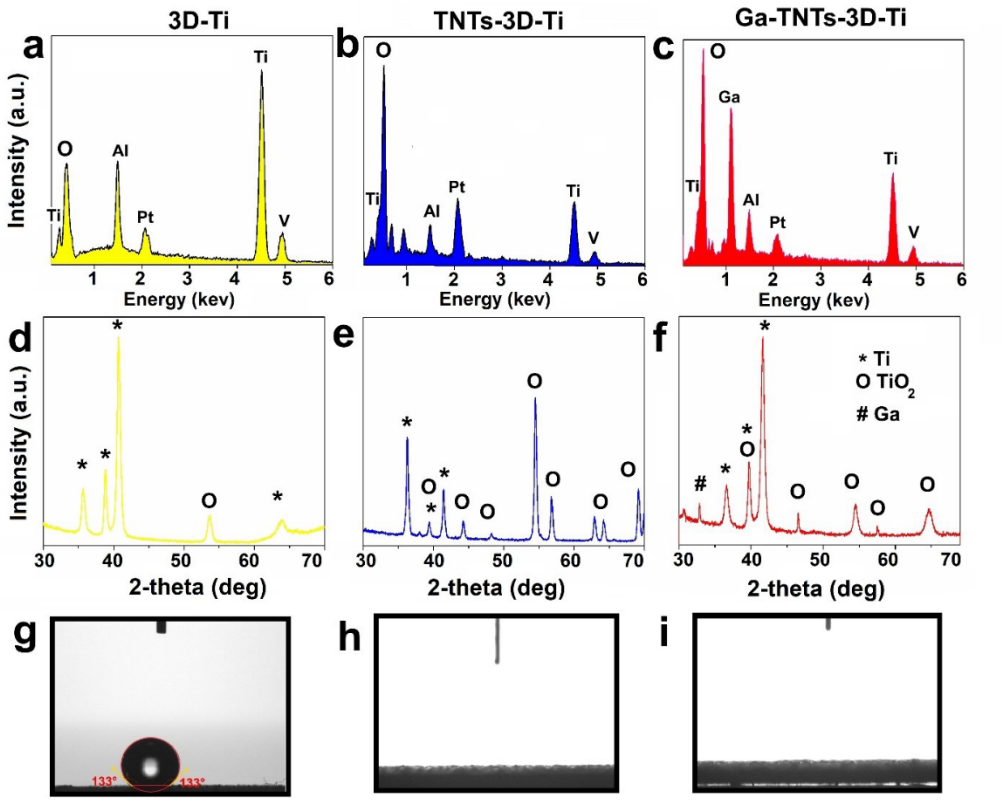

Figure 4. Characterization and surface properties of 3D-Ti, TNTs-3D-Ti and Ga-TNTs-3D-Ti. (a–c) EDX spectra, (d–f) XRD patterns with peaks corresponding to Ti, anatase TiO_2 and Ga^{3+} layer, and (g–i) wetting properties of each respective surface as confirmed by water contact angle (WCA). (TNT: titania nanotubes. Ga: gallium)

>90 nm could impair cell spreading and adhesion due to the inhibition of integrin clustering and reduction of focal adhesion contact point formation.[5,29] Next, cytotoxicity of the fabricated Ti implants was assessed toward MG-63 cells as a function of their cell membrane integrity. As was similarly observed from the results of the MTS assay, Figure 6b shows no significant difference between LDH release from cells attached on 3D-Ti and TNTs-3D-Ti at day 1. However, at longer incubation times, TNTs-3D-Ti showed a significant ($p<0.05$) increase of cytotoxicity toward MG 63 cells compared to the glass control. After 4 and 7 days, cells cultured on TNTs-3D-Ti released a significantly higher amount of LDH compared to 3D-Ti and glass, indicating cell membrane damage to attached cells, which agrees with the lower cell viability observed from MTS assay results.

Live/dead fluorescent staining was then applied to directly confirm cell viability and attachment density at 1-, 4- and 7-days incubation (Figure 6c). After 24 h, the percentage of viable cells on 3D-Ti was approximately 25–30% higher than on TNTs-3D-Ti. There was a significant ($p<0.0001$) increase in the number of viable cells observed on 3D-Ti at day 7 (Figure 6d). A similar trend was observed for cell density (cell number/cm^2), Figure 6e, in which the cell density on TNTs-3D-Ti was significantly lower ($p<0.0001$) than on 3D-Ti after 7 days of culture. The density increased significantly on 3D-Ti at day 7 compared to days 1 and 4, while cell numbers remained relatively unchanged on TNTs-3D-Ti over the course of 7 days. All these data confirm that the fabricated TNTs with tube diameters ~100 nm can significantly reduce bone overgrowth on the surface compared to the smooth surface of 3D-Ti.

Investigation of the changes to the cell cytoskeleton by fluorescent labelling of F-actin revealed obvious deformation of the actin network structure of cells attached on TNTs-3D-Ti surfaces (Figure 6c, last column). Quantification of the focal adhesion sites by labelling of vinculin further showed MG-63 cells on 3D-Ti having a higher number (31 ± 12) of focal adhesions compared to cells on TNTs-3D-Ti (14 ± 5 focal adhesions). The reduction in the number of focal adhesion sites on TNTs-3D-Ti can be attributed to a reduction in the number of cell anchorage sites due to the gaps corresponding to TNTs pores. This, in turn, can be translated into reduced attachment of osteoblasts on the surface, as confirmed by cell attachment and viability results (*vide supra*)[14,29b].

ChemMedChem
Full Papers
doi.org/10.1002/cmdc.202100580
Chemistry Europe
European Chemical Societies Publishing

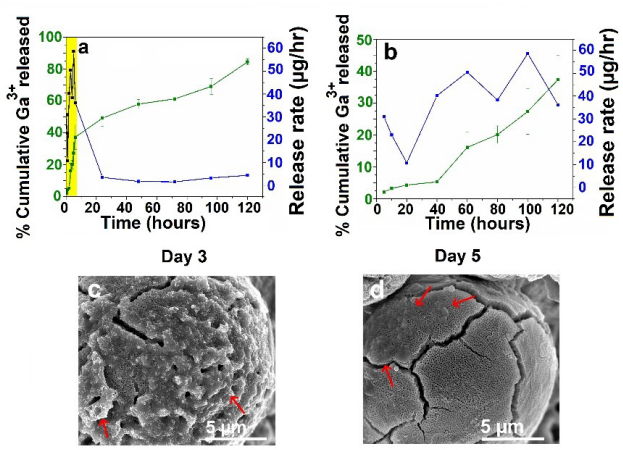

Figure 5. *In-vitro* Ga^{3+} release profiles from Ga-TNTs-3D-Ti showing % cumulative Ga^{3+} released and release rate for (a) 5 days and (b) 6 h (burst release) presenting magnified view of the yellow rectangle shown in (a), (total Ga^{3+} ~683 µg/disc). (c–d) SEM images showing dissolution of the gallium nitrate layer after 3 and 5 days. The gallium layer dissolves gradually with the TNTs surface partially exposed after 3 days while almost all the Ga^{3+} layer was dissolved within 5 days. Red arrows denoting Ga^{3+} containing layer on surface Values are expressed as the mean ± SD for at least 3 triplicates.

Next, the impact of TNTs on cell morphology and proliferation was visually examined under high resolution SEM, as shown in Figure 7. At day 1, the few cells detected on TNTs-3D-Ti exhibited a rounded morphology and were mostly attached under the shield of the microsphere structures, Figure 7b, which serves to indicate that the TNT surface is not favored by the cells. On the contrary, MG-63 cells on 3D-Ti showed the production of numerous cell extensions, forming multiple focal adhesions on the surface, as shown in Figure 7a. After 4 days of incubation, more cells showing a polygonal shape were observed on 3D-Ti, Figure 7c. At day 7, Figure 7e and f show a high density of cell spreading on 3D-Ti in contrast to TNTs-3D-Ti where only a few rounded cells were detected, as shown by the red arrows.

Based on the above results, we can conclude that the nanoporous structures of TNTs-3D-Ti did not support cell attachment. As a result, TNTs-3D-Ti could be potentially used for temporary fracture fixation to reduce bone cell overgrowth on the implant surface.[30] Another potential application of TNTs-3D-Ti surface is that they may hamper the growth of cancer cells, thus, they can be placed at the cancer site to provide temporal support and anti-cancer drug release, as we showed before. The implants can be subsequently removed easily after cancer treatment to allow the healthy bone tissue to regenerate.[22,31] It is important to note that this application will need further studies to be confirmed.

Antibacterial performance of Ga^{3+} coated (Ga-TNTs-3D-Ti) implants

To evaluate the antibacterial activity of Ga-TNTs-3D-Ti surfaces toward *S. aureus* and *P. aeruginosa*, standard plate count techniques were employed to assess CFU mL^{-1} following a 5 h bacterial incubation. Ga-TNTs-3D-Ti showed 100% eradication of both bacterial strains as compared to polystyrene and Ga^{3+} free TNTs-3D-Ti surfaces as control substrata, Figure 8a. Owing to the structural similarity between Ga^{3+} and iron (Fe), bacterial cells uptake Ga^{3+} instead of Fe which results in inhibition of Fe-dependent oxidation and reduction reactions essential for bacterial DNA synthesis, ultimately causing bacterial cell death.[12c] Notably, Ga^{3+} can also enhance osteoblast growth and inhibit bone breakdown. These characteristics make Ga^{3+} a potential candidate for coating additives and composite materials that simultaneously protect against bone infections while promoting bone healing.[11a,12c,d]

The bactericidal activity of Ga^{3+} ions released during the in-*vitro* experiments was also evaluated. Solutions containing released Ga^{3+} ions were collected after surfaces had been maintained in PBS for 5 days. Aliquots of Ga^{3+} containing physiological buffer was then incubated with *S. aureus* and *P. aeruginosa* bacterial suspensions. A significant reduction ($p < 0.0001$) of bacterial cells was observed, as shown in Figure 8b, confirming the antibacterial efficacy of dissolved Ga^{3+}. Based on the Ga^{3+} release pattern and its significant antibacterial activity, it is expected that Ga^{3+} will be effective against bacterial infection arising during the surgical procedure or after implant insertion from infected wounds or haematogenous seeding within the patient's body.[32]

ChemMedChem
Full Papers
doi.org/10.1002/cmdc.202100580
Chemistry Europe
European Chemical Societies Publishing

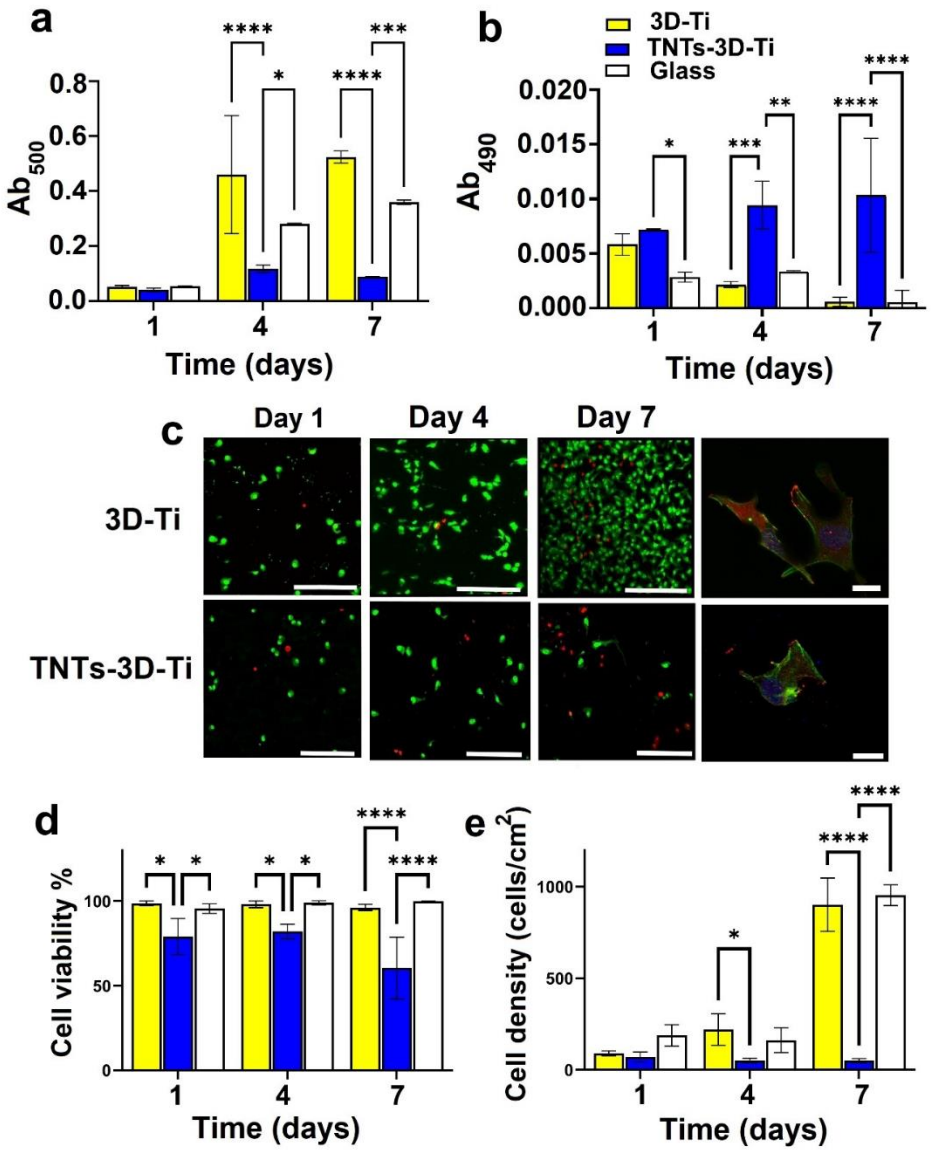

Figure 6. The viability and attachment density of osteoblast-like MG-63 cells after 1-, 4- and 7-days incubation on 3D-Ti and TNTs-3D-Ti in comparison to the control group (glass). (a) MTS assay showing cell viability on days 1, 4 and 7, (b) LDH release from MG-63 cells (normalized with cells numbers) after 1, 4 and 7 days, (c) *First three columns*, representative images of live/dead staining of MG-63 (live cells, red; dead cells, green). Scale bars = 200 μm, *last column*: confocal images showing cytoskeletal morphology and distribution of focal adhesion sites in MG-63 after 4 days of incubation. Phalloidin labelled F-actin (green), Alexa Fluor 594 labelled vinculin staining for the observation of focal adhesion (red) and TO-PRO-3 nuclear stain (blue) are shown. Scale bars = 20 μm. (d) cell viability (quantified by calculating live and dead cell numbers from the confocal images, cell viability (%) = number of live cells/number of total cells ×100%), and (e) Cell density. Values are expressed as the mean ± SD for at least 3 replicates. Statistically significant differences are labelled as *: $p < 0.05$; **: $p < 0.01$; ***: $p < 0.001$, ****: $p < 0.0001$. (TNTs: titania nanotubes)

After the dissolution of the gallium nitrate layer, TNTs will be exposed to the surrounding environment inside the body. Thus, we then examined TNTs generated on 3D-Ti for their potential physical antibacterial activity toward *S. aureus* and *P. aeruginosa*. The TNTs-3D-Ti surfaces were incubated with bacteria for 18 h and then the bacterial attachment and viability on surface were assessed using CLSM. Fluorescence microscopy was used in comparison to plate count techniques to assess the

ChemMedChem
Full Papers
doi.org/10.1002/cmdc.202100580
Chemistry Europe
European Chemical Societies Publishing

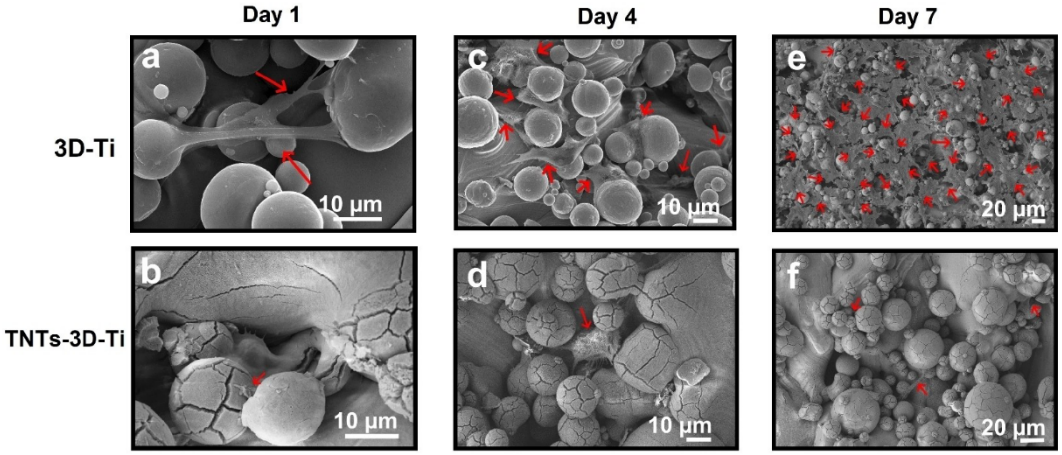

Figure 7. The morphology of MG-63 cells grown on 3D-Ti and TNTs-3D-Ti. High resolution SEM images showing the attachment and spreading of MG-63 osteoblast-like cells (indicated by the red arrows) with only a few cells attached on TNTs-3D-Ti (TNTs: titania nanotubes).

physical antibacterial action of surface nanostructures by direct observation of cell attachment and membrane integrity. Fluorescent micrographs of the bacterial attachment and proportion of live *vs* dead bacteria, as determined by live/dead staining using Syto9 (green, viable) and propidium iodide (red, non-viable) are shown in Figure 8c. Bacterial attachment, as calculated from CLSM images, show no significant difference between attachment of *S. aureus* to 3D-Ti and TNTs-3D-Ti; however, TNTs-3D-Ti experienced significantly ($p < 0.0001$) reduced levels of *P. aeruginosa* attachment with $\sim 16 \times 10^3 \pm 11 \times 10^3$ cells/mm^2 compared to 3D-Ti with $\sim 58 \times 10^3 \pm 16 \times 10^3$ attached cells/mm^2, Figure 8d.

The ability of the surface topography to physically inactivate bacteria significantly varied according to bacterial strain. TNTs-3D-Ti displayed high antibacterial efficiency against *P. aeruginosa* cells compared to *S. aureus*. This variation in antibacterial activity could be attributed to the difference in structure and thickness of the bacterial envelope between *S. aureus* (gram positive) and *P. aeruginosa* (gram negative). Gram negative bacteria are surrounded by a thin outer membrane made of lipopolysaccharide which can be easily damaged, causing bacterial death.[33] Despite the lack of such membrane in Gram positive bacteria, they are encapsuled by several layers of peptidoglycan which are ~5 times thicker than that of gram-negative bacteria. The presence of this stiff peptidoglycan layer protects *S. aureus* against the physical damage induced by TNTs.[33] In addition, both *S. aureus*. and *P. aeruginosa* appeared deformed on TNTs-3D-Ti compared to 3D-Ti as shown in SEM images, Figure 9.

Overall, the results confirm the significant influence of TNTs on the degree of bacterial retention, which was dependent on the bacterial strain (i.e., more obvious for *P. aeruginosa* than *S. aureus*). Accordingly, it can be concluded that TNTs-3D-Ti could relatively reduce the occurrence of bacterial attachment and kill bacteria that do attach on implants surface compared to smooth 3D-Ti surface.

Conclusion

The fabrication of 3D-printed Ti implants with arrays of TNTs by combination of selective laser melting and electrochemical anodization followed by Ga^{3+} coating was successfully demonstrated as a new concept proposed for a short-term implant application with enhanced bactericidal efficacy and reduced bone cell attachment. Our results showed that TNTs with tailored pore diameters (~100 nm) can be used to control the attachment and overgrowth of bone cells on the surface of the implant. This structural property makes them suitable for application as a temporary implant material intended to be removed from the body.

Superior antibacterial activity of the fabricated implant models was successfully achieved by coating of Ga^{3+} as a non-conventional antibacterial agent that demonstrated the ability to provide sufficient concentrations of Ga^{3+} able to effectively eradicate 100% of bacteria. Interestingly, the physical (mechano-)bactericidal activity of TNTs was significantly dependent on the bacterial strain; Ga^{3+} free 3D-Ti-TNTs surfaces could significantly kill *P. aeruginosa* while simultaneously reducing their surface attachment, in contrast to *S. aureus*, which were more resistant to the mechanical bactericidal action.

The presented work confirms the potential of a new generation of low-cost, removable implants whose performance can be enhanced by dual combination of surface topography and drug-releasing functionality that enables control of bone cell response while effectively inhibiting bacterial colonization. Nevertheless, further studies are required for optimization of cellular response and tuning of the antibacterial performances

ChemMedChem
Full Papers
doi.org/10.1002/cmdc.202100580
Chemistry Europe
European Chemical Societies Publishing

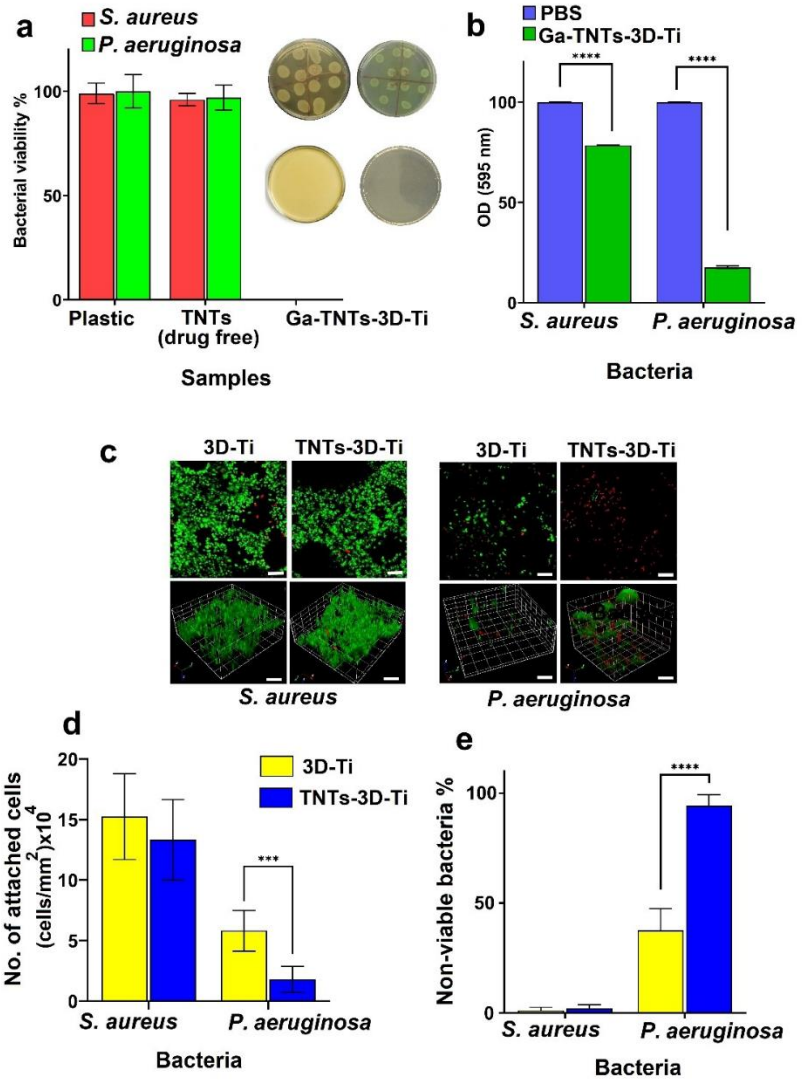

Figure 8. Antibacterial activity of Ga^{3+} coated discs and TNTs showing (a) 100% bacterial eradication on Ga-TNTs-3D-Ti compared to controls. (b) Significant reduction of bacterial proliferation when exposed to solutions containing the *in-vitro* release of Ga^{3+} in PBS for 5 days against both bacterial strains. (c) Representative CLSM micrographs of *S. aureus* and *P. aeruginosa* bacterial growth (upper raw), 3D reconstructions of the CLSM z-series (bottom raw), scale bars = 10 μm. (d) Attachment of *S. aureus* and *P. aeruginosa* on 3D-Ti and TNTs-3D-Ti and (e) antibacterial activity of 3D-Ti and TNTs-3D-Ti against both bacterial strains. Values are expressed as the mean ± SD for at least 3 replicates. Statistically significant differences are labelled as *: $p < 0.05$; **: $p < 0.01$; ***: $p < 0.001$, ****: $p < 0.0001$. (TNTs: titania nanotubes)

of fabricated 3D-printed implantable Ti materials; however, we have successfully validated their potential to be transformed into the next stage of *in-vivo* and clinical studies.

Experimental Section

Fabrication of 3D Ti implants

Ti6Al4 V powder (Titanium grade 5, TLS Technik GmbH & Co. Spezialpulver, Germany) was used to fabricate 3D-Ti discs of size 1.5 × 1.5 cm^2 using SLM machine (ProX 200 Production 3D Printer, Phenix Systems PXM (USA), equipped with a 300 W Laser (1070 nm at 50% power)) under inert argon atmosphere. Details of the

ChemMedChem
Full Papers
doi.org/10.1002/cmdc.202100580
Chemistry Europe
European Chemical Societies Publishing

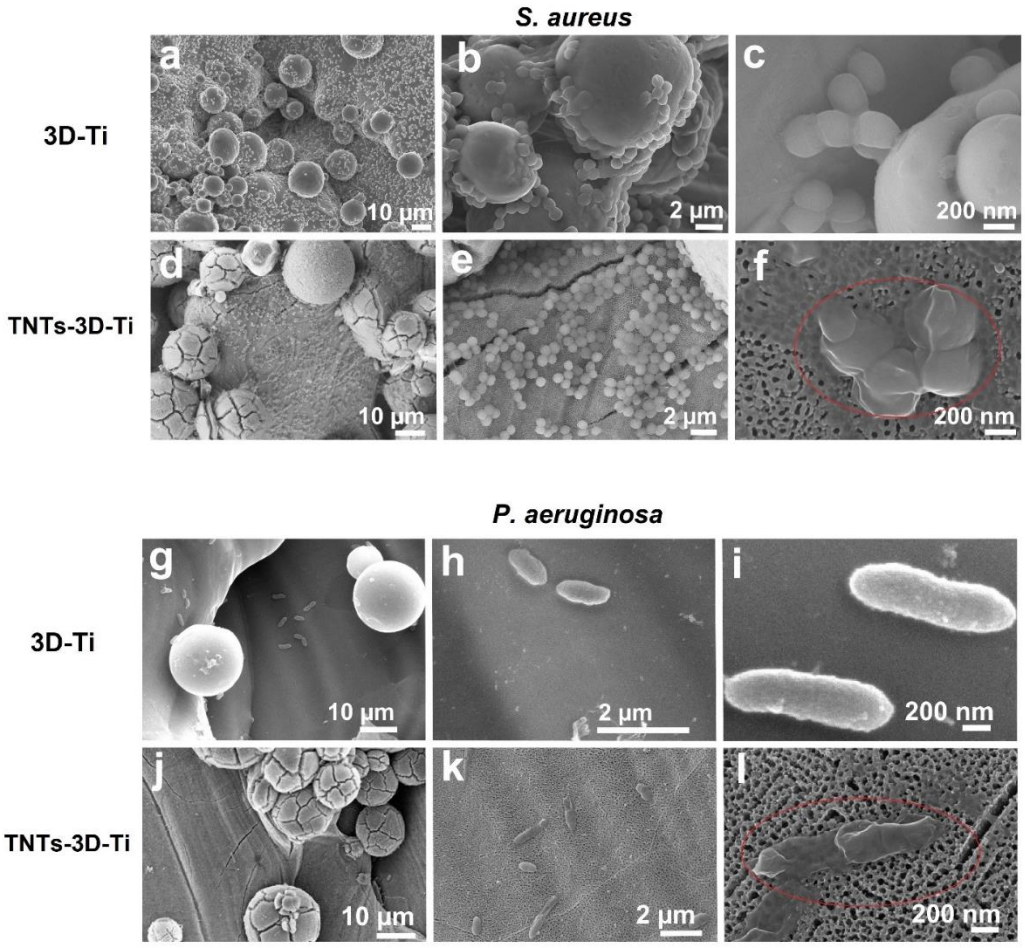

Figure 9. Attachment pattern and morphology of *S. aureus* (a-f) and *P. aeruginosa* (g-l) on 3D-Ti and TNTs-3D-Ti surfaces. SEM images showing the morphology of bacterial cells that appear healthy on 3D-Ti, in contrast to TNTs-3D-Ti in which bacterial cells appear deformed, as marked by red circles. (TNTs: titania nanotubes)

fabrication and the average diameter of particles were reported in our previous study.[22] After fabrication, the discs were cleaned by sonication in acetone for 10 min to eliminate any loosely attached powder particles. The resulting discs will be referred to as "3D-Ti".

Titania nanotubes fabrication on 3D-Ti

Titanium nanotubes (TNTs) were generated on the surface of 3D-Ti discs through electrochemical anodization (EA) process under a temperature-controlled system designed in our laboratory as described elsewhere.[22] Briefly, 3D-Ti discs were anodized in ethylene glycol electrolyte solution containing NH_4F (0.1 M), lactic acid (1.5 M) and water (5% w/w), (Chem-Supply, Australia) at 20, 40 or 60 V for 15 min with constant stirring at 60 °C. The applied voltage was controlled by programmable power supply (Agilent, USA) and current change was recorded using the LabView program (National Instruments). After anodization, the 3D-Ti discs with TNTs on top (TNTs-3D-Ti) were sonicated in Milli-Q water for 5 min to remove any remaining chemicals.

All samples (*i.e.*, 3D-Ti and TNTs-3D-Ti) were placed in Milli-Q water for 2 weeks prior to bacterial studies to ensure the complete removal of any residual chemicals from the fabrication process.

Gallium nitrate coating onto TNTs-3D-Ti

Gallium nitrate was coated on TNTs-3D-Ti by application of 10 µL of gallium nitrate solution (10 mg mL^{-1}) on the surface and leaving to dry under vacuum for 1 h at room temperature to remove air gaps inside the TNTs. Each disc was loaded with 2500 µg of gallium nitrate (equivalent to ~683 µg of Ga^{3+}/disc) by repeating this step 25 times.

ChemMedChem
Full Papers
doi.org/10.1002/cmdc.202100580
Chemistry Europe
European Chemical Societies Publishing

Characterization

High resolution images of the fabricated Ti implants (3D-Ti and TNTs-3D-Ti) were recorded using focused ion beam (FIB)-scanning electron microscopy (SEM) (FEI Helios Nanolab 600 Dual Beam, Thermo Fisher Scientific, Australia). The chemical composition of the surface was analyzed using energy-dispersive X-ray spectroscopy (EDX, Oxford Ultim Max Large Area SDD EDS detector, Oxford instruments, USA). All substrata were coated with platinum (5 nm) prior to imaging. X-ray diffraction spectra (XRD, Rigaku MiniFlex 600, Japan) were obtained to show crystallinity of the surface micro-nano structures at a scanning rate of 10 degrees per min using $Cu_{k\alpha}$ radiation over the range of 30–80°. Water contact angle (WCA) measurements were also recorded using sessile drop method at room temperature using a tension theta optical tensiometer (KSV instruments, Finland). Three samples were tested with at least three separate measurements were taken for each one. WCA was measured over 10 seconds using 5 μl of Milli-Q water.

In-vitro Ga^{3+} release

The *in-vitro* Ga^{3+} release was assessed by placing gallium nitrate coated discs (Ga-TNTs-3D-Ti) in 4 mL of PBS (pH 7.4) at 37 °C for 5 days. At a predetermined time, 400 μL of solution containing Ga^{3+} was collected and replaced with fresh PBS to maintain sink conditions.[34]

All collected release samples were stored at 4 °C until further analysis. Gallium content was analyzed using inductively coupled plasma mass spectrometry (ICP-MS Triple Quad, Agilent 8900, USA). Prior to analysis, all samples were diluted 100 times with 2% HNO_3 and then filtered with 0.22 Millipore filter prior to analysis. A calibration curve was constructed using ICP standard solution for gallium. TNTs-3D-Ti discs (*i.e.*, Ga^{3+} fee) were also placed in PBS as a blank under the same conditions. All experiments were repeated in triplicates and the data were analyzed for statistical significance.

Cell culture

Human osteosarcoma (osteoblast-like) MG-63 cells were purchased from Sigma-Aldrich (USA). Cells were cultured in 75 cm^2 cell culture (T75) flasks with Dulbecco's Modified Eagle Medium with GlutaMAX™ (Life Technologies, Inc.), supplemented with 10% fetal bovine serum, 1% Penicillin-Streptomycin (Sigma) at 37 °C in a humidified atmosphere with 5% CO_2. Cells were passaged for subculture when the cell density achieved 90% confluency. Prior to cell seeding, Ti discs and glass slides (positive control groups) were sterilized with 70% (v/v) ethanol for 10 minutes and washed twice with sterile PBS then allowed to dry overnight. MG-63 cells were subsequently seeded on the samples at a density of 2×10^4 cells cm^{-2} and incubated at 37 °C in a humidified atmosphere with 5% CO_2. The cell density was calculated using a hemocytometer.

Cell proliferation

Cell proliferation was studied using 3-(4,5-dimethylthiazol-2-yl)-5-(3-carboxymethoxyphenyl)-2-(4-sulfophenyl)-2 h tetrazolium (MTS) assay. Samples were collected after 1, 4 and 7 days of incubation and gently washed twice with PBS buffer to remove unattached cells. Afterward, the samples were transferred to a sterile well plate and incubated in DMEM with 20% (v/v) MTS reagent (Promega, WI, USA) at 37 °C in a humidified atmosphere with 5% CO_2 for 1.5 h. During incubation, tetrazolium salt is reduced by viable cells into a colored formazan dye. This reaction is mediated by NAD(P)H-dependent dehydrogenase enzymes in mitochondrial respiratory chain. The supernatant from each sample was then collected and the absorbance was measured at 500 nm using a POLARstar Omega microplate reader (BMG Labtech, Ortenberg, Germany).

Cytotoxicity assay

The concentration of extracellular lactate dehydrogenase (LDH) released from the cells seeded on 3D-Ti, TNTs-3D-Ti, and glass as a planar control surface was measured using UV/VIS spectrophotometry. At predetermined times 1, 4 and 7 days of incubation, 50 μL from the supernatant of each sample were collected and incubated for 30 min at room temperature with 50 μL of CytoTox 96® reagent (Non-Radioactive Cytotoxicity Assay Promega) in a new well-plate. The absorbance was then measured at 490 nm.

Dead/Live cell stain

After 1, 4 and 7 days of cells incubation, discs were washed twice with PBS and then covered with staining solution containing calcein AM (2 μM) and ethidium homodimer-1 (4 μM) (Life Technologies, Inc.) for 30 min in the dark at room temperature. Subsequently, the samples were rinsed and immersed in PBS followed by imaging *via* confocal microscopy (Olympus FluoView™ FV3000). Counts of live and dead cells were quantified using Matlab software, CellC. The cell viability percentage was measured as the ratio of the number of viable cells to total number of cells on the surface. At least 20 fluorescence images were taken for each sample (image size is 500 μm^2 and images were taken in a stepwise manner over the entirety of the 1 cm^2 sample) and each experiment was repeated in triplicate. Then, the cell numbers per independent replicate are averaged.

Immunocytochemistry and cytoskeleton staining

On the 4th day of cell culture, samples were washed twice with PBS and then fixed with 4% paraformaldehyde for 15 min. For permeabilization, samples were covered with 0.2% Triton X-100 for 15 min. After that, 1% bovine serum albumin (BSA) was used to block the samples for 30 min. Next, samples were incubated at room temperature with primary antibody, anti-Vinculin (mouse)(-Sigma-Aldrich) and secondary antibody, anti-Mouse IgG in 5% goat serum (Life Technologies, Inc) at room temperature for 1 h. Actin filaments and cell nuclei were stained with phalloidin (Invitrogen) for 20 min followed by TO-PRO™-3 Iodide (Invitrogen) for 30 min, respectively. Cells were imaged using confocal laser scanning microscopy (CLSM; LSM710 NLO, Carl Zeiss, Oberkochen),Germany.

SEM imaging

The morphology of cells attached on 3D-Ti and TNTs-3D-Ti was assessed using SEM. Samples were gently rinsed with Milli-Q water after incubation for 1, 4 and 7 days and fixed with 2.5% v/v glutaraldehyde (Sigma) and were then rinsed 2 times with Milli-Q water. The cells were dehydrated with ethanol at increasing concentrations (30, 50, 70, 90, and 100%v/v) for 10 min each and an additional 10 min in 100 v/v% ethanol. After that, samples were immersed in hexamethyldisilazane (HMDS) (Sigma) for 10 min. The samples were left to air-dry and then sputter-coated with 5 nm gold for imaging. High resolution images were recorded using the SEM capabilities of a Raith150 two direct write ultra-high-resolution electron beam lithography tool (Raith, GmBH) under high vacuum at an accelerating voltage of 3 kV.

ChemMedChem | Full Papers doi.org/10.1002/cmdc.202100580 | Chemistry Europe European Chemical Societies Publishing

Antibacterial activity assays

Bacterial strains and growth conditions

S. aureus ATCC 25923 was purchased from American Type Culture Collection (Manassas, VA, USA). *P. aeruginosa* (clinical isolate from a chronic rhinosinusitis patient) was obtained from Adelaide Pathology Partners (Mile End, Australia). The use of bacterial isolates was approved by The Local Institutional Human Research Ethics Committee (HREC/15/TQEH/132). Both bacterial stocks were stored at −80 °C in frozen glycerol broth. Prior to each experiment, 100 μL of the *S. aureus* and *P. aeruginosa* bacteria from stocks was plated on Tryptone Soy Agar (TSA) and Nutrient Agar (NA) plates, respectively, and grown overnight at 37 °C.

Antibacterial activity of gallium coated Ti implants

Ga^{3+} coated discs (Ga-TNTs-3D-Ti) were first sterilized under UV irradiation for 30 min before testing and placed in 24-well plate. Bacterial suspensions of either *S. aureus* or *P. aeruginosa* were prepared by resuspending a single colony of bacteria in broth medium to reach 0.5 MacFarland units (approximately 1.5×10^8 colony forming units (CFU)/mL)). The bacterial suspensions of *S. aureus* and *P. aeruginosa* were then diluted 1:100 in TSB and NA, respectively to obtain a final bacterial concentration of approximately 1.5×10^6 CFU mL^{-1}. Next, the surface of the samples was covered with 20 μL of bacterial suspension and were then incubated for 5 h at 37 °C. After 5 h, the samples were placed in 980 μL of sterilized saline and shaken together for 1 min to collect viable bacteria remaining on the surface.[35] After that, ten-fold serial dilution of collected bacterial suspension was plated onto agar plates (TSA for *S. aureus* and Cetrimide agar for *P. aeruginosa*) and then incubated for 24 h at 37 °C. Finally, CFU were counted. Ga^{3+} free samples (TNTs-3D-Ti) were also treated in the same way while empty plastic wells were used as positive controls taken as 100% viability. Thus, % bacterial cells viability was calculated based on the following formula:

$$\%\ \text{Bacterial Cell Viability} = \frac{CFUs}{CFUc}\ \text{x100}$$

Where *CFUs* is the average number of CFU recorded for each sample and *CFUc* is the average CFU for plastic

Antibacterial activity of the release solution

After 5 days of Ga^{3+} release, the release solutions were collected to assess the bactericidal action of the Ga^{3+}. For each sample, 0.5 mL of collected solution was mixed with 0.5 mL of bacterial suspension containing 10^4 CFU mL^{-1} and then incubated for 5 h. After that, 200 μL of the incubate were transferred to 96 well-plate and the optical density (OD) of the bacterial suspension was determined at 595 nm using a FLUOstar OPTIMA plate reader (BMG Labtech, Ortenberg, Germany), PBS with no bacteria was used as a blank and each experiment was repeated in triplicates followed by statistically analysis.[36]

Antibacterial activity of TNTs-3D-Ti implants

3D-Ti and TNTs-3D-Ti were immersed in 1 mL of bacterial suspension (adjusted to an OD_{600} 0.1 in nutrient broth) in sterile 12-well plates for 18 h at 27 °C in dark and static conditions. Discs were then rinsed gently with PBS and stained with Live/Dead Baclight (Invitrogen) and imaged with confocal laser scanning microscopy to detect the proportion of live/dead bacteria on the surface. Images were then analyzed using Matlab software, CellC to determine the bacterial counts. SEM imaging of samples with attached bacteria, after 18 h of incubation, were processed as described above.

Statistical analysis

All the results presented in this study were statistically treated and expressed as mean ± standard deviation (SD) of at least three independent experiments. Unpaired t-test and two-way ANOVA were used to analyze the data. The level for significance was set to $p < 0.05$ for all the comparisons.

Acknowledgements

The authors acknowledge the financial support provided to S.M. by Australian Research Council (ARC) (IH 15010003) grant, the Australian Government Training Program Scholarship, and Forrest George and Sandra Lynne Young Supplementary Scholarship. The authors acknowledge the contribution of Sandy Liao from RMIT for preparing cell cultures for this study. The authors are grateful to the School of Chemical Engineering at the University of Adelaide for support of this research. Authors gratefully acknowledge the RMIT Microscopy and Microanalysis Facility (RMMF) for providing access to their analytical instruments.

Conflict of Interest

The authors declare no conflict of interest.

Keywords: Titanium implants · additive manufacturing · 3D-printing · titania nanotubes · antibacterial · gallium

[1] E. N. Feins, Y. Lee, E. D. O'Cearbhaill, N. V. Vasilyev, S. Shimada, I. Friehs, D. Perrin, P. E. Hammer, H. Yamauchi, G. Marx, A. Gosline, V. Arabagi, J. M. Karp, P. J. del Nido, *Nat. Biomed. Eng.* **2017**, *1*, 818–825.
[2] a) N. G. Grün, P. L. Holweg, N. Donohue, T. Klestil, A.-M. Weinberg, *Innovative Surgical Sciences* **2018**, *3*, 119–125; b) E. A. Gorter, D. I. Vos, C. F. M. Sier, I. B. Schipper, *Eur J Trauma Emerg Surg* **2011**, *37*, 623–627; c) Z. Gugala, R. Lindsey, *Orthopaedic Knowledge Online Journal* **2015**, *13*, 1–20.
[3] a) S. Maher, A. Mazinani, M. R. Barati, D. Losic, *Expert Opin. Drug Delivery* **2018**, *15*, 1021–1037; b) J. Lincks, B. D. Boyan, C. R. Blanchard, C. H. Lohmann, Y. Liu, D. L. Cochran, D. D. Dean, Z. Schwartz, *Biomaterials* **1998**, *19*, 2219–2232; c) K. Rabel, R.-J. Kohal, T. Steinberg, P. Tomakidi, B. Rolauffs, E. Adolfsson, P. Palmero, T. Fürderer, B. Altmann, *Sci. Rep.* **2020**, *10*, 12810; d) Y. Hou, L. Yu, W. Xie, L. C. Camacho, M. Zhang, Z. Chu, Q. Wei, R. Haag, *Nano Lett.* **2020**, *20*, 748–757.
[4] E. A. Cavalcanti-Adam, T. Volberg, A. Micoulet, H. Kessler, B. Geiger, J. P. Spatz, *Biophys. J.* **2007**, *92*, 2964–2974.
[5] Y. He, Z. Li, X. Ding, B. Xu, J. Wang, Y. Li, F. Chen, F. Meng, W. Song, Y. Zhang, *Bioact. Mater.* **2021**.
[6] a) J. G. Lyons, M. A. Plantz, W. K. Hsu, E. L. Hsu, S. Minardi, *Frontiers in Bioengineering and Biotechnology* **2020**, *8*; b) L. Liang, P. Krieg, F. Rupp, E. Kimmerle-Müller, S. Spintzyk, M. Richter, G. Richter, A. Killinger, J. Geis-Gerstorfer, L. Scheideler, *Adv. Mater. Interfaces* **2019**, *6*, 1801720; c) D. Campoccia, L. Montanaro, C. R. Arciola, *Biomaterials* **2006**, *27*, 2331–2339.
[7] J. S. Hayes, I. M. Khan, C. W. Archer, R. G. Richards, *European cells & materials* **2010**, *20*, 98–108; materials **2010**, 20, 98–108.

ChemMedChem
Full Papers
doi.org/10.1002/cmdc.202100580
Chemistry Europe
European Chemical Societies Publishing

[8] X. Li, B. Wu, H. Chen, K. Nan, Y. Jin, L. Sun, B. Wang, *J. Mater. Chem. B* **2018**, *6*, 4274–4292.
[9] a) Y. Li, Y. Yang, R. Li, X. Tang, D. Guo, Y. a. Qing, Y. Qin, *Int. J. Nanomed.* **2019**, *14*, 7217–7236; b) M. Gimeno, P. Pinczowski, M. Pérez, A. Giorello, M. Á. Martínez, J. Santamaría, M. Arruebo, L. Luján, *Eur. J. Pharm. Biopharm.* **2015**, *96*, 264–271.
[10] D. Losic, M. S. Aw, A. Santos, K. Gulati, M. Bariana, *Expert Opin. Drug Delivery* **2015**, *12*, 103–127.
[11] a) B. W. Stuart, G. E. Stan, A. C. Popa, M. J. Carrington, I. Zgura, M. Necsulescu, D. M. Grant, *Bioactive Materials* **2021**; b) D. Campoccia, L. Montanaro, P. Speziale, C. R. Arciola, *Biomaterials* **2010**, *31*, 6363–6377.
[12] a) E. Zhang, X. Zhao, J. Hu, R. Wang, S. Fu, G. Qin, *Bioact. Mater.* **2021**, *6*, 2569–2612; b) A. Cochis, B. Azzimonti, R. Chiesa, L. Rimondini, M. Gasik, *ACS Biomater. Sci. Eng.* **2019**, *5*, 2815–2820; c) L. Li, H. Chang, N. Yong, M. Li, Y. Hou, W. Rao, *J. Mater. Chem. B* **2021**, *9*, 85–93; d) L. C. S. Antunes, F. Imperi, F. Minandri, P. Visca, *Antimicrob. Agents Chemother.* **2012**, *56*, 5961–5970.
[13] D. Campoccia, L. Montanaro, C. R. Arciola, *Biomaterials* **2013**, *34*, 8533–8554.
[14] T. L. Clainche, D. Linklater, S. Wong, P. Le, S. Juodkazis, X. L. Guével, J.-L. Coll, E. P. Ivanova, V. Martel-Frachet, *ACS Appl. Mater. Interfaces* **2020**, *12*, 48272–48283.
[15] K. Gulati, M. S. Aw, D. Losic, *Nanoscale Res. Lett.* **2011**, *6*, 571–576.
[16] a) J. Ni, H. Ling, S. Zhang, Z. Wang, Z. Peng, C. Benyshek, R. Zan, A. K. Miri, Z. Li, X. Zhang, J. Lee, K. J. Lee, H. J. Kim, P. Tebon, T. Hoffman, M. R. Dokmeci, N. Ashammakhi, X. Li, A. Khademhosseini, *Mater. Today Bio* **2019**, *3*, 100024; b) C. Cai, X. Wu, W. Liu, W. Zhu, H. Chen, J. C. D. Qiu, C. N. Sun, J. Liu, Q. Wei, Y. Shi, *J. Mater. Sci. Technol.* **2020**, *57*, 51–64.
[17] S. H. Ko, H. Pan, C. P. Grigoropoulos, C. K. Luscombe, J. M. J. Fréchet, D. Poulikakos, *Nanotechnology* **2007**, *18*, 345202.
[18] a) Z. Jing, R. Ni, J. Wang, X. Lin, D. Fan, Q. Wei, T. Zhang, Y. Zheng, H. Cai, Z. Liu, *Bioactive Materials* **2021**, *6*, 4542–4557; b) D. Zhang, D. Qiu, M. A. Gibson, Y. Zheng, H. L. Fraser, D. H. StJohn, M. A. Easton, *Nature* **2019**, *576*, 91–95; c) L. Yuan, S. Ding, C. Wen, *Bioact. Mater.* **2019**, *4*, 56–70.
[19] C. Yin, T. Zhang, Q. Wei, H. Cai, Y. Cheng, Y. Tian, H. Leng, C. Wang, S. Feng, Z. Liu, *Bioact. Mater.* **2021**.
[20] a) J. Park, S. Bauer, K. von der Mark, P. Schmuki, *Nano Lett.* **2007**, *7*, 1686–1691; b) S. Minagar, J. Wang, C. C. Berndt, E. P. Ivanova, C. Wen, *J. Biomed. Mater. Res. Part A* **2013**, *101 A*, 2726–2739; c) C. von Wilmowsky, S. Bauer, R. Lutz, M. Meisel, F. W. Neukam, T. Toyoshima, P. Schmuki, E. Nkenke, K. A. Schlegel, *J. Biomed. Mater. Res. Part B* **2009**, *89B*, 165–171.
[21] M. Ribeiro, F. J. Monteiro, M. P. Ferraz, *Biomatter* **2012**, *2*, 176–194.
[22] S. Maher, G. Kaur, L. Lima-Marques, A. Evdokiou, D. Losic, *ACS Appl. Mater. Interfaces* **2017**, *9*, 29562–29570.
[23] K. Gulati, A. Santos, D. Findlay, D. Losic, *J. Phys. Chem. C* **2015**, *119*, 16033–16045.
[24] S. Maher, A. R. Wijenayaka, L. Lima-Marques, D. Yang, G. J. Atkins, D. Losic, *ACS Biomater. Sci. Eng.* **2021**, *7*, 441–450.
[25] J. Drelich, E. Chibowski, *Langmuir* **2010**, *26*, 18621–18623.
[26] Y. Yuan, M. P. Hays, P. R. Hardwidge, J. Kim, *RSC Adv.* **2017**, *7*, 14254–14261.
[27] J.-H. Kim, S. Kim, J.-H. So, K. Kim, H.-J. Koo, *ACS Appl. Mater. Interfaces* **2018**, *10*, 17448–17454.
[28] J. Dong, D. Fang, L. Zhang, Q. Shan, Y. Huang, *Materialia* **2019**, *5*, 100209.
[29] a) B. Voltrova, V. Hybasek, V. Blahnova, J. Sepitka, V. Lukasova, K. Vocetkova, V. Sovkova, R. Matejka, J. Fojt, L. Joska, M. Daniel, E. Filova, *RSC Adv.* **2019**, *9*, 11341–11355; b) K. S. Brammer, S. Oh, C. J. Cobb, L. M. Bjursten, H. v. d. Heyde, S. Jin, *Acta Biomater.* **2009**, *5*, 3215–3223; c) Y. Q. Hao, S. J. Li, Y. L. Hao, Y. K. Zhao, H. J. Ai, *Appl. Surf. Sci.* **2013**, *268*, 44–51.
[30] a) H. A. Peterson, *Journal of pediatric orthopedics* **2005**, *25*, 107–115; b) G. Reith, V. Schmitz-Greven, K. O. Hensel, M. M. Schneider, T. Tinschmann, B. Bouillon, C. Probst, *BMC Surg.* **2015**, *15*, 96–96.
[31] G. Kaur, T. Willsmore, K. Gulati, I. Zinonos, Y. Wang, M. Kurian, S. Hay, D. Losic, A. Evdokiou, *Biomaterials* **2016**, *101*, 176–188.
[32] P. Izakovicova, O. Borens, A. Trampuz, *EFORT Open Reviews* **2019**, *4*, 482–494.
[33] a) T. J. Silhavy, D. Kahne, S. Walker, *Cold Spring Harbor Perspect. Biol.* **2010**, *2*, a000414; b) C. E. Harper, C. J. Hernandez, *APL Bioeng* **2020**, *4*, 021501–021501.
[34] M. Gibaldi, S. Feldman, *J. Pharm. Sci.* **1967**, *56*, 1238–1242.
[35] W. Zhang, S. Zhang, H. Liu, L. Ren, Q. Wang, Y. Zhang, *J. Mater. Sci. Technol.* **2021**, *88*, 158–167.
[36] a) D. Gan, T. Xu, W. Xing, X. Ge, L. Fang, K. Wang, F. Ren, X. Lu, *Adv. Funct. Mater.* **2019**, *29*, 1805964; b) D. Gan, W. Xing, L. Jiang, J. Fang, C. Zhao, F. Ren, L. Fang, K. Wang, X. Lu, *Nat. Commun.* **2019**, *10*, 1487.

Manuscript received: September 2, 2021
Revised manuscript received: September 29, 2021
Accepted manuscript online: October 4, 2021
Version of record online: November 3, 2021

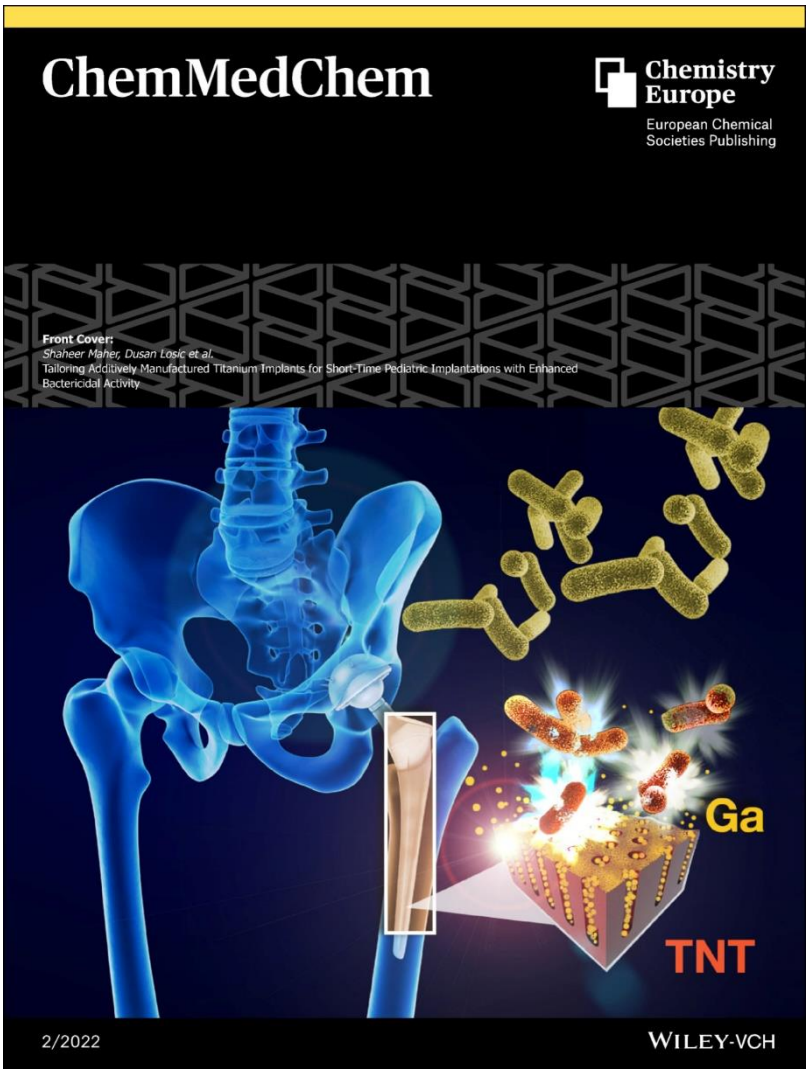
ChemMedChem
Chemistry Europe
European Chemical Societies Publishing
Front Cover:
Shaheer Maher, Dusan Losic et al.
Tailoring Additively Manufactured Titanium Implants for Short-Time Pediatric Implantations with Enhanced Bactericidal Activity
Ga
TNT
2/2022
WILEY-VCH

Statement of Authorship

Title of Paper	Micro- and Nano-structured 3D Printed Titanium Implants with Hydroxyapatite Coating for Improved Osseointegration
Publication Status	☑ Published ☐ Accepted for Publication ☐ Submitted for Publication ☐ Unpublished and Unsubmitted w ork w ritten in manuscript style
Publication Details	Jie Qin, Dongqing Yang,Shaheer Maher, Luis Lima-Marques,Yanmin Zhou, Yujie Chen, Gerald J. Atkins, and Dusan Losic, Micro- and nano-structured 3D printed titanium implants with a hydroxyapatite coating for improved osseointegration. Journal of Materials Chemistry B, 2018. 6(19): p. 3136-3144.

Principal Author

Name of Principal Author (Candidate)	Shaheer Maher (*also known* as Shaheer Makar)		
Contribution to the Paper	Participated in implants fabrication, characterization and revised the manuscript		
Overall percentage (%)	30% (Equally contributed secondary author)		
Certification:	This paper reports on original research I conducted during the period of my Higher Degree by Research candidature and is not subject to any obligations or contractual agreements with a third party that would constrain its inclusion in this thesis. I am the primary author of this paper.		
Signature		Date	09/09/2021

Co-Author Contributions

By signing the Statement of Authorship, each author certifies that:

i. the candidate's stated contribution to the publication is accurate (as detailed above);

ii. permission is granted for the candidate in include the publication in the thesis; and

iii. the sum of all co-author contributions is equal to 100% less the candidate's stated contribution.

Name of Co-Author	Jie Qin		
Contribution to the Paper	Primary author, performed fabrication, characterisation and cell studies Author can not be reached, signed by corresponding author on their behalf		
Signature		Date	09/09/2021

Name of Co-Author			
Contribution to the Paper			
Signature		Date	

Please cut and paste additional co-author panels here as required.

Statement of Authorship

Title of Paper	Micro- and Nano-structured 3D Printed Titanium Implants with Hydroxyapatite Coating for Improved Osseointegration
Publication Status	☑ Published ☐ Accepted for Publication ☐ Submitted for Publication ☐ Unpublished and Unsubmitted w ork w ritten in manuscript style
Publication Details	Jie Qin, Dongqing Yang,Shaheer Maher, Luis Lima-Marques,Yanmin Zhou, Yujie Chen, Gerald J. Atkins, and Dusan Losic, Micro- and nano-structured 3D printed titanium implants with a hydroxyapatite coating for improved osseointegration. Journal of Materials Chemistry B, 2018. 6(19): p. 3136-3144.

Principal Author

Name of Principal Author (Candidate)	Shaheer Maher (*also known as* Shaheer Makar)		
Contribution to the Paper	Participated in implants fabrication, characterization and revised the manuscript		
Overall percentage (%)	30%(equally contributed secondary author)		
Certification:	This paper reports on original research I conducted during the period of my Higher Degree by Research candidature and is not subject to any obligations or contractual agreements with a third party that would constrain its inclusion in this thesis. I am the primary author of this paper.		
Signature		Date	09/09/2021

Co-Author Contributions

By signing the Statement of Authorship, each author certifies that:

i. the candidate's stated contribution to the publication is accurate (as detailed above);

ii. permission is granted for the candidate in include the publication in the thesis; and

iii. the sum of all co-author contributions is equal to 100% less the candidate's stated contribution.

Name of Co-Author	Dongqing Yang		
Contribution to the Paper	Particiapted in cell study and revised the manuscript		
Signature		Date	09/09/2021

Name of Co-Author	Luis Lima-Marques		
Contribution to the Paper	Supervised 3D-printing manufacturing process		
Signature		Date	09/09/2021

Please cut and paste additional co-author panels here as required.

Statement of Authorship

Title of Paper	Micro- and Nano-structured 3D Printed Titanium Implants with Hydroxyapatite Coating for Improved Osseointegration
Publication Status	☑ Published ☐ Accepted for Publication ☐ Submitted for Publication ☐ Unpublished and Unsubmitted w ork w ritten in manuscript style
Publication Details	Jie Qin, Dongqing Yang,Shaheer Maher, Luis Lima-Marques,Yanmin Zhou, Yujie Chen, Gerald J. Atkins, and Dusan Losic, Micro- and nano-structured 3D printed titanium implants with a hydroxyapatite coating for improved osseointegration. Journal of Materials Chemistry B, 2018. 6(19): p. 3136-3144.

Principal Author

Name of Principal Author (Candidate)	Shaheer Maher (*also known* as Shaheer Makar)
Contribution to the Paper	Participated in implants fabrication, characterization and revised the manuscript
Overall percentage (%)	30% Equally contributed secondary author)
Certification:	This paper reports on original research I conducted during the period of my Higher Degree by Research candidature and is not subject to any obligations or contractual agreements with a third party that would constrain its inclusion in this thesis. I am the primary author of this paper.
Signature	Date 09/09/2021

Co-Author Contributions

By signing the Statement of Authorship, each author certifies that:

i. the candidate's stated contribution to the publication is accurate (as detailed above);

ii. permission is granted for the candidate in include the publication in the thesis; and

iii. the sum of all co-author contributions is equal to 100% less the candidate's stated contribution.

Name of Co-Author	Gerald J. Atkins
Contribution to the Paper	Supervised the development of cell study and revised the manuscript
Signature	Date 09/09/2021

Name of Co-Author	Dusan Losic
Contribution to the Paper	Supervised the development of study, revised the manuscript and acted as corresponding author
Signature	Date 09/09/2021

Please cut and paste additional co-author panels here as required.

Statement of Authorship

Title of Paper	Micro- and Nano-structured 3D Printed Titanium Implants with Hydroxyapatite Coating for Improved Osseointegration
Publication Status	☑ Published ☐ Accepted for Publication ☐ Submitted for Publication ☐ Unpublished and Unsubmitted w ork w ritten in manuscript style
Publication Details	Jie Qin, Dongqing Yang,Shaheer Maher, Luis Lima-Marques,Yanmin Zhou, Yujie Chen, Gerald J. Atkins, and Dusan Losic, Micro- and nano-structured 3D printed titanium implants with a hydroxyapatite coating for improved osseointegration. Journal of Materials Chemistry B, 2018. 6(19): p. 3136-3144.

Principal Author

Name of Principal Author (Candidate)	Shaheer Maher (*also known* as Shaheer Makar)		
Contribution to the Paper	Participated in implants fabrication, characterization and revised the manuscript		
Overall percentage (%)	30% (Equally contributed secondary author)		
Certification:	This paper reports on original research I conducted during the period of my Higher Degree by Research candidature and is not subject to any obligations or contractual agreements with a third party that would constrain its inclusion in this thesis. I am the primary author of this paper.		
Signature		Date	09/09/2021

Co-Author Contributions

By signing the Statement of Authorship, each author certifies that:

i. the candidate's stated contribution to the publication is accurate (as detailed above);

ii. permission is granted for the candidate in include the publication in the thesis; and

iii. the sum of all co-author contributions is equal to 100% less the candidate's stated contribution.

Name of Co-Author	Yanmin Zhou		
Contribution to the Paper	Particiapted in characterization experiments The co-author can not be reacher, signed by corresponding author on their behalf		
Signature		Date	09/09/2021

Name of Co-Author	Yujie Chen		
Contribution to the Paper	Particiapted in characterization experiments The co-author can not be reacher, signed by corresponding author on their behalf		
Signature		Date	09/09/2021

Please cut and paste additional co-author panels here as required.

Journal of Materials Chemistry B

PAPER

View Article Online
View Journal | View Issue

Cite this: J. Mater. Chem. B, 2018, 6, 3136

Micro- and nano-structured 3D printed titanium implants with a hydroxyapatite coating for improved osseointegration

Jie Qin, [ab] Dongqing Yang,†[c] Shaheer Maher,†[af] Luis Lima-Marques,[d] Yanmin Zhou,[b] Yujie Chen,[e] Gerald J. Atkins*[c] and Dusan Losic *[a]

Received 17th December 2017,
Accepted 12th April 2018

DOI: 10.1039/c7tb03251j

rsc.li/materials-b

With the increasing demand for low-cost and more efficient dental implants, there is an urgent need to develop new manufacturing approaches and implants with better osseointegration performance. 3D printing technology provides enormous opportunities for the rapid fabrication of a new generation of patient-tailored dental implants with significantly reduced costs. This study presents the demonstration of a unique model of titanium implants based on 3D printing technology with improved osseointegration properties. Titanium alloy (Ti6Al4V) implants with a micro-structured surface are fabricated using a selective laser-melting process followed by further nano-structuring with electrochemical anodization to form titania nanotubes (TNT) and subsequent bioactivation by a hydroxyapatite (HA) coating. The osseointegration properties of the fabricated implants were examined using human primary osteoblasts and cell line models. The results showed significantly increased protein adsorption, cell adhesion and cell spreading. The expression of the late osteoblast/osteocyte genes *GJA1* and *PHEX* was also enhanced, indicating a cell maturation effect and the promotion of mineralization on the surface. These results suggest that 3D printing technology combined with electrochemical nano-structuring and HA modification is a promising approach for the fabrication of Ti implants with improved osseointegration and provides potential alternatives to conventional dental implants.

1. Introduction

The number of dental implant procedures is steadily increasing worldwide, reaching about one million operations every year.[1] This rising demand poses a great challenge to the conventional dental implant industry. Manufacturing by casting or machining, the conventional implant production approach is complicated, expensive, and time consuming.[2] Furthermore, current implants are only available in a fixed set of dimensions and therefore may not be suitable for every patient. In addition, the requirement of storing a large variety of pre-made implants could result in serious wastage of resources due to expiration, therefore making implants more expensive.[2] Thus, a more efficient approach for implant production, custom made on demand, is highly desirable.

Three-dimensional (3D) printing is currently attracting increasing attention across many sectors, opening new horizons for the fabrication of various biomedical implants and tissue engineering.[3] This technology directly utilizes computer-aided design models to fabricate any desired structure, saving significant time and cost.[4] The application of 3D printing to fabricate patient tailored implants with desirable properties will result in revolutionary improvements, among which is the flexibility in implant design to obtain different shapes of implants with tuned dimensions.[5] More importantly, 3D printing will allow production on demand and personalized implants using computed tomography (CT) scans to create a precisely defined shape to replace a missing tooth, which can be designed especially for each patient and be fabricated very quickly in a clinical environment.[4] At the same time, the implant manufacturing companies using this technology will be able to deliver implants on request instead of undertaking mass production and storage of implants. Accordingly, 3D printing technology is emerging as a promising tool for producing a new generation of medical implants. However, before putting

[a] School of Chemical Engineering, The University of Adelaide, 5005, Australia. E-mail: dusan.losic@adelaide.edu.au
[b] Departments of Dental Implantology, School and Hospital of Stomatology, Jilin University, 130021, China
[c] Centre for Orthopaedic and Trauma Research, Adelaide Medical School, Discipline of Orthopaedics and Trauma, The University of Adelaide, 5005, Australia. E-mail: gerald.atkins@adelaide.edu.au
[d] The Institute for Photonics and Advanced Sensing, The University of Adelaide, SA 5005, Australia
[e] School of Mechanical Engineering, The University of Adelaide, 5005, Australia
[f] Faculty of Pharmacy, Assiut University, Assiut, 71526, Egypt
† These authors equally contributed to the work.

View Article Online
Paper Journal of Materials Chemistry B

such 3D printed dental implants into real application, it is important to investigate and optimize their performance in terms of osseointegration, a critical prerequisite for the stability and long-term survival rate of dental implants.[6]

Since the implant surface comes directly in contact with bone after insertion, many efforts have been made to modify the surface properties to improve their biointegration.[7,8] Early work by Buser *et al.*[9] showed that a micro-roughened surface prepared by sandblasting and acid etching significantly increased osseointegration compared to smooth surfaces. Such rough topographies are believed to provide mechanical interlocking with cells. Considering that the major components of bone are nano-scale materials, it is proposed that implants with nano-surface topography could provide superior osseointegration features.[10]

Titania nanotube (TNT) structures prepared by electrochemical anodization of titanium are recognized as a remarkable representative of these nanostructures.[11] These arrays of tiny tubes which are open at the top and closed at the bottom can be prepared with good control over dimensions (diameters 10–300 nm and lengths 0.5 to 300 μm) and they have been well explored for drug-delivery applications.[12] Electrochemical anodization is a scalable, cost-effective and simple fabrication process that can be implemented for modifications of medical implants using most clinically proved metals at the industrial scale.[13] Several studies have demonstrated that TNT structures could promote osteoblastic cell adhesion, proliferation and enhance the ingrowth of bone and vascular tissues.[14–17] Additionally, the residual fluoride in TNT resulting from the anodization process could also favor implant osseointegration.[1] The first concept to demonstrate engineering of new 3D printed Ti implants (3D-Ti) for drug delivery applications was recently reported by our group, showing promising applications for the delivery of anti-cancer drugs and localized cancer therapy.[18]

In this work we propose an approach to further improve the osseointegration performance of 3D printed Ti alloy implants by combining 3D printing technology, surface nanoengineering and chemical modification. The concept is based on the idea of developing advanced 3D printed implants with dual micro- and nano-topography (3D-Ti-TNT) fabricated by 3D printing and electrochemical anodization, followed by hydroxyapatite (HA) surface functionalization as depicted in Fig. 1. The enhancement of osseointegration performance of 3D implants using HA is proposed due to its chemical similarities to bone mineral.[19–21] HA is clinically approved for surface coating of medical implants to promote bone healing and apposition, leading to faster fixation and better clinical outcomes.[19–21] Successful synthesis of HA on titania nanotubes has been achieved by a simple and efficient alternative immersion method (AIM), consisting of successive immersion of the implants into $Ca(OH)_2$ and $(NH_4)_2HPO_4$ for repeated cycles.[22] The implants after each fabrication step were characterized by different techniques to show surface morphology and chemical composition. The osseointegration properties of fabricated implants were evaluated by protein adsorption, cell adhesion, morphology and gene expression. The results obtained suggest that the fabricated implants could be a promising alternative for the fabrication of patient-specific dental implants.

2. Experimental

2.1. 3D printing of Ti implants

Titanium alloy powder (Ti6Al4V) was used for printing the implants in the form of square strips (1.2 × 1.2 cm^2) with a selective laser melting machine (3D System ProX 200 (Phenix Systems PXM)), equipped with a 300 W Laser (1070 nm at 50% power), in the presence of an Argon atmosphere (~500 ppm O_2). A thin even layer of the metal powder was deposited across a build plate and then the selected areas of the powder were precisely melted by the high power focused laser. This process is repeated, building up layer by layer until the desired thickness (~0.6 mm) is reached, generating the implants accordingly. The resulting implants are referred to as 3D-Ti throughout this study. Commercially available Titanium foil (Sigma-Aldrich, Sydney, Australia), referred to as Ti, was also cut in the same size as the control.

2.2. Fabrication of 3D printed Ti implants with TNT layers

3D-Ti was cleaned by sonication in ethanol for 10 min, followed by drying in N_2. After this, a TNT layer was fabricated on the surface by electrochemical anodization. During the process,

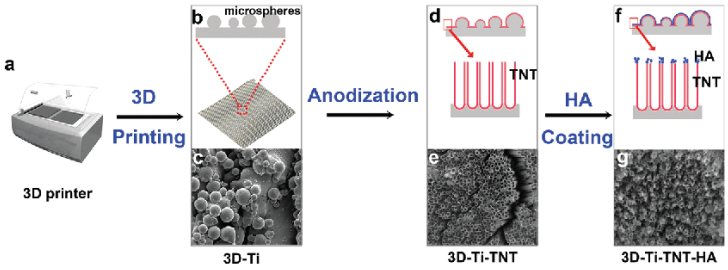

Fig. 1 Scheme showing the fabrication of 3D printed Ti alloys implants with dual micro- and nano-topography fabricated by combining 3D printing, electrochemical anodization, and bioactivation by a hydroxyapatite (HA) coating. (a) 3D printer. (b and c) Scheme and SEM image showing typical surface topography of the 3D printed implants. (d and e) Scheme and SEM image of electrochemically engineered implants with a titania nanotube layer. (f and g) Scheme and SEM image of implants after HA coating.

View Article Online
Journal of Materials Chemistry B Paper

3D-Ti served as the anode and a thin Ti foil served as the cathode. Both of the electrodes were immersed in ethylene glycol electrolyte containing ammonium fluoride (0.1 M), lactic acid (1.5 M) and water (5 vol%). A special electrochemical setup designed in our laboratory was used, and the whole system was maintained at 60 °C under constant stirring with a magnetic stirrer (50 rpm). A constant voltage of 60 V was applied for 15 min. A computer-aided power supply (Agilant) was used to supply the desired voltage and was controlled using the LabView program (National Instruments). After anodization, the samples were washed with MilliQ water thoroughly and dried in air. The resulting implants are referred to as 3D-Ti-TNT.

2.3. Surface functionalization of 3D-Ti-TNT with a hydroxyapatite (HA) coating

HA coating of the 3D-Ti-TNT was performed by Kodama's alternative immersion method (AIM).[22] Fifteen implants were separately placed onto a custom designed holder, which allowed all TNT layers to be exposed. The holder was first manually immersed in 200 ml of saturated $Ca(OH)_2$ for 1 min at room temperature. Subsequently, it was manually immersed in 200 ml of $(NH_4)_2HPO_4$ (0.02 M) for the same time. This was repeated for 5 cycles. Between each soaking step and after each cycle, the implants were dipped in 200 ml of MilliQ water for 1 min without any shaking. Finally, the implants were left to dry at room temperature and are referred to as 3D-Ti-TNT-HA throughout this study.

2.4. Characterization of prepared implants

The surface morphology of the prepared implants was characterized by a field emission scanning electron microscope (SEM, FEI Quanta 450) working at 10 kV. Prior to SEM examination, implants were coated with platinum (5 nm thickness). Energy-dispersive X-ray spectroscopy (EDS) was also recorded to analyse the elemental composition of the implants. X-ray Diffraction (XRD) patterns were also measured using a Rigaku Miniflex diffractometer operating at 40 kV and 15 mA. The scan range was from 30° to 80° (2θ) with a step size of 0.02°. The mechanical properties of the implants were assessed by a nanoindentation system (IBIS, M/S Fisher-Cripps Laboratory, Australia). Load-controlled indentation with a maximum load of 200 mN was performed on the polished surface of the implants, with a loading rate of 2.5 mN s^{-1}, which represented the static response of the material.[23] The Oliver–Pharr method was used to quantify the elastic modulus (E) and hardness (H).

2.5. Protein adsorption

All implants were cut to a standard size (6 × 6 mm^2) and sterilized by UV irradiation for 1 h on both sides. A protein solution, also used as culture media, was prepared with α-modified minimal essential medium (α-MEM, Gibco, NY, USA) supplemented by foetal bovine serum (10 vol%), HEPES (10 mM), L-glutamine (0.2 M) and penicillin/streptomycin (1 vol%). Each Ti, 3D-Ti, 3D-Ti-TNT, and 3D-Ti-TNT-HA implant (in triplicate) was placed in a single well of the 48-well plate. 250 μl of the protein solution was added onto each implant surface and they were incubated at 37 °C for 1.5 h. Unattached proteins were washed away with PBS. Attached proteins were fixed with neutral formalin (10%) and stained with crystal violet (1%) for 20 min. The excess stain was removed by washing in water. The protein-associated stain was then extracted with acetic acid (10 vol%, 200 μl $well^{-1}$) for 20 min and the absorbance at 570 nm was measured by spectrophotometry.

2.6. Cell adhesion

Human osteoblast-like cells grown from bone samples were obtained with patient informed consent, as previously described.[24] Cells were cultured in α-modified minimal essential medium (α-MEM, Gibco, NY, USA) supplemented with foetal bovine serum (10 vol%), HEPES (10 mM), L-glutamine (0.2 M) and penicillin/streptomycin (1 vol%) (all from Life Technologies). After reaching confluence, osteoblast cells were removed from culture flasks using collagenase-2, trypsin, and suspended at a density of 2 × 10^5 cells ml^{-1}. A 250 μl aliquot (containing 5 × 10^4 cells) was added onto each implant (Ti, 3D-Ti, 3D-Ti-TNT, and 3D-Ti-TNT-HA (in triplicate)). After incubating for 2 h, unattached cells were removed by PBS washing. Attached cells were fixed with neutral formalin (10%) and stained with 4′,6-diamidino-2-phenylindole (DAPI) (1 μg ml^{-1}). Cell numbers in three random fields from each sample were counted under a fluorescence microscope (Olympus BX51).

2.7. Cell morphology study by confocal microscopy

Cells were seeded on to each implant (Ti, 3D-Ti, 3D-Ti-TNT, and 3D-Ti-TNT-HA) in a 48-well plate. 24 h after seeding, the media were removed. Implants with cells on the surface were gently washed by PBS and fixed with neutral buffered formalin (10%). Attached cells were stained with phalloidin-TRITC (10 μM) (Sigama) and DAPI (1 μg ml^{-1}) in PBS for 1 h. Cell morphology was observed under a confocal laser-scanning microscope (Olympus FV3000). Phalloidin-TRITC was excited at 561 nm and DAPI at 405 nm.

2.8. Cell morphology study by SEM

Cells were seeded on to each implant (Ti, 3D-Ti, 3D-Ti-TNT, and 3D-Ti-TNT-HA) at a density of 5 × 10^4 in a 48-well plate. 3 days after seeding, the media were removed and changed to differentiation media (α-MEM with foetal bovine serum (10%), ascorbate-2-phosphate (50 μg ml^{-1}) and potassium dihydrogen phosphate (1.8 mM)). 7 days later, implants with cells on the surface were gently washed by PBS and fixed in glutaraldehyde (1.25%) (Sigma-Aldrich, Sydney, Australia) for 24 h. A post-fix in osmium tetroxide (2%) for 30 min was also performed. After that, cells were dehydrated serially in 70%, 90%, 100% ethanol, 100% hexamethyldisilazane (HMDS) : 100% ethanol (1 : 1) solution, and 100% HMDS. After drying, implants were mounted on SEM holders, coated with a 5 nm thick layer of platinum, and observed under a SEM.

2.9. Gene expression analysis

The expression of *GJA1* and *PHEX* was analysed by using reverse transcription-quantitative polymerase chain reaction (RT-qPCR).

View Article Online

Paper

Journal of Materials Chemistry B

SaOS2 human osteoblast-like cells, a well-established cell line for gene analysis,[25] were seeded onto each implant at a density of 1×10^6. After reaching confluence, the media were changed to differentiation media as described above. The media were replaced at 3 or 4-day intervals. After 7 days of differentiation, RNA was harvested from each sample using Trizol reagent (Life Technologies, NY, USA) and was reverse transcribed into cDNA using the iScript RT kit (BioRad, CA, USA) as described elsewhere.[25] SYBR Green Fluor qPCR Mastermix (Qiagen, Limburg, The Netherlands) was used to perform RT-qPCR in a CFX Connect thermocycler (BioRad) with the primer sequences published previously.[26] Primers were synthesized by Geneworks (Thebarton, SA, Australia). Relative gene expression was calculated using the $2^{-\Delta\Delta Ct}$ method and normalized to the expression of 18S rRNA.

2.10. Statistical analysis

Data are expressed as the mean ± SEM and were analysed using one-way analysis of variance (ANOVA) with Tukey's multiple comparison test. A p-value <0.05 was considered to indicate a statistically significant difference.

3. Results and discussion

3.1. Characterization of nanostructured and HA functionalized 3D printed implants

Scanning electron microscope (SEM) images of the surface morphology of prepared implants are presented in Fig. 2. As shown in Fig. 2a, 3D printed Ti implants (3D-Ti) were covered by numerous microspheres of sizes ranging from 5–20 μm (average ~12 μm) in diameter. Higher resolution images showed that these structures were fused to the underlying surface, and were highly interconnected (Fig. 2b), suggestive of a stable, micro-rough surface. These microspheres result from partial melting of the alloy powder used during the selective laser melting process. This topography contrasted sharply with that of commercially available Ti (Ti), which possessed a relatively smooth surface as seen in Fig. 2c.

As a result of electrochemical anodization, a well-ordered titania nanotube (TNT) layer was generated on the entire surface of the 3D printed Ti implant, including the microspheres (Fig. 2d and e) and the underlying surface (Fig. 2e and f). A powder sintering route using the space-hold technique has

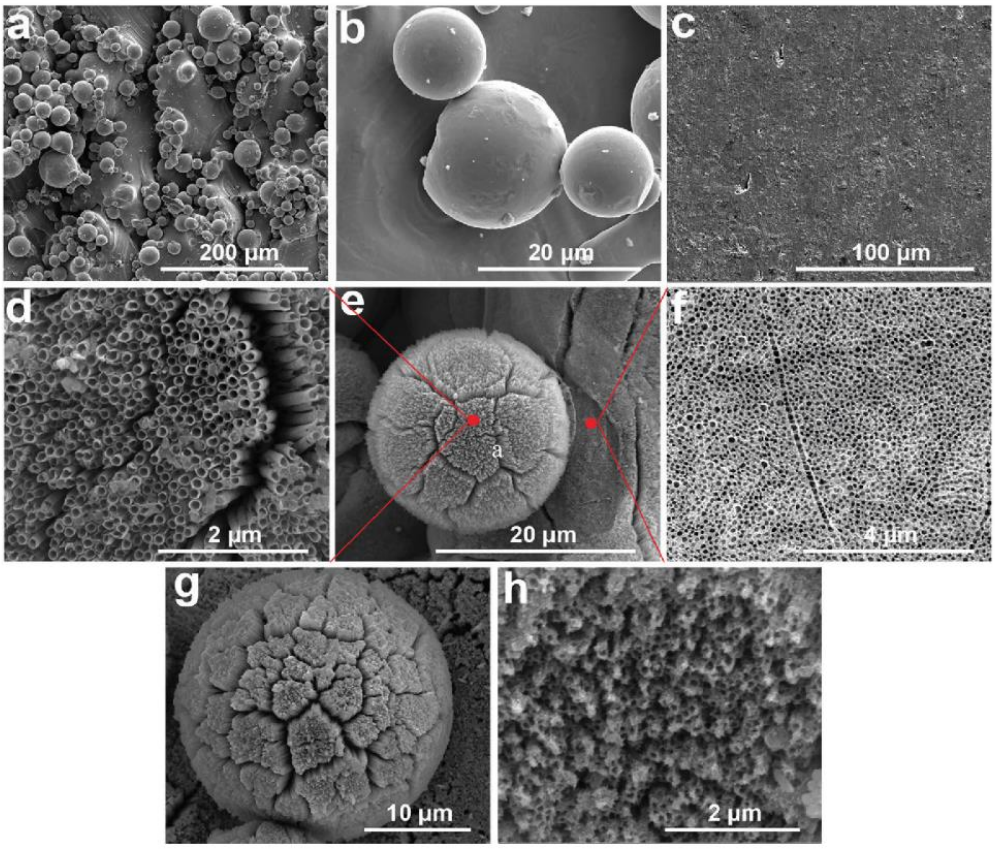

Fig. 2 SEM images of 3D-Ti (a and b), Ti (c), 3D-Ti-TNT (d–f) and 3D-Ti-TNT-HA (g and h). (a) 3D-Ti was covered by microspheres of various sizes. (b) High resolution image showing that microspheres were fused to the underlying surface, and were highly interconnected. (c) Pure Ti foil possessing a relatively smooth surface (*i.e.* no micro-features). (d–f) TNT formed on the entire surface of 3D Ti, including the microspheres (d and e) and the underlying surfaces (e and f). (g) Crystalline deposits were found on the implant surface and (h) the nanotubes were still visible after HA coating.

View Article Online
Journal of Materials Chemistry B Paper

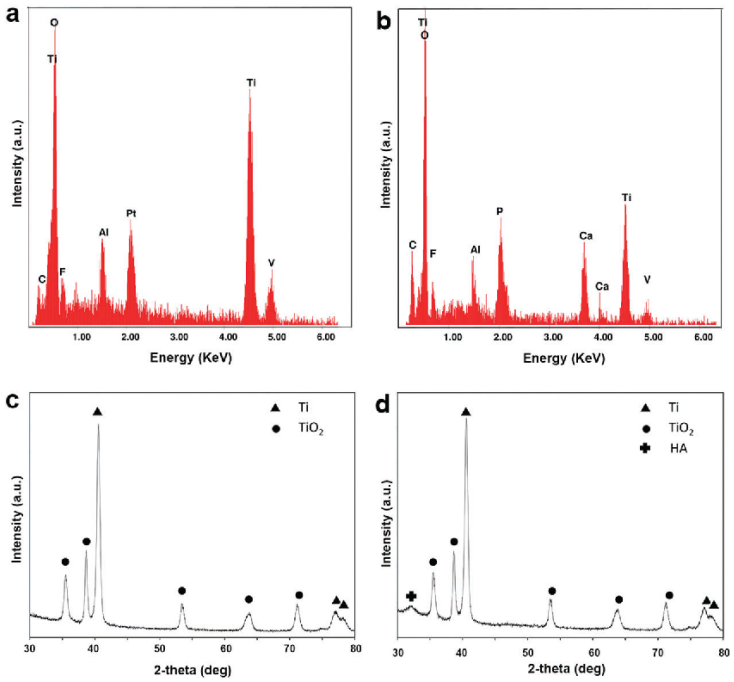

Fig. 3 (a and b) EDS and (c and d) XRD spectra. EDS spectrum of 3D-Ti-TNT before (a) and after (b) HA treatment. Significant Ca and P peaks appeared after HA treatment (b). XRD spectrum of 3D Ti TNT before (c) and after (d) HA treatment. HA peaks appeared after HA treatment (d).

also been reported to produce porous Ti implants.[27] However, the pore-size in such implants is distributed within a wide range. Therefore, reproducing the porous structures to control the physicochemical properties of the implant is challenging. By comparison, the implant in this study was fabricated with reproducibly uniform nanotubes with an average individual tube diameter of ~120 nm, a length of ~3 μm and a density of $\sim 5 \times 10^9$ nanotubes per cm^2. As expected, cracks were evident on the TNT layers due to the radial outgrowth of nanotubes on the curved surfaces. However, these cracks do not compromise the stability of the TNT layer and potentially allow for additional amounts of therapeutics to be loaded.[18,28–30] These findings confirm the successful fabrication of an advanced implant with combined dual micro- and nano-topography, represented by the microspheres and TNT, respectively.

SEM images of the prepared 3D-Ti-TNT implants after HA immersion treatment are presented in Fig. 2g and h. Crystalline deposits were found homogenously distributed on the implant surface (Fig. 2g). TNT structures were still visible as shown in the higher resolution image (Fig. 2h). These results are in accordance with Kodama's work, in which a HA coating was successfully fabricated on TNT by HA immersion treatment.[21] Gu *et al.*[31] proposed that the mechanism of HA formation results from the reaction of the titanium oxide layer with hydroxide to form hydrogen metatitanate: $TiO_2 + OH \rightarrow HTiO_3$. The resulting negatively charged surface promoted adsorption of Ca^{2+} and formation of calcium titanate. This titanate then adsorbed HPO_4^{2} in the solution of $(NH_4)_2HPO_4$ to form calcium phosphate nuclei. Subsequent HA formation and crystallization would then readily occur.

To evaluate the chemical nature of the crystalline deposits on the implant surface, energy dispersive X-ray spectroscopy (EDS) was performed before (Fig. 3a) and after (Fig. 3b) the HA treatment. Fig. 3b shows significant peaks of Ca and P after HA treatment, indicating the successful formation of a Ca–P deposit with a Ca : P ratio of 1.53, which approximates the theoretical Ca : P ratio (1.67) of HA, confirming the formation of a HA layer on the implant surface.[32] It is noteworthy that fluoride peaks appeared on the surface of the implant with TNT. These fluoride ions were derived from the anodization electrolyte and incorporated into the TNT structures. It is worth mentioning that the presence of F^{-1} ions is claimed to be favorable for the osseointegration of implants.[33]

X-ray diffraction (XRD) graphs were also recorded before (Fig. 3c) and after (Fig. 3d) the HA treatment. According to the reference data JCPDS-0432, HA peaks were present after the HA treatment (Fig. 3d). This additionally confirmed the formation of HA on the implant surface.

The elastic modulus (E) of the implant was measured to be 109.9 ± 1.8 GPa, which was consistent with the reported values of the biomedical Ti6Al4V alloy (110–114 GPa).[34] The hardness (H) of the implant reached 4.84 ± 0.12 GPa, compared to 3.28–3.39 GPa in the wrought Ti6Al4V.[34,35] According to the relationship between yield strength (σ_y) and hardness, $H = 3\sigma_y$[5], the yield strength of the implant was estimated to be ~1.6 GPa, which clearly surpassed the American Society for Testing and

View Article Online

Paper

Journal of Materials Chemistry B

Materials (ASTM) standard (795 MPa).[36] Compared with the porous implant produced by the space-hold technique, which has a yield strength of 60 MPa,[27] the 3D printed implant in this study could provide much higher yield strength. It is presumably strong enough to resist handling during implantation and *in vivo* loading. Notably, the wear resistance is closely related to the ratio between H and E, the so-called plasticity index.[37] Materials with a higher plasticity index exhibit greater wear resistance. Therefore, one could expect that, compared to wrought Ti6Al4V, our 3D printed Ti6Al4V with similar elastic modulus but higher hardness would exhibit increased wear resistance.[38]

3.2. Protein adsorption

When a material is implanted, proteins in the surrounding tissues and plasma would be expected to spontaneously adsorb onto the implant surface. This protein layer could mediate the subsequent cell performance, playing an important role during the osseointergration process.[39] The protein adsorption properties were therefore tested and found to be: 3D-Ti-TNT-HA > 3D-Ti-TNT > 3D-Ti > Ti (Fig. 4a). The increase in protein adsorption on 3D-Ti and 3D-Ti-TNT could be attributed to increased surface roughness due to the microspheres and nanostructures.[40]

Another noteworthy finding in these experiments was that 3D-Ti-TNT-HA had a significant increase in protein adsorption compared with others samples. The total protein adsorbed on 3D-Ti-TNT-HA was 92-fold that of Ti, 60-fold that of 3D-Ti, and 5-fold that of 3D-Ti-TNT. This is in accordance with a recent study in which serum proteins preferably adsorbed onto a HA coated surface but not onto Ti.[41] Wang *et al.* pointed out that the possible reason might be electrostatic force.[42] Ionic Ca^{2+} and PO_4^{3} groups on HA surfaces could serve as protein binding sites, with calcium sites binding negatively charged groups, such as the carboxylate group and carbonyl group, and phosphate sites binding positively charged groups, including amino, aromatic and guanido groups, on the protein molecules.[42]

3.3. Cell adhesion

Cell adhesion is a critical event that occurs when bone cells come into contact with an implant surface, which is crucially important for influencing subsequent cellular behaviour.[43] Additionally, early adhesion of bone cells could competitively inhibit bacterial adhesion.[44] Therefore, cell adhesion on Ti, 3D-Ti, 3D-Ti-TNT, and 3D-Ti-TNT-HA was evaluated after 2 h of incubation. As shown in Fig. 4b, 3D-Ti-TNT-HA exhibited significantly increased cell adhesion. This is in accordance with the above protein adsorption results. Previous studies reported a similar correlation, proposing that this occurrs due to the adhered proteins being extracellular matrix proteins, such as fibronectin and vitronectin, which efficiently promote cell attachment.[41,45]

3.4. Cell morphology

The response of osteoblastic cells to these surfaces was tested using human primary bone-derived cells, previously termed 'NHBC'. These represent a spectrum of early osteoblast-osteocyte differentiation stages and provide a clinically relevant model for the current application since they are derived from patients receiving an orthopaedic implant.[46,47] The morphology of osteoblasts on the different implant surfaces at an early stage (24 h) was examined by confocal microscopy (Fig. 5). The cytoskeleton was stained with phalloidin-TRITC (red) and the nucleus was stained with DAPI (blue). Results indicated that cells on Ti spread widely, whereas cells on the other (3D) surfaces appeared to retain a smaller footprint, with an increased number of dendritic-like connections between adjacent cells. In the bone, such intercellular connectivity allows for the transfer of biochemical signals between cells, and in mature bone interconnected osteocytes form a functional syncytial network in this way.[48,49] Moreover, cells on 3D-Ti, 3D-Ti-TNT and 3D-Ti-TNT-HA had a larger nuclear : cytoplasm ratio compared with those on Ti, consistent with a more differentiated cell phenotype.[50] Confocal microscopy was not able to distinguish the cell morphologies when the cell number increased with time, due to the general high degree of confluency of the cultures. SEM was therefore employed to examine cell morphology after 7 days culturing (Fig. 6). Cells on Ti spread in a 2D manner and remained flat and spindle shaped (Fig. 6a), whereas those on 3D-Ti exhibited a plump, polygonal morphology (Fig. 6b). Cells on 3D-Ti-TNT began to exhibit a stellate shape with long, slender dendritic processes, suggesting a further differentiated morphology (Fig. 6c).[51]

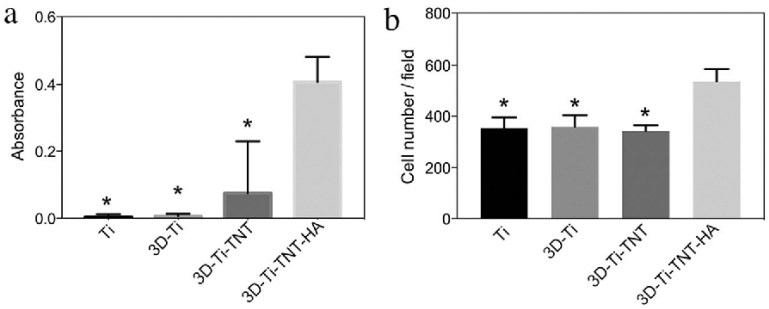

Fig. 4 (a) Protein adsorption and (b) cell adhesion on Ti, 3D-Ti, 3D-Ti-TNT, and 3D-Ti-TNT-HA. (a) 3D-Ti-TNT-HA had a significant increase in protein adsorption. (b) 3D-Ti-TNT-HA significantly increased cell adhesion. Data shown are means ± SEM. A significant difference to 3D-Ti-TNT-HA is indicated by * ($p < 0.05$).

View Article Online
Journal of Materials Chemistry B Paper

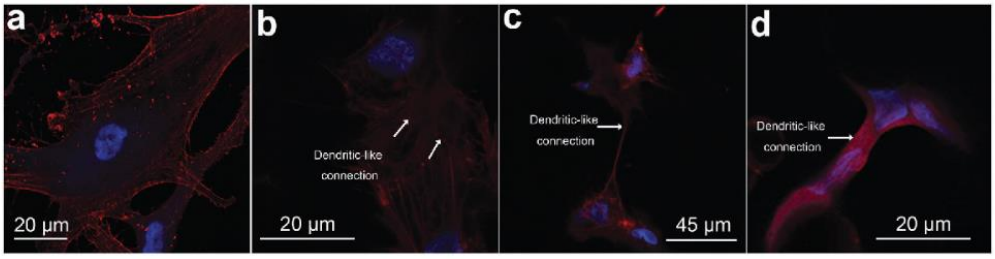

Fig. 5 Confocal microscopy images of human primary osteoblasts on (a) Ti, (b) 3D-Ti, (c) 3D-Ti-TNT, and (d) 3D-Ti-TNT-HA after 24 h of culture. (a) Cells on Ti spread widely. (b–d) Cells on 3D surfaces had a larger nuclear : cytoplasm ratio and retained a smaller footprint, with an increased number of dendritic-like connections between adjacent cells, indicative of a more differentiated cell phenotype.

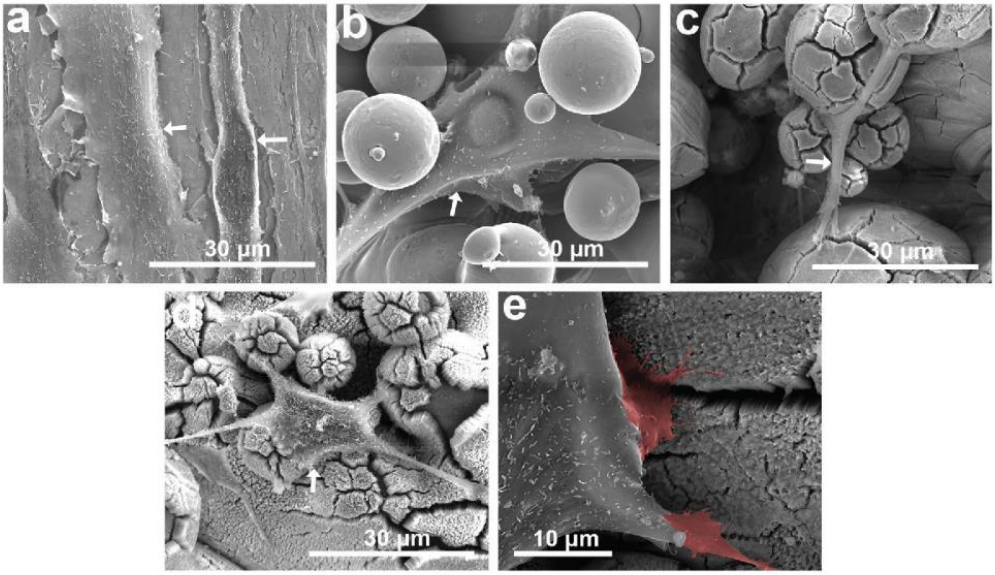

Fig. 6 SEM images of human primary osteoblasts on (a) Ti, (b) 3D-Ti, (c) 3D-Ti-TNT, and (d and e) 3D-Ti-TNT-HA after 7 days of culture. (a) Cells on Ti spread flatly and remained a spindle-like shape. (b) Cells on 3D-Ti showed a plump, polygonal shape. (c) Cells on 3D-Ti-TNT exhibited a stellate shape with long dendritic processes. (d) Cells on 3D-Ti-TNT-HA exhibited a more prominent stellate shape, with many cell processes and pseudopodia (e) suggesting a further differentiated morphology. White arrows indicate cells. Red colours indicate pseudopodia.

Cells cultured on 3D-Ti-TNT-HA exhibited a more prominent stellate shape, with many cell processes and pseudopodia (Fig. 6d and e). Similar observations were reported by Kim *et al.*, who found that the direction of cell spreading was more diverse on Ti if a HA coating was applied.[52] Overall, our findings suggest that cells cultured on 3D-Ti-TNT-HA had a more mature and differentiated, osteocyte-like morphology.[53] This finding is consistent with the study of Gu *et al.*,[31] indicating the superior differentiated morphology of osteoblasts on a HA-deposited TNT surface. The advantage of our material lies in that, instead of fabricating TNT onto a flat Ti surface as performed by Gu *et al.*, we fabricated TNT onto 3D-Ti. This 3D-Ti has an osseoinductive micro-rough surface and can be tailored to any desired dimension.

3.5. Gene expression

The expression of *GJA1*, encoding connexin 43 (Cx43), the principal protein component of functional gap-junctions in

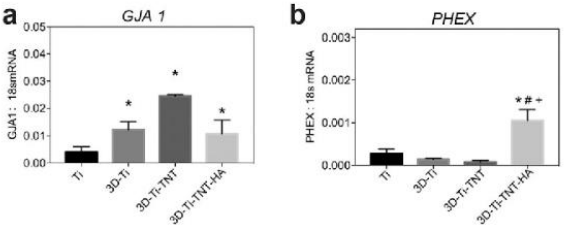

Fig. 7 Gene expression of *GJA1* and *PHEX* in SAOS2 cells plated on different implant surfaces after 7 days of culture. (a) The expression of *GJA1* was increased on the 3D structure. (b) The expression of *PHEX* was significantly increased on 3D-Ti-TNT-HA. Data shown are means of three experimental replicates ± SEM. Significant differences to expression on Ti are indicated by * ($p < 0.05$). Significant differences to expression on 3D-Ti are indicated by # ($p < 0.05$). Significant differences to expression on 3D-Ti-TNT are indicated by + ($p < 0.05$).

bone cell networking and a marker of mature osteocytes, [26] was increased in cultures on 3D-Ti, 3D-Ti-TNT, and 3D-Ti-TNT-HA, suggesting a maturation effect of the 3D structure (Fig. 7a). The expression of the gene *PHEX*, encoding a phosphate-regulating gene with homologies to endopeptidases on the X chromosome, an osteocyte maker that promotes mineralization,[54] was also significantly increased in cultures on 3D-Ti-TNT-HA compared with the other three surfaces (Fig. 7b), indicating that this surface could better promote osteoblast/osteocyte-mediated mineralization and differentiation. Both calcium and phosphate ions, which could be released from the HA substrate, are known promoters of biomineralisation and osteoblast/osteocyte differentiation.[55,56]

4. Conclusions

This current study presents advanced 3D printed and nanostructured Ti alloy implants modified with HA, to provide improved osseointegration properties based on enhanced protein adsorption, cell adhesion, cell spreading and mature osteoblast gene expression patterns. These implants were fabricated using a combination of 3D printing technology, electrochemical surface nanoengineering and chemical coating using HA. 3D printed Ti implants have characteristic micro-scale roughness, due to the presence of microspherical structures from the laser sintering process combined with an array of nanotubular structures additionally introduced by electrochemical anodization while retaining the micro-particle arrangement. These implants were further functionalized by a HA coating *via* an alternative immersion method in order to further improve their bone integration performance. The resulting implants significantly promoted protein adsorption, osteoblast cell adhesion, spreading, and increased the expression of certain genes related to osteoblast differentiation and mineralisation. These results are explained by the combined and synergistic impact of dual topography and HA chemistry. The results suggest that nanostructured and functionalised 3D-Ti-TNT-HA has promise in the manufacture of improved dental implants compared to current conventional implants. In addition, a 3D-Ti-TNT-HA implant could be developed as a drug releasing system with additional therapeutic functions, achieved by loading drugs (*e.g.* anti-inflammatory drugs, and antibiotics) into the titania nanotubes. Further bone response studies using an animal model are required before the clinical application of this implant.

Conflicts of interest

There are no conflicts of interest to declare.

Acknowledgements

The authors acknowledge the financial support provided to S. M. by the Australian Government Training Program Scholarship, ARC grant funded supplementary scholarship and Forrest George and Sandra Lynne Young Supplementary Scholarship. This work was performed in part at the OptoFab node of the Australian National Fabrication Facility utilizing Commonwealth and SA State Government funding. The authors thank Dr Animesh Basak, Dr Agatha Labrinidis, Ms Ruth Williams, and Mr Ken Neubauer from Adelaide Microscopy (AM) center for providing technical support for confocal microscopy and SEM. Also acknowledged is the support from Prof. Zonghan Xie at School of Mechanical Engineering, The University of Adelaide, and Drs Asiri R. Wijenayaka and Matthew Prideaux at the Centre for Orthopaedic and Trauma Research, The University of Adelaide.

References

1 L. Le Guehennec, A. Soueidan, P. Layrolle and Y. Amouriq, *Dent. Mater.*, 2007, **23**, 844–854.
2 V. Bhasin and M. R. Bodla, *Dissertation*, Massachusetts Institute of Technology, 2014.
3 U. Kalsoom, P. N. Nesterenko and B. Paull, *RSC Adv.*, 2016, **6**, 60355–60371.
4 D. Radenkovic, A. Solouk and A. Seifalian, *Med. Hypotheses*, 2016, **87**, 30–33.
5 C. L. Ventola, *P T*, 2014, **39**, 704–711.
6 R. Adell, U. Lekholm, B. Rockler and P. I. Branemark, *Int. J. Oral Surg.*, 1981, **10**, 387–416.
7 N. Jiang, S. S. Zhu, J. H. Li, L. Zhang, Y. M. Liao and J. Hu, *RSC Adv.*, 2016, **6**, 49954–49965.
8 M. M. Lu, D. Shao, P. Wang, D. Y. Chen, Y. D. Zhang, M. Q. Li, J. H. Zhao and Y. M. Zhou, *RSC Adv.*, 2016, **6**, 82688–82697.
9 D. Buser, R. K. Schenk, S. Steinemann, J. P. Fiorellini, C. H. Fox and H. Stich, *J. Biomed. Mater. Res.*, 1991, **25**, 889–902.
10 G. Mendonca, D. B. Mendonca, F. J. Aragao and L. F. Cooper, *Biomaterials*, 2008, **29**, 3822–3835.
11 M. Karlsson, E. Palsgard, P. R. Wilshaw and L. Di Silvio, *Biomaterials*, 2003, **24**, 3039–3046.
12 K. Gulati, M. S. Aw, D. Findlay and D. Losic, *Ther. Deliv.*, 2012, **3**, 857–873.
13 D. Losic and S. Simovic, *Expert Opin. Drug Deliv*, 2009, **6**, 1363–1381.
14 K. Gulati, S. Maher, D. M. Findlay and D. Losic, *Nanomedicine (Lond)*, 2016, **11**, 1847–1864.
15 D. Losic, M. S. Aw, A. Santos, K. Gulati and M. Bariana, *Expert Opin. Drug Deliv*, 2015, **12**, 103–127.
16 R. A. Gittens, T. McLachlan, R. Olivares-Navarrete, Y. Cai, S. Berner, R. Tannenbaum, Z. Schwartz, K. H. Sandhage and B. D. Boyan, *Biomaterials*, 2011, **32**, 3395–3403.
17 S. L. Wu, Z. Y. Weng, X. M. Liu, K. W. K. Yeung and P. K. Chu, *Adv. Funct. Mater.*, 2014, **24**, 5464–5481.
18 S. Maher, G. Kaur, L. Lima-Marques, A. Evdokiou and D. Losic, *ACS Appl. Mater. Interfaces*, 2017, **9**, 29562–29570.
19 R. S. Faeda, R. Spin-Neto, E. Marcantonio, A. C. Guastaldi and E. Marcantonio Jr, *Microsc. Res. Tech.*, 2012, **75**, 940–948.
20 R. A. Surmenev, M. A. Surmeneva and A. A. Ivanova, *Acta Biomater.*, 2014, **10**, 557–579.
21 I. H. Orenstein, D. P. Tarnow, H. F. Morris and S. Ochi, *J. Periodontol.*, 1998, **69**, 1404–1412.

22 A. Kodama, S. Bauer, A. Komatsu, H. Asoh, S. Ono and P. Schmuki, *Acta Biomater.*, 2009, **5**, 2322–2330.
23 S. O'Brien, J. Shaw, X. Zhao, P. V. Abbott, P. Munroe, J. Xu, D. Habibi and Z. Xie, *J. Biomech.*, 2014, **47**, 1060–1066.
24 G. J. Atkins, K. J. Welldon, A. R. Wijenayaka, L. F. Bonewald and D. M. Findlay, *Am J Physiol-Cell Ph*, 2009, **297**, C1358–C1367.
25 M. Prideaux, A. R. Wijenayaka, D. D. Kumarasinghe, R. T. Ormsby, A. Evdokiou, D. M. Findlay and G. J. Atkins, *Calcif. Tissue Int.*, 2014, **95**, 183–193.
26 D. Yang, A. G. Turner, A. R. Wijenayaka, P. H. Anderson, H. A. Morris and G. J. Atkins, *Mol. Cell. Endocrinol.*, 2015, **412**, 140–147.
27 C. Caparros, M. Ortiz-Hernandez, M. Molmeneu, M. Punset, J. A. Calero, C. Aparicio, M. Fernandez-Fairen, R. Perez and F. J. Gil, *J. Mater. Sci.: Mater. Med.*, 2016, **27**, 151.
28 K. Gulati, M. Kogawa, M. Prideaux, D. M. Findlay, G. J. Atkins and D. Losic, *Mat Sci Eng C-Mater*, 2016, **69**, 831–840.
29 K. Gulati, M. S. Aw and D. Losic, *Nanoscale Res. Lett.*, 2011, **6**, 571.
30 K. Gulati, G. J. Atkins, D. M. Findlay and D. Losic, *Proc. SPIE*, 2013, **8812**, 88120C.
31 Y. X. Gu, J. Du, J. M. Zhao, M. S. Si, J. J. Mo and H. C. Lai, *J. Biomed. Mater. Res. B Appl. Biomater*, 2012, **100**, 2122–2130.
32 G. Ciapetti, G. Di Pompo, S. Avnet, D. Martini, A. Diez-Escudero, E. B. Montufar, M. P. Ginebra and N. Baldini, *Acta Biomater.*, 2017, **50**, 102–113.
33 L. F. Cooper, Y. Zhou, J. Takebe, J. Guo, A. Abron, A. Holmen and J. E. Ellingsen, *Biomaterials*, 2006, **27**, 926–936.
34 M. Niinomi, *Materials Science and Engineering: A*, 1998, **243**, 231–236.
35 N. Poondla, T. S. Srivatsan, A. Patnaik and M. Petraroli, *J. Alloys Compd.*, 2009, **486**, 162–167.
36 ASTM International, 2002.
37 A. Leyland and A. Matthews, *Wear*, 2000, **246**, 1–11.
38 S. K. Kim, J. B. Lee, J. Y. Koak, S. J. Heo, K. R. Lee, L. R. Cho and S. S. Lee, *J. Oral Rehabil.*, 2005, **32**, 346–350.
39 E. N. Mpoyi, M. Cantini, P. M. Reynolds, N. Gadegaard, M. J. Dalby and M. Salmeron-Sanchez, *ACS Nano*, 2016, **10**, 6638–6647.
40 D. D. Deligianni, N. Katsala, S. Ladas, D. Sotiropoulou, J. Amedee and Y. F. Missirlis, *Biomaterials*, 2001, **22**, 1241–1251.
41 K. L. Kilpadi, P. L. Chang and S. L. Bellis, *J. Biomed. Mater. Res.*, 2001, **57**, 258–267.
42 K. Wang, C. Zhou, Y. Hong and X. Zhang, *Interface Focus*, 2012, **2**, 259–277.
43 B. Joddar and Y. Ito, *J. Mater. Chem.*, 2011, **21**, 13737–13755.
44 A. G. Gristina, *Science*, 1987, **237**, 1588–1595.
45 D. M. Rivera-Chacon, M. Alvarado-Velez, C. Y. Acevedo-Morantes, S. P. Singh, E. Gultepe, D. Nagesha, S. Sridhar and J. E. Ramirez-Vick, *J. Biomed. Nanotechnol.*, 2013, **9**, 1092–1097.
46 S. Gronthos, A. C. Zannettino, S. E. Graves, S. Ohta, S. J. Hay and P. J. Simmons, *J. Bone Miner. Res.*, 1999, **14**, 47–56.
47 G. J. Atkins, P. Kostakis, B. Pan, A. Farrugia, S. Gronthos, A. Evdokiou, K. Harrison, D. M. Findlay and A. C. Zannettino, *J. Bone Miner. Res.*, 2003, **18**, 1088–1098.
48 S. L. Dallas, M. Prideaux and L. F. Bonewald, *Endocr. Rev.*, 2013, **34**, 658–690.
49 G. Atkins and D. Findlay, *Osteoporosis Int.*, 2012, **23**, 2067–2079.
50 J. Cubo, M. Hui, F. Clarac and A. Quilhac, *J. Morphol.*, 2017, **278**, 621–628.
51 H. Chen, T. Senda and K. Y. Kubo, *Med. Mol. Morphol.*, 2015, **48**, 61–68.
52 H. W. Kim, H. E. Kim and J. C. Knowles, *Biomaterials*, 2004, **25**, 3351–3358.
53 T. A. Franz-Odendaal, B. K. Hall and P. E. Witten, *Dev. Dyn.*, 2006, **235**, 176–190.
54 G. J. Atkins, P. S. Rowe, H. P. Lim, K. J. Welldon, R. Ormsby, A. R. Wijenayaka, L. Zelenchuk, A. Evdokiou and D. M. Findlay, *J. Bone Miner. Res.*, 2011, **26**, 1425–1436.
55 Y. L. Chang, C. M. Stanford and J. C. Keller, *J. Biomed. Mater. Res.*, 2000, **52**, 270–278.
56 K. J. Welldon, D. M. Findlay, A. Evdokiou, R. T. Ormsby and G. J. Atkins, *Mol. Cell Endocrinol.*, 2013, **376**, 85–92.

CHAPTER 5

ENGINEERING OF SURFACE NANOPILLARS ON 3D-PRINTED TITANIUM IMPLANTS

5.1. Overview

Bacterial infection is one of the leading causes of implant failure which mainly treated through systemic administration of antibiotics. Excessive antibiotics administration could result in severe adverse effect as well as development of antibiotic resistant bacteria.

This chapter presents a new surface engineering approach aiming to generate bioinspired micro- to nanostructures on surfaces on 3D-printed Ti implants fabricated by combining selective laser melting technology, electrochemical anodization, and hydrothermal (HT) processes.

Results showed that incorporating structural templates of TNTs created by electrochemical anodization on the surface served as seed promotors and initiators for the vertical growth of sharp nanostructures. The resulting implants display unique surfaces with a distinctive dual micro- to nano-topography composed of micron-sized spherical features and vertically aligned nanoscale pillar structures. The fabricated surface topography was capable to enhance hydroxyapatite like mineral deposition from simulated body fluid (SBF) compared to control. In addition, normal human osteoblast-like cells (NHBCs) showed strong surface adhesion while displayed greater propensity to mineralize compared to control surfaces.

The outcome of this chapter shows that the fabricated nature-inspired multiscale-structured surface could offer desired features for improving osseointegration while possessing antibacterial performance.

This chapter has been published as:

- **Shaheer Maher,** Asiri R. Wijenayaka, Luis Lima-Marques, Dongqing Yang, Gerald J. Atkins and Dusan Losic (2021), Advancing of additive-manufactured titanium implants with bioinspired micro- to nanotopographies. ACS Biomaterials Science & Engineering 7(2): 441-450.

Statement of Authorship

Title of Paper	Advancing of Additive-Manufactured Titanium Implants with Bioinspired Micro- to Nanotopographies
Publication Status	☑ Published ☐ Accepted for Publication ☐ Submitted for Publication ☐ Unpublished and Unsubmitted w ork w ritten in manuscript style
Publication Details	S. Maher, A.R. Wijenayaka, L. Lima-Marques, D. Yang, G.J. Atkins, D. Losic, Advancing of Additive-Manufactured Titanium Implants with Bioinspired Micro- to Nanotopographies, ACS Biomaterials Science & Engineering 7(2) (2021) 441-450.

Principal Author

Name of Principal Author (Candidate)	Shaheer Maher (*also known as* Shaheer Makar)		
Contribution to the Paper	Study design, samples preparation, performed characterization on all samples, interpreted data and wrote manuscript		
Overall percentage (%)	85%		
Certification:	This paper reports on original research I conducted during the period of my Higher Degree by Research candidature and is not subject to any obligations or contractual agreements with a third party that would constrain its inclusion in this thesis. I am the primary author of this paper.		
Signature		Date	19/08/2021

Co-Author Contributions

By signing the Statement of Authorship, each author certifies that:

i. the candidate's stated contribution to the publication is accurate (as detailed above);

ii. permission is granted for the candidate in include the publication in the thesis; and

iii. the sum of all co-author contributions is equal to 100% less the candidate's stated contribution.

Name of Co-Author	Asiri R. Wijenayaka		
Contribution to the Paper	Helped in cell study		
Signature		Date	19/08/2021

Name of Co-Author	Luis Lima-Marques		
Contribution to the Paper	Supervised 3D-printing process		
Signature		Date	19/08/2021

Please cut and paste additional co-author panels here as required.

Statement of Authorship

Title of Paper	Advancing of Additive-Manufactured Titanium Implants with Bioinspired Micro- to Nanotopographies
Publication Status	☑ Published ☐ Accepted for Publication ☐ Submitted for Publication ☐ Unpublished and Unsubmitted w ork w ritten in manuscript style
Publication Details	S. Maher, A.R. Wijenayaka, L. Lima-Marques, D. Yang, G.J. Atkins, D. Losic, Advancing of Additive-Manufactured Titanium Implants with Bioinspired Micro- to Nanotopographies, ACS Biomaterials Science & Engineering 7(2) (2021) 441-450.

Principal Author

Name of Principal Author (Candidate)	Shaheer Maher (*also known as* Shaheer Makar)
Contribution to the Paper	Study design, samples preparation, performed characterization on all samples, interpreted data and wrote manuscript
Overall percentage (%)	85%
Certification:	This paper reports on original research I conducted during the period of my Higher Degree by Research candidature and is not subject to any obligations or contractual agreements with a third party that would constrain its inclusion in this thesis. I am the primary author of this paper.
Signature	Date 23/08/2021

Co-Author Contributions

By signing the Statement of Authorship, each author certifies that:

i. the candidate's stated contribution to the publication is accurate (as detailed above);

ii. permission is granted for the candidate in include the publication in the thesis; and

iii. the sum of all co-author contributions is equal to 100% less the candidate's stated contribution.

Name of Co-Author	Dongqing Yang
Contribution to the Paper	Helped in cell study
Signature	Date 23/08/2021

Name of Co-Author	Gerald J. Atkins
Contribution to the Paper	Supervised cell studies, revised the final manuscript
Signature	Date 09/09/2021

Please cut and paste additional co-author panels here as required.

Statement of Authorship

Title of Paper	Advancing of Additive-Manufactured Titanium Implants with Bioinspired Micro- to Nanotopographies
Publication Status	☑ Published ☐ Accepted for Publication ☐ Submitted for Publication ☐ Unpublished and Unsubmitted work written in manuscript style
Publication Details	S. Maher, A.R. Wijenayaka, L. Lima-Marques, D. Yang, G.J. Atkins, D. Losic, Advancing of Additive-Manufactured Titanium Implants with Bioinspired Micro- to Nanotopographies, ACS Biomaterials Science & Engineering 7(2) (2021) 441-450.

Principal Author

Name of Principal Author (Candidate)	Shaheer Maher (*also known* as Shaheer Makar)		
Contribution to the Paper	Study design, samples preparation, performed characterization on all samples, interpreted data and wrote manuscript		
Overall percentage (%)	85%		
Certification:	This paper reports on original research I conducted during the period of my Higher Degree by Research candidature and is not subject to any obligations or contractual agreements with a third party that would constrain its inclusion in this thesis. I am the primary author of this paper.		
Signature		Date	23/08/2021

Co-Author Contributions

By signing the Statement of Authorship, each author certifies that:

i. the candidate's stated contribution to the publication is accurate (as detailed above);

ii. permission is granted for the candidate in include the publication in the thesis; and

iii. the sum of all co-author contributions is equal to 100% less the candidate's stated contribution.

Name of Co-Author	Dusan Losic		
Contribution to the Paper	Supervised the development of work, edited and revised the manuscript and acted as the corresponding author		
Signature		Date	23/08/2021

Name of Co-Author			
Contribution to the Paper			
Signature		Date	

Please cut and paste additional co-author panels here as required.

ACS Biomaterials SCIENCE & ENGINEERING

pubs.acs.org/journal/abseba Article

Advancing of Additive-Manufactured Titanium Implants with Bioinspired Micro- to Nanotopographies

Shaheer Maher, Asiri R. Wijenayaka, Luis Lima-Marques, Dongqing Yang, Gerald J. Atkins, and Dusan Losic*

Cite This: *ACS Biomater. Sci. Eng.* 2021, 7, 441−450 Read Online

ACCESS | Metrics & More | Article Recommendations

ABSTRACT: There is an increasing demand for low-cost and more efficient titanium (Ti) medical implants that will provide improved osseointegration and at the same time reduce the likelihood of infection. In the past decade, additive manufacturing (AM) using metal selective laser melting (SLM) or three-dimensional (3D) printing techniques has emerged to enable novel implant geometries or properties to overcome such potential challenges. This study presents a new surface engineering approach to create bioinspired multistructured surfaces on SLM-printed Ti alloy (Ti6Al4V) implants by combining SLM technology, electrochemical anodization, and hydrothermal (HT) processes. The resulting implants display unique surfaces with a distinctive dual micro- to nano-topography composed of micron-sized spherical features, fabricated by SLM and vertically aligned nanoscale pillar structures as a result of combining anodization and HT treatment. The fabricated implants enhanced hydroxyapatite-like mineral deposition from simulated body fluid (SBF) compared to control. In addition, normal human osteoblast-like cells (NHBCs) showed strong adhesion to the nano-/microstructures and displayed greater propensity to mineralize compared to control surfaces. This engineering approach and the resulting nature-inspired multiscale-structured surface offers desired features for improving osseointegration and antibacterial performance toward the development of next-generation orthopedic and dental implants.

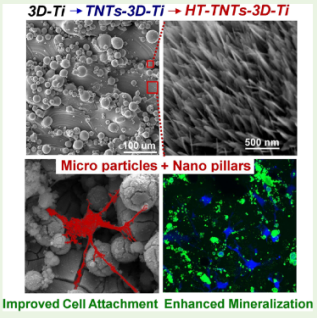

KEYWORDS: *additive manufacturing (AM), titanium implants, bioinspired materials, dual topography, nanostructures, selective laser melting (SLM)*

1. INTRODUCTION

The emerging field of bioinspired materials, connecting materials science and engineering with biology, is rapidly advancing the availability of new materials for broad applications.[1] Nature provides an unlimited source of inspiration for the design of many new materials based on the structures and properties mastered through evolution over millions of years.[2] These concepts of nature's material designs and their translation through engineering new artificial materials offer the potential to solve many problems across broad sectors, including the field of biomedical implants, which has strong needs for developing a new generation of implants with improved performance and functionality.[2]

Titanium (Ti) and its alloys have been broadly employed for many applications because of their remarkable mechanical properties, chemical stability, and unique corrosion resistance.[3,4] Many of these applications, such as protective coatings, electrodes, energy catalysis, and medical implants, are directed by their surface structures, functions and interfacial properties.[5,6] Ti is the most commonly used metal in medical implants also because of its excellent biocompatibility.[7] Although Ti-based medical implants have a long history of successful clinical use, they still face challenges related to their integration into the host tissues and longevity after implantation.[8−10] The failure of orthopedic implants can occur because of various reasons, including inflammation, poor osseointegration resulting in loosening, as well as bacterial infection, which are mainly related to implant surface properties.[11−13] The implant surface is the first site to come in contact with the surrounding tissue, and interfacial interactions with the biological environment play the most critical role in determining the fate of the implant inside the body. When bone implants fail, they may require repeated surgeries, carrying the risk of further morbidity and considerable socioeconomic cost.

Most surface engineering strategies to address Ti implant failure are focused on improving biointegration or preventing bacterial contamination and biofilm formation, with limited research devoted to combined approaches addressing both

Received: August 16, 2020
Accepted: January 6, 2021
Published: January 25, 2021

https://dx.doi.org/10.1021/acsbiomaterials.0c01210
ACS Biomater. Sci. Eng. 2021, 7, 441−450

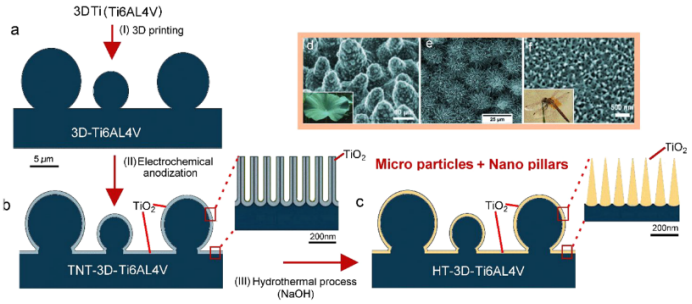

Figure 1. (a) Schematic presentation of the proposed concept for the fabrication of Ti materials with multistructured surfaces combining AM and surface-modification techniques, 3D printing (generating surface with microspheres), electrochemical anodization (generating a surface with vertically aligned TNTs), and hydrothermal process (generating an array of vertically aligned nanostructures). Examples of similar multistructured surfaces combining microbumps and sharp nanostructures occur in nature: (d) *Nelumbo nucifera* (Indian lotus) (reproduced with permission from ref[31] Copyright 2011 Beilstein Publishing), (e) wax rod-shaped structure on the surface of cabbage leaf (reproduced with permission from ref[32] Copyright 2014 The Royal Society of Chemistry (RSC)), and (f) dragonfly surface with nanopillar structures (reproduced with permission from ref[33] Copyright 2013 John Wiley & Sons, Inc.).

problems. To enhance cellular functions in response to the implant surface, both micro and nanoscale topographies have been suggested to be important features, although the influence of the specific topography, particular size, and geometry is still in debate.[14] Several conventional processes have been adopted to achieve a micro-rough surface, including mechanical spraying, laser sintering, and plasma processing.[15,16] Recently, more advanced surface modifications were explored, showing successful structural engineering of Ti and Ti alloys with micro- and nanoscale structures with a broad range of size and geometries, including spheres, particles, tubes, rods, pillars, spikes, and wires.[17,18] This was achieved using several processes, such as electrochemical etching, anodization, plasma and metal deposition, and hydrothermal (HT) processing.[19−22] They result in creating Ti materials with many new properties, including increased surface area and porosity and improved photocatalytic and interfacial properties beneficial for many applications, in particular, for biomedical implants.[9,11]

As a result of recent advancements in low-cost additive manufacturing (AM) techniques and their translation into numerous pharmaceutical and medical applications (e.g., new drug-delivery and tissue engineering),[23,24] it was reasonable to integrate these surface-engineering AM technologies in order to further improve and extend the properties and functionalities of resulting Ti medical implants. Motivated by these prospects, our team pioneered the combination of a selective laser melting (SLM) three-dimensional (3D) printing technique and electrochemical anodization to fabricate Ti alloys with unique surfaces composed of microspheres and arrays of titania nanotubes (TNTs) vertically aligned to the microstructured surface.[24−26] The specific aim of this study was to evaluate bone cell interaction and integration with these multiscale structures in order to improve cell adhesion, proliferation, and osseointegration, beyond what is achievable on the unmodified surfaces of conventional Ti implants.[24−26]

Following our previous studies on AM-Ti implants focused on improving biointegration properties, herein, we present another concept to fabricate a new type of multiscale-structured implant surface inspired by the goal of improving their osseointegration and antibacterial properties. The proposed concept is to implement the bioinspired multistructured surface on 3D-printed Ti alloys that combine microspheres and an array of nanosharp nanostructures. The latter feature is motivated by recent studies showing that such nanostructures developed in nature (for example, on insect wings) can kill bacteria by the physical disruption of their cell membranes.[27−29] To fabricate this type of multistructured surface, we applied AM technologies to the Ti alloy, establishing a microsphere topography followed by surface modification by electrochemical anodization and HT processing in NaOH to generate vertically aligned, sharp nanostructures over the entire surface. It is worth mentioning that these surface-modification techniques are cheaper, time-efficient, and more diverse in providing surfaces with a broad range of nanostructures compared to other techniques, such as plasma coating which requires specific expensive hardware, time-consuming procedures to adjust the coating parameters (e.g., vacuum, inert gas, temperature, etc.), and is problematic for coating complex shapes.[30] The proposed concept is summarized in Figure 1. In addition to the novel production process, i.e. combining three diverse methods to fabricate this unique multistructured surface, our approach involves the production of a template to induce the surface growth of titanate nanostructures with specific two-dimensional (2D) structures by a specific HT process, which, to our knowledge, has not been previously reported. Structural templates from TNTs created by electrochemical anodization on the surface act as seed promotors and initiators for the vertical growth of sharp nanostructures using the HT process. The HT process with the specific alkali NaOH was selected based on previous studies, showing that this promotes the relatively uniform vertical growth of titanate structures from the surface.[7,11,31−33] The fabricated multistructured surfaces of titania using this integrated and scalable process are similar to the natural structures found in plants, such as Indian lotus (*Nelumbo nucifera*), and the wings of insects, such as the dragonfly, display exciting properties and functionalities that have been translated into new material designs (Figure 1d−f).[34−36] The morphologic features of these fabricated surfaces are characterized in terms of their promotion of hydroxyapatite (HA) growth, mineralization, and bone cell growth ability.

2. EXPERIMENTAL SECTION

2.1. Fabrication of SLM or 3D Ti Implants. Titanium wafers (0.61 ± 0.01 mm thickness) in the form of square strips (1.2 × 1.2

https://dx.doi.org/10.1021/acsbiomaterials.0c01210
ACS Biomater. Sci. Eng. 2021, 7, 441−450

cm^2) were printed using Ti6Al4V powder (titanium grade 5, TLS Technik GmbH & Co. Spezialpulver, Germany) with an SLM machine (ProX 200 Production 3D Printer, Phenix Systems PXM (USA), equipped with 300 W Laser (1070 nm at 50% power)) under an inert argon atmosphere. The Ti6Al4V alloy powder material used in the fabrication process is characterized by the average particle diameter as follows: D[90%] = 31.32 μm, D[50%] = 24.07 μm, and D[10%] = 10.69 μm; where D[90%] indicates 90% of volume distribution below that value, D[50%] indicates 50% of volume distribution, while D[10%] indicates 10% of volume distribution below the value. The Ti wafers (3D-Ti) were then thoroughly cleaned by ultrasonication in acetone for 10 min to remove any nonattached particles from the surface followed by drying using a N_2 gun.

2.2. Surface Modification. The electrochemical anodization of the 3D-Ti samples was performed, as previously described,[25,26] using a temperature-controlled electrochemical cell designed in our laboratory. During the anodization process, 3D-Ti served as the anode, and a thin Ti foil served at as the cathode. The system was maintained at 60 °C under constant stirring. A constant voltage of 60 V was applied for 15 min. Voltage control was achieved using a computer-aided power supply (Agilent, USA), and change in current was recorded through the LabView program (National Instruments). After the formation of surface TNTs, the wafers were immersed in Milli-Q water (Option Q—Purelabs (Australia) for 7 days to remove any remaining electrolyte.

The HT reaction was carried out according to the procedures described previously,[11,31,32,37] with some modifications. Briefly, 3D-Ti or TNTs-3D-Ti were immersed in 50 ml of NaOH (1 M) (Chem-Supply, Australia) inside a Teflon vessel housed inside a 100 ml stainless-steel autoclave, which was then placed in an oven at 160 °C for different times ranging from 0.5 to 6 h. Subsequently, the vessels were allowed to cool to room temperature, and the samples were rinsed three times with Milli-Q water. The samples were then immersed in 0.6 M HCl solution for 1 h followed by calcination inside a tube furnace at 300 °C for 3 h under atmospheric conditions. This process was used to convert sodium titanate into hydrogen titanate, which has many valuable properties (catalytic, semiconductive properties). Unmodified 3D-Ti wafers were used as controls for all the experiments, and each experiment was repeated in triplicates.

2.3. Surface Characterization. Surface characterization was performed using focused-ion beam (FIB)—scanning electron microscopy (SEM) (FEI Helios Nanolab 600 Dual Beam, Thermo Fisher Scientific, Australia) and energy-dispersive X-ray spectroscopy (EDX, Oxford Ultim Max Large Area SDD EDS detector, Oxford instruments, USA). The samples were coated with platinum (5 nm) prior to imaging with SEM. X-ray diffraction (XRD) spectra (Rigaku MiniFlex 600, Japan) and the water contact angle (WCA), using a tension theta optical tensiometer (KSV instruments, Finland), of the samples were also recorded.

2.4. Hydroxyapatite-like Mineral Formation in Simulated Body Fluid. Simulated body fluid (SBF) was prepared by dissolving NaCl, $NaHCO_3$, KCl, $K_2HPO_4{\cdot}3H_2O$, $MgCl_2{\cdot}6H_2O$, $CaCl_2$, and Na_2SO_4 (Chem-Supply, Australia) in Milli-Q water at 36.5 °C with tris-hydroxymethyl aminomethane (Tris), and pH was adjusted to 7.4 using 1 M HCl. SBF ion concentrations (in mM) were as follows: N^+:142, K^+:5, Mg^{2+}:1.5, Ca^{+2}:2.5, Cl^-:147.8, HCO_3^-:4.2, HPO_4^{2-}:1, SO_4^{2-}: 0.5. The wafers were immersed in SBF for 28 days at 37 °C.[34] After that, the samples were removed from the solution, gently rinsed with Milli-Q water, and allowed to dry at room temperature. Surface microanalysis was then performed by XRD and SEM/EDX imaging.

2.5. Cell Culture. Normal human osteoblast-like cells (NHBCs) were obtained from patients who underwent total hip replacement surgery with patient-informed consent and with the approval of the Human Ethics Committee of the Royal Adelaide Hospital, as previously described.[38] NHBCs were passaged in a proliferation medium consisting of αMEM containing FCS (10% v/v), penicillin (50 U/ml), streptomycin (50 μg/ml), and ascorbate-2-phosphate (100 μM). All the cell culture chemicals were purchased from Life Technologies Pty Ltd. (Australia) unless otherwise specified. The cells were maintained at 37 °C in 5% CO_2 with 95% relative humidity. For differentiating experiments, the cells were cultured in a differentiation medium, consisting of αMEM, FCS (5% v/v), penicillin (50 U/ml), streptomycin (50 μg/ml), ascorbate-2-phosphate (100 μM), and KH_2PO_4 (1.8 mM) for up to 28 days to achieve an osteocyte-like phenotype, as previously described.[39]

Prior to seeding cells, alloy substrates were sterilized by immersion in 70% (v/v) ethanol for 5 min and air-drying in a Class II biohazard hood for 3 h followed by washing in sterile water thrice. Triplicate substrates were placed in a single well of a 6-well tissue culture plate. The NHBCs were seeded at 2×10^5 cells per well in 2 ml of proliferation media. The following day, the samples were moved to a new 6-well tissue culture plates containing the differentiation medium. Differentiation medium was replenished every 3 days for the duration of the experiment. Plates were maintained at 37 °C in a humidified incubator containing 5% CO_2.

Cell morphology, viability, and proliferation were studied using a live-cell-imaging approach on days 9 and 28 of differentiation. All samples for imaging were rinsed with PBS for 5 min at 37 °C and moved to a fresh 6-well plate containing the staining solution of CellTrace Calcein Violet, AM (500 nM; Thermo Fisher Scientific). Calcein Violet is a cell-permeant dye that is converted into fluorescent calcein after intracellular esterases remove the acetoxymethyl esters in the viable cells. Mineral deposition in the same samples was evaluated by adding Calcein Green (50 μM; Thermo Fisher Scientific) 24 h prior to imaging. Calcein Green is a cell-nonpermeant dye that fluoresces when it is bound to calcium crystals. The samples were inverted into 24-well imaging plates with 25 μm thin film bottom (Eppendorf) containing PBS buffer, and images were acquired using an Olympus FV3000 confocal imaging system with a silicon immersion objective (30x, Olympus, Australia). A 405 nm laser was used to excite Calcein Violet, and emission was collected in the range between 410 and 470 nm. A 488 nm laser was used to excite Calcein Green, and emission was collected in the range between 490 and 575 nm. Confocal microscopy images were also recorded, and the fluorescence intensity of each image was established using ImageJ (public domain program developed at the RSB of the NIH).[40,41] The results from ImageJ were statistically treated and expressed as mean ± standard deviation (SD). The unpaired *t*-test was used to analyze the data. The level of significance was set to $p < 0.05$ for all comparisons.

The cells were then fixed in 4% v/v paraformaldehyde (ProSciTech, Australia) and 1.25% v/v glutaraldehyde (Electron Microscopy Sciences, USA), washed with PBS, and sequentially dehydrated in ethanol (70, 90, and 100% for 15 min each). The samples were then immersed in hexamethyl disilazane (HMDS, Sigma-Aldrich, Australia):100% ethanol (1:1) solution for 10 min and then in 100% HMDS twice for 10 min. The samples were then dried and coated with platinum (5 nm) for SEM imaging.

3. RESULTS AND DISCUSSION

The SEM images of the surface morphology of the 3D-printed Ti alloy (3D-Ti) before and after the anodization process are presented in Figure 2. Figure 2a–c shows the typical surface of 3D-Ti with randomly dispersed microsphere structures, which result from an incomplete melting of metal powders used in the laser sintering process.[25,26] During this process, the laser melts Ti alloy powder (particles) in a layer-by-layer fashion to create the Ti alloy bulk structure, leaving microparticles on top of the last layer that is partially melted. The average diameter of these microparticles is ~12 μm, with the range from 5 to 20 μm, as measured by SEM. It is worth mentioning that these surface microparticles are strongly attached to the surface, which is confirmed by high resolution and cross-sectional SEM imaging (Figure 2c). In addition, any unattached or loosely attached particles were removed during the sonication step in acetone.

The SEM images of the 3D-printed surface after the anodization process are presented in Figure 2d–f. These

https://dx.doi.org/10.1021/acsbiomaterials.0c01210
ACS Biomater. Sci. Eng. 2021, 7, 441−450

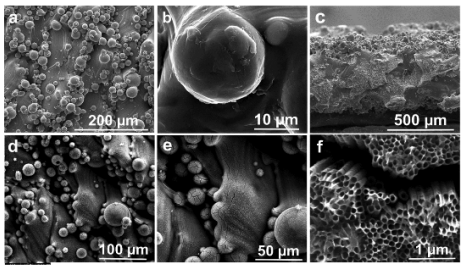

Figure 2. SEM images showing (a–c) top surface and the cross-section of the fabricated 3D-Ti alloys with spherical particles and their size. The conversion of their surface into the TiO_2 oxide layer with an array of vertically aligned nanotubes (TNTs) by electrochemical anodization is presented in SEM images that show the top surface in (d–f). This anodization layer is used as a template to grow an array of sharp nanostructures.

images confirm the formation of a layer of vertically aligned, well-ordered array of TNTs covering the whole surface, including the microsphere surface and the flat surface between them, as previously described.[26] The TNTs fabrication process yielded TNTs of dimensions ~120 ± 10 nm in diameter and 1 μm in length, which can be tailored by the anodization parameters, as reported previously in our previous work.[25] The mechanism of TNTs formation was previously described, involving balancing of two processes: one is the dissolution of Ti by the effect of fluoride ions and the other is the formation of a TiO_2 layer that leads to the formation of TNTs by a self-ordered process.[19,20] The fabricated TNTs serve as a template of TiO_2 to promote the nucleation required for the reaction with NaOH to generate nanopillared structures. In addition, the electrochemical anodization process will make the surface more corrosion-resistant and hence enhance its stability and longevity upon insertion into the body.[42,43]

The comparative surface morphologies after the hydrothermal process (1 M NaOH at 160 °C, followed by 0.6 M HCl and annealing) obtained after different HT times (0.5 to 6 h) on 3D-Ti and anodized 3D-Ti (i.e., TNTs-3D-Ti) are summarized in Figure 3. These images show that the majority of the surface of both the surfaces (3D-Ti and TNTs-3D-Ti) is covered with nanostructures as result of the HT process, although with different morphologies. For clarity, the SEM images mainly from the flat surface are presented, but the same nanostructures are created on microparticles as well. While on the anodized TNTs-3D-Ti surface, we can see the formation of vertical nanostructures (Figure 3f,h,j,l), and the non-anodized HT surface consisted of flat sheet-like structures (Figure 3e,g,i,k). These results support our hypothesis that the underlying layer of TNTs and their surface patterns could act as a template and direct the pattern of the vertical growth of nanostructures compared with the flat surface that promotes the horizontal growth (i.e., nanopillars vs nanosheets). This growth during the HT process is shown to be time-dependent, starting from small protrusions or bumps (0.5–1 h) to vertically aligned, sharp nanostructures 200–500 nm in height created at 4 h, which is consistent with previous studies.[37,44] With a longer duration of the HT process (6 h), the growth of a longer, sharp structure of several microns was observed on the TNT-3D-Ti surface (Figure 3l), showing that the size of these nanostructures can be temporally controlled. In this study, we found that the optimized HT time is 4 h, providing

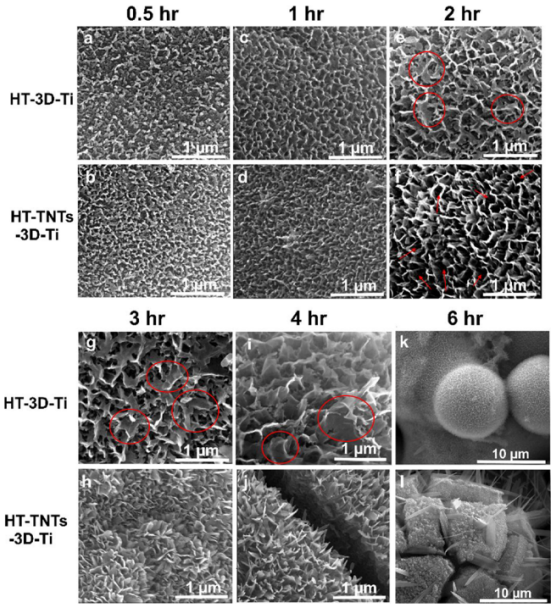

Figure 3. Comparative SEM images of nanostructured surface 3D-Ti (HT-3D-Ti) and TNTs-3D-Ti (HT-TNTs-3D-Ti) created by after the HT process (1 M NaOH) at different times (0.5, 1, 2,3, 4, and 6 h), showing the formation of different nanostructures. The arrows in figure (f) indicate the voids corresponding to the TNTs underlying the template. The circles denote the nanosheet structures.

the most desirable nanostructure, which could have the potential for mechano-bactericidal actions, as reported previously.[22,44,45]

High-resolution SEM images showing the optimized surface (HT at 4 h on TNTs-3D-Ti) are presented in Figure 4a to provide more details of the geometry and dimensions of the generated nanostructures from the HT process. The morphology of the generated nanostructures appears to have a 2D geometry with a sharp triangular shape. These nanostructures have a wide base, ranging from 50 to 100 nm, with sharp edges and sharp tips, and they can be described with different terms, such as nanospears or nanoswords. SEM images (Figure 4a,b). The length of these nanostructures increases as a function of the duration of the HT process, from 100 to 550 nm (4 h), which agrees with previous studies, showing that the growth rate of titanate nanostructures during the HT process is time-dependent.[22] Interestingly, after 6 h (Figure 3l), the surface nanostructures could grow into extensive sheets of titanate of length of ~5 μm. The interdistance between the top tips of these structures was measured to be around 50–250 nm. The distance increased within the first 2 h, after which the interdistance started to decrease again. This could be attributed to the initial fast dissolution of Ti^{4+} from TNTs during the hydrothermal process, as explained in the mechanism (vide infra), which leads to an increase in the distance between the tips, compared to $Na_2Ti_3O_7$ crystal formation. After this, the rate of crystal formation is increased, leading to a faster growth of the nanostructure (in length and width) with a subsequent decrease in the interdistance. The effect of the presence of TNTs could be also confirmed through the similarities between the TNTs diameters and the void spaces between

https://dx.doi.org/10.1021/acsbiomaterials.0c01210
ACS Biomater. Sci. Eng. 2021, 7, 441–450

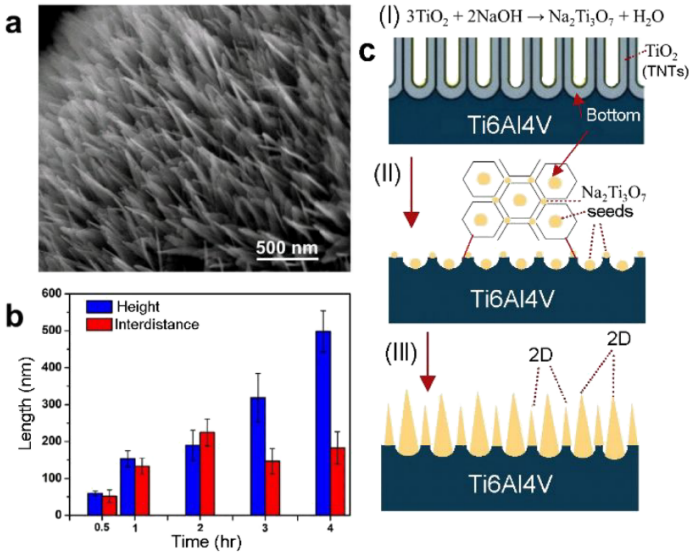

Figure 4. (a) High-resolution SEM images showing the high density of the vertically aligned nanostructure fabricated on the surface of TNTs-3D-Ti using the HT process with NaOH for 4 h. (b) Influence of HT time on the length and the interdistance of fabricated nanostructures. (c) Mechanism of the template-induced growth of the sodium-titanate nanostructure during the HT process with three stages: dissolution of TNTs, titanate seed formation on the underlying template, and the growth of nanostructures.

the nanostructures corresponding to the nanotube openings with a diameter of ~130 ± 18 nm (Figure 3f). This indicates that the nanostructures are induced by the specific geometry and the TiO_2 content of the underlying TNT pattern, confirming our proposed concept of surface-controlled HT growth.

These fabricated nanostructures are similar to those fabricated on black silicon, Ti, gold, and polymers fabricated using various methods, all of which have been shown to possess antibacterial properties based on their ability to kill bacteria by mechanical modes of action.[46,47] These 2D geometries with a combination of sharp edges and sharp tips are expected to be more efficient for the destruction of bacteria, providing multiple levels of sharp structures that can disrupt the bacterial cell walls. Most previous studies show a physical mode of action based on either sharp tips/spikes (e.g., black silicon[46]) or sharp edges (graphene[48]), but not on a combination of these two structures. A recent study by Ivanova et al. indicates that having a mixed topography increases antibacterial performance.[49,50] These nanostructures, generating a very high surface area, are also expected to have very strong catalytic properties potentially valuable for applications other than bone implants.[51]

The mechanism of surface modification during the HT process is complex and not yet fully understood, as it is influenced by many parameters, such as the substrate type, seeding, electrolyte concentration, temperature, time, electrolyte steering and pressure.[11,31] Most previous studies focused on the influence of electrolyte concentration (e.g., NaOH or KOH), temperature and duration on the creation of different morphologies. Our hypothesis presented in this study (illustrated in Figure 4c) is that the growth of specific nanosharp geometries can also be controlled by the substrate structure obtained before HT modification, which has not been considered previously. Our presented results strongly support this hypothesis, showing that the 3D-Ti printed substrate with an array of TNT structures can act as a template to facilitate the nucleation reaction and the growth of the observed nanostructures. We hypothesize that the process of the TNT template-induced growth occurred in three stages. In the first stage, the Ti^{4+} ions were generated from the dissolution of the TiO_2 oxide layer (TNTs) by NaOH (Figure 4c, Stage I). These Ti^{4+} ions under high temperature and pressure during the HT process recrystallize in the form of the initial crystals of $Na_2Ti_3O_7$ (sodium titanate) on the underlying Ti alloy surface (Stage II).[52] We postulate that the underlying template of TNTs structures have a crucial role in this recrystallization process, promoting and locating these seeds on their central and connecting edges. When these initial crystals form at these locations, they act as nucleation sites for further growth of well-defined nanostructures (Stage III, Figure 4c). The scheme of the proposed mechanism presented in Figure 4c, showing the generated nanostructures and their distribution on the surface and interdistance, are in a good agreement with the pattern of TNTs structures and observed nanostructures from the SEM images (Figure 4a). In contrast, in the case of the 3D-Ti-only substrates, the generated HT structures appear as the condensed layers of a nanosheet network with preferred horizontal growth, as seen in Figure 3.

Figure 5 summarizes the contact angle, as well as the EDX and XRD results from fabricated 3D-Ti and HT-TNTs-3D-Ti. The WCA of the 3D-Ti surface was 133° ± 3°, indicating the highly hydrophobic nature of the untreated surface. After the HT treatment, this surface is transformed into a super-hydrophilic surface where no WCA could be measured because of the formation of a hydrophilic titanate layer. Such a hydrophilic surface could improve bone cell adhesion and protein binding, which translates into enhanced osseointegration.[53] At the same time, it could significantly reduce bacterial attachment to the surface, as a result of a reduction in the

https://dx.doi.org/10.1021/acsbiomaterials.0c01210
ACS Biomater. Sci. Eng. 2021, 7, 441−450

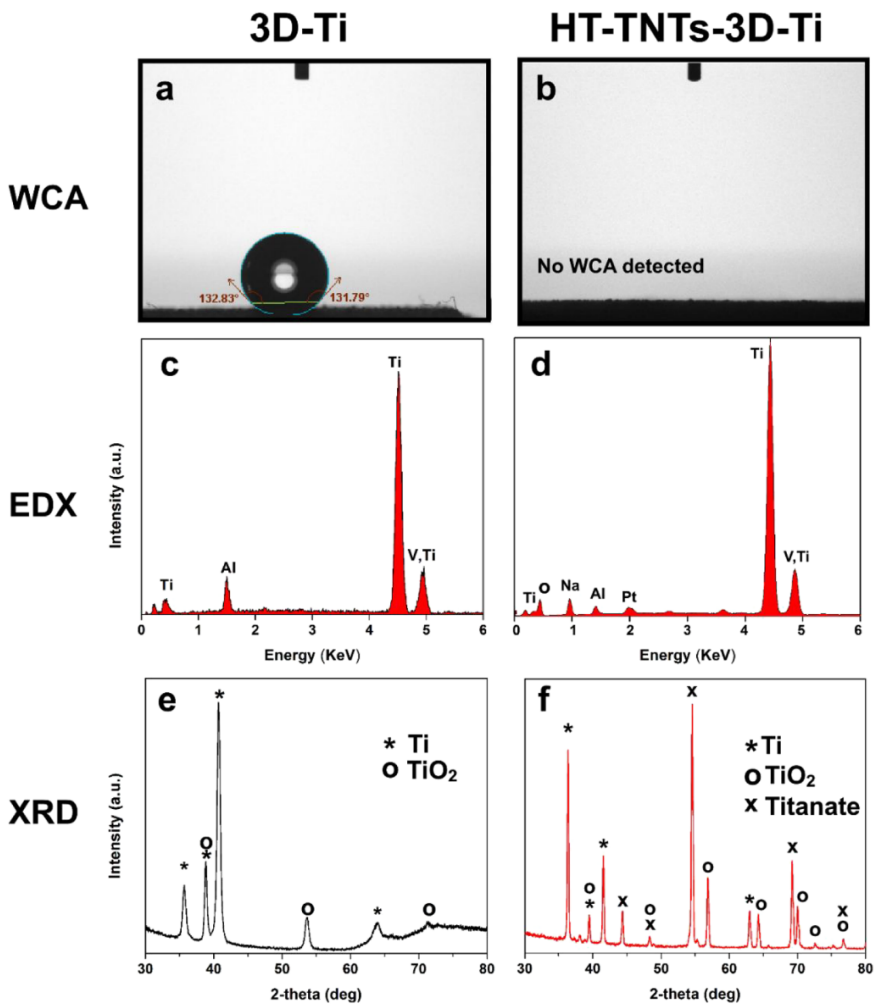

Figure 5. Surface properties and chemical characterization of fabricated 3D-Ti, before and after the HT process (HT-TNTs-3D-Ti) showing (a, b) wetting properties by WCA, (c, d) chemical composition by EDX, and (e, f) crystallinity by XRD. TiO_2 exists in anatase and rutile phases.

hydrophobic interaction and repulsion between the surface and bacteria, as previously shown.[54]

The comparative EDX analysis of the 3D-printed Ti6Al4V alloy before and after the HT process showed expected peaks for Ti, Al, and V, and the peaks of Na of titanate formed (Figure 5c,d). Furthermore, comparative XRD graphs showed sharp, high-intensity diffraction peaks, indicating the crystallinity of HT-TNTs-3D-Ti after annealing. Prominent Ti peaks appear in both 3D-Ti and HT-TNTs-3D-Ti, while prominent titanate peaks only appeared after the HT reaction. The peaks of HT-TNTs-3D-Ti also indicate the appearance of TiO_2 as anatase (JCPDS 21−1272) and rutile (JCPDS 21−1276) phases after the HT reaction, following annealing at 300 °C (Figure 5e,f). The results are in agreement with the standard peak patterns of titatnate $Na_2Ti_3O_7$ (JCPDS 31−1329) and $H_2Ti_3O_7$ (JCPDS 36−0654).[32,55] It is worth mentioning that there is an overlap between the XRD peaks of $Na_2Ti_3O_7$ produced after HT and those of $H_2Ti_3O_7$ produced after the reaction with HCl. At the same time, longer immersion times of samples, up to 72 h, in HCl is usually required to convert all $Na_2Ti_3O_7$ to $H_2Ti_3O_7$, as described by Bela et al.[55]

The fabricated HT-TNTs-3D-Ti dual micro to nano-structured surface was further studied to confirm its ability to support hydroxyapatite-like mineral (HAP) formation in vitro. HAP formation on the implant's surface is predictive of the host tissue response in vivo. Many studies confirmed that in vitro HAP formation from SBF, with an equal content of inorganic ions as plasma, shows strong agreement with in vivo studies.[56,57] The SEM images of HT-TNTs-3D-Ti that was immersed in SBF for 28 days show the deposition of HAP, in contrast to the 3D-Ti surface which appeared smooth with undetected deposition (Figure 6a,b). EDX analysis of the surface showed Ca and P peaks in the case of HT-TNTs-3D-Ti, as shown in Figure 6c, while no such peaks were detected for the 3D-Ti surface (i.e., the EDX pattern appeared similar to that shown in Figure 5c). These results were confirmed by XRD (Figure 6d), showing the specific HAP peak corresponding to the crystalline HA (JCPDS-0432). These results confirm that nano-rough structures (i.e., nano-pillars) could signifi-

https://dx.doi.org/10.1021/acsbiomaterials.0c01210
ACS Biomater. Sci. Eng. 2021, 7, 441−450

ACS Biomaterials Science & Engineering pubs.acs.org/journal/abseba Article

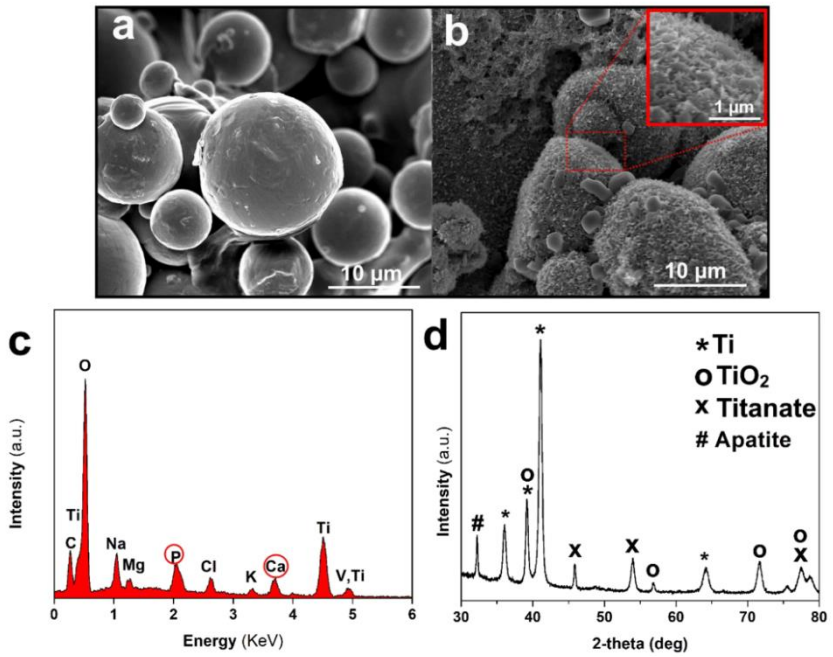

Figure 6. HAP-like formation in SBF, (a) SEM image showing the 3D-Ti surface with no HAP deposits after immersion in SBF for 28 days, (b) SEM image showing HAP-like deposition on the HT-TNTs-3D-Ti surface, (c) EDX analysis of HT-TNTs-3D-Ti showing the peaks of Ca and P, and (d) XRD of the HT-TNTs-3D-Ti surface after HAP-like deposition.

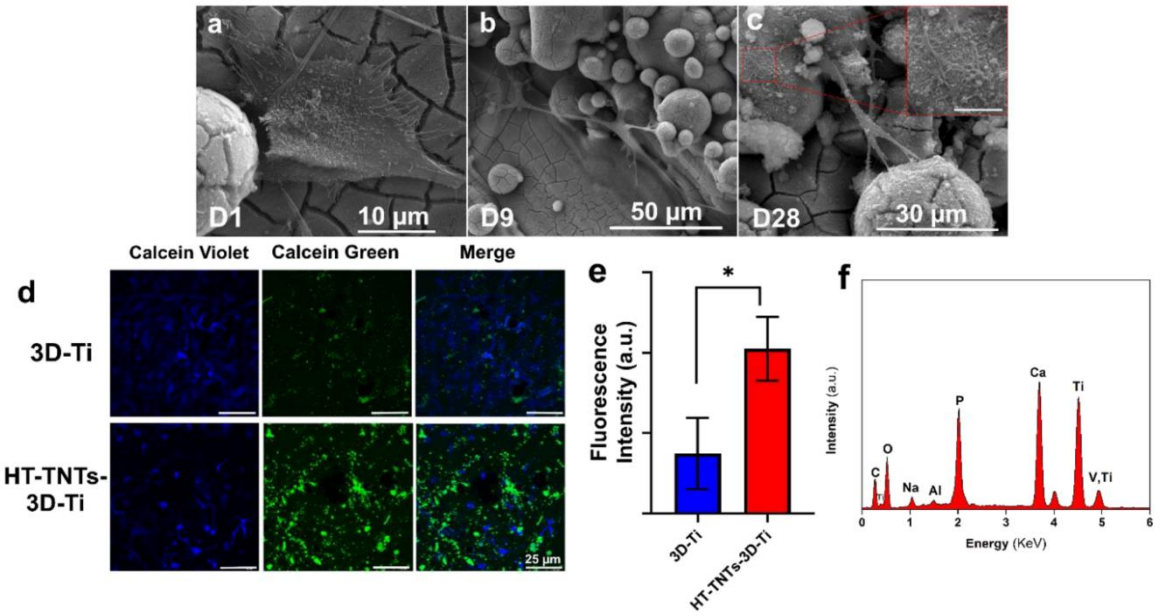

Figure 7. Cell culture of NHBCs, (a–c) SEM images showing NHBCs attached and their morphology on HT-TNTs-3D-Ti after incubation for 1, 9, and 28 days, respectively (inset in (c) showing higher magnification of extracellular matrix (ECM) fibers, scale bar 5 μm), (d) confocal microscopy images of NHBCs after culture on HT-TNTs-3D-Ti and 3D-Ti for 28 days showing viable cells in purple (Calcein Violet) and mineral deposition in green (Calcein Green), (e) bar chart showing the intensity of fluorescence measured from the confocal microscopy images (n = 3; mean ± SD); statistically significant difference is indicated by * ($p < 0.05$), and (f) EDX surface analysis of HT-TNTs-3D-Ti after 28 days of cell culture showing calcium and phosphorus peaks.

https://dx.doi.org/10.1021/acsbiomaterials.0c01210
ACS Biomater. Sci. Eng. 2021, 7, 441−450

cantly enhance the nucleation and growth of HAP residues, which is expected to support the process of osseointegration. In addition, rapid nucleation of HAP could be also attributed to ion exchange from HT-TNTs-3D-Ti with the H_3O^+ ions in SBF, which results in the formation of Ti-OH groups. These groups subsequently combine with Ca^+ and phosphate ions to build up HAP-like crystals.[58]

The ultimate goal of using bone implants is to provide the required mechanical support and induce bone healing. This should be preceded by osseointegration in which the surrounding bone cells first interact with the implant surface. Recent studies have confirmed that micro/nanosurface topography could induce cell adhesion and attachment compared to smooth surfaces.[59,60] To ensure that the fabricated HT-TNTs-3D-Ti implants could support cell adhesion and proliferation, we examined the growth of NHBCs on their surface. Figure 7a−c shows NHBCs attached on the "peak and valley"-like structure of HT-TNTs-3D-Ti. The firm attachment could be confirmed by the presence of cytoskeletal stress fibers (actin-filaments), which could translate into effective osseointegration.[61] It is worth mentioning that the NHBCs morphology changed with time from day 1 to day 28. Plump, polygonal cells appeared on day 1, as seen in Figure 7a. After this time, the cells exhibited a stellate structure with more numerous and longer pseudopodia and cell processes, denoting a further differentiated morphology (Figure 7b,c).

Furthermore, NHBCs seeded on HT-TNTs-3D-Ti showed increased mineralization compared to those attached to the control samples, as detected by the Calcein Green stain (Figure 7d,e). These results were also confirmed by EDX analysis of the HT-TNTs-3D-Ti surface after 28 days of cell culture. Figure 7f shows prominent peaks for Ca and P deposited on the surface, which are the two main components of HAP. Increased mineralization suggests the differentiation of NHBCs into mature osteocyte-like cells.[62,63] During the differentiation process, extracellular matrix (ECM) rich in collagen is formed, which is subsequently followed by the deposition of a HAP-like, mineralized protein composite. Such ECM could be detected in the form of a network of fibers covering the entire surface (Figure 7c, inset).

4. CONCLUSIONS

In conclusion, this study presents the fabrication of unique bioinspired surfaces with multiscale micro- to nanotopography on Ti alloy, which is achieved by a combination of AM or SLM techniques, electrochemical anodization and HT processing. This type of surface topography composed of randomly dispersed spherical microspheres covered by vertically aligned sharp nanostructures (nano-spears) has nature's signature used by plants and insects for protective purposes. The study revealed, for the first time, the template-aided fabrication of arrays of distinct nanostructures by HT processing, which is achieved using TNTs to act as nucleation sites for their growth. The time-dependent growth of these nanostructures was confirmed, which opens the possibility to further tune and optimize their length relevant to the desired biological response (cell growth, proliferation, differentiation, antibacterial response, etc.). A considerable enhancement of HAP-like mineral deposition from the SBF solution compared to control is confirmed, which is the critical requirement for Ti implants. Finally, studies using NHBCs showed strong bone cell adhesion to this mixed micro to nanostructure and significantly greater propensity to mineralize compared to the control surfaces. These results indicate several valuable advantages of dual micro−nano topographies, which are important for orthopedic and dental implants, showing their ability to provide multiple benefits; they not only support host cell attachment and bone mineralization, demonstrated here, but also potentially provide antibacterial protection that will be explored in further studies. In addition, the AM technology with the implant design flexibility will allow "on demand" low-cost production of desired medical implants with customized shapes and dimensions, specifically for individual needs ready to use, without the need for mass production, storage and shelf-life problems, which is not possible with current processes. Final determination of the effectiveness of these new types of implants with unique nanostructures requires further experimental studies to evaluate long-term interactions with human bone cells, together with their effectiveness against different bacterial strains.

AUTHOR INFORMATION

Corresponding Author

Dusan Losic − *School of Chemical Engineering and Advanced Materials, The University of Adelaide, Adelaide, South Australia 5005, Australia;* orcid.org/0000-0002-1930-072X; Email: dusan.losic@adelaide.edu.au

Authors

Shaheer Maher − *School of Chemical Engineering and Advanced Materials, The University of Adelaide, Adelaide, South Australia 5005, Australia;* orcid.org/0000-0002-2556-1096

Asiri R. Wijenayaka − *Centre for Orthopaedic and Trauma Research, Adelaide Medical School, Discipline of Orthopaedics and Trauma, The University of Adelaide, Adelaide, South Australia 5005, Australia*

Luis Lima-Marques − *The Institute for Photonics and Advanced Sensing, The University of Adelaide, Adelaide, South Australia 5005, Australia*

Dongqing Yang − *Centre for Orthopaedic and Trauma Research, Adelaide Medical School, Discipline of Orthopaedics and Trauma, The University of Adelaide, Adelaide, South Australia 5005, Australia*

Gerald J. Atkins − *Centre for Orthopaedic and Trauma Research, Adelaide Medical School, Discipline of Orthopaedics and Trauma, The University of Adelaide, Adelaide, South Australia 5005, Australia;* orcid.org/0000-0002-3123-9861

Complete contact information is available at: https://pubs.acs.org/10.1021/acsbiomaterials.0c01210

Author Contributions

The manuscript was written through contributions of all authors. All authors have given approval to the final version of the manuscript.

Notes

The authors declare the following competing financial interest(s): All fabrication procedures used in this paper were previously developed by the authors or adapted from the literature. While the authors have no competing interests to declare, we acknowledge our involvement in an Innovative Manufacturing Collaborative Research Centre (IMCRC) project entitled 'An Antimicrobial Nanosurface for Orthopaedic Implants' (2018−2020); no financial, technical or other resource from that project was used to support this study.

https://dx.doi.org/10.1021/acsbiomaterials.0c01210
ACS Biomater. Sci. Eng. 2021, 7, 441−450

■ ACKNOWLEDGMENTS

The authors acknowledge the financial support provided to S.M. by the Australian Government Training Program Scholarship, Australian research Council (IH 15000003) grant, and Forrest George and Sandra Lynne Young Supplementary Scholarship. The authors are grateful to the School of Chemical Engineering at the University of Adelaide for support of this research.

■ REFERENCES

(1) Koch, K.; Bhushan, B.; Barthlott, W. Diversity of structure, morphology and wetting of plant surfaces. *Soft Matter* **2008**, *4*, 1943−1963.
(2) Sun, Y.; Guo, Z. Recent advances of bioinspired functional materials with specific wettability: from nature and beyond nature. *Nanoscale Horiz.* **2019**, *4*, 52−76.
(3) Chouirfa, H.; Bouloussa, H.; Migonney, V.; Falentin-Daudré, C. Review of titanium surface modification techniques and coatings for antibacterial applications. *Acta Biomater.* **2019**, *83*, 37−54.
(4) Geetha, M.; Singh, A. K.; Asokamani, R.; Gogia, A. K. Ti based biomaterials, the ultimate choice for orthopaedic implants − A review. *Prog. Mater. Sci.* **2009**, *54*, 397−425.
(5) Jiang, X.; Zhang, Y.; Li, Z.; Ren, Y.; Zhang, M.; He, G.; Song, X.; Sun, Z. Microstructure, optical and photoelectron-chemical properties of TiO2 microspheres prepared by hydrothermal method. *J. Mater. Sci.: Mater. Electron.* **2015**, *26*, 2070−2075.
(6) Chaguetmi, S.; Achour, S.; Mouton, L.; Decorse, P.; Nowak, S.; Costentin, C.; Mammeri, F.; Ammar, S. TiO_2 nanofibers supported on Ti sheets prepared by hydrothermal corrosion: effect of the microstructure on their photochemical and photoelectrochemical properties. *RSC Adv.* **2015**, *5*, 95038−95046.
(7) Cai, K.; Lai, M.; Yang, W.; Hu, R.; Xin, R.; Liu, Q.; Sung, K. L. P. Surface engineering of titanium with potassium hydroxide and its effects on the growth behavior of mesenchymal stem cells. *Acta Biomater.* **2010**, *6*, 2314−2321.
(8) Wennerberg, A.; Albrektsson, T. Effects of titanium surface topography on bone integration: a systematic review. *Clin. Oral Implants Res.* **2009**, *20*, 172−184.
(9) Maher, S.; Mazinani, A.; Barati, M. R.; Losic, D. Engineered titanium implants for localized drug delivery: recent advances and perspectives of Titania nanotubes arrays. *Expert Opin. Drug Deliv.* **2018**, *15*, 1021−1037.
(10) Campoccia, D.; Montanaro, L.; Arciola, C. R. A review of the biomaterials technologies for infection-resistant surfaces. *Biomaterials* **2013**, *34*, 8533−8554.
(11) Mohandas, A.; Krishnan, A. G.; Biswas, R.; Menon, D.; Nair, M. B. Antibacterial and cytocompatible nanotextured Ti surface incorporating silver via single step hydrothermal processing. *Mater. Sci. Eng. C Mater. Biol. Appl.* **2017**, *75*, 115−124.
(12) Mas-Moruno, C.; Su, B.; Dalby, M. J. Multifunctional Coatings and Nanotopographies: Toward Cell Instructive and Antibacterial Implants. *Adv. Healthcare Mater.* **2019**, *8*, No. 1801103.
(13) Orapiriyakul, W.; Young, P. S.; Damiati, L.; Tsimbouri, P. M. Antibacterial surface modification of titanium implants in orthopaedics. *J Tissue Eng* **2018**, *9*, No. 204173141878983.
(14) Li, Y.; Liu, C. Nanomaterial-based bone regeneration. *Nanoscale* **2017**, *9*, 4862−4874.
(15) Staruch, R.; Griffin, M. F.; Butler, P. Nanoscale Surface Modifications of Orthopaedic Implants: State of the Art and Perspectives. *Open Orthop. J.* **2016**, *10*, 920−938.
(16) Pałka, K.; Pokrowiecki, R. Porous Titanium Implants: A Review. *Adv. Eng. Mater.* **2018**, *20*, No. 1700648.
(17) Gulati, K.; Aw, M. S.; Findlay, D.; Losic, D. Local drug delivery to the bone by drug-releasing implants: perspectives of nano-engineered titania nanotube arrays. *Ther. Deliv.* **2012**, *3*, 857−873.
(18) Hasan, J.; Jain, S.; Chatterjee, K. Nanoscale Topography on Black Titanium Imparts Multi-biofunctional Properties for Orthopedic Applications. *Sci. Rep.* **2017**, *7*, No. 41118.
(19) Roy, P.; Berger, S.; Schmuki, P. TiO2 nanotubes: synthesis and applications. *Angew. Chem., Int. Ed.* **2011**, *50*, 2904−2939.
(20) Losic, D.; Aw, M. S.; Santos, A.; Gulati, K.; Bariana, M. Titania nanotube arrays for local drug delivery: recent advances and perspectives. *Expert Opin. Drug Deliv.* **2015**, *12*, 103−127.
(21) Gulati, K.; Maher, S.; Findlay, D. M.; Losic, D. Titania nanotubes for orchestrating osteogenesis at the bone−implant interface. *Nanomedicine* **2016**, *11*, 1847−1864.
(22) Wandiyanto, J. V.; Cheeseman, S.; Truong, V. K.; Kobaisi, M. A.; Bizet, C.; Juodkazis, S.; Thissen, H.; Crawford, R. J.; Ivanova, E. P. Outsmarting superbugs: bactericidal activity of nanostructured titanium surfaces against methicillin- and gentamicin-resistant Staphylococcus aureus ATCC 33592. *J. Mater. Chem. B* **2019**, *7*, 4424−4431.
(23) Jamróz, W.; Szafraniec, J.; Kurek, M.; Jachowicz, R. 3D Printing in Pharmaceutical and Medical Applications - Recent Achievements and Challenges. *Pharm. Res.* **2018**, *35*, 176−176.
(24) Gulati, K.; Prideaux, M.; Kogawa, M.; Lima-Marques, L.; Atkins, G. J.; Findlay, D. M.; Losic, D. Anodized 3D−printed titanium implants with dual micro- and nano-scale topography promote interaction with human osteoblasts and osteocyte-like cells. *J. Tissue Eng. Regen. Med.* **2017**, *11*, 3313−3325.
(25) Maher, S.; Kaur, G.; Lima-Marques, L.; Evdokiou, A.; Losic, D. Engineering of Micro- to Nanostructured 3D-Printed Drug-Releasing Titanium Implants for Enhanced Osseointegration and Localized Delivery of Anticancer Drugs. *ACS Appl. Mater. Interfaces* **2017**, *9*, 29562−29570.
(26) Qin, J.; Yang, D.; Maher, S.; Lima-Marques, L.; Zhou, Y.; Chen, Y.; Atkins, G. J.; Losic, D. Micro- and nano-structured 3D printed titanium implants with a hydroxyapatite coating for improved osseointegration. *J. Mater. Chem. B* **2018**, *6*, 3136−3144.
(27) Elbourne, A.; Crawford, R. J.; Ivanova, E. P. Nano-structured antimicrobial surfaces: From nature to synthetic analogues. *J. Colloid Interface Sci.* **2017**, *508*, 603−616.
(28) Jaggessar, A.; Shahali, H.; Mathew, A.; Yarlagadda, P. K. D. V. Bio-mimicking nano and micro-structured surface fabrication for antibacterial properties in medical implants. *J. Nanobiotechnol.* **2017**, *15*, 64.
(29) Michalska, M.; Gambacorta, F.; Divan, R.; Aranson, I. S.; Sokolov, A.; Noirot, P.; Laible, P. D. Tuning antimicrobial properties of biomimetic nanopatterned surfaces. *Nanoscale* **2018**, *10*, 6639−6650.
(30) Fox, K. E.; Tran, N. L.; Nguyen, T. A.; Nguyen, T. T.; Tran, P. A., Surface modification of medical devices at nanoscale—recent development and translational perspectives. In *Biomaterials in Translational Medicine*, Yang, L.; Bhaduri, S. B.; Webster, T. J., Eds. Academic Press: 2019; 163−189. DOI: 10.1016/B978-0-12-813477-1.00008-6.
(31) Anitha, V. C.; Banerjee, A. N.; Joo, S. W.; Min, B. K. Morphology-dependent low macroscopic field emission properties of titania/titanate nanorods synthesized by alkali-controlled hydrothermal treatment of a metallic Ti surface. *Nanotechnology* **2015**, *26*, No. 355705.
(32) Pavasupree, S.; Onoda, K.; Yoshikawa, S.; Simpraditpan, A.; Pecharapa, W. Characterization of Flower-like Titanate and Titania Nanowires on Titanium Plate Substrate. *Energy Procedia* **2013**, *34*, 555−562.
(33) Clements, L. R.; Wang, P.-Y.; Harding, F.; Tsai, W.-B.; Thissen, H.; Voelcker, N. H. Mesenchymal stem cell attachment to peptide density gradients on porous silicon generated by electrografting. *Phys. Status Solidi A* **2011**, *208*, 1440−1445.
(34) Ensikat, H. J.; Ditsche-Kuru, P.; Neinhuis, C.; Barthlott, W. Superhydrophobicity in perfection: the outstanding properties of the lotus leaf. *Beilstein J. Nanotechnol.* **2011**, *2*, 152−161.
(35) Ramachandran, R.; Nosonovsky, M. Surface micro/nano-topography, wetting properties and the potential for biomimetic icephobicity of skunk cabbage Symplocarpus foetidus. *Soft Matter* **2014**, *10*, 7797−7803.

https://dx.doi.org/10.1021/acsbiomaterials.0c01210
ACS Biomater. Sci. Eng. 2021, 7, 441−450

(36) Gao, C.-Y.; Meng, G.-X.; Li, X.; Wu, M.; Liu, Y.; Li, X.-Y.; Zhao, X.; Lee, L.; Feng, X. Wettability of dragonfly wings: the structure detection and theoretical modeling. *Surf. Interface Anal.* **2013**, *45*, 650−655.
(37) Cao, Y.; Su, B.; Chinnaraj, S.; Jana, S.; Bowen, L.; Charlton, S.; Duan, P.; Jakubovics, N. S.; Chen, J. Nanostructured titanium surfaces exhibit recalcitrance towards Staphylococcus epidermidis biofilm formation. *Sci. Rep.* **2018**, *8*, 1071.
(38) Atkins, G. J.; Kostakis, P.; Pan, B.; Farrugia, A.; Gronthos, S.; Evdokiou, A.; Harrison, K.; Findlay, D. M.; Zannettino, A. C. RANKL Expression Is Related to the Differentiation State of Human Osteoblasts. *J. Bone Miner. Res.* **2003**, *18*, 1088−1098.
(39) Prideaux, M.; Wijenayaka, A. R.; Kumarasinghe, D. D.; Ormsby, R. T.; Evdokiou, A.; Findlay, D. M.; Atkins, G. J. SaOS2 Osteosarcoma cells as an in vitro model for studying the transition of human osteoblasts to osteocytes. *Calcif. Tissue Int.* **2014**, *95*, 183−193.
(40) Kelley, J. B.; Paschal, B. M. Fluorescence-based quantification of nucleocytoplasmic transport. *Methods* **2019**, *157*, 106−114.
(41) Jensen, E. C. Quantitative analysis of histological staining and fluorescence using ImageJ. *Anat. Rec.* **2013**, *296*, 378−381.
(42) Kim, K.; Lee, B.-A.; Piao, X.-H.; Chung, H.-J.; Kim, Y.-J. Surface characteristics and bioactivity of an anodized titanium surface. *J. Periodontal. Implant Sci.* **2013**, *43*, 198−205.
(43) Singh, A.; Singh, B. P.; Wani, M. R.; Kumar, D.; Singh, J. K.; Singh, V. Effect of anodization on corrosion behaviour and biocompatibility of Cp-titanium in simulated body fluid. *Bull. Mater. Sci.* **2013**, *36*, 931−937.
(44) Diu, T.; Faruqui, N.; Sjöström, T.; Lamarre, B.; Jenkinson, H. F.; Su, B.; Ryadnov, M. G. Cicada-inspired cell-instructive nanopatterned arrays. *Sci. Rep.* **2014**, *4*, 7122.
(45) Linklater, D. P.; Baulin, V. A.; Juodkazis, S.; Crawford, R. J.; Stoodley, P.; Ivanova, E. P. Mechano-bactericidal actions of nanostructured surfaces. *Nat. Rev. Microbiol.* **2020**, *19*, 8−22.
(46) Ivanova, E. P.; Hasan, J.; Webb, H. K.; Gervinskas, G.; Juodkazis, S.; Truong, V. K.; Wu, A. H. F.; Lamb, R. N.; Baulin, V. A.; Watson, G. S.; Watson, J. A.; Mainwaring, D. E.; Crawford, R. J. Bactericidal activity of black silicon. *Nat. Commun.* **2013**, *4*, 2838.
(47) Wandiyanto, J. V.; Tamanna, T.; Linklater, D. P.; Truong, V. K.; Al Kobaisi, M.; Baulin, V. A.; Joudkazis, S.; Thissen, H.; Crawford, R. J.; Ivanova, E. P. Tunable morphological changes of asymmetric titanium nanosheets with bactericidal properties. *J. Colloid Interface Sci.* **2020**, *560*, 572−580.
(48) Nine, M. J.; Tran, D. N. H.; ElMekawy, A.; Losic, D. Interlayer growth of borates for highly adhesive graphene coatings with enhanced abrasion resistance, fire-retardant and antibacterial ability. *Carbon* **2017**, *117*, 252−262.
(49) Abdul Rahman, N. R.; Muniandy, L.; Adam, F.; Iqbal, A.; Ng, E. P.; Lee, H. L. Detailed photocatalytic study of alkaline titanates and its application for the degradation of methylene blue (MB) under solar irradiation. *J. Photochem. Photobiol., A* **2019**, *375*, 219−230.
(50) Le Clainche, T.; Linklater, D.; Wong, S.; Le, P.; Juodkazis, S.; Le Guével, X.; Coll, J.-; Ivanova, E.P.; Martel-Frachet, V. Mechano-Bactericidal Titanium Surfaces for Bone Tissue Engineering. *ACS Appl. Mater. Interfaces* **2020**, *12*, 48272−48283.
(51) Ivanova, E. P.; Linklater, D. P.; Werner, M.; Baulin, V. A.; Xu, X. M.; Vrancken, N.; Rubanov, S.; Hanssen, E.; Wandiyanto, J.; Truong, V. K.; Elbourne, A.; Maclaughlin, S.; Juodkazis, S.; Crawford, J. The multi-faceted mechano-bactericidal mechanism of nanostructured surfaces. *Proc. Natl. Acad. Sci.* **2020**, *117*, 12598−12605.
(52) Huang, J.; Cao, Y.; Deng, Z.; Tong, H. Formation of titanate nanostructures under different NaOH concentration and their application in wastewater treatment. *J. Solid State Chem.* **2011**, *184*, 712−719.
(53) Ercan, B.; Taylor, E.; Alpaslan, E.; Webster, T. J. Diameter of titanium nanotubes influences anti-bacterial efficacy. *Nanotechnology* **2011**, *22*, No. 295102.
(54) Yuan, Y.; Hays, M. P.; Hardwidge, P. R.; Kim, J. Surface characteristics influencing bacterial adhesion to polymeric substrates. *RSC Adv.* **2017**, *7*, 14254−14261.
(55) Bela, S.; Wong, A. S. W.; Ho, G. W. Hydrolysis and ion exchange of titania nanoparticles towards large-scale titania and titanate nanobelts for gas sensing applications. *J. Phys. D: Appl. Phys.* **2010**, *43*, No. 035401.
(56) Kokubo, T.; Takadama, H. How useful is SBF in predicting in vivo bone bioactivity? *Biomaterials* **2006**, *27*, 2907−2915.
(57) Chen, L.; Komasa, S.; Hashimoto, Y.; Hontsu, S.; Okazaki, J. In Vitro and In Vivo Osteogenic Activity of Titanium Implants Coated by Pulsed Laser Deposition with a Thin Film of Fluoridated Hydroxyapatite. *Int. J. Mol. Sci.* **2018**, *19*, 1127.
(58) Miyazaki, T.; Kim, H.-M.; Kokubo, T.; Ohtsuki, C.; Kato, H.; Nakamura, T. Mechanism of bonelike apatite formation on bioactive tantalum metal in a simulated body fluid. *Biomaterials* **2002**, *23*, 827−832.
(59) Liu, H.; Huang, X.; Yu, H.; Yang, X.; Zhang, X.; Hang, R.; Tang, B. A cytocompatible micro/nano-textured surface with Si-doped titania mesoporous arrays fabricated by a one-step anodization. *Mater. Sci. Eng., C* **2017**, *73*, 120−129.
(60) Moon, B.-S.; Kim, S.; Kim, H.-E.; Jang, T.-S. Hierarchical micro-nano structured Ti6Al4V surface topography via two-step etching process for enhanced hydrophilicity and osteoblastic responses. *Mater. Sci. Eng., C* **2017**, *73*, 90−98.
(61) Tojkander, S.; Gateva, G.; Lappalainen, P. Actin stress fibers assembly, dynamics and biological roles. *J. Cell Sci.* **2012**, *125*, 1855−1864.
(62) Boskey, A. L.; Roy, R. Cell culture systems for studies of bone and tooth mineralization. *Chem. Rev.* **2008**, *108*, 4716−4733.
(63) Atkins, G. J.; Rowe, P. S.; Lim, H. P.; Welldon, K. J.; Ormsby, R.; Wijenayaka, A. R.; Zelenchuk, L.; Evdokiou, A.; Findlay, D. M. Sclerostin is a locally acting regulator of late-osteoblast/preosteocyte differentiation and regulates mineralization through a MEPE-ASARM-dependent mechanism. *J. Bone Miner. Res.* **2011**, *26*, 1425−1436.

https://dx.doi.org/10.1021/acsbiomaterials.0c01210
ACS Biomater. Sci. Eng. 2021, 7, 441−450

CHAPTER 6

ANTIBACTERIAL ACTIVITY OF SURFACE NANOPILLARS FABRICATED ON 3D-PRINTED TITANIUM IMPLANTS

6.1. Overview

Since systemic administration of antibiotics to treat infection at site of the implant is limited with poor drug bioavailability, systemic side effects and the chance of development of resistant strains of bacteria. This chapter aims to explore a highly efficacious antibacterial surface combining physical and chemical antibacterial mechanisms in order to create long-term antibacterial protection on Ti implant. The potential antibacterial activity of surface nanopillars (physical bactericidal effect) fabricated on the surface of 3D-printed Ti implants was explored against two of the most common bacterial pathogens; *Staphylococcus aureus* and *Pseudomonas aeruginosa.* In addition, enhanced antibacterial performance was achieved through loading the fabricated implants with gallium nitrate as a non-conventional antibacterial agent which has less potential to develop bacterial resistance.

Results confirm significant antibacterial performance of Ga^{3+} loaded substrates with eradication of 100% bacteria. Moreover, nanopillars significantly prevented bacterial attachment and biofilm formation while killing bacteria remaining on the surface. Furthermore, 3D-printed surfaces with microspheres of diameter between 5-30 µm and interspaces of 12-35 µm favoured the attachment of osteoblast-like MG-63 cells.

The outcomes of this chapter will pave the way towards the generation of dual antibacterial implants that could be designed to enhance bone cell attachment while protecting from bacterial infection.

This chapter has been published as:

- **Shaheer Maher**, Denver Linklater, Hadi Rastin, Sandy Liao, Karolinne Martins, de Sousa, Luis Lima-Marques, Peter Kingshott, Helmut Thissen, Elena P. Ivanova and Dusan Losic (2021), Advancing of 3D-printed titanium implants with combined antibacterial protection using ultrasharp nanostructured surface and gallium-releasing agents. ACS Biomaterials Science & Engineering 8(1): 314–327.

Statement of Authorship

Title of Paper	Advancing of 3D-printed titanium implants with combined antibacterial protection using ultra-sharp nanostructured surface and gallium releasing agents
Publication Status	☐ Published ☐ Accepted for Publication ☑ Submitted for Publication ☐ Unpublished and Unsubmitted w ork w ritten in manuscript style
Publication Details	Advancing of 3D-printed titanium implants with combined antibacterial protection using ultra-sharp nanostructured surface and gallium releasing agents, Shaheer Maher, Denver Linklater, Hadi Rastin, Sandy Liao, Karolinne Martins de Sousa, Luis Lima-Marques, Peter Kingshott, Helmut Thissen, Elena P. Ivanova,Dusan Losic

Principal Author

Name of Principal Author (Candidate)	Shaheer Maher (*also known as* Shaheer Makar)		
Contribution to the Paper	Study design, samples preparation, performed characterization on all samples, participated in bacterial studies, interpreted data and wrote manuscript		
Overall percentage (%)	85%		
Certification:	This paper reports on original research I conducted during the period of my Higher Degree by Research candidature and is not subject to any obligations or contractual agreements with a third party that would constrain its inclusion in this thesis. I am the primary author of this paper.		
Signature		Date	31/08/2021

Co-Author Contributions

By signing the Statement of Authorship, each author certifies that:

i. the candidate's stated contribution to the publication is accurate (as detailed above);

ii. permission is granted for the candidate in include the publication in the thesis; and

iii. the sum of all co-author contributions is equal to 100% less the candidate's stated contribution.

Name of Co-Author	Denver Linklater		
Contribution to the Paper	Cell culture and bacterial study, revised the manuscript		
Signature		Date	31/8/2021

Name of Co-Author	Hadi Rastin		
Contribution to the Paper	Participated in bacterial study		
Signature		Date	31/08/2021

Please cut and paste additional co-author panels here as required.

Statement of Authorship

Title of Paper	Advancing of 3D-printed titanium implants with combined antibacterial protection using ultra-sharp nanostructured surface and gallium releasing agents
Publication Status	☐ Published ☐ Accepted for Publication ☑ Submitted for Publication ☐ Unpublished and Unsubmitted w ork w ritten in manuscript style
Publication Details	Advancing of 3D-printed titanium implants with combined antibacterial protection using ultra-sharp nanostructured surface and gallium releasing agents, Shaheer Maher, Denver Linklater, Hadi Rastin, Sandy Liao, Karolinne Martins de Sousa, Luis Lima-Marques, Peter Kingshott, Helmut Thissen, Elena P. Ivanova,Dusan Losic

Principal Author

Name of Principal Author (Candidate)	Shaheer Maher (*also known as* Shaheer Makar)
Contribution to the Paper	Study design, samples preparation, performed characterization on all samples, participated in bacterial studies, interpreted data and wrote manuscript
Overall percentage (%)	85%
Certification:	This paper reports on original research I conducted during the period of my Higher Degree by Research candidature and is not subject to any obligations or contractual agreements with a third party that would constrain its inclusion in this thesis. I am the primary author of this paper.
Signature	Date 31/08/2021

Co-Author Contributions

By signing the Statement of Authorship, each author certifies that:

i. the candidate's stated contribution to the publication is accurate (as detailed above);

ii. permission is granted for the candidate in include the publication in the thesis; and

iii. the sum of all co-author contributions is equal to 100% less the candidate's stated contribution.

Name of Co-Author	Peter Kinshott
Contribution to the Paper	Revised the final manuscript
Signature	Date 31/8/2021

Name of Co-Author	Helmut Thissen
Contribution to the Paper	Revised the final manuscript
Signature	Date 31/08/2021

Please cut and paste additional co-author panels here as required.

Statement of Authorship

Title of Paper	Advancing of 3D-printed titanium implants with combined antibacterial protection using ultra-sharp nanostructured surface and gallium releasing agents
Publication Status	☐ Published ☐ Accepted for Publication ☑ Submitted for Publication ☐ Unpublished and Unsubmitted w ork w ritten in manuscript style
Publication Details	Advancing of 3D-printed titanium implants with combined antibacterial protection using ultra-sharp nanostructured surface and gallium releasing agents, Shaheer Maher, Denver Linklater, Hadi Rastin, Sandy Liao, Karolinne Martins de Sousa, Luis Lima-Marques, Peter Kingshott, Helmut Thissen, Elena P. Ivanova,Dusan Losic

Principal Author

Name of Principal Author (Candidate)	Shaheer Maher (*also known as* Shaheer Makar)		
Contribution to the Paper	Study design, samples preparation, performed characterization on all samples, participated in bacterial studies, interpreted data and wrote manuscript		
Overall percentage (%)	85%		
Certification:	This paper reports on original research I conducted during the period of my Higher Degree by Research candidature and is not subject to any obligations or contractual agreements with a third party that would constrain its inclusion in this thesis. I am the primary author of this paper.		
Signature		Date	31/08/2021

Co-Author Contributions

By signing the Statement of Authorship, each author certifies that:

i. the candidate's stated contribution to the publication is accurate (as detailed above);

ii. permission is granted for the candidate in include the publication in the thesis; and

iii. the sum of all co-author contributions is equal to 100% less the candidate's stated contribution.

Name of Co-Author	Sandy Liao		
Contribution to the Paper	Participated in Cell culture study		
Signature		Date	31/8/2021

Name of Co-Author	Karolinne Martins de Sous		
Contribution to the Paper	Participated in cell culture study		
Signature		Date	31/08/2021

Please cut and paste additional co-author panels here as required.

Statement of Authorship

Title of Paper	Advancing of 3D-printed titanium implants with dual anti-bactericidal protection using ultra-sharp nanostructured surface and gallium releasing agent
Publication Status	☐ Published ☐ Accepted for Publication ☑ Submitted for Publication ☐ Unpublished and Unsubmitted w ork w ritten in manuscript style
Publication Details	

Principal Author

Name of Principal Author (Candidate)	Shaheer Maher (*also known as* Shaheer Makar)
Contribution to the Paper	Study design, samples preparation, performed characterization on all samples, interpreted data and wrote manuscript
Overall percentage (%)	85%
Certification:	This paper reports on original research I conducted during the period of my Higher Degree by Research candidature and is not subject to any obligations or contractual agreements with a third party that would constrain its inclusion in this thesis. I am the primary author of this paper.
Signature	Date: 20/08/2021

Co-Author Contributions

By signing the Statement of Authorship, each author certifies that:

i. the candidate's stated contribution to the publication is accurate (as detailed above);

ii. permission is granted for the candidate in include the publication in the thesis; and

iii. the sum of all co-author contributions is equal to 100% less the candidate's stated contribution.

Name of Co-Author	Luis Lima-Marques
Contribution to the Paper	Supervised 3D-printing process
Signature	Date: 20/08/2021

Name of Co-Author	
Contribution to the Paper	
Signature	Date:

Please cut and paste additional co-author panels here as required.

Statement of Authorship

Title of Paper	Advancing of 3D-printed titanium implants with combined antibacterial protection using ultra-sharp nanostructured surface and gallium releasing agents
Publication Status	☐ Published ☐ Accepted for Publication ☑ Submitted for Publication ☐ Unpublished and Unsubmitted w ork w ritten in manuscript style
Publication Details	Advancing of 3D-printed titanium implants with combined antibacterial protection using ultra-sharp nanostructured surface and gallium releasing agents, Shaheer Maher, Denver Linklater, Hadi Rastin, Sandy Liao, Karolinne Martins de Sousa, Luis Lima-Marques, Peter Kingshott, Helmut Thissen, Elena P. Ivanova,Dusan Losic

Principal Author

Name of Principal Author (Candidate)	Shaheer Maher (*also known* as Shaheer Makar)		
Contribution to the Paper	Study design, samples preparation, performed characterization on all samples, participated in bacterial studies, interpreted data and wrote manuscript		
Overall percentage (%)	85%		
Certification:	This paper reports on original research I conducted during the period of my Higher Degree by Research candidature and is not subject to any obligations or contractual agreements with a third party that would constrain its inclusion in this thesis. I am the primary author of this paper.		
Signature		Date	31/08/2021

Co-Author Contributions

By signing the Statement of Authorship, each author certifies that:

i. the candidate's stated contribution to the publication is accurate (as detailed above);

ii. permission is granted for the candidate in include the publication in the thesis; and

iii. the sum of all co-author contributions is equal to 100% less the candidate's stated contribution.

Name of Co-Author	Elena P. Ivanova		
Contribution to the Paper	Supervised cell and bacterial studies, revised the final manuscript		
Signature		Date	31/8/2021

Name of Co-Author	Dusan Losic		
Contribution to the Paper	Supervised the development of work, edited and revised the manuscript and acted as the corresponding author		
Signature		Date	31/08/2021

Please cut and paste additional co-author panels here as required.

ACS Biomaterials SCIENCE & ENGINEERING

pubs.acs.org/journal/abseba Article

Advancing of 3D-Printed Titanium Implants with Combined Antibacterial Protection Using Ultrasharp Nanostructured Surface and Gallium-Releasing Agents

Shaheer Maher,[○] Denver Linklater,[○] Hadi Rastin, Sandy Tzu-Ying Liao, Karolinne Martins de Sousa, Luis Lima-Marques, Peter Kingshott, Helmut Thissen, Elena P. Ivanova,* and Dusan Losic*

Cite This: https://doi.org/10.1021/acsbiomaterials.1c01030 Read Online

ACCESS | Metrics & More | Article Recommendations | Supporting Information

ABSTRACT: This paper presents the development of advanced Ti implants with enhanced antibacterial activity. The implants were engineered using additive manufacturing three-dimensional (3D) printing technology followed by surface modification with electrochemical anodization and hydrothermal etching, to create unique hierarchical micro/nanosurface topographies of microspheres covered with sharp nanopillars that can mechanically kill bacteria in contact with the surface. To achieve enhanced antibacterial performance, fabricated Ti implant models were loaded with gallium nitrate as an antibacterial agent. The antibacterial efficacy of the fabricated substrates with the combined action of sharp nanopillars and locally releasing gallium ions (Ga^{3+}) was evaluated toward *Staphylococcus aureus* and *Pseudomonas aeruginosa*. Results confirm the significant antibacterial performance of Ga^{3+}-loaded substrates with a 100% eradication of bacteria. The nanopillars significantly reduced bacterial attachment and prevented biofilm formation while also killing any bacteria remaining on the surface. Furthermore, 3D-printed surfaces with microspheres of diameter 5−30 μm and interspaces of 12−35 μm favored the attachment of osteoblast-like MG-63 cells, as confirmed via the assessment of their attachment, proliferation, and viability. This study provides important progress toward engineering of next-generation 3D-printed implants, that combine surface chemistry and structure to achieve a highly efficacious antibacterial surface with dual cytocompatibility to overcome the limitations of conventional Ti implants.

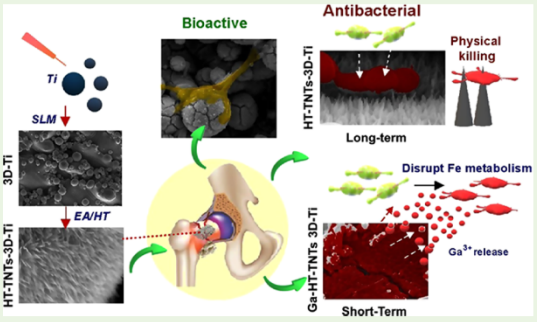

KEYWORDS: *titanium implants, antibacterial surfaces, osseointegration, additive manufacturing, selective laser melting, electrochemical anodization, hydrothermal, gallium nitrate*

1. INTRODUCTION

The use of titanium (Ti) medical implants to replace or heal nonfunctional bone tissues is a common worldwide healthcare practice due to their biocompatibility, corrosion resistance, and desired mechanical properties.[1,2] Despite their long history of application, Ti and Ti alloy implants (e.g., dental implants, screws, hip and knee replacements, rods, etc.) are still far from ideal and continue to suffer from poor osseointegration and bacterial infection.[1,3,4] These issues ultimately result in implant failure, which requires prolonged hospitalization and, in many cases, surgical replacement of the failed implant. This, in turn, significantly affects patients' quality of life, limiting their ability to work and perform essential daily tasks while adding a significant economic burden on the healthcare system (~69 000$ AUD per patient).[4,5] To address the challenges of the currently used implants, there is an urgent need for engineering a new generation of Ti implants that can prevent bacterial infection while simultaneously supporting bone cell attachment.[6,7]

Regarding implant-associated infection, the most common and routine approach to eliminate bacteria at the implant site is based on systemic antibiotic administration (e.g., gentamicin) prior to, and after, orthopedic surgery. This approach can cause systemic toxicity, resulting in severe adverse effects to the kidneys and liver, especially in elderly patients.[8] Also, the formation of bacterial biofilms and insufficient blood supply at the implant site can inhibit antibiotic activity.[9] Another approach is the local administration of antibiotics in the form of antibiotic-loaded implants or bone cement.[8] Nevertheless, the presence of antibiotics at high concentrations at the implant site can interfere with bone cell−surface interactions[8]

Received: August 13, 2021
Accepted: December 16, 2021

ACS Biomaterials Science & Engineering pubs.acs.org/journal/abseba Article

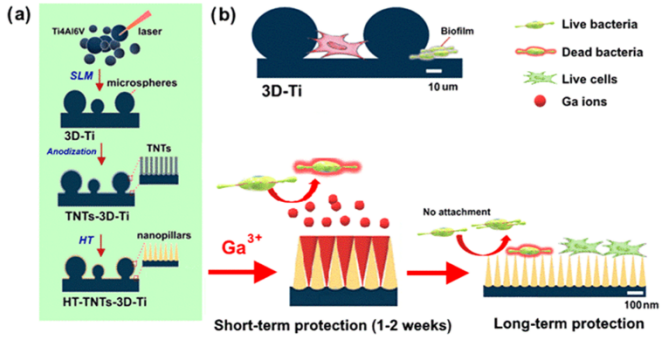

Figure 1. (a) Schematic representation of 3D-printed Ti implant fabrication by selective laser melting (SLM) followed by electrochemical anodization and hydrothermal processing (HT) to generate a unique surface with microparticles combined with nanopillars able to provide a dual mode of antibacterial protection. (b) Schematic representation showing these two modes of antibacterial protection achieved by releasing Ga^{3+} to kill surrounding bacteria and sharp nanostructures to kill bacteria in case they encounter the surface. This combination of microsphere and nanopillars structures was designed based on the rationale to provide balanced antibacterial and osseointegration performances.

and introduces a significant risk of the development of antimicrobial resistance (AMR) in bacterial pathogens, such as methicillin-resistant *Staphylococcus aureus* (MRSA).[10]

Owing to the limitations of conventional antibiotic applications, different surface modification approaches have been explored to modify implants to provide inherent bactericidal activity based on changes to their physicochemical properties (i.e., surface chemistry, surface charge, topography, and roughness).[8,11] Recently, a new and appealing approach was introduced based on the development of specific surface nanostructures that mimic the topography of insect wing (e.g., cicadas and dragonflies) surfaces that are able to mechanically kill bacteria through disruption of their cell membranes, creating a new perspective for the design of next-generation Ti implants.[12,13] These nanostructures are efficient at killing bacteria that come into direct contact with the surface; however, they are not capable of inhibiting bacterial infections within the bone microenvironment surrounding the implant.[11,14] As a result, an ideal implant should possess dual antibacterial activity; eradicating bacterial infection that could arise in the surrounding tissues during, or after, surgery and inhibiting any bacterial growth on its surface.[8]

Several nonconventional antibacterial agents such as silver (Ag), copper (Cu), gallium III ions (Ga^{3+}), and cerium have been explored as potential antimicrobial agents for Ti-implantable materials.[3,4,15] Recent studies showed that Ga^{3+} exhibits broad-spectrum antimicrobial activity against drug-resistant pathogens such as MRSA based on its ability to substitute iron, thus disrupting iron-dependent oxidation and reduction reactions required for bacterial DNA synthesis.[10] By contrast, Ag has shown some toxic side effects in *in vitro* studies.[16,17] In addition, Ga^{3+} has been used as an FDA-approved antitumor and antihypercalcemia drug.[18] Studies have confirmed that Ga^{3+} could promote bone cell growth and prevent osteoclastic activity, thus inhibiting bone breakdown.[19,20] Ga^{3+} can also enhance collagen synthesis and bone tissue formation.[19] These properties make Ga^{3+} a suitable candidate for preventing and eradicating implant-associated infections while also promoting bone tissue formation. Nonetheless, it has not been explored in combination with other antibacterial mechanisms on Ti implantable materials.

Indeed, most of the current research toward developing antibacterial strategies for Ti implants focuses on killing bacteria either by physical contact with the surface nanostructures or through chemical means (the release of surface-attached antibacterial agents), and only a few studies have focused on their combination.[21]

New structural manufacturing technology, called additive manufacturing (AM) technology (a.k.a. three-dimensional (3D) printing), has been recently explored for the manufacture of biomedical implants.[22−25] Despite the use of AM in the development of metal implants still being relatively underutilized, this technology offers many advantages over conventional fabrication techniques. For example, AM enables design flexibility with the ability to fabricate customized implants rapidly on demand with complex and optimized geometry to fit the requirements of the body and mimic bone porosity.[22,24,26] Selective laser melting (SLM) may be considered as an ideal AM process for the fabrication of Ti implants with much lower costs, minimized waste, and lower energy footprint compared to conventional implant manufacturing based on casting or machining.[22,27] We recently demonstrated the surface modification of 3D-printed implants possessing an array of nanopillar surface structures through combined electrochemical anodization and hydrothermal etching, which showed excellent mineralization of bone cells.[28]

Herein, we present a comprehensive study on the engineering of new surface topographies with micro−nano hierarchical structures on titania surfaces using a low-cost 3D-printing technology followed by further structural and chemical surface modifications to advance their antibacterial protection, as shown schematically in Figure 1. This study aimed to explore the creation of a new generation of Ti materials possessing a dual mode of antibacterial action based on the mechano-bactericidal action of sharp nanostructures and localized release of Ga^{3+}. The rationale of our proposed dual antibacterial approach is to provide, in the first step, a highly confident short-term antibacterial protection by the localized release of highly efficient antibacterial agent to kill any bacteria present on the implant, thus preventing any bacterial attachment or colonization over the first few days of the implant insertion, which carries the most risk for infection. In addition, long-term protection is provided by the sharp

https://doi.org/10.1021/acsbiomaterials.1c01030
ACS Biomater. Sci. Eng. XXXX, XXX, XXX−XXX

nanostructures on the implant surface, providing an additional insurance policy by minimizing any bacterial infection during the life of the implant inside the body. The bactericidal activity of fabricated 3D-printed implant models with and without releasing antibacterial agent (Ga^{3+}) was evaluated against two common human bacterial pathogens, *S. aureus* and *Pseudomonas aeruginosa*, together with the response of osteoblast-like cells. The results of this study will provide a better understanding of the development of bioactive surfaces with dual micro-nanotopography and their impact on both cells and bacteria. More importantly, this work provides a valuable contribution toward engineering a new generation of advanced bone implants manufactured by the SLM technology that is expected to disrupt existing conventional implant manufacturing technology.

2. MATERIALS AND METHODS

2.1. Fabrication of 3D-Ti Implant Models. Ti6Al4V implant models (1.5 × 1.5 cm^2) were fabricated with an SLM machine (ProX 200 Production 3D Printer, Phenix Systems PXM, equipped with a 270 W laser (1070 nm at 50% power, spot size 70 nm), scanning velocity: 1800 mm/s) under inert argon atmosphere with a chamber pressure of 24 mbar. Ti6Al4V alloy powder (Titanium grade 5, TLS Technik GmbH & Co. Spezialpulver, Germany) was used in the fabrication process as described previously.[29] The powder was spread in the form of which was then selectively melted by a laser beam to form a 30 nm thick layer. Successive layers were added till the desired thickness was achieved. After fabrication, the substrates were sonicated in acetone for 10 min to remove any unattached powder particles. The resulting samples with microstructured surface will be referred to as "3D-Ti" throughout this paper.

2.2. Fabrication of Nanopillar Structures on 3D-Ti (Mechanical Antibacterial Action). To fabricate nanopillars structures on the surface of 3D-Ti substrates, titania nanotubes (TNTs) were created on the surface using a temperature-controlled electrochemical cell designed in our laboratory as described elsewhere.[29,30] Briefly, 3D-Ti substrates were placed inside the cell as the anode while a Ti plate served as a counter electrode (i.e., cathode). The electrodes were immersed in ethylene glycol electrolyte solution containing lactic acid (1.5 M), water (5% w/w), and NH_4F (0.1 M) and maintained at 60 °C with an applied voltage of 60 V for 15 min under constant stirring. After anodization, the substrates (TNTs-3D-Ti) were cleaned by sonication in Milli-Q water for 5 min to remove any remaining electrolyte.

The hydrothermal process to make nanopillar structures and achieve mechanical antibacterial function was performed using an adapted procedure as described previously.[31−33] Briefly, TNTs-3D-Ti substrates were submerged in 50 mL of NaOH (1 M) (Chem-Supply, Australia) placed in a Teflon vessel housed inside a stainless-steel autoclave. The samples were hydrothermally etched for 4 h at 160 °C. Afterward, the samples were removed from the oven and allowed to cool to room temperature, rinsed three times with Milli-Q water, and allowed to dry at room temperature overnight. Subsequently, the samples were annealed inside a tube furnace at 300 °C for 3 h under atmospheric conditions. These hydrothermally modified substrates are referred to as HT-TNTs-3D-Ti throughout the text. All prepared substrates were placed in Milli-Q water for 2 weeks prior to cell and bacteria studies to ensure the complete removal of any chemicals that could be adsorbed during their fabrication.

2.3. Gallium Nitrate Loading on 3D-Printed Implants with Nanopillar Structures (Chemical Antibacterial Protection). To achieve the chemical antibacterial protection, HT-TNTs-3D-Ti, with nanopillar structures, were loaded by antibacterial agent Ga^{3+} by placing 10 μL of gallium nitrate solution (10 mg/mL) on the implant surfaces. The substrates were dried under vacuum for 1 h at room temperature to eliminate air gaps between the surface nanopillars and maximize loading. The previous step was repeated 25 times; thus, each substrate will be loaded with ∼2500 μg of gallium nitrate (equivalent to ∼683 μg of Ga^{3+}). These final fabricated models of drug-releasing substrates were referred to as Ga-HT-TNTs-3D-Ti.

2.4. Surface Characterization. High-resolution images of fabricated substrates in all steps were obtained using focused ion beam (FIB)-scanning electron microscopy (SEM) (FEI Helios Nanolab 600 Dual Beam, Thermo Fisher Scientific, Australia) operated at 10 kV. The samples were coated with platinum (5 nm) prior to imaging with SEM. The microsphere's average diameter and interdistances were measured from SEM images using ImageJ (public domain program developed at the RSB of the NIH). The surface chemical analysis was performed using energy-dispersive X-ray spectroscopy (EDX, Oxford Ultim Max Large Area SDD EDS detector, Oxford Instruments). X-ray diffraction spectra (XRD, Rigaku MiniFlex 600, Japan, with a tube voltage value of 40 kV and a tube current value of 15 mA) was obtained to show crystallinity of the surface micro−nanostructures. XRD spectra were obtained under ambient conditions at scanning rate of 10°/min using $Cu_{K\alpha}$ radiation for the range of 30−80°. Surface roughness was measured by noncontact laser profilometry (Contour GT-K, Bruker) and the roughness average (R_a − arithmetic mean of the absolute values of all points of the profile) was recorded. The surface water contact angle (WCA) was recorded using the sessile drop method at room temperature with a tension theta optical tensiometer (KSV instruments, Finland) equipped with an automated stage, droplet dispenser and a digital camera. Milli-Q water (resistivity 18.2 Ω) with a drop size of 2 μL was used. Three different spots for three different substrates were tested. The images were analyzed using OneAttension software (Ver 3.2, Biolin Scientific).

2.5. *In Vitro* Ga^{+3} Release Study and Kinetics. Drug-loaded substrates (Ga-HT-TNTs-3D-Ti) were immersed in 4 mL of PBS (pH 7.4) at 37 °C for 5 days. At a predetermined time, 400 μL of release solution was removed and replaced with fresh PBS to maintain sink conditions.[34]

All collected release samples were stored at 4 °C till analysis. Inductively coupled plasma mass spectrometry (ICP-MS Triple Quad, Agilent 8900) was used for quantitative analysis of released gallium ions. Calibration curve was obtained using ICP standard solution for gallium with different concentrations. All samples were diluted 100 times with 2% HNO_3 and then filtered with a 0.22 Millipore filter prior to analysis. Blank samples were prepared by placing HT-TNTs-3D-Ti substrates (i.e., drug fee) in PBS under the same conditions. All of the aforementioned experiments were repeated in triplicate, and the data were statistically treated.

2.6. Antibacterial Assays. *2.6.1. Bacterial Strains and Growth Conditions.* *P. aeruginosa* ATCC 9721 and *S. aureus* CIP 65.8^T were obtained from American Type Culture Collection and Pasteur Institute France, respectively. Frozen stocks were refreshed on nutrient agar at 37 °C for 24 h. Prior to experiments, bacteria were freshly subcultured on nutrient agar (Oxoid) for 24 h at 37 °C.

2.6.2. Antibacterial Activity of Ga^{3+}-Loaded Implant Models. To evaluate the antibacterial activity of Ga-HT-TNTs-3D-Ti, the samples were challenged against *S. aureus* and *P. aeruginosa* bacteria. First, the samples were sterilized under UV irradiation for 30 min before testing and placed in a 24-well plate. A single colony of bacteria was resuspended in broth medium to reach 0.5 MacFarland Unit (∼1.5 × 10^8 colony forming units (CFU)/mL). The suspension of *S. aureus* and *P. aeruginosa* was subsequently diluted 1:100 in TSB and NA, respectively to obtain a final bacterial concentration of ∼1.5 × 10^6 CFU/mL. Next, 20 μL of bacterial suspension was added on the sample's surface to cover the whole surface. The samples were then incubated at 37 °C for 5 h. After that, 980 μL of sterilized saline was added onto the sample's surface and shaken together for 1 min to resuspend the viable bacteria remaining on the surface.[35] Following this, 10-fold serial dilution of collected bacterial suspension was plated onto agar plates (TSA for *S. aureus* and Cetrimide agar for *P. aeruginosa*) and then incubated for 24 h at 37 °C. Afterward, the CFU were counted on each plate. Drug-free samples (HT-TNTs-3D-Ti) were also tested in the same way, while empty plastic wells were used as controls taken as 100% viability. The % bacterial cells viability was calculated based on eq 1

https://doi.org/10.1021/acsbiomaterials.1c01030
ACS Biomater. Sci. Eng. XXXX, XXX, XXX−XXX

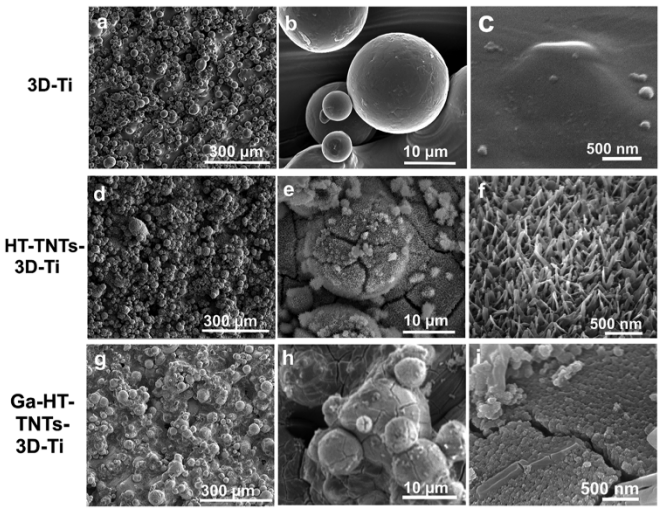

Figure 2. SEM images showing (a–c) the top surface of micro-smooth 3D-Ti, (d–f) HT-TNTs-3D-Ti with nanopillar structures generated after electrochemical anodization and hydrothermal processing of 3D-Ti, and (g–i) Ga-HT-TNTs-3D-Ti with gallium nitrate layer covering the surface. Images confirm the microstructure stability after both electrochemical anodization and hydrothermal etching (HT: hydrothermally treated, TNT: titania nanotubes, Ga: gallium).

$$\%\ \text{bacterial cell viability} = \frac{\text{CFUs}}{\text{CFUc}} \times 100 \quad (1)$$

where CFUs is the average number of CFU recorded for each sample and CFUc is the average CFU for plastic

2.6.3. Antibacterial Activity of the Release Solution. At the end of the drug release experiment (i.e., 5 days), the release solutions were collected to evaluate the antibacterial activity of the gallium ions released from the substrates. The sample solution (0.5 mL) was mixed with 0.5 mL of bacterial suspension (10^4 CFU/mL) and left in an incubator for 5 h. Then, 200 μL of each sample was transferred to a 96-well plate and the optical density (OD) of the bacterial suspension was measured at 595 nm using a FLUOstar OPTIMA plate reader (BMG Labtech, Ortenberg, Germany). Each experiment was repeated in triplicate, followed by statistical analysis.[36,37]

2.6.4. Antibacterial Activity of Surface Nanopillars. Bacterial suspensions of *P. aeruginosa* and *S. aureus* cells (adjusted to an OD_{600} 0.1 in nutrient broth (Oxoid)), were made up from freshly subcultured colonies on nutrient agar plates. The samples were incubated in 1 mL (sufficient to submerge the samples) of bacterial suspension in sterile 12-well plates for 18 h at 27 °C in dark and static conditions. The samples were then washed gently with distilled water, stained with LIVE/DEAD BacLight (Invitrogen), and imaged using confocal laser scanning microscopy. Counts of live and dead cells were quantified using Matlab software, CellC. Images were analyzed using ICY (Institut Pasteur, France) ver. 2.0.3.0.

2.6.5. Scanning Electron Microscopy (SEM) Imaging. The morphology of bacterial cells attached on different samples was assessed using SEM. The samples were gently rinsed with Milli-Q H_2O after incubation with bacteria, fixed with 2.5% v/v glutaraldehyde (Sigma), and were then rinsed two times with Milli-Q water. The samples were then dehydrated with ethanol at different concentrations (30, 50, 70, 90, and 100% v/v) for 10 min each and an additional 10 min in 100 v/v% ethanol. Afterward, the samples were immersed in hexamethyldisilazane (HMDS) (Sigma) for 10 min. The samples were left to air-dry and then sputter-coated with gold for imaging. High-resolution images were recorded using the SEM capabilities of a Raith150 Two direct-write ultrahigh-resolution electron beam lithography tool (Raith, GmBH) under high vacuum at an accelerating voltage of 3 kV.

2.7. Hydroxyapatite-like Mineral Formation in SBF. Simulated body fluid (SBF) was prepared by dissolving KCl, NaCl, $NaHCO_3$, $K_2HPO_4{\cdot}3H_2O$, $MgCl_2{\cdot}6H_2O$, $CaCl_2$, and Na_2SO_4 (Chem-Supply, Australia) in Milli-Q water with Tris-hydroxymethyl aminomethane (Tris) at 36.5 °C. pH was then adjusted to 7.4 using 1 M HCl. SBF ion concentrations (in mM) were as follows: N^+: 142, K^+: 5, Mg^{2+}: 1.5, Ca^{+2}: 2.5, Cl^-: 147.8, HCO_3^-: 4.2, HPO_4^{2-}: 1, SO_4^{2-}: 0.5. Gallium nitrate-loaded substrates were placed in a 12-well plate while immersed in 3 mL of SBF for 28 days at 37 °C.[38] After that, the samples were removed from the solution, gently rinsed with Milli-Q water, and allowed to dry at room temperature. Surface microanalysis was then performed by SEM/EDX imaging.

2.8. Cell Culture. Human osteosarcoma (osteoblast-like) MG-63 cells were obtained from Sigma-Aldrich. The cells were cultured in 75 cm^2 cell culture (T75) flasks with Dulbecco's modified Eagle's medium with GlutaMAX (Life Technologies, Inc.), supplemented with 10% fetal bovine serum, 1% penicillin–streptomycin (Sigma) at 37 °C in a humidified atmosphere with 5% CO_2. The cells were passaged for subculture when the cell density achieved 90% confluency. Prior to cell seeding, Ti samples and glass slides as positive control groups were sterilized with 70% (v/v) ethanol for 10 min and washed twice with sterile PBS. MG-63 cells were subsequently seeded on the samples at a density of 2×10^4 cells/cm^2. The cell density was calculated using a hemocytometer (Cells). The cells were incubated with Ga^{3+} free samples at 37 °C in a humidified atmosphere with 5% CO_2.

2.8.1. Cell Proliferation by MTS Assay. After 1, 4, and 7 days of incubation, the samples (Ga^{13} free) were gently washed twice with PBS to remove any unattached cells. The samples were then placed in a new well plate and immersed in DMEM with 20% (v/v) of the MTS reagent (Promega, WI) at 37 °C in a humidified atmosphere with 5% CO_2 for 1.5 h. During incubation, viable cells reduce tetrazolium salt into a colored formazan dye. This reaction is mediated by NAD(P)H-dependent dehydrogenase enzymes in the mitochondrial respiratory chain. The supernatant from each sample was then transferred to a new well plate (Sigma) and the absorbance was measured at 500 nm using a POLARstar Omega microplate reader (BMG Labtech, Ortenberg, Germany).

2.8.2. Cytotoxicity Assay. Using a CytoTox 96 Non-Radioactive Cytotoxicity Assay (Promega), the amount of extracellular lactate

https://doi.org/10.1021/acsbiomaterials.1c01030
ACS Biomater. Sci. Eng. XXXX, XXX, XXX–XXX

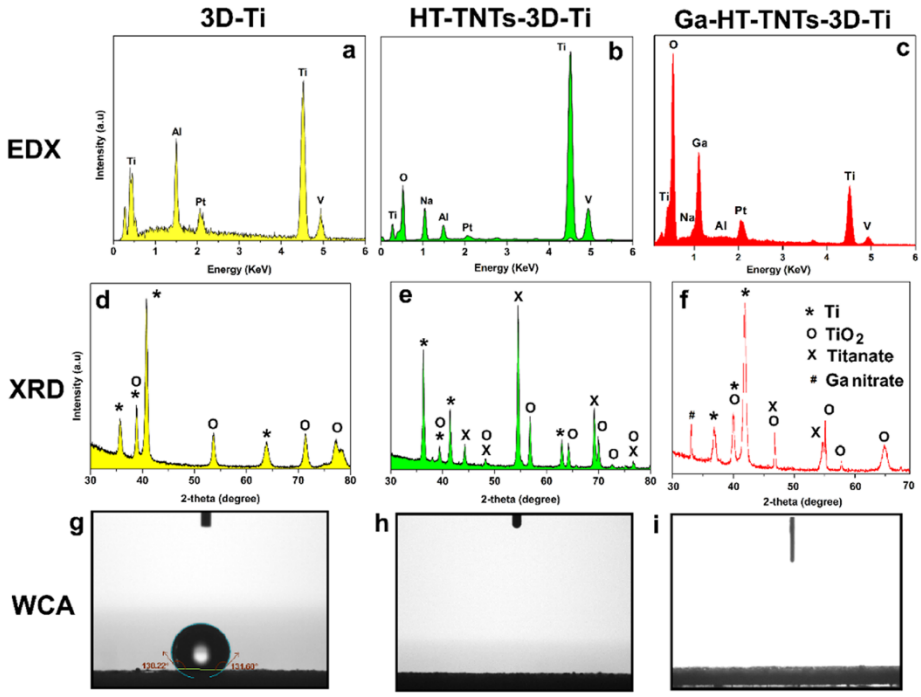

Figure 3. Chemical characterization and surface properties of 3D-Ti, HT-TNTs-3D-Ti, and Ga-HT-TNTs-3D-Ti showing (a–c) EDX spectra showing surface chemical composition; (d–f) XRD patterns with peaks corresponding to Ti, anatase TiO_2, $Na_2Ti_3O_7$, and Ga nitrate; and (g–i) wetting properties of these surfaces by water contact angle (WCA) (HT: hydrothermally treated, TNT: titania nanotubes, Ga: gallium).

dehydrogenase (LDH) released from the cells incubated on the 3D-Ti, HT-TNTs-3D-Ti, and control surfaces was measured using UV/VIS spectrophotometry. After 1, 4, and 7 days of incubation, 50 μL aliquots from the supernatant of each sample were transferred into a new well plate followed by 50 μL of CytoTox 96 reagent. The plate was then incubated for 30 min at room temperature and the absorbance was measured at 490 nm.

2.8.3. Dead/Live Cell Stain. Ti substrates were washed twice using PBS after incubation with MG-63 cells for 1, 4, and 7 days. Calcein AM (2 μM) and ethidium homodimer-1 (4 μM) (Life Technologies, Inc.) were mixed in PBS to create the staining solution. The samples were covered with the dye solution for 30 min in the dark at RT. The samples were subsequently rinsed and immersed in PBS and then imaged via confocal microscopy (Olympus FluoView FV3000). Counts of live and dead cells were quantified using Matlab software, CellC.

2.8.4. Immunocytochemistry and Cytoskeleton Staining. On the 4th day of incubation, the samples with attached cells were rinsed twice with PBS and then fixed with 4% paraformaldehyde for 15 min. For permeabilization, the cells were covered in 0.2% Triton X-100 for 15 min. Next, the samples were blocked in 1% bovine serum albumin (BSA) for 30 min. Afterward, the samples were incubated at room temperature for 1 h with primary antibody, anti-Vinculin (mouse) (Sigma-Aldrich) and secondary antibody, anti-Mouse IgG in goat serum (Life Technologies, Inc.) at RT for 1 h. Subsequently, actin filaments were stained with phalloidin (Invitrogen) for 20 min followed by cell nuclei staining by TO-PRO-3 Iodide (Invitrogen) for 30 min. The cells were imaged using confocal laser scanning microscopy. Results of at least 10 fields of view per sample were analyzed with ImageJ.

For SEM imaging, Ti surfaces incubated with cells for 1, 4, and 7 days were gently rinsed and processed for imaging as described above in Section 2.6.5.

2.9. Statistical Analysis. All of the results presented in this study are statistically treated and expressed as mean ± standard deviation (SD) of at least three independent experiments. One-way and two-way ANOVA were used to analyze the data. The level of significance was set to $p < 0.05$ for all of the comparisons.

3. RESULTS AND DISCUSSION

3.1. Fabrication and Characterization of the Fabricated Implant Models. The morphology and structural details of the fabricated implant models, 3D-Ti, HT-TNTs-3D-Ti, and Ga-HT-TNTs-3D-Ti, were analyzed by scanning electron microscopy (SEM) and are presented in Figures 2 and S1. The typical microstructured surface of the 3D-Ti substrates is covered with randomly arranged microspheres with diameters ranging from 5 to 30 μm (Figure 2a,b). The microsphere size distribution on the surface was measured and is represented in Figure S1c. Variable interspace distances were formed between the randomly dispersed microspheres on the surface ranging from <1 to ~50 μm (Figure S2). During the SLM process, the laser beam melts successive layers of Ti alloy powders (microparticles) to generate a composite structure consisting of templates with microparticles attached on the top surface. The cross section in Figure S3 shows the interconnected layers of the microparticles, which were successively melted during SLM. High-resolution SEM images (Figure 2b,e,h) confirm the firm anchoring of these microparticles to the surface. In addition, all samples were used after extensive sonication in acetone to remove any loosely attached particles from the surface. The average roughness value (R_a) was 17 ± 3 μm, as shown in Figure S4, and other surface

https://doi.org/10.1021/acsbiomaterials.1c01030
ACS Biomater. Sci. Eng. XXXX, XXX, XXX−XXX

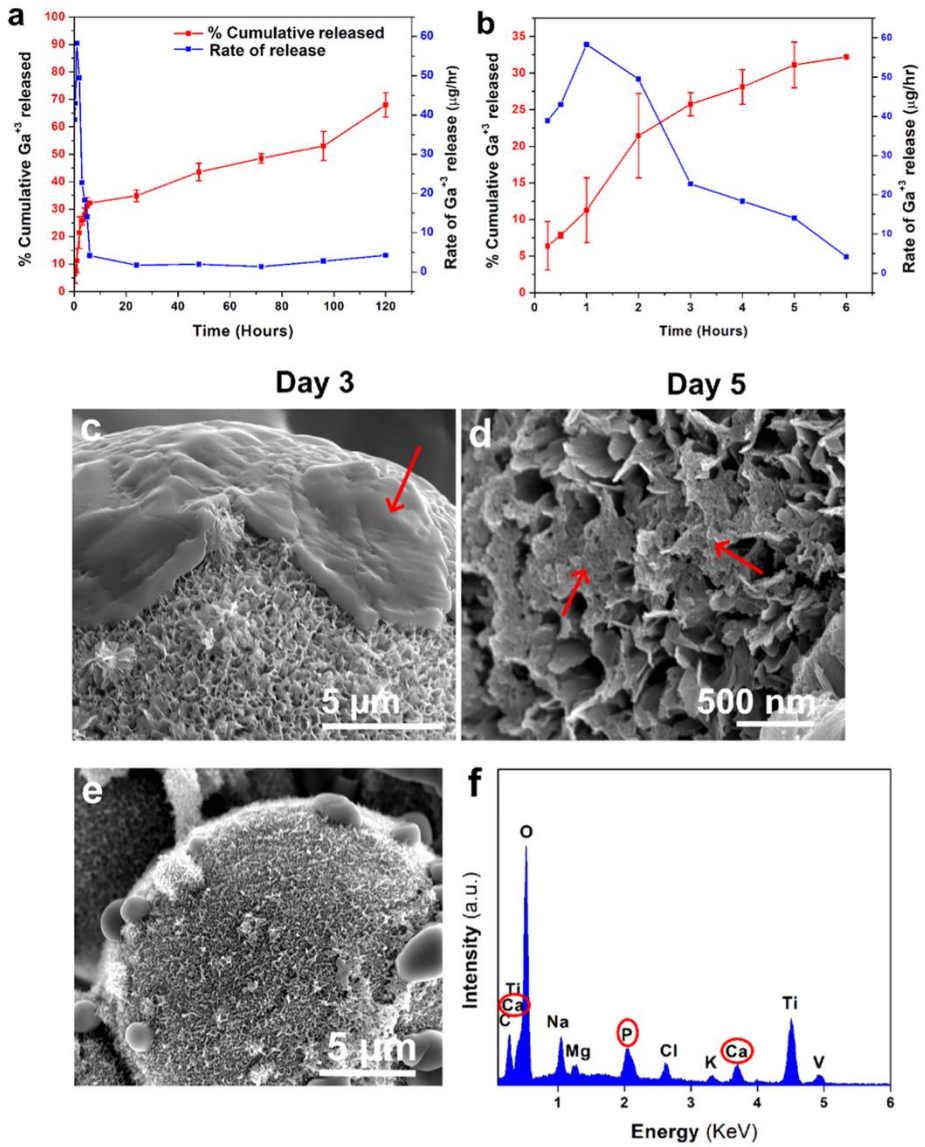

Figure 4. *In vitro* drug release profiles of Ga^{3+} from Ga-HT-TNTs-3D-Ti showing % cumulative Ga^{3+} released and release rate for (a) 5 days and (b) 6 h (burst release) presenting a magnified view of the yellow rectangle shown in (a). SEM images showing the surface of Ga-HT-TNTs-3D-Ti, (c) after 3 days and (d) after 5 days of drug release experiment. Gallium nitrate dissolves gradually with the surface significantly exposed after 3 days while almost all gallium nitrate is dissolved within 5 days. Red arrows indicate gallium nitrate crystals remaining on the surface. (e) SEM image showing hydroxyapatite-like deposition on the surface of Ga-HT-TNTs-3D-Ti. (f) EDX analysis of Ga-HT-TNTs-3D-Ti showing peaks of Ca and P after HAP deposition.

roughness parameters can be found in the Supporting Information. Apart from the microparticles, the peaks and valley structures of the surface appeared smooth, exhibiting no nanostructures.

The surface topography of HT-TNTs-3D-Ti with nanopillar structures fabricated using successive modification steps (i.e., electrochemical anodization and hydrothermal etching) are shown in Figures 2d–f and S5. SEM images show nanopillars with an average length of 550 ± 50 nm and an average interspace distance of 130 ± 50 nm. First, electrochemical anodization was used to generate a titanium oxide (TiO_2) layer in the form of TNTs on the microparticles' surface (Figure S3d–f), followed by hydrothermal processing with NaOH at 160 °C for 4 h. During the HT process, the TNT structures act as a template to promote the nucleation of nanopillar features. The Ti^{4+} ions, generated from the dissolution of the TiO_2 layer

https://doi.org/10.1021/acsbiomaterials.1c01030
ACS Biomater. Sci. Eng. XXXX, XXX, XXX−XXX

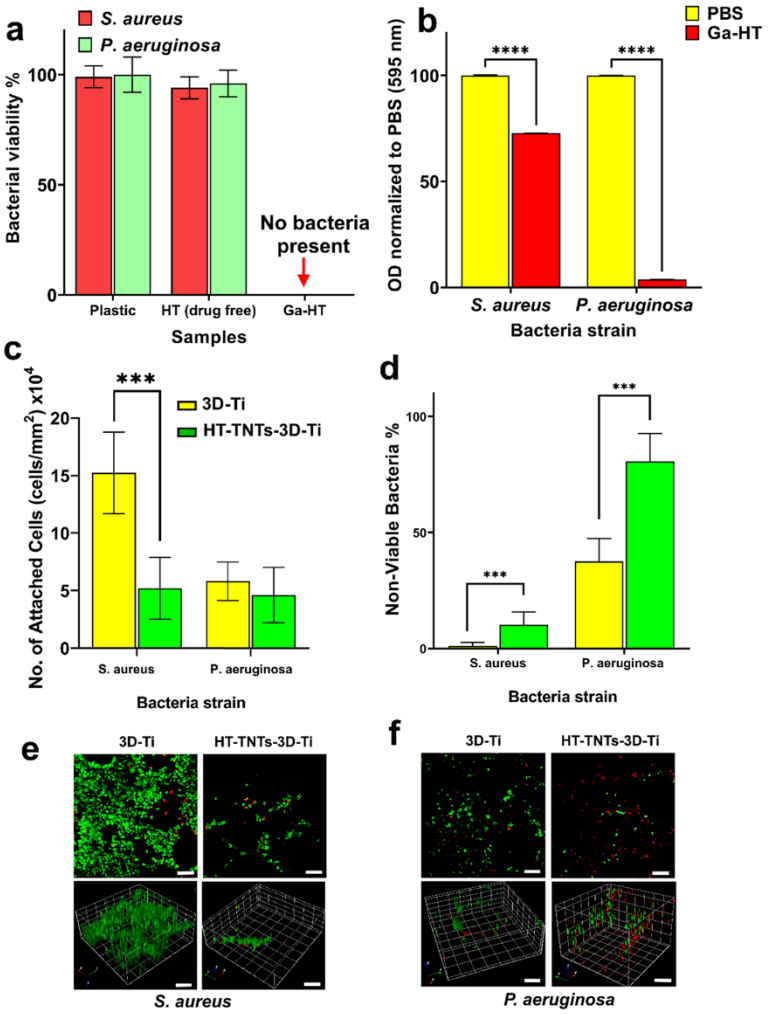

Figure 5. Antibacterial study results showing (a) absence of any viable bacteria in the case of Ga^{3+}-loaded samples compared to Ga^{3+}-free samples; (b) significant antibacterial activity of Ga^{3+} after *in vitro* release for 5 days against both bacterial strains; (c) attachment of bacterial cells on $Ga3^{+}$-free surfaces with a significant reduction of *S. aureus* and *P. aeruginosa* attachment on HT-TNTs-3D-Ti and compared to 3D-Ti; (d) significant antibacterial activity of HT-TNTs-3D-Ti against both bacterial strains; and (e, f) representative CLSM micrographs of *S. aureus* and *P. aeruginosa* bacterial growth (top row), 3D reconstructions of the CLSM z-series (bottom row). Scale bars = 10 μm. Values are expressed as mean ± SD for at least three replicates. Statistically significant differences are labeled as $^{*}p < 0.05$; $^{**}p < 0.01$; $^{***}p < 0.001$, $^{****}p < 0.0001$ (HT: hydrothermally treated, TNT: titania nanotubes).

(TNTs) by NaOH, recrystallize under the effect of high temperature and pressure forming sodium titanate ($Na_2Ti_3O_7$) crystals on the underlying surface that continue to grow into nanopillars.[28,39] Figure 2g–i shows the surface topography of Ga-HT-TNTs-3D-Ti, created after deposition of gallium nitrate on the surface of HT-TNTs-3D-Ti. As observed from these images, the Ga nitrate layer completely covered the surface nanostructures, confirming the successful loading of the antibacterial agent.

The physical and chemical properties of 3D-Ti, HT-TNTs-3D-Ti, and Ga-HT-TNTs-3D-Ti were characterized using EDX, XRD, and WCA measurements. EDX spectra of all samples displayed the typical peaks of Ti, Al, and V, as shown in Figure 3a–c. In addition, a Na peak could be detected corresponding to sodium titanate ($Na_2Ti_3O_7$) formation in the case of HT-TNTs-3D-Ti (Figure 3b). After Ga nitrate loading, a prominent Ga peak was also observed, confirming successful loading (Figure 3c).

The crystal structure of the Ti samples was assessed by XRD and through the analysis of the distinct diffraction peaks shown in Figure 3d–f. All samples showed Ti peaks (JCPDS 44-1294), while anatase TiO_2 peaks (JCPDS 21-1272) and $Na_2Ti_3O_7$ (JCPDS 31-1329) peaks were evident after hydrothermal processing (Figure 3e). In addition, a peak

https://doi.org/10.1021/acsbiomaterials.1c01030
ACS Biomater. Sci. Eng. XXXX, XXX, XXX−XXX

corresponding to gallium nitrate appeared in Ga-HT-TNTs-3D-Ti confirming the deposition of gallium on surface peaks (JCPDS 06-0180) (Figure 3f).

The wettability of the surface is a critical feature influencing the interaction between cells or bacteria and the implant surface. Previous studies showed that hydrophilicity causes a significant reduction in bacterial cell attachment to the surface of implants due to inhibition of hydrophobic interactions, promoting the repulsion between the surface and bacteria.[26,40] In addition, combining nanostructures with hydrophilicity can enhance protein adsorption and improve osseointegration.[41] We measured the WCA of the samples as demonstrated in Figure 3g–i. 3D-Ti possessed a hydrophobic surface with a WCA of 133 ± 1°. On the contrary, the water droplets spread rapidly (WCA of <5–10°) over the surface of HT-TNTs-3D-Ti and Ga-HT-TNTs-3D-Ti samples, indicating superhydrophilic surfaces. The high surface wettability could be attributed to the presence of an oxide layer on the surface. In addition, the presence of micro/nano-rough structures on the surface also increases the wetting properties of hydrophilic surfaces.[42]

3.2. *In Vitro* Release of Antibacterial Agents (Ga^{3+} Ions). An *in vitro* release study of gallium ions from the Ga-HT-TNTs-3D-Ti model implants was performed in PBS at 37 °C for 5 days; results are shown in Figure 4. The drug release exhibits a typical two-phase release pattern; with burst release for the first few hours followed by slower release with zeroth-order kinetics over the study period (5 days). Burst release was attributed to the dissolution of the gallium nitrate layer covering the surface while the slower release occurred because of the dissolution and release of gallium nitrate entrapped within the voids between the nanopillars. The burst release with a high rate of Ga^{3+} release (average ~50 μg/h) is expected to be beneficial for eradicating any bacterial cells that might be present in the vicinity of the implant within the first few hours post implantation, especially those arising from the operating theater environment, surgical equipment, clothing of medical and paramedical staff, resident bacteria on the patient's skin.[43] After that, a slow release with a lower rate (~2 μg/h) over a relatively longer period will provide ongoing critical antibacterial protection in the early stages after surgery when the majority of infections usually happen. Based on the release rate, it is expected that the gallium nitrate layer will be completely dissolved within 10 days. These observed release characteristics can be described as highly favorable for real application after insertion of implants which is currently performed by high dosages of systemic therapy using conventional antibiotics that is well known to have many adverse side effects.[11]

To further explore how the gallium nitrate layer will act under physiological conditions, Ga-HT-TNTs-3D-Ti samples were collected at different time points (3 and 5 days) of the release and were analyzed using SEM. After 3 days, SEM images showed significant removal of the gallium nitrate layer and the exposure of the surface nanostructures, as shown in Figure 4c,d. It is worth mentioning that the thickness of the gallium layer can be controlled by changing the number of loading cycles. This allows control of the localized dosage of the antimicrobial agent over time to meet the required therapeutic window after implant insertion and post-surgical recovery which are both high risk for bacterial infection. At the end of the release experiment (e.g., 5 days), complete removal of the gallium nitrate layer occurred exposing the surface nanopillars as shown in Figure 4d, which would allow the healthy bone cells to attach and interact with the implant surface without interference from the deposited gallium layer. As seen in Figure 4d, only a few crystals are remaining on the surface that are expected to be totally removed later leaving a clean surface after ~10 days. Thus, the addition of a Ga^{3+} releasing surface is expected to provide enough local concentration of Ga^{3+} ions to successfully destroy bacteria by interfering with bacterial metabolism. It is worth mentioning that Ga^{3+} ions were previously confirmed to be nontoxic for other cells and will not make any structural interruption to the implant surface for cell attachment and integration, thus, this was not further studied in this work.[18]

3.3. Characterization of *In Vitro* HAP Depositions. Many studies have confirmed the *in vitro* HAP deposition on the surface of Ti implant materials to lead to a successful *in vivo* implant-bone cell attachment.[38,44] Here, we tested the ability of gallium nitrate-loaded implant models to support *in vitro* deposition of hydroxyapatite-like minerals (HAP) from SBF for 28 days. SEM images show deposition of HAP for Ga-HT-TNTs-3D-Ti (Figure 4e). EDX analysis of the surface also showed peaks of calcium and phosphorus, as shown in Figure 4f, confirming the formation of HAP.[45]

3.4. Antibacterial Activity of Ga^{3+}-Loaded Implant Models (Ga-HT-TNTs-3D-Ti). The antibacterial efficacy of Ga-HT-TNTs-3D-Ti surfaces toward *S. aureus* and *P. aeruginosa* was evaluated using the plate count enumeration method after a 5 h incubation. The bactericidal activity of Ti surfaces with and without gallium nitrate loading is shown in Figure 5a. Ga-HT-TNTs-3D-Ti showed 100% eradication of bacteria compared to plastic and samples without Ga^{3+}. These results indicate that the release of Ga^{3+} could significantly eliminate all viable bacterial cells surrounding the surface.

The antibacterial efficacy of Ga^{3+} released into PBS was then assessed. Buffer containing dissolved Ga^{3+} was collected after 5 days and then incubated with bacterial suspensions. A significant reduction ($p < 0.0001$) in both strains of bacteria was observed, as shown in Figure 5b, indicating that Ga^{3+} is effective even after 5 days. Thus, the data presented provide evidence that Ga^{3+} release over the study period could successfully secure sufficient antibacterial protection. It is also worth noting that the release can be modified or triggered as we showed previously.[46]

3.5. Influence of Micro/Nanosurface Topographies on Antibacterial Activity. The nanopillar structures on HT-TNTs-3D-Ti were expected to possess antibacterial properties based on their ability to kill bacteria by a mechanical mode of action.[12,13] Increasing evidence indicates that the processes of osseointegration and bacterial infection are related.[47] The concept of "the race to the surface" explains the competition between the bacteria, trying to attach on the surface to develop a biofilm, and human cells, endeavoring to interact and adhere to the implant.[7] As we explained earlier, the rationale of our approach is to use this mechanical mode of action to provide sustained antibacterial activity that will prevent bacterial colonization and biofilm formation during the life of the implant in the body. To assess the antibacterial efficacy of the surface nanopillars, Ga^{3+}-free Ti surfaces were selected to avoid any interference from Ga^{3+}. HT-TNTs-3D-Ti were incubated with bacteria for 18 h, followed by evaluation of bacterial attachment and antibacterial activity.

The quantification of bacterial cell viability and attachment, as calculated from confocal laser scanning microscopy (CLSM), is shown in Figure 5c–f. HT-TNTs-3D-Ti

https://doi.org/10.1021/acsbiomaterials.1c01030
ACS Biomater. Sci. Eng. XXXX, XXX, XXX–XXX

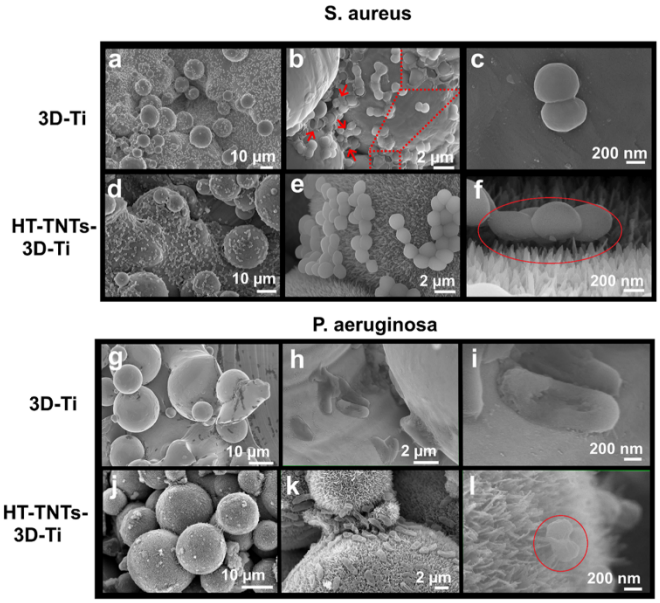

Figure 6. SEM images showing the morphology of *S. aureus* (a–f) and *P. aeruginosa* (g–l) on different Ti surfaces. Bacterial cells appear healthy on 3D-Ti, in contrast to HT-TNTs-3D-Ti in which bacterial cells appear deformed as marked by red circles. Red arrows in (b) indicate extracellular polymeric substances (EPS), while the inset represents a higher magnification of *S. aureus* showing EPS on 3D-Ti (HT: hydrothermally treated).

demonstrated a significantly reduced level of *S. aureus* attachment of $35.9 \times 10^3 \pm 29.4 \times 10^3$ cells/mm^2 compared to 3D-Ti control surfaces with $164.6 \times 10^3 \pm 51.8 \times 10^3$ attached cells/mm^2. SEM micrographs also revealed the presence of extracellular polymeric substance (EPS) production (Figure 6b) as an indication of biofilm formation, which is contrary to observations for HT-TNTs-3D-Ti. Bacterial biofilm is a structured accumulation of bacterial cells encapsulated in a self-produced extracellular polymeric substance that protects the bacteria from the host's immune system and can inhibit the efficacy of antibiotics. Once a biofilm is established on an implant surface, it can be very difficult to eradicate and could eventually result in chronic inflammation and implant failure.[9,48] As a result, it is essential for the surface to prevent bacterial attachment or kill any attached bacteria before a biofilm is formed.[48]

In the case of *P. aeruginosa*, 3D-Ti and HT-TNTs-3D-Ti displayed comparable levels of bacterial attachment with $58.2 \times 10^3 \pm 16.7 \times 10^3$ and $49.7 \times 10^3 \pm 21.7 \times 10^3$ cells/mm^2, respectively (Figure 5c).

The ability of the surface topography to mechanically inactivate bacteria significantly varied with different surface topography. The presence of nanopillars on the surface of HT-TNTs-3D-Ti significantly reduced *S. aureus* and *P. aeruginosa* viability compared to smooth 3D-Ti, as shown in Figure 5d. The SEM images in Figure 6 show the tendency for bacteria to settle in the crevices formed between the Ti microspheres. Moreover, the SEM images confirmed the nanostructure-induced membrane damage inflicted on attached *P. aeruginosa* bacterial cells, as seen in Figure 6l. Overall, it can be concluded that HT-TNTs-3D-Ti could significantly reduce the occurrence of bacterial attachment and eradicate those bacterial cells that do attach on implants surface compared to 3D-Ti.

3.6. Influence of Micro/Nanosurface Topography on MG-63 Viability, Proliferation, and Morphology. Since the surface is the first site of interaction with living tissues, many studies have shown that topography can strongly influence cell adhesion, proliferation, and differentiation.[49,50] However, the influence of the specific dimensions and geometry of surface topography (e.g., micro- or nanosurface) on bone tissue formation remains inconclusive due to the lack of uniformity of fabrication that results in widely variable surface structures, making it difficult to compare the cell response to different topographies.[51−53]

The effect of the surface topography of HT-TNTs-3D-Ti substrata on eukaryotic cell response was tested using human MG-63 osteoblast-like cells. Since we had previously confirmed that the gallium nitrate layer would completely dissolve under physiological conditions, Ga^{3+} free surfaces (HT-TNTs-3D-Ti) were used to evaluate the viability and proliferation of cells at 1, 4, and 7 days of culture, as shown in Figure 7a. On day 1, no significant difference in cell viability was observed between HT-TNTs-3D-Ti, 3D-Ti, and the glass control. On day 4, the cell viability on 3D-Ti was significantly higher than HT-TNTs-3D-Ti. Cell viability on HT-TNTs-3D-Ti increased significantly from day 1 to day 4 ($p < 0.001$) and was further increased on day 7, where no significant difference was observed on day 7 compared to 3D-Ti and glass coverslips (used as a positive control for cellular attachment and proliferation).

LDH activity in culture media (DMEM) was also measured as an indication of cell membrane integrity. Figure 7b shows no significant difference between all tested samples on day 1. Notably, the amount of LDH released on days 4 and 7 in the case of HT-TNTs-3D-Ti was less than that released on day 1,

https://doi.org/10.1021/acsbiomaterials.1c01030
ACS Biomater. Sci. Eng. XXXX, XXX, XXX−XXX

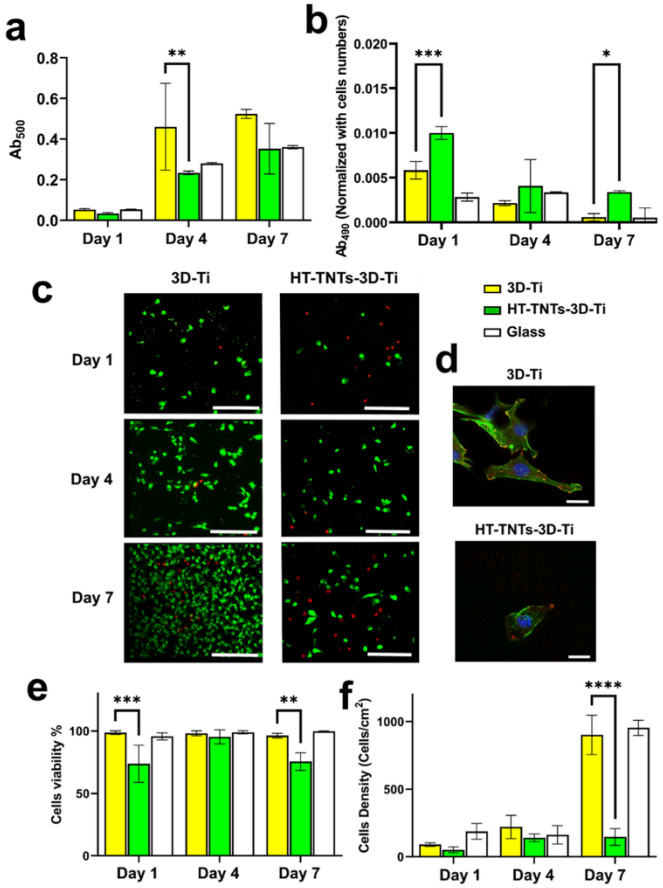

Figure 7. Viability and attachment density of osteoblast-like MG-63 cells after 1, 4, and 7 days incubation on HT-TNTs-3D-Ti, 3D-Ti, and glass. (a) MTS assay showing viability on days 1, 4, and 7; (b) LDH release from MG-63 cells after 1, 4, and 7 days of growth; and (c) representative images of live/dead staining of MG-63 (live cells, red; dead cells, green). Scale bar = 200 μm. (d) Representative confocal fluorescence images showing MG-63 cell morphology and focal adhesion points after 4 days incubation. Phalloidin-labeled F-actin (green), Alexa Fluor 594-labeled vinculin staining for the observation of focal adhesions (red) and TO-PRO-3 nuclear stain (blue) are shown. Scale bars are 20 μm. (e) Cell viability (quantified by calculating live and dead cell numbers from the confocal images, cell viability (%) = number of live cells/number of total cells × 100% (eq 2)), and (f) cell density. Values are expressed as mean ± SD for at least three replicates. Statistically significant differences are labeled as $^{*}p < 0.05$; $^{**}p < 0.01$; $^{***}p < 0.001$; and $^{****}p < 0.0001$ (HT: hydrothermally treated, TNT: titania nanotubes).

which agrees with MTS assay results in which cell viability was higher on those days compared to day 1.

The cell viability and density were confirmed by live/dead fluorescent staining (Figure 7c). The quantified results of MG-63 cell viability and total cell density are shown in Figure 7e,f. After day 1, the cell viability percentage (measured as the ratio between the number of viable cells to the total number of cells) on 3D-Ti was ca. 25−30% greater than on HT-TNTs-3D-Ti with no difference observed between all samples on day 4.

Concerning the cell density (number/cm^2), Figure 7f shows a similar trend to the viability data for all surfaces on day 1. Compared to day 1, the cell density increased on day 4 approximately 2 and 3 times for 3D-Ti and HT-TNTs-3D-Ti, respectively. By day 7, the density of cells on 3D-Ti increased significantly but remained constant on HT-TNTs-3D-Ti. The higher cell density on 3D-Ti could be explained by an increase in the number of attached cells owing to the formation of more focal adhesion sites. The quantification of focal adhesion sites via fluorescent labeling of vinculin (Figure 7d) showed MG-63 cells with a higher number of focal adhesions on 3D-Ti compared to HT-TNTs-3D-Ti. On average, the cells exhibited 31 ± 12 and 9 ± 3 focal adhesion points per cell on 3D-Ti and HT-TNTs-3D-Ti, respectively. The reduction in the number of focal adhesion sites on HT-TNTs-3D-Ti can be explained by the influence of nanotopography on integrin expression. Studies have shown that nano-rough surfaces reduce integrin expression.[54] Transmembrane integrins act as a bridge binding extracellular matrix proteins and linker proteins of focal adhesions such as vinculin within the cell membrane. In addition, a reduced number of focal adhesions could result from fewer anchoring sites due to spaces between the nanopillars.[12,55] Although previous data confirmed the influence of surface topography on cellular response,[56,57] it is difficult to obtain a distinctive comparison between results

https://doi.org/10.1021/acsbiomaterials.1c01030
ACS Biomater. Sci. Eng. XXXX, XXX, XXX−XXX

from other studies owing to variations of cell lines, surface features, and chemistry between different studies. In our case, we suggest that MG-63 cells are still in the proliferative phase (increasing in number) on 3D-Ti during the period of study (i.e., 7 days), whereas they started to differentiate (not increasing in number) into a more mature state on the HT-TNTs-3D-Ti surface by day 7.[58] This explains the significantly higher density of cells on 3D-Ti compared to HT-TNTs-3D-Ti after 7 days, which confirms that surface topography can significantly control cellular behavior. These results agree with previous data showing that MG-63 cells on micro/nano-rough surfaces exhibit decreased proliferation, increased differentiation with higher levels of late differentiation markers (osteoprotegerin, vascular endothelial growth factor, and osteocalcin), compared to microstructured surfaces.[7,58,59]

Next, high-resolution SEM imaging was utilized to visually identify the influence of topographical features of various surface structures indicative of cell morphology and proliferation and to investigate the change of cell morphology over time, as shown in Figure 8. After 24 h incubation, the cells on

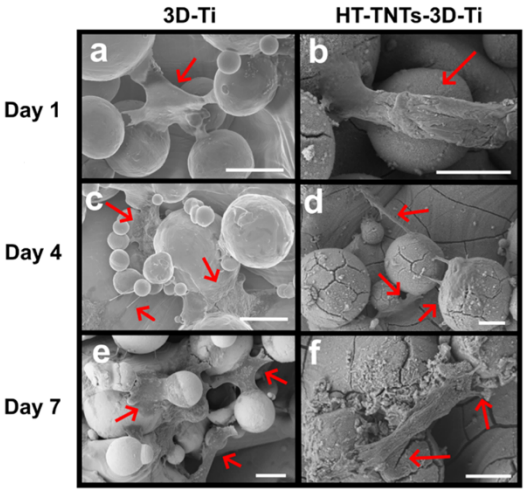

Figure 8. Morphology of MG-63 cells grown on 3D-Ti and HT-TNTs-3D-Ti. High-resolution SEM images showing the attachment and spreading of MG-63 osteoblast-like cells (indicated by the red arrows) at 1, 4, and 7 days of incubation. Scale bars = 10 μm (HT: hydrothermally treated).

HT-TNTs-3D-Ti were found to exhibit a more spread morphology compared to cells on 3D-Ti (Figure 8b). After 4 days of cultivation, cells mainly showing a polygonal shape were observed on 3D-Ti (Figure 8c). The cells were observed to interact primarily around the spherical islands. The cells on HT-TNTs-3D-Ti exhibited an elongated morphology, attaching on multiple spheres simultaneously with their extended cytoplasmic processes and filopodia. This confirms the firm anchoring of the cells with the surface features together with the appearance of cytoskeletal stress fibers (actin filaments), which could eventually be translated into effective osseointegration.[60] On day 7 (Figure 8e,f), highly spread cells with numerous filopodia were observed on the 3D-Ti samples while, in the case of HT-TNTs-3D-Ti, the cells mainly presented with an elongated bipolar morphology; cell length did not further extend compared with the cell shape analyzed at the previous time points.

The presence of randomly arranged microspheres on the surface, with variable interspace, enabled us to observe the effect of surface interspaces on cell spreading to estimate the suitable dimensions to enhance attachment and spreading. We observed the spreading patterns of the cell and correlated them to microsphere interspaces. The whole body of the cell was able to attach between spheres with interspace dimensions ranging from 12−35 μm as seen in Figures 8a−f and S2. In the case of microspheres with an interspace distance of less than 12 μm, the cells spread on top of the microspheres (Figure S2e). On the other hand, if the distance was quite large, the cells usually spread on the flat surface while extending their filopodia until reaching the nearest microsphere, as seen in Figure S2f. It was also noticed that the microspheres can act as bridges to allow cell extension, as seen in Figures 8b and S2c, thus providing more anchorage points to the surface.

Based on these results, we can conclude that both the micro- and nanosurface features are critical for cell attachment and proliferation. For example, microspheres with optimum interspaces were able to provide more attachment for cells. Both 3D-Ti and HT-TNTs-3D-Ti surfaces could support cell growth and provide long-term attachment required for permanent implants (e.g., dental implants, hip and bone replacements). It has previously been demonstrated that surfaces with microtopography have improved bone fixation and greater pull-out strength *in vivo*.[61,62] Additionally, recent findings show that cells (e.g., osteoblasts) respond to surface nanoscale features that mimic the hierarchical bone microenvironment to promote bone cell activity and consequently strengthen cell attachment. Moreover, surface nanotopography showed excellent biocompatibility through enhancing protein adsorption, bone apatite formation, and providing sufficient space for cell anchoring and proliferation.[15]

Thus, we hypothesize that the formation of hierarchical surface topography exhibiting both micro- and nanoscale roughness could enable regulation of cell growth and development, leading to improved osseointegration, while simultaneously exhibiting antibacterial activity. Despite the ability of 3D-Ti to support cell growth, higher bacterial attachment of both tested pathogens and the ability of *S. aureus* to form a biofilm make 3D-Ti a less appealing choice for implants as schematically represented in Figure S6. By contrast, HT-TNTs-3D-Ti demonstrated good mammalian cell support and bactericidal and antibiofouling activity.

4. CONCLUSIONS

In summary, we present a fabrication concept for the next generation of a unique surface of micro-rough implants where TNTs were used as the template to generate specific and novel 2D sharp nanopillar structures through combining additive manufacturing (i.e., selective laser melting) approach with scalable and low-cost surface modification techniques; electrochemical anodization and hydrothermal processing. The fabrication of hierarchical micro- to nanotopography 3D-printed Ti implants (HT-TNTs-3D-Ti) was demonstrated to achieve combined antibacterial protection based on the mechano-bactericidal action of sharp nanostructures and localized release of Ga^{3+}. Short-term antibacterial protection was provided by loading of antibacterial agent Ga^{3+}, which was shown to have favorable localized drug release kinetics and the ability to effectively destroy bacteria (100%) in the vicinity of

https://doi.org/10.1021/acsbiomaterials.1c01030
ACS Biomater. Sci. Eng. XXXX, XXX, XXX−XXX

the implant over 5 days, providing initial protection from bacterial infection. Additionally, HT-TNTs-3D-Ti implant models with a micro−nanostructured surface with sharp nanopillars showed the successful killing of attached bacteria while simultaneously preventing their attachment and biofilm formation on the surface. The combination of these two modes of antibacterial action is complementary and can be further tuned by controlling Ga^{3+} release, if required. We also confirmed that both micro- and nanosurface features critically influence the response of osteoblast-like MG-63 cell response in which microfeatures with interspaces suitable to accommodate cells improved cell attachment.

Thus, we present a new concept for the manufacture of Ti implants with a dual mode of antibacterial action, while simultaneously supporting the enhanced attachment and growth of osteoblasts. This work will pave the way for further development of a new generation of low-cost 3D-printed Ti implants whose performance can be significantly upgraded by a combination of mechano-bactericidal surface topography and drug-releasing functionality for the development of the ideal implant that can dually control bone cell response while effectively inhibiting bacterial infection. Further optimization and tuning of the antibacterial and bio-integration performances of the fabricated 3D-printed implant are still required; however, we have successfully demonstrated their potential to be translated into the next stage of *in vivo* and clinical studies.

■ ASSOCIATED CONTENT

Supporting Information

The Supporting Information is available free of charge at https://pubs.acs.org/doi/10.1021/acsbiomaterials.1c01030.

Camera image of 3D-Ti and HT-TNTs-3D-Ti plates; size distribution of microspheres dispersed on top of 3D-Ti as measured from SEM images; high-resolution SEM images showing cell spreading on the surface of 3D-Ti and HT-TNTs-3D-Ti; high-resolution SEM images showing cross section of 3D-Ti and TNTs-3D-Ti; 3D reconstructed interferometer image of 3D-Ti; high-resolution SEM images showing nanopillar structures on HT-TNTs-3D-Ti; schematic illustration showing the effect of surface structures on MG-63 cell and bacteria; HT-TNTs-3D-Ti showed bactericidal activity while bacterial biofilms were formed on 3D-Ti; and both 3D-Ti and HT-TNts-3D-Ti supported the adhesion of MG-36 (PDF)

■ AUTHOR INFORMATION

Corresponding Authors

Elena P. Ivanova − *College of STEM, School of Science, RMIT University, Melbourne, VIC 3000, Australia; Australian Research Council (ARC) Training Centre in Surface Engineering for Advanced Materials (SEAM), Swinburne University of Technology, Hawthorn, VIC 3122, Australia;* orcid.org/0000-0002-5509-8071; Email: elena.ivanova@rmit.edu.au

Dusan Losic − *School of Chemical Engineering and Advanced Materials, The University of Adelaide, Adelaide, SA 5005, Australia;* orcid.org/0000-0002-1930-072X; Email: dusan.losic@adelaide.edu.au

Authors

Shaheer Maher − *School of Chemical Engineering and Advanced Materials, The University of Adelaide, Adelaide, SA 5005, Australia; Faculty of Pharmacy, Assiut University, Assiut 71526, Egypt;* orcid.org/0000-0002-2556-1096

Denver Linklater − *College of STEM, School of Science, RMIT University, Melbourne, VIC 3000, Australia;* orcid.org/0000-0003-1433-3685

Hadi Rastin − *School of Chemical Engineering and Advanced Materials, The University of Adelaide, Adelaide, SA 5005, Australia*

Sandy Tzu-Ying Liao − *College of STEM, School of Science, RMIT University, Melbourne, VIC 3000, Australia; Department of Chemistry and Biotechnology, School of Science, Swinburne University of Technology, Hawthorn, VIC 3022, Australia; Australian Research Council (ARC) Training Centre in Surface Engineering for Advanced Materials (SEAM), Swinburne University of Technology, Hawthorn, VIC 3122, Australia*

Karolinne Martins de Sousa − *College of STEM, School of Science, RMIT University, Melbourne, VIC 3000, Australia*

Luis Lima-Marques − *The Institute for Photonics and Advanced Sensing, The University of Adelaide, Adelaide, SA 5005, Australia*

Peter Kingshott − *Department of Chemistry and Biotechnology, School of Science, Swinburne University of Technology, Hawthorn, VIC 3022, Australia; Australian Research Council (ARC) Training Centre in Surface Engineering for Advanced Materials (SEAM), Swinburne University of Technology, Hawthorn, VIC 3122, Australia;* orcid.org/0000-0001-5882-5804

Helmut Thissen − *Australian Research Council (ARC) Training Centre in Surface Engineering for Advanced Materials (SEAM), Swinburne University of Technology, Hawthorn, VIC 3122, Australia; CSIRO Manufacturing, Clayton, VIC 3168, Australia;* orcid.org/0000-0002-3254-6855

Complete contact information is available at: https://pubs.acs.org/10.1021/acsbiomaterials.1c01030

Author Contributions

○S.M. and D. Linklater contributed equally. The manuscript was written through contributions of all authors. All authors have given approval to the final version of the manuscript.

Notes

The authors declare no competing financial interest.

■ ACKNOWLEDGMENTS

The authors acknowledge the financial support provided to S.M. by Australian Research Council (ARC) (IH 15000003) grant, the Australian Government Training Program Scholarship, and Forrest George and Sandra Lynne Young Supplementary Scholarship. Funding from the Australian Research Council (ARC) Industrial Transformation Research Hubs Scheme (ARC Research Hub for Australian Steel Manufacturing, Project Number IH130100017) and ARC Industrial Transformation Training Centre (ITTC) scheme (Project Number IC180100005) is gratefully acknowledged. The authors are grateful to the School of Chemical Engineering at the University of Adelaide for support of this research. They gratefully acknowledge the RMIT Microscopy

https://doi.org/10.1021/acsbiomaterials.1c01030
ACS Biomater. Sci. Eng. XXXX, XXX, XXX−XXX

and Microanalysis Facility (RMMF) for providing access to their analytical instruments.

REFERENCES

(1) Garg, D.; Matai, I.; Sachdev, A. Toward Designing of Anti-infective Hydrogels for Orthopedic Implants: From Lab to Clinic. *ACS Biomater. Sci. Eng.* **2021**, *7*, 1933−1961.
(2) Zhang, L.-C.; Chen, L.-Y. A Review on Biomedical Titanium Alloys: Recent Progress and Prospect. *Adv. Eng. Mater.* **2019**, *21*, No. 1801215.
(3) Zhang, E.; Zhao, X.; Hu, J.; Wang, R.; Fu, S.; Qin, G. Antibacterial metals and alloys for potential biomedical implants. *Bioact. Mater.* **2021**, *6*, 2569−2612.
(4) Qu, X.; Yang, H.; Jia, B.; Wang, M.; Yue, B.; Zheng, Y.; Dai, K. Zinc alloy-based bone internal fixation screw with antibacterial and anti-osteolytic properties. *Bioact. Mater.* **2021**, *6*, 4607−4624.
(5) Sousa, A.; Carvalho, A.; Pereira, C.; Reis, E.; Santos, A. C.; Abreu, M.; Soares, D.; Fragoso, R.; Ferreira, S.; Reis, M.; Sousa, R. Economic Impact of Prosthetic Joint Infection - an Evaluation Within the Portuguese National Health System. *J. Bone Joint Infect.* **2018**, *3*, 197−202.
(6) Maher, S.; Mazinani, A.; Barati, M. R.; Losic, D. Engineered titanium implants for localized drug delivery: recent advances and perspectives of Titania nanotubes arrays. *Expert Opin. Drug Delivery* **2018**, *15*, 1021−1037.
(7) Long, E. G.; Buluk, M.; Gallagher, M. B.; Schneider, J. M.; Brown, J. L. Human mesenchymal stem cell morphology, migration, and differentiation on micro and nano-textured titanium. *Bioact. Mater.* **2019**, *4*, 249−255.
(8) Li, X.; Wu, B.; Chen, H.; Nan, K.; Jin, Y.; Sun, L.; Wang, B. Recent developments in smart antibacterial surfaces to inhibit biofilm formation and bacterial infections. *J. Mater. Chem. B* **2018**, *6*, 4274−4292.
(9) Li, Y.; Yang, Y.; Li, R.; Tang, X.; Guo, D.; Qing, Ya.; Qin, Y. Enhanced antibacterial properties of orthopedic implants by titanium nanotube surface modification: a review of current techniques. *Int. J. Nanomed.* **2019**, *14*, 7217−7236.
(10) Stuart, B. W.; Stan, G. E.; Popa, A. C.; Carrington, M. J.; Zgura, I.; Necsulescu, M.; Grant, D. M. New solutions for combatting implant bacterial infection based on silver nano-dispersed and gallium incorporated phosphate bioactive glass sputtered films: A preliminary study. *Bioact. Mater.* **2021**, *8*, 325−340.
(11) Ghimire, A.; Song, J. Anti-Periprosthetic Infection Strategies: From Implant Surface Topographical Engineering to Smart Drug-Releasing Coatings. *ACS Appl. Mater. Interfaces* **2021**, *13*, 20921−20937.
(12) Clainche, T. L.; Linklater, D.; Wong, S.; Le, P.; Juodkazis, S.; Guével, X. L.; Coll, J.-L.; Ivanova, E. P.; Martel-Frachet, V. Mechano-Bactericidal Titanium Surfaces for Bone Tissue Engineering. *ACS Appl. Mater. Interfaces* **2020**, *12*, 48272−48283.
(13) Linklater, D. P.; Baulin, V. A.; Juodkazis, S.; Crawford, R. J.; Stoodley, P.; Ivanova, E. P. Mechano-bactericidal actions of nanostructured surfaces. *Nat. Rev. Microbiol.* **2020**, *19*, 8−22.
(14) Prathapachandran, J.; Suresh, N. Management of peri-implantitis. *Dent. Res. J.* **2012**, *9*, 516−521.
(15) Cochis, A.; Azzimonti, B.; Chiesa, R.; Rimondini, L.; Gasik, M. Metallurgical Gallium Additions to Titanium Alloys Demonstrate a Strong Time-Increasing Antibacterial Activity without any Cellular Toxicity. *ACS Biomater. Sci. Eng.* **2019**, *5*, 2815−2820.
(16) Li, P.-W.; Kuo, T.-H.; Chang, J.-H.; Yeh, J.-M.; Chan, W.-H. Induction of cytotoxicity and apoptosis in mouse blastocysts by silver nanoparticles. *Toxicol. Lett.* **2010**, *197*, 82−87.
(17) Mao, B.-H.; Chen, Z.-Y.; Wang, Y.-J.; Yan, S.-J. Silver nanoparticles have lethal and sublethal adverse effects on development and longevity by inducing ROS-mediated stress responses. *Sci. Rep.* **2018**, *8*, No. 2445.
(18) Dong, J.; Fang, D.; Zhang, L.; Shan, Q.; Huang, Y. Gallium-doped titania nanotubes elicit anti-bacterial efficacy in vivo against *Escherichia coli* and *Staphylococcus aureus* biofilm. *Materialia* **2019**, *5*, No. 100209.
(19) Li, L.; Chang, H.; Yong, N.; Li, M.; Hou, Y.; Rao, W. Superior antibacterial activity of gallium based liquid metals due to Ga3+ induced intracellular ROS generation. *J. Mater. Chem. B* **2021**, *9*, 85−93.
(20) Antunes, L. C. S.; Imperi, F.; Minandri, F.; Visca, P. In Vitro and In Vivo Antimicrobial Activities of Gallium Nitrate against Multidrug-Resistant Acinetobacter baumannii. *Antimicrob. Agents Chemother.* **2012**, *56*, 5961−5970.
(21) Losic, D. Advancing of titanium medical implants by surface engineering: recent progress and challenges. *Expert Opin. Drug Delivery* **2021**, *18*, 1355−1378.
(22) Ni, J.; Ling, H.; Zhang, S.; Wang, Z.; Peng, Z.; Benyshek, C.; Zan, R.; Miri, A. K.; Li, Z.; Zhang, X.; Lee, J.; Lee, K. J.; Kim, H. J.; Tebon, P.; Hoffman, T.; Dokmeci, M. R.; Ashammakhi, N.; Li, X.; Khademhosseini, A. Three-dimensional printing of metals for biomedical applications. *Mater. Today Bio* **2019**, *3*, No. 100024.
(23) Li, N.; Huang, S.; Zhang, G.; Qin, R.; Liu, W.; Xiong, H.; Shi, G.; Blackburn, J. Progress in additive manufacturing on new materials: A review. *J. Mater. Sci. Technol.* **2019**, *35*, 242−269.
(24) Jing, Z.; Ni, R.; Wang, J.; Lin, X.; Fan, D.; Wei, Q.; Zhang, T.; Zheng, Y.; Cai, H.; Liu, Z. Practical strategy to construct anti-osteosarcoma bone substitutes by loading cisplatin into 3D-printed titanium alloy implants using a thermosensitive hydrogel. *Bioact. Mater.* **2021**, *6*, 4542−4557.
(25) Zhang, D.; Qiu, D.; Gibson, M. A.; Zheng, Y.; Fraser, H. L.; StJohn, D. H.; Easton, M. A. Additive manufacturing of ultrafine-grained high-strength titanium alloys. *Nature* **2019**, *576*, 91−95.
(26) Yin, C.; Zhang, T.; Wei, Q.; Cai, H.; Cheng, Y.; Tian, Y.; Leng, H.; Wang, C.; Feng, S.; Liu, Z. Surface treatment of 3D printed porous Ti6Al4V implants by ultraviolet photofunctionalization for improved osseointegration. *Bioact. Mater.* **2021**, *7*, 26−38.
(27) Cai, C.; Wu, X.; Liu, W.; Zhu, W.; Chen, H.; Qiu, J. C. D.; Sun, C. N.; Liu, J.; Wei, Q.; Shi, Y. Selective laser melting of near-α titanium alloy Ti-6Al-2Zr-1Mo-1V: Parameter optimization, heat treatment and mechanical performance. *J. Mater. Sci. Technol.* **2020**, *57*, 51−64.
(28) Maher, S.; Wijenayaka, A. R.; Lima-Marques, L.; Yang, D.; Atkins, G. J.; Losic, D. Advancing of Additive-Manufactured Titanium Implants with Bioinspired Micro- to Nanotopographies. *ACS Biomater. Sci. Eng.* **2021**, *7*, 441−450.
(29) Maher, S.; Kaur, G.; Lima-Marques, L.; Evdokiou, A.; Losic, D. Engineering of Micro- to Nanostructured 3D-Printed Drug-Releasing Titanium Implants for Enhanced Osseointegration and Localized Delivery of Anticancer Drugs. *ACS Appl. Mater. Interfaces* **2017**, *9*, 29562−29570.
(30) Qin, J.; Yang, D.; Maher, S.; Lima-Marques, L.; Zhou, Y.; Chen, Y.; Atkins, G. J.; Losic, D. Micro- and nano-structured 3D printed titanium implants with a hydroxyapatite coating for improved osseointegration. *J. Mater. Chem. B* **2018**, *6*, 3136−3144.
(31) Mohandas, A.; Krishnan, A. G.; Biswas, R.; Menon, D.; Nair, M. B. Antibacterial and cytocompatible nanotextured Ti surface incorporating silver via single step hydrothermal processing. *Mater. Sci. Eng. C* **2017**, *75*, 115−124.
(32) Anitha, V. C.; Banerjee, A. N.; Joo, S. W.; Min, B. K. Morphology-dependent low macroscopic field emission properties of titania/titanate nanorods synthesized by alkali-controlled hydrothermal treatment of a metallic Ti surface. *Nanotechnology* **2015**, *26*, No. 355705.
(33) Pavasupree, S.; Onoda, K.; Yoshikawa, S.; Simpraditpan, A.; Pecharapa, W. Characterization of Flower-like Titanate and Titania Nanowires on Titanium Plate Substrate. *Energy Procedia* **2013**, *34*, 555−562.
(34) Gibaldi, M.; Feldman, S. Establishment of sink conditions in dissolution rate determinations. Theoretical considerations and application to nondisintegrating dosage forms. *J. Pharm. Sci.* **1967**, *56*, 1238−1242.

https://doi.org/10.1021/acsbiomaterials.1c01030
ACS Biomater. Sci. Eng. XXXX, XXX, XXX−XXX

(35) Zhang, W.; Zhang, S.; Liu, H.; Ren, L.; Wang, Q.; Zhang, Y. Effects of surface roughening on antibacterial and osteogenic properties of Ti-Cu alloys with different Cu contents. *J. Mater. Sci. Technol.* **2021**, *88*, 158−167.
(36) Gan, D.; Xu, T.; Xing, W.; Ge, X.; Fang, L.; Wang, K.; Ren, F.; Lu, X. Mussel-Inspired Contact-Active Antibacterial Hydrogel with High Cell Affinity, Toughness, and Recoverability. *Adv. Funct. Mater.* **2019**, *29*, No. 1805964.
(37) Gan, D.; Xing, W.; Jiang, L.; Fang, J.; Zhao, C.; Ren, F.; Fang, L.; Wang, K.; Lu, X. Plant-inspired adhesive and tough hydrogel based on Ag-Lignin nanoparticles-triggered dynamic redox catechol chemistry. *Nat. Commun.* **2019**, *10*, No. 1487.
(38) Kokubo, T.; Takadama, H. How useful is SBF in predicting in vivo bone bioactivity? *Biomaterials* **2006**, *27*, 2907−2915.
(39) Huang, J.; Cao, Y.; Deng, Z.; Tong, H. Formation of titanate nanostructures under different NaOH concentration and their application in wastewater treatment. *J. Solid State Chem.* **2011**, *184*, 712−719.
(40) Yuan, Y.; Hays, M. P.; Hardwidge, P. R.; Kim, J. Surface characteristics influencing bacterial adhesion to polymeric substrates. *RSC Adv.* **2017**, *7*, 14254−14261.
(41) Kopf, B. S.; Ruch, S.; Berner, S.; Spencer, N. D.; Maniura-Weber, K. The role of nanostructures and hydrophilicity in osseointegration: In-vitro protein-adsorption and blood-interaction studies. *J. Biomed. Mater. Res., Part A* **2015**, *103*, 2661−2672.
(42) Drelich, J.; Chibowski, E. Superhydrophilic and Superwetting Surfaces: Definition and Mechanisms of Control. *Langmuir* **2010**, *26*, 18621−18623.
(43) Ribeiro, M.; Monteiro, F. J.; Ferraz, M. P. Infection of orthopedic implants with emphasis on bacterial adhesion process and techniques used in studying bacterial-material interactions. *Biomatter* **2012**, *2*, 176−194.
(44) Chen, L.; Komasa, S.; Hashimoto, Y.; Hontsu, S.; Okazaki, J. In Vitro and In Vivo Osteogenic Activity of Titanium Implants Coated by Pulsed Laser Deposition with a Thin Film of Fluoridated Hydroxyapatite. *Int. J. Mol. Sci.* **2018**, *19*, No. 1127.
(45) Yang, Z.; Si, S.; Zeng, X.; Zhang, C.; Dai, H. Mechanism and kinetics of apatite formation on nanocrystalline TiO2 coatings: A quartz crystal microbalance study. *Acta Biomater.* **2008**, *4*, 560−568.
(46) Gulati, K.; Maher, S.; Chandrasekaran, S.; Findlay, D. M.; Losic, D. Conversion of titania (TiO2) into conductive titanium (Ti) nanotube arrays for combined drug-delivery and electrical stimulation therapy. *J. Mater. Chem. B* **2016**, *4*, 371−375.
(47) Wandiyanto, J. V.; Truong, V. K.; Al Kobaisi, M.; Juodkazis, S.; Thissen, H.; Bazaka, O.; Bazaka, K.; Crawford, R. J.; Ivanova, E. P. The Fate of Osteoblast-Like MG-63 Cells on Pre-Infected Bactericidal Nanostructured Titanium Surfaces. *Materials* **2019**, *12*, No. 1575.
(48) Olson, M. E.; Ceri, H.; Morck, D. W.; Buret, A. G.; Read, R. R. Biofilm bacteria: formation and comparative susceptibility to antibiotics. *Can. J. Vet. Res.* **2002**, *66*, 86−92.
(49) Lyons, J. G.; Plantz, M. A.; Hsu, W. K.; Hsu, E. L.; Minardi, S. Nanostructured Biomaterials for Bone Regeneration. *Front. Bioeng. Biotechnol.* **2020**, *8*, No. 922.
(50) Wang, Q.; Zhou, P.; Liu, S.; Attarilar, S.; Ma, R. L.-W.; Zhong, Y.; Wang, L. Multi-Scale Surface Treatments of Titanium Implants for Rapid Osseointegration: A Review. *Nanomaterials* **2020**, *10*, No. 1244.
(51) Wennerberg, A. The importance of surface roughness for implant incorporation. *Int. J. Mach. Tools Manuf.* **1998**, *38*, 657−662.
(52) Wennerberg, A.; Albrektsson, T. Effects of titanium surface topography on bone integration: a systematic review. *Clin. Oral Implants Res.* **2009**, *20*, 172−184.
(53) Hohmann, J. K.; von Freymann, G. Influence of Direct Laser Written 3D Topographies on Proliferation and Differentiation of Osteoblast-Like Cells: Towards Improved Implant Surfaces. *Adv. Funct. Mater.* **2014**, *24*, 6573−6580.
(54) Yim, E. K.; Darling, E. M.; Kulangara, K.; Guilak, F.; Leong, K. W. Nanotopography-induced changes in focal adhesions, cytoskeletal organization, and mechanical properties of human mesenchymal stem cells. *Biomaterials* **2010**, *31*, 1299−1306.
(55) Brammer, K. S.; Oh, S.; Cobb, C. J.; Bjursten, L. M.; van der Heyde, H.; Jin, S. Improved bone-forming functionality on diameter-controlled TiO2 nanotube surface. *Acta Biomater.* **2009**, *5*, 3215−3223.
(56) Neoh, K. G.; Hu, X.; Zheng, D.; Kang, E. T. Balancing osteoblast functions and bacterial adhesion on functionalized titanium surfaces. *Biomaterials* **2012**, *33*, 2813−2822.
(57) Milner, K. R.; Siedlecki, C. A. Fibroblast response is enhanced by poly(L-lactic acid) nanotopography edge density and proximity. *Int. J. Nanomed.* **2007**, *2*, 201−211.
(58) Boyan, B. D.; Bonewald, L. F.; Paschalis, E. P.; Lohmann, C. H.; Rosser, J.; Cochran, D. L.; Dean, D. D.; Schwartz, Z.; Boskey, A. L. Osteoblast-mediated mineral deposition in culture is dependent on surface microtopography. *Calcif. Tissue Int.* **2002**, *71*, 519−529.
(59) Gittens, R. A.; Olivares-Navarrete, R.; Cheng, A.; Anderson, D. M.; McLachlan, T.; Stephan, I.; Geis-Gerstorfer, J.; Sandhage, K. H.; Fedorov, A. G.; Rupp, F.; Boyan, B. D.; Tannenbaum, R.; Schwartz, Z. The roles of titanium surface micro/nanotopography and wettability on the differential response of human osteoblast lineage cells. *Acta Biomater.* **2013**, *9*, 6268−6277.
(60) Tojkander, S.; Gateva, G.; Lappalainen, P. Actin stress fibers assembly, dynamics and biological roles. *J. Cell Sci.* **2012**, *125*, 1855−1864.
(61) Aparicio, C.; Padrós, A.; Gil, F. J. In vivo evaluation of micro-rough and bioactive titanium dental implants using histometry and pull-out tests. *J. Mech. Behav. Biomed. Mater.* **2011**, *4*, 1672−1682.
(62) Vilani, G. N. L.; de Oliveira Ruellas, A. C.; Elias, C. N.; Mattos, C. T. Stability of smooth and rough mini-implants: clinical and biomechanical evaluation - an in vivostudy. *Dent. Press J. Orthod.* **2015**, *20*, 35−42.

https://doi.org/10.1021/acsbiomaterials.1c01030
ACS Biomater. Sci. Eng. XXXX, XXX, XXX−XXX

Advancing of 3D-printed titanium implants with combined antibacterial protection using ultra-sharp nanostructured surface and gallium releasing agents

Shaheer Maher [1,2,‡], Denver Linklater [3,‡], Hadi Rastin [1], Tzuying Liao [3,4,5], Karolinne Martins de Sousa [3], Luis Lima-Marques [7], Peter Kingshott [4,5], Helmut Thissen [5,6], Elena P. Ivanova[3,5,], Dusan Losic [1*]*

[1] School of Chemical Engineering and Advanced Materials, The University of Adelaide, Adelaide SA 5005, Australia

[2] Faculty of Pharmacy, Assiut University, Assiut, 71526, Egypt

[3] College of STEM, School of Science, RMIT University, Melbourne VIC 3000, Australia

[4] Department of Chemistry and Biotechnology, School of Science, Swinburne University of Technology, Hawthorn VIC 3022, Australia

[5] Australian Research Council (ARC) Training Centre in Surface Engineering for Advanced Materials (SEAM), Swinburne University of Technology, Hawthorn VIC 3122, Australia

[6] CSIRO Manufacturing, Clayton VIC 3168, Australia

[7] The Institute for Photonics and Advanced Sensing, The University of Adelaide, Adelaide SA 5005, Australia

*** Corresponding Author:**

Dusan Losic: dusan.losic@adelaide.edu.au

Elena P. Ivanova: elena.ivanova@rmit.edu.au

The number of pages: 7

Number of figures: 6

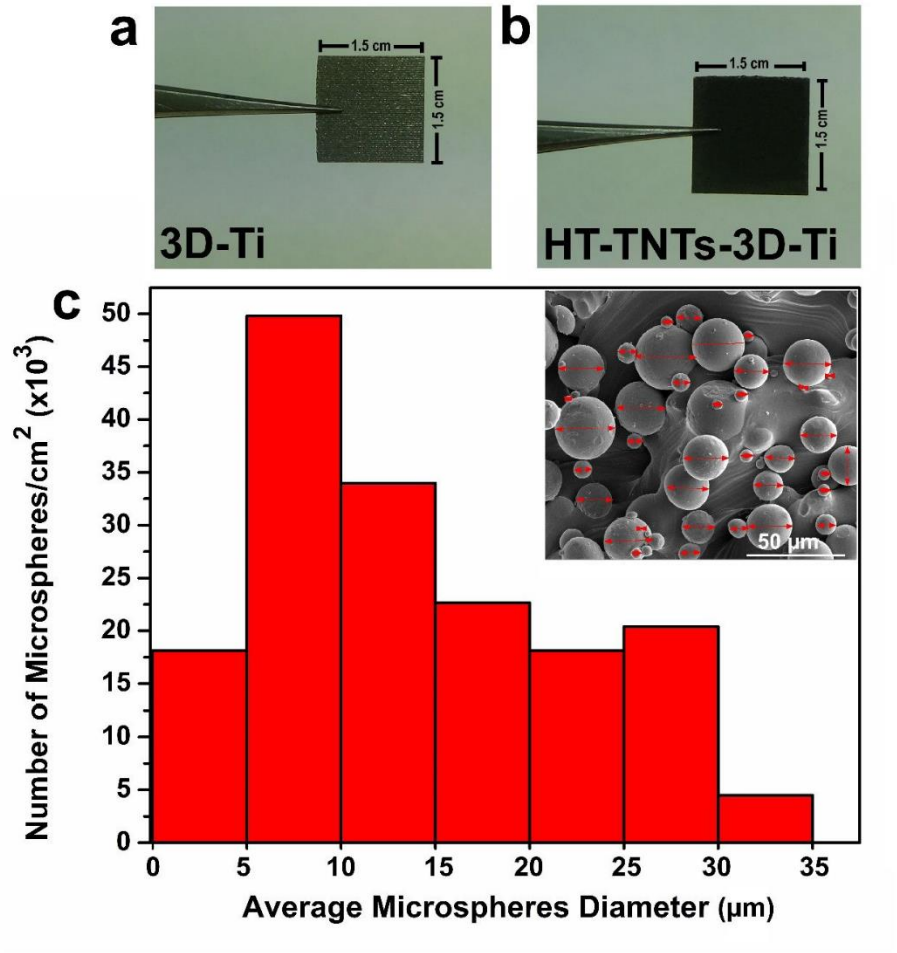

Figure S1. (a-b) camera image of 3D-Ti and HT-TNTs-3D-Ti plates (c) Size distribution of microspheres dispersed on top of 3D-Ti as measured from SEM images, inset showing SEM of 3D-Ti

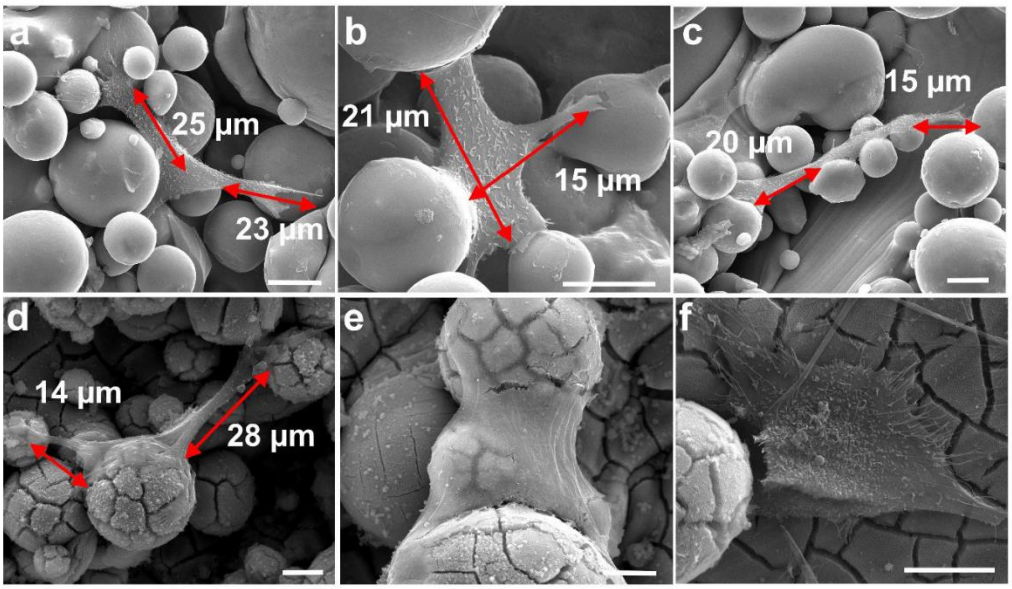

Figure S2. High resolution SEM images showing cells spreading on the surface of (a-c) 3D-Ti and (d-f) HT-TNTs-3D-Ti. The interspaces between microspheres were measured using ImageJ software from SEM images. Scale bars = 10 µm.

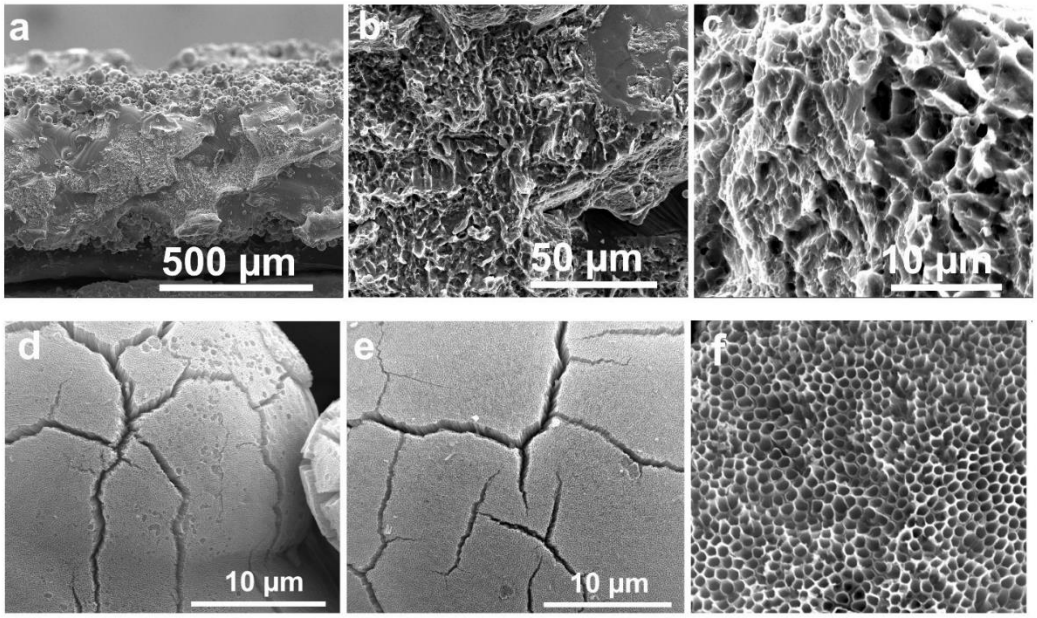

Figure S3: High resolution SEM images showing cross section of 3D-Ti. Microparticles appear firmly attached as seen in (a). (d-f) High resolution SEM image showing TNTs

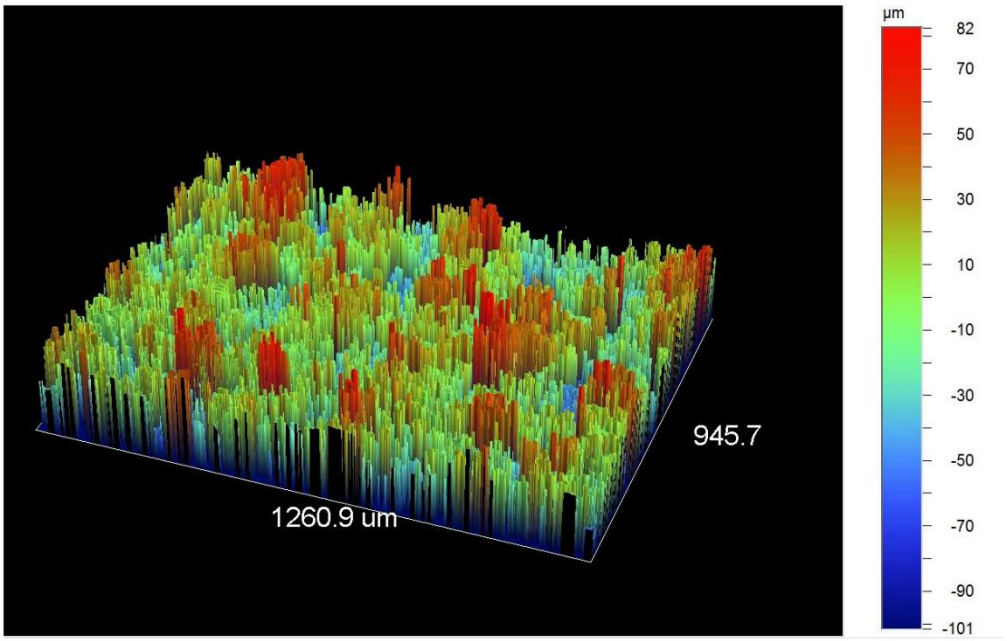

Figure S4. 3D reconstructed interferometer image of 3D-Ti

Rv (maximum valley depth) = 99.04 ±43 µm

Rt (Maximum peak height) = 69 ±12 µm

S5

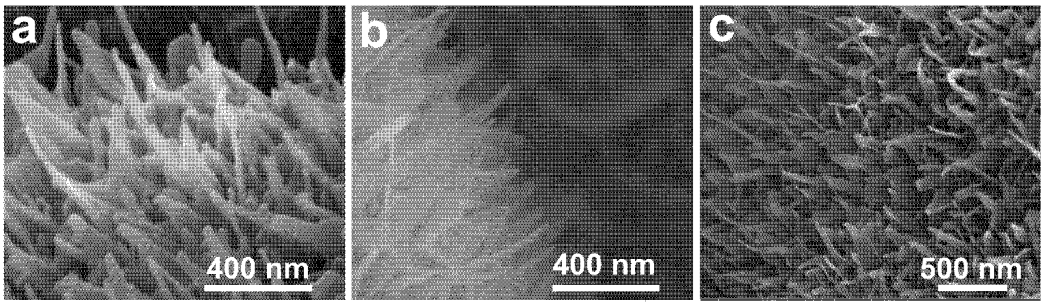

Figure S5: High resolution SEM images showing nanopillars structures on HT-TNTs-3D-Ti

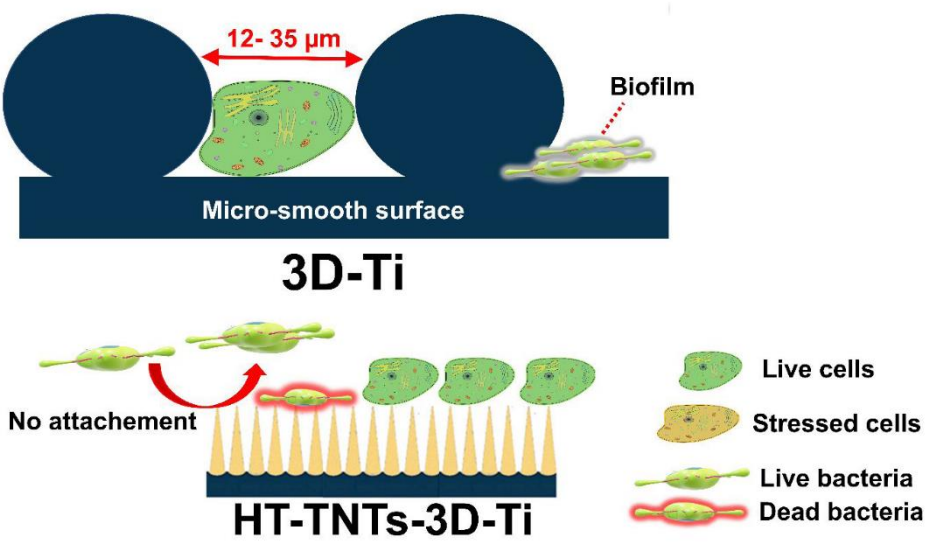

Figure S6. Schematic illustration showing effect of surface structures on MG63 cell and bacteria. HT-TNTs-3D-Ti showed bactericidal activity while bacterial biofilms were formed on 3D-Ti. Both 3D-Ti and HT-TNts-3D-Ti supported the adhesion of MG-36.

CHAPTER 7

CONCLUSIONS AND PERSPECTIVE

7.1 Conclusions:

The research described in this thesis contributes to the development of novel biomedical titanium implants by combining additive manufacturing technology (*i.e.,* selective laser melting) followed by post-fabrication surface manufacturing techniques of electrochemical anodization and a hydrothermal process, which are cost-effective and scalable. The fabricated implants were designed to address the current challenges facing the use of titanium implants for dental and orthopaedic applications. This study also explores the potential applications of Ti implants for localized drug delivery of therapeutics to overcome the drawbacks of systemic drug administration. In addition, multiple approaches were investigated to address the problem of bacterial infection at the implant surface through application of a non-conventional antibacterial agent (gallium ions), which has less potential to develop bacterial resistance than conventional antibiotics [1, 2], and through incorporating surface nano-features (*e.g.*, nanopillars and TNTs), that could reduce bacterial attachment while possessing inherent antibacterial properties. Finally, the ability of the surface features, either nano- or micro-scale, were assessed to control the process of bone cell attachment and proliferation.

Results obtained from this thesis will pave the way for further development of a new generation of low-cost, 3D-printed Ti implants, whose performance can be significantly upgraded by the combination of a mechano-bactericidal surface topography and drug-releasing functionality that is needed for an optimized implant, in order to dually control bone cell responses while effectively inhibiting bacterial colonization.

Three main concepts can be summarized based on research outcomes:

1- ***Localized drug delivery applications of TNTs (Chapter 3):***

New 3D-printed Ti alloy-based drug releasing implants with a unique combination of microspherical and nanotopography were fabricated. TNTs were grown on the surface of 3D-

printed Ti implants using an electrochemical anodization process. Chemotherapeutic agents doxorubicin (DOX) and apoptosis-inducing ligand (Apo2L/TRAIL) were then loaded into TNTs and tested for their cytotoxic activity [3].

Results confirmed the successful fabrication of well-ordered nanotube arrays covering the entire surface of a test implant of diameter 120 ± 10 nm and length 3.25 ±0.2 μm. Fibroblasts were then used to test if cell attachment to TNTs would significantly affect the release of the loaded drugs.

In-vitro drug release experiments confirmed the capacity of TNTs to release their drug loads. In addition, the release efficacy of chemotherapeutic agents from TNTs was unaffected by fibroblast adhesion, as confirmed by *in-vitro* cytotoxicity studies. At the same time, the loaded naturally occurring anticancer agent, Apo2L/TRAIL, was able to eradicate MDA-MB-231-TXSA human breast cancer cells while sparing normal fibroblasts attached on the surface.

It is worth mentioning that using fibroblasts, a connective tissue cell type found in numerous soft tissues, may not give accurate information about the attachment of bone cells on the surface of the implant since cell attachment may differ according to the type of cell used [4]. As a result, human primary osteoblasts and osteoblast-like MG-63 cells were used in the ensuing studies described throughout the thesis. However, the use of fibroblasts in Chapter 3 served the purpose to show that drugs loaded inside TNTs could be effectively released even when cells are attached on the surface

2- ***Controlling bone cell attachment and growth on surface of the implants (Chapters 4 and 6)***:

A major challenge associated with bone implants is uncontrolled bone cell growth and attachment on their surfaces. As discussed in Chapters 1 and 2, implants differ in their applications and intended duration inside the body [5]. Thus, the ability to direct (either promote or reduce) bone cell attachment and growth is important in the design of implants. As a result, the attachment and growth of human primary osteoblasts and MG-63 cells were tested on

different implant surfaces, including smooth 3D-Ti, 3D-Ti implants coated with TNTs (TNTs-3D-Ti) (Chapter 4), TNTs coated with HA (Chapter 4) and TNTs modified into nanopillars (Chapter 6). In addition, this research tried to find the specific microscale features that could promote cell adhesion, as discussed in Chapter 6.

Results revealed that TNTs showed significant reduction in MG-63 cell attachment and proliferation, suggesting that TNTs could be used for short-term implants where surface on-growth of bone cells is not desirable [6]. On the other hand, HA coating of TNTs significantly enhanced protein adsorption, cell adhesion and cell spreading on the surface, supported also by the expression of the late osteoblast/osteocyte genes *GJA1* and *PHEX [7]*.

Results from Chapters 5 and 6 revealed that the presence of surface nanopillars (HT-TNTs-3D-Ti) significantly enhanced HA deposition from SBF compared to smooth 3D-Ti [8, 9]. Cells also displayed greater propensity to mineralize compared to control surfaces. Moreover, 3D-printed surfaces with microspheres of diameter between 5-30 μm and interspaces of 12-35 μm favoured the attachment of osteoblast-like MG-63 cells, as confirmed by assessment of their attachment, proliferation, and viability in Chapter 6 [9].

3- ***Enhancing the antibacterial properties of Ti implants (Chapters 4 and 6)***:

Bacterial infection is considered one of the main reasons for implant failure and the need for their surgical removal. As previously discussed, systemically administered antibiotics may not efficiently reach the implant site to eradicate the bacteria due to impaired blood supply or formation of bacterial biofilms. Moreover, the excessive use of systemic antibiotics can have severe side-effects, especially on elderly patients or those with underlying poor health. To address this, the design of implants with multiple antibacterial actions was investigated. In this context, the antibacterial action of gallium nitrate loaded implants was studied. In addition, the bactericidal activity of surface nanostructures based on mechanical disruption of bacteria was also explored.

Results of Chapters 4 and 6 confirmed the antibacterial activity of gallium ions released from the surface of TNTs-3D-Ti and HT-TNTs-3D-Ti implants, in which 100% of the bacteria were effectively eradicated in case of *Staphylococcus aureus* and *Pseudomonas aeruginosa*. In addition, the *in-vitro* release study showed that Ga^{3+} could be effectively released for up to 5 days which is expected to be sufficient to prevent bacterial infection during the first few days of the life of the implant [6, 9].

On studying the inherent antibacterial activity of TNTs and nanopillars to provide long-term bactericidal protection, results confirmed that nanopillars significantly reduced bacterial attachment and prevented biofilm formation while killing bacteria remaining on the surface for both tested bacterial strains of *S. aureus* and *P. aeruginosa.* On the other hand, TNTs showed significantly high antibacterial activity against *P. aeruginosa* in contrast to *S. aureus*, which was more resistant [6]. This highlights the potential variability of the response of different bacterial species or strains to physical antibacterial mechanisms, as confirmed in Chapters 4 and 6.

7.2 Recommendations for future work

This research project marked a new advanced manufacturing process, which combines 3D-printing with surface nanoengineering technology to produce advanced Ti implants with dual micro- and nano-topography. Such implants are expected to control bio-integration post-surgery, as well as the implants featuring tuneable drug releasing properties to provide localized therapeutics for conditions such as bacterial infection and bone cancer. Furthermore, on demand production of highly customizable implants will reduce the high costs involved in implant post-processing procedures currently required in order to fit the specific needs of individual patients. This study opened many directions for future studies and several key aspects are recommended to translate this research into the development of the next generation of Ti implants and their progress into the next stages of *in-vivo* (pre-clinical) and clinical studies:

1- Exploring new surface functionalization approaches to achieve dual antibacterial and osseointegration properties:

One potential modification of the implant surfaces developed in this thesis is to incorporate graphene, owing to its attractive biocompatibility and mechanical properties with high surface area. Recent research confirmed that graphene can promote bone generation while inhibiting bacterial growth [10, 11]. Decorating the surface of Ti implants with graphene through a silanization treatment of the surface was recently reported, which appears to be an attractive strategy to combine the desirable properties of graphene into the surface of Ti implants [11].

2- In-vivo assessment of osseointegration, antibacterial, drug releasing ability and long-term toxicity of the fabricated implants:

TNTs and nanopillars fabricated in this study demonstrated great potential to control cell adhesion and growth. At the same time, they showed potential antibacterial and drug releasing capabilities. However, the behaviour of the fabricated nanostructures should be tested *in-vivo* to determine their actual efficacy and safety in terms of their integration in living tissues

and their ability to inhibit bacterial infection within biological environment. Therefore *in-vivo* studies are logical step forward for further development and implementation of outcomes on development of these 3D-printed implants.

3- Implementation of triggered release of drug loaded implants:

Triggered drug release is sometimes more desired than direct or immediate release. For example, in cases of bacterial infection that may occur after several months after implant insertion, the ability of triggering the release of antibacterial agents from the implant would be of great value. Triggered release is also highly desirable for anticancer agents which can be only released in response to specific triggering mechanisms [12, 13]. This was demonstrated by our team and others through a variety of techniques such as magnetic [14], electrical [15], ultrasonic [16], or pH triggering release mechanisms [17]. Thus, an appealing next step is to implement these triggering mechanisms into the multifunctional 3D-printed implants designed throughout this thesis.

4- Improvement of gallium loading and release for 3D-printed Ti implants*:*

In this thesis, gallium ions were effectively loaded and released on the surface of the fabricated implants. Their antibacterial efficacy was confirmed *in-vitro*. Although release of Ga^{3+} lasted for at least 5 days, the incorporation of gallium into the crystal structure of the implant itself could result in significantly prolonged antibacterial activity, a desirable property for long-term implants. Possible methods to achieve this is through hydrothermal ion-exchange processes [18] or by including gallium into Ti alloy powder that is used in the fabrication of the implants during SLM [19].

5- Exploring the sensing and monitoring capabilities of TNTs and nanopillars*:*

Ti implants could also provide real-time, non-invasive sensing capabilities within the microenvironment of the bone implant. This could help to monitor loading or pressure on the implants, bone healing or any change within the bone microenvironment that could suggest

early detection of infection, inflammation or other signs of implant failure, such as the formation of particulate wear or lack of bone integrations [20, 21]. However, *in-vivo* non-invasive sensing is very challenging problem [22] that requires implementation of specific sensing probes or wireless systems [21, 23] within the implants that can provide relevant signals monitored externally by devices such as radio frequency identification (RFID) [24]. This type of smart implants will reduce the huge costs which result from complications, facilitate real-time treatment and significantly reduce the recovery times [25]. Incorporating sensors into the design of 3D-printed implants fabricated in this thesis can result in multifunctional implants that can combine therapeutic benefits (*e.g.*, support and localized drug delivery functions) together with diagnostic functions.

6- Improving the mechanical strength by surface modification of Ti implants by microarc oxidation (MAO), also known as plasma electrolytic oxidation (PEO):

PEO is considered an innovative technique for surface coating of Ti and its alloys. Recent studies showed that PEO is an efficient strategy to improve Ti implant biocompatibility through application of Ca/P coatings [26]. It can also be used to functionalize the surface with antibacterial agents. Incorporating different antibacterial or bioactive materials during PEO process is a promising technique for the development of multifunctional implants, which is expected to be one of our research focuses in the future.

7- Exploring other antibacterial mechanisms of TNTs:

This thesis explored the physical antibacterial activity of TNTs. However, other antibacterial mechanisms should be also explored. TiO_2 nanoparticles have been previously studied for their ability to generate reactive oxygen species (ROS) under ultrasound stimulation, which resulted in inhibition of cancer cell growth [27]. The same property could be explored for TNTs, which could therefore be used as a potential mechanism to trigger on demand bactericidal or anticancer effects at the site of the implant.

References:

[1] E. Zhang, X. Zhao, J. Hu, R. Wang, S. Fu, G. Qin, Antibacterial metals and alloys for potential biomedical implants, Bioactive Materials 6(8) (2021) 2569-2612.

[2] X. Qu, H. Yang, B. Jia, M. Wang, B. Yue, Y. Zheng, K. Dai, Zinc alloy-based bone internal fixation screw with antibacterial and anti-osteolytic properties, Bioactive Materials 6(12) (2021) 4607-4624.

[3] S. Maher, G. Kaur, L. Lima-Marques, A. Evdokiou, D. Losic, Engineering of Micro- to Nanostructured 3D-Printed Drug-Releasing Titanium Implants for Enhanced Osseointegration and Localized Delivery of Anticancer Drugs, ACS Appl Mater Interfaces 9(35) (2017) 29562-29570.

[4] F.-Y. Teng, C.-L. Ko, H.-N. Kuo, J.-J. Hu, J.-H. Lin, C.-W. Lou, C.-C. Hung, Y.-L. Wang, C.-Y. Cheng, W.-C. Chen, A comparison of epithelial cells, fibroblasts, and osteoblasts in dental implant titanium topographies, Bioinorganic chemistry and applications 2012 (2012) 687291-687291.

[5] S. Maher, A. Mazinani, M.R. Barati, D. Losic, Engineered titanium implants for localized drug delivery: recent advances and perspectives of Titania nanotubes arrays, Expert Opin Drug Deliv 15(10) (2018) 1021-1037.

[6] S. Maher, D. Linklater, H. Rastin, P. Le Yap, E.P. Ivanova, D. Losic, Tailoring Additively Manufactured Titanium Implants for Short-Time Pediatric Implantations with Enhanced Bactericidal Activity, ChemMedChem 17(2) (2022) e202100580.

[7] J. Qin, D. Yang, S. Maher, L. Lima-Marques, Y. Zhou, Y. Chen, G.J. Atkins, D. Losic, Micro- and nano-structured 3D printed titanium implants with a hydroxyapatite coating for improved osseointegration, Journal of Materials Chemistry B 6(19) (2018) 3136-3144.

[8] S. Maher, A.R. Wijenayaka, L. Lima-Marques, D. Yang, G.J. Atkins, D. Losic, Advancing of Additive-Manufactured Titanium Implants with Bioinspired Micro- to Nanotopographies, ACS Biomaterials Science & Engineering 7(2) (2021) 441-450.

[9] S. Maher, D. Linklater, H. Rastin, S.T.-Y. Liao, K. Martins de Sousa, L. Lima-Marques, P. Kingshott, H. Thissen, E.P. Ivanova, D. Losic, Advancing of 3D-Printed Titanium Implants with Combined Antibacterial Protection Using Ultrasharp Nanostructured Surface and Gallium-Releasing Agents, ACS Biomaterials Science & Engineering 8(1) (2022) 314-327.

[10] X. Cheng, Q. Wan, X. Pei, Graphene Family Materials in Bone Tissue Regeneration: Perspectives and Challenges, Nanoscale research letters 13(1) (2018) 289-289.

[11] J. Sun, X. Liu, C. Lyu, Y. Hu, D. Zou, Y.-S. He, J. Lu, Synergistic antibacterial effect of graphene-coated titanium loaded with levofloxacin, Colloids and Surfaces B: Biointerfaces 208 (2021) 112090.

[12] M. Huo, Y. Chen, J. Shi, Triggered-release drug delivery nanosystems for cancer therapy by intravenous injection: where are we now?, Expert Opinion on Drug Delivery 13(9) (2016) 1195-1198.

[13] A. Jayasree, S. Ivanovski, K. Gulati, ON or OFF: Triggered therapies from anodized nano-engineered titanium implants, Journal of Controlled Release 333 (2021) 521-535.

[14] M.S. Aw, J. Addai-Mensah, D. Losic, Magnetic-responsive delivery of drug-carriers using titania nanotube arrays, Journal of Materials Chemistry 22(14) (2012) 6561-6563.

[15] K. Gulati, S. Maher, S. Chandrasekaran, D.M. Findlay, D. Losic, Conversion of titania (TiO2) into conductive titanium (Ti) nanotube arrays for combined drug-delivery and electrical stimulation therapy, Journal of Materials Chemistry B 4(3) (2016) 371-375.

[16] M.S. Aw, D. Losic, Ultrasound enhanced release of therapeutics from drug-releasing implants based on titania nanotube arrays, International journal of pharmaceutics 443(1) (2013) 154-162.

[17] T. Wang, X. Liu, Y. Zhu, Z.D. Cui, X.J. Yang, H. Pan, K.W.K. Yeung, S. Wu, Metal Ion Coordination Polymer-Capped pH-Triggered Drug Release System on Titania Nanotubes for Enhancing Self-antibacterial Capability of Ti Implants, ACS Biomaterials Science & Engineering 3(5) (2017) 816-825.

[18] M.D. Wadge, B.W. Stuart, K.G. Thomas, D.M. Grant, Generation and characterisation of gallium titanate surfaces through hydrothermal ion-exchange processes, Materials & Design 155 (2018) 264-277.

[19] A. Cochis, B. Azzimonti, R. Chiesa, L. Rimondini, M. Gasik, Metallurgical Gallium Additions to Titanium Alloys Demonstrate a Strong Time-Increasing Antibacterial Activity without any Cellular Toxicity, ACS Biomaterials Science & Engineering 5(6) (2019) 2815-2820.

[20] G. Bergmann, F. Graichen, J. Dymke, A. Rohlmann, G. Duda, P. Damm, High-Tech Hip Implant for Wireless Temperature Measurements In Vivo, PLoS ONE 7 (2012) e43489.

[21] A. Hassanzadeh, A. Moulavi, A. Panahi, A New Capacitive Sensor for Histomorphometry Evaluation of Dental Implants, IEEE Sens. J. 21(13) (2021) 14515-14521.

[22] E.H. Ledet, B. Liddle, K. Kradinova, S. Harper, Smart implants in orthopedic surgery, improving patient outcomes: a review, Innov Entrep Health 5 (2018) 41-51.

[23] B.D. Nelson, S.S. Karipott, Y. Wang, K.G. Ong, Wireless Technologies for Implantable Devices, Sensors (Basel) 20(16) (2020) 4604.

[24] H. Aubert, RFID technology for human implant devices, Comptes Rendus Physique 12(7) (2011) 675-683.

[25] J. Andreu-Perez, D.R. Leff, H.M. Ip, G.Z. Yang, From Wearable Sensors to Smart Implants--Toward Pervasive and Personalized Healthcare, IEEE Trans. Biomed. Eng. 62(12) (2015) 2750-62.

[26] M. Aliofkhazraei, D.D. Macdonald, E. Matykina, E.V. Parfenov, V.S. Egorkin, J.A. Curran, S.C. Troughton, S.L. Sinebryukhov, S.V. Gnedenkov, T. Lampke, F. Simchen, H.F. Nabavi, Review of plasma electrolytic oxidation of titanium substrates: Mechanism, properties, applications and limitations, Applied Surface Science Advances 5 (2021) 100121.

[27] D.G. You, V.G. Deepagan, W. Um, S. Jeon, S. Son, H. Chang, H.I. Yoon, Y.W. Cho, M. Swierczewska, S. Lee, M.G. Pomper, I.C. Kwon, K. Kim, J.H. Park, ROS-generating TiO2

nanoparticles for non-invasive sonodynamic therapy of cancer, Scientific Reports 6(1) (2016) 23200.